

THE ROLE OF PROTEIN DEGRADATION IN NEURONAL CELL DEATH

Thesis submitted for the degree of
Doctor of Philosophy
At the University of Leicester

by

Joanna Marie Norman
MRC Toxicology Unit

September 2008

The Role of Protein Degradation in Neuronal Cell Death

Joanna Norman, MRC Toxicology Unit, University of Leicester, Leicester, LE1 9HN

In neuronal systems, the degradation of intracellular proteins, controlled by the ubiquitin-proteasome system and autophagy, is of paramount importance for normal cellular homeostasis. The dysfunction of either of these pathways leads to the accumulation of protein aggregates, as seen in neurodegenerative conditions, culminating in neuronal cell death. In the current study I investigated the cleavage of the proteasome subunits, S1, S6' and S5a in cerebellar granule neurons induced to undergo apoptosis through the withdrawal of potassium. The cleavage of S1 and S6' and the loss of proteasomal activity corresponded with the activation of caspase-3; however the role of the proteasome was shown to be limited in this model as cells had passed the death commitment point. In addition, I developed a multiubiquitinated fluorescent sensor for the analysis of the proteasomal function on a single cell level, and characterised its use in SH-SY5Y cells. I have also constructed epitope-tagged plasmids encoding the autophagy-related proteins and examined their potential regulation by cell death proteases in an *in vitro* cleavage assay. Most of the autophagy-related proteins were cleaved in the *in vitro* model and the potential cleavage sites were identified for mutagenesis. The cleavage of Beclin 1 was also observed in apoptotic cerebellar granule neuron lysates. Finally, I investigated the mechanisms by which the HDACi, TSA, exerts a neuroprotective effect in cerebellar granule neurons. I have demonstrated that it increases the expression of a number of BCL2 family proteins, in particular MCL1, which was hypothesised to contribute to the neuroprotection observed. Taken together, I have demonstrated in this thesis that there are multiple levels of control during cell death; defining their importance is essential for the development of future drug targets.

Acknowledgements

Firstly, I would like to thank my supervisors: Profs Gerry Cohen and Pierluigi Nicotera for giving me the opportunity to carry out this work in their laboratories. To Dr Edward Bampton, my 'third' supervisor, I am so grateful for all the advice and guidance that you have given me in both my lab work and in the writing of this thesis, I appreciate it so much. Many thanks to Dr Mike Mulheran for his invaluable help with the statistical analysis. Also, thanks to the Mechanisms of Neuronal Apoptosis and Neurodegeneration, and the Mechanisms of Apoptosis groups, both of which I have had the pleasure of working with at the MRC.

I would also like to thank Dr Satoshi Inoue, Dr Nick Harper, Dr Michael Butterworth and Kathrin Weber for their invaluable help, support and friendship, especially the 'vodka/San Miguel nights' that we have shared and the discussions on football and rugby – I will miss them a lot!! Maria Azucena Guerra-Martin, thank-you for your continued help and guidance with the culturing of the CGNs throughout these four years. A special thanks to Dr Davina Twiddy who dealt with a lot of tears and frustration, and gave me so much help and advice, I wouldn't have lasted six months in the lab if it wasn't for your support. I can not find the words to describe how grateful I am.

Thank-you to my Mum and Dad, who have always had an unwavering belief in me and encouraged me to do the best that I can, and to Carrie; everything that you have achieved has made me so proud. Finally, to my boyfriend, Rob; there is so much that I want to thank you for. Thank-you for being there no matter what, always knowing the right things to say and for putting up with my tantrums! I am so grateful for your support, love and understanding throughout the last four years.

Table of Contents

Title Page.....	1
Abstract.....	2
Acknowledgements.....	3
Table of Contents.....	4
Table of Figures.....	10
Abbreviations.....	14

Chapter 1

Introduction.....	20
1.1. Apoptosis.....	21
1.1.2. Morphological and Biochemical features of Apoptosis.....	22
1.1.3. The Caspase Family.....	22
1.1.3.1. The Initiator Caspases.....	23
1.1.3.2. The Effector Caspases.....	23
1.1.4. The Extrinsic Pathway.....	25
1.1.5. The Intrinsic Pathway of Apoptosis.....	28
1.1.6. The BCL2 family.....	29
1.1.7. The Calpain Family.....	31
1.1.8. Neuronal Apoptosis.....	32
1.2. Protein and Organelle Degradation.....	33
1.2.1. The Ubiquitin-Proteasome System.....	34
1.2.1.1. The Ubiquitin Conjugation Pathway.....	34
1.2.1.1.1. Variations on Ubiquitination.....	39
1.2.1.1.2. Ubiquitin-like (UBL) proteins.....	39
1.2.1.2. Deubiquitinating enzymes.....	40
1.2.1.3. The 26S Proteasome.....	40
1.2.1.3.1. The 20S Core Particle.....	40
1.2.1.3.2. The 19S Regulatory Particle.....	41
1.2.1.4. Inhibitors of Proteasomal Activity.....	43
1.2.1.5. The Proteasome and Apoptosis.....	44
1.2.2. The Autophagy Pathway.....	44
1.2.2.1 Morphological features.....	45
1.2.2.2. The Autophagic Process.....	46
1.2.2.2.1. The Phagophore Assembly Site.....	46
1.2.2.2.2. The Target of Rapamycin (TOR)-dependent and independent induction of autophagy.....	47

1.2.2.2.3. Atg1 Kinase Complex.....	48
1.2.2.2.4. Atg9, Atg2 and Atg18	51
1.2.2.2.5. The Phosphatidylinositol 3-Kinase Complex	51
1.2.2.2.6. The Ubiquitin-like Protein Conjugation Systems	52
1.2.2.2.7. Maturation of the Autophagosome and Fusion with the Lysosome	53
1.2.2.3. Autophagy and Apoptosis	54
1.2.2.4. Degradation in the Nervous System.....	55
1.3. The HDAC Family	56
1.4. Aims	58

Chapter 2

Materials and Methods.....	59
2.1. Primary Culture of Mouse Cerebellar Granule Neurons	60
2.2. Potassium (K ⁺) withdrawal-induced apoptosis	60
2.3. Treatment with inhibitors of histone deacetylases (HDACi)	61
2.4. Assessment of neuronal viability	61
2.5. Preparation of CGN whole cell extracts for immunoblot	62
2.6. Preparation of isolated cerebella for immunoblot.....	62
2.7. Bradford Assay.....	62
2.8. SDS-Polyacrylamide Gel Electrophoresis (SDS-PAGE).....	63
2.9. Coomassie Blue Staining	63
2.10. Western blotting	63
2.11. Assay of Caspase-3/7 Activity.....	65
2.12. Assay of the Chymotrypsin-like Activity of the 20S Proteasome.....	66
2.13. Production and Purification of Recombinant Caspase-3.....	66
2.14. Construction of 26S Proteasome Sensor	68
2.15. Extraction of RNA from HeLa cells.....	70
2.16. Reverse Transcription-PCR	70
2.17. Construction of plasmids for hAtg3, 4A, 4B, 4C, 4D, 5, Beclin 1, 7, LC3, GABARAP, 9, 10 and 12.....	70
2.18. <i>In Vitro</i> Translation (TNT Reaction)	71
2.19. <i>In Vitro</i> Protease Cleavage Assays.....	74
2.20. SH-SY5Y Cell Culture	74
2.21. Transfection of SH-SY5Y cells.....	74
2.22. FACS Analysis for the measurement of YFP expression.....	75

2.23. Mouse Embryonic Fibroblast Cell Culture	75
2.24. Treatment of MEFs with HDACi	75
2.25. HDAC4 activity following immunoprecipitation	75
2.26. Statistical Analysis	75

Chapter 3

S1 and S6' are Cleaved in CGNs during K ⁺ Withdrawal-induced Cell Death	77
3.1. Introduction	78
3.2. Results	80
3.2.1. The caspase-3 cleavage sites in S1 and S6' are conserved in the mouse.	80
3.2.2 The proteasomal subunits S1 and S6' are cleaved by recombinant caspase-3 in CGN lysates <i>in vitro</i> .	80
3.2.3. The loss of CGN viability correlates with the activation of caspase-3/7.	85
3.2.4. The detection of the cleavage fragments of S1 and S6' correlate with the peak in caspase-3/7 activity.	89
3.2.5. The loss of 20S proteasomal activity is restored by caspase inhibitors.	94
3.2.6. The proteasome inhibitor MG132 delays the cell death stimulated by withdrawal of K ⁺ in CGNs.	99
3.2.7. The induction of autophagy is an early event in K ⁺ withdrawal in CGNs...	101
3.2.8. The construction of a proteasome sensor for single cell analysis of proteasomal degradation and its <i>in vitro</i> characterisation.	104
3.2.9. The characterisation of the proteasome sensor constructs in SH-SY5Y cells.	108
3.3. Discussion	113

Chapter 4

The <i>In Vitro</i> Cleavage of the hAtg Proteins by Cell Death Proteases.	118
4.1. Introduction	119
4.2. Results	121
4.2.1. The hAtg plasmids are expressed in an <i>in vitro</i> transcription-translation system.	121
4.2.2. The recombinant enzymes for <i>in vitro</i> characterisation are active.	121
4.2.3. Recombinant caspases and calpain 1 cleave numerous hAtg proteins <i>in vitro</i>	124
4.2.4. The cleavage of the hAtg constructs are further confirmed; and the potential cleavage sites identified.	127

4.2.4.1. Beclin 1 is cleaved at its N-terminus by rCaspase-3 and -6, and in the middle of the protein by rCalpain 1.....	127
4.2.4.2. hAtg9 was weakly expressed, despite efforts to increase its expression.	130
4.2.4.3. rCapase-3 and rCalpain 1 cleave in the middle of hAtg7.	130
4.2.4.4. hAtg12 is cleaved by rCalpain 1 at its N-terminus; the cleavage of hAtg5 is predicted to fall in its hAtg16-interacting domains.....	133
4.2.4.5. rCalpain 1 cleaves hAtg10 at its N-terminus.	133
4.2.4.5. hAtg4A is cleaved at its N-terminus by rCalpain 1 and rCaspase-3 cleaves its C-terminus.	136
4.2.4.6. hAtg4B is cleaved at the N-terminus by rCaspase-3; rCalpain 1 cleaves at the C-terminus.....	136
4.2.4.7. rCaspase-3 cleaves hAtg4C at its canonical N-terminal DEVD site; rCalpain 1 cleavage occurs in the middle of hAtg4C.....	139
4.2.4.8. GABARAP is cleaved at the C-terminus by rCalpain 1.	139
4.2.4.9. rAtg3 cleavage by rCaspase-3, -6 and -8, and rCalpain 1 occurs in the middle of the protein.....	142
4.2.5. A minor amount of Beclin 1 is cleaved during K ⁺ withdrawal-induced cell death in CGNs.....	144
4.3. Discussion.....	146

Chapter 5

The Modulation of the BCL2 Family Proteins by HDACi in CGNs	153
5.1. Introduction	154
5.2. Results	156
5.2.1. Multiple HDACs are expressed in CGNs.	156
5.2.2. The HDACi, TSA, induces rapid cell death in CGNs treated at DIV1, yet survival is maintained when treated at DIV7.	156
5.2.3. The 'switch' between the induction of cell death or the continued survival of CGNs after 24 h treatment with TSA is at approximately DIV4.....	162
5.2.4. TSA modulates the protein level of MCL1, BIM _{EL} , BID and BAX in CGNs at DIV7	167
5.2.5. The majority of HDAC activity in CGNs is the result of Class I HDACs. ...	171
5.2.6. BCL2 family protein expression is developmentally regulated in the cerebellum.....	174
5.3. Discussion.....	177

Chapter 6

General Discussion	182
6.1. General Discussion	183
6.2. Future Work	190
References.....	192

Table of Figures

Chapter 1

Figure 1.1.1: Schematic of caspase structure and maturation.....	24
Figure 1.1.2: The Extrinsic and Intrinsic Pathways of Apoptosis.....	26
Figure 1.1.3: Schematic of BCL2 family structure and the BH3-only protein binding specificity.....	30
Figure 1.2.1: The Ubiquitination Pathway.....	36
Figure 1.2.2: The Autophagy Pathway.....	49

Chapter 2

Figure 2.14.1: Purification profile of recombinant His6- Caspase-3 using Ni-NTA beads.....	67
Figure 2.16.1: Schematic of the construction of the proteasome sensor – p4xubi(G76V)-EYFP.....	69
Figure 2.19.1: Schematic of the construction of the hAtg plasmids for <i>in vitro</i> expression.....	72
Figure 2.19.2: Schematics of the hAtg constructs.....	73

Chapter 3

Figure 3.2.1: Sequence alignment of the human S1, S6' and S5a proteins with those from the mouse.....	81
Figure 3.2.2: Active rCaspase-3 is able to cleave S1 and S6' in mouse CGN lysates.....	83
Figure 3.2.3: Time course of K ⁺ withdrawal in CGNs.....	87
Figure 3.2.4: Caspase-3/7 activity peaks at 16 h in CGNs in low K ⁺	90
Figure 3.2.5: Active caspase-3 is evident at 8 h in low K ⁺	91
Figure 3.2.6: S1 and S6' are cleaved by 16 h in low K ⁺	93
Figure 3.2.7: Protease inhibitors restore proteasomal activity lost after 8 h in low K ⁺	95
Figure 3.2.8: The S1/S6' cleavage fragments are lost in the presence of caspase inhibitors.....	98
Figure 3.2.9: MG132 delays low K ⁺ induced cell death in CGNs.....	100
Figure 3.2.10: There is evidence of autophagy during the early stages of K ⁺ withdrawal cell death in CGNs.....	103
Figure 3.2.11: Schematic representation of the multi-ubiquitinated sensors prepared.....	105
Figure 3.2.12: The <i>in vitro</i> characterisation of constructed proteasome sensors.....	107

Figure 3.2.13: The characterisation of the proteasome sensors in SH-SY5Y cells....	109
Figure 3.2.14: Proteasome inhibitors cause the accumulation of EYFP in SH-SY5Y cells, confirming their use as a proteasome sensor.....	111

Chapter 4

Figure 4.2.1: The prepared Atg constructs are expressed in an <i>in vitro</i> transcription-translation system.....	122
Figure. 4.2.2: The recombinant proteases cleave substrates in a concentration-dependent manner.....	123
Figure 4.2.3: All hAtg proteins are cleaved by proteases <i>in vitro</i>	125
Figure 4.2.4: Beclin 1 is cleaved rCaspase-3, -6 and rCalpain 1.....	128
Figure 4.2.5: The expression of hAtg9 is weak in the TNT reaction.....	131
Figure 4.2.6: hAtg7 is cleaved by rCaspase-3 and rCalpain 1.....	132
Figure 4.2.7: The cleavage of hAtg12 by rCalpain 1 and hAtg5 by rCaspase-3.....	134
Figure 4.2.8: hAtg10 is cleaved by rCalpain 1 at its N-terminus.....	135
Figure 4.2.9: hAtg4A is cleaved by rCaspase-3 and rCalpain 1.....	137
Figure 4.2.10: The cleavage of hAtg4B by rCalpain 1 may fall in the vector sequence.....	138
Figure 4.2.11: hAtg4C is cleaved by rCaspase-3 and rCalpain 1.....	140
Figure 4.2.12: GABARAP is cleaved by rCalpain 1.....	141
Figure 4.2.13: hAtg3 is cleaved by rCaspase-3, -6, -8 and rCalpain 1.....	143
Figure 4.2.14: Beclin 1 is cleaved in CGNs undergoing cell death through K ⁺ withdrawal.....	145
Figure 4.3.1: The cleavage of the hAtg proteins by active caspases.....	147
Figure 4.3.2: The cleavage of the hAtg proteins by calpain 1.....	150

Chapter 5

Figure 5.2.1: HDAC protein expression in CGNs, MEFs and SH-SY5Y cells.....	157
Figure 5.2.2: TSA induces apoptosis at DIV1.....	159
Figure 5.2.3: TSA induces caspase cleavage in immature CGNs.....	160
Figure 5.2.4: The survival of mature CGNs (DIV7) is maintained up to 72 h after TSA treatment.....	161
Figure 5.2.5: The 'switch' in the differential response of CGNs to TSA occurs around DIV4.....	163
Figure 5.2.6: The BCL2 family proteins are differentially expressed between DIV1-7.....	165
Figure 5.2.7: MCL1, BIM _{EL} , BID and BAX are modulated by TSA in CGNs at DIV7	

.....	168
Figure 5.2.8: TSA induces the loss of BCL2 family proteins in CGNs at DIV1.....	170
Figure 5.2.9: The accumulation of AcTub cannot be used to confirm Class II HDAC inhibition in CGNs.....	172
Figure 5.2.10: The BCL2 family proteins are differentially expressed during the development of the cerebellum.....	175

Chapter 6

Figure 6.1.1: Schematic of the proposed processes in this investigation.....	184
--	-----

Abbreviations

A1/BCL2A1	BCL2-related protein A1
Ac-DEVD.AFC	Acetyl-Aspartic acid-Glutamine-Valine-Aspartic acid-7-amino-4-trifluoromethylcoumarin
AcH3	Acetylated Histone-3
AcTub	Acetylated Tubulin
AD	Alzheimer's Disease
AFC	7-amino-4-trifluoromethylcoumarin
Ala	Alanine
ALLN	N-Acetyl-Leu-Leu-Norleucinal
ALS	Amyotrophic Lateral Sclerosis
AMC	7-amino-4-methylcoumarin
AMPK	Adenosine monophosphate (AMP)-activated protein kinase
Apaf-1	Apoptotic Protease Activating Factor-1
APC	Anaphase Promoting Complex
Ape-1	Aminopeptidase I
APF	ATP-dependent Proteolysis factor (ubiquitin)
APG	Autophagy genes
Arg	Arginine
ATCC	American Type Culture Collection
Atg	Autophagy-related protein
ATG	Autophagy-related protein
ATP	Adenosine Triphosphate
AUG	Autophagocytosis genes
BAD	BCL2-antagonist of cell death
BAX	BCL2-associated X protein
BBC3/PUMA	BCL2-binding component-3
BCL2	B-cell lymphoma-2
BCLW	BCL2-like-2
Beclin 1	mammalian homologue of Atg6
BH	BCL2 Homology Domain
BID	BH3-interacting domain death agonist
Bif-1	Endophilin B1
BIK/BLK/NBK	BCL2-interacting killer
BIM	BCL2-like 11
BOK	BCL2-Ovarian Killer
BSA	Bovine Serum Albumin
Ca ²⁺	Calcium
CaCl ₂	Calcium Chloride
CAD	Caspase-activated DNase
CaMK	Calcium/calmodulin-dependent protein kinase
CaMKK	Calcium/calmodulin-dependent protein kinase kinase
CARD	Caspase Activation and Recruitment Domain
Caspase	Cysteiny aspartate-specific protease
CBP	CREB-binding Protein
CDK	Cyclin Dependent Protein Kinase
cDNA	Complementary Deoxyribonucleic acid
Ced	Cell Death Defective Gene (<i>C. elegans</i>)
CED	Cell Death Defective Protein (<i>C. elegans</i>)
CFP	Cyan Fluorescent Protein
CGN	Cerebellar Granule Neurons
CHAPS	3-[(3-cholamidopropyl)dimethylammonio]-propanesulphonate
CNS	Central Nervous System
CO ₂	Carbon Dioxide
CP	Proteasome 20S Core Particle
CREB	cAMP response element binding protein

CSS	Control Salt Solution
Cvt	Cytoplasm-to-vacuole
Cys	Cysteine
Cyt	Cytochrome
DD	Death Domain
DED	Death Effector Domain
DEVdase	Ability to process the fluorogenic substrate Aspartic acid-Glutamine-Valine-Aspartic Acid-7-amino-4-trifluoromethylcoumarin
DEVd.fmk	Z-Asp(OMe)-Glu(OMe)-Val-Asp(OMe)-fluoromethylketone
DIABLO	Direct IAP binding protein with low pI
DISC	Death-Inducing Signalling Complex
DIV	Days <i>in vitro</i>
DMEM	Dulbecco's Modified Eagle's Medium
DMSO	Dimethyl sulphoxide
DNA	Deoxyribonucleic acid
DP5	Death Protein-5
DTT	Dithiothreitol
DUB	Deubiquitinating Enzyme
4E-BP	4E- Binding Proteins
E1	Ubiquitin-activating Enzyme
E2	Ubiquitin-Conjugating Enzyme
E3	Ubiquitin-Ligases
E6-AP	E6-Associated Protein
ECACC	European Collection of Animal Cell Cultures
ECL	Enhanced Chemiluminescence
ECD	Evolutionary Conserved Domain
EDTA	Diaminoethanetetra-acetic acid
Egl-1	Egg-laying defective-1 gene
Egl-1	Egg-laying defective-1 protein
EGTA	1, 2-Di(2-aminoethoxy)ethane-N, N, N', N'-tetra-acetic acid
eIF2 α	Eukaryotic Initiation Factor 2 α
EM	Electron Microscopy
EMEA	European Medicines Agency
EYFP	Enhanced Yellow Fluorescent Protein
FACS	Fluorescence-Activated Cell Sorter
FADD	Fas receptor Associated Death Domain
FasL	Fas Ligand
FBS	Fetal Bovine Serum
FDA	Food and Drug Administration
FRET	Fluorescence Resonance Energy Transfer
G76V	glycine to valine mutation in ubiquitin
GABARAP	GABA _A Receptor Associated Protein
GAPDH	Glyceraldehyde-3-phosphate Dehydrogenase
GATE-16	Golgi Associated ATPase Enhancer of 16 kDa
GFAP	Glial Fibrillary Acidic Protein
GFP	Green Fluorescent Protein
Glu	Glutamine
Gly	Glycine
GSK	Glycogen Synthase Kinase
GTPase	Guanosine Triphosphatase
H33342/SYTOX	nuclear staining with Hoechst 33342/SYTOX Orange
h	Hour
H	Hoechst
HAT	Histone Acetylase

HCl	Hydrochloric acid
HD	Huntington's Disease
HDAC	Histone Deacetylase
HDACi	Histone Deacetylase Inhibitor/s
HDM	human homologue of MDM2
HECT	Homologous to E6-AP C-terminus
HeLa	Human Cervix Adenocarcinoma Cell Line
HEPES	N-[2-Hydroxyethyl]piperazine-N'-[2-ethanesulphonic acid]
His	Histidine
His ₆	6-Histidine residue tag
HRP	Horseradish Peroxidase
HRK	Harakiri
HRP	Horseradish Peroxidase
HSP	Heat Shock Protein
Htt	Huntingtin Protein
IAP	Inhibitor of Apoptosis Proteins
IB	Immunoblot
ICAD	Inhibitor of caspase-activated DNase
ICE	Interleukin-1-converting enzyme
IETD.AFC	N-acetyl-Asp-Glu-Val-Asp-7-amino-4-trifluoromethylcoumarin
IFN- γ	Interferon- γ
IgG	Immunoglobulin Gamma
IGL	Internal Granule Layer
IL-1 β	Interleukin-1 β
Ile	Isoleucine
IGF-1	Insulin-like growth factor
IM	Isolation Membrane
IP	Immunoprecipitation
IP ₃	Inositol-1, 4, 5-Triphosphate
IPTG	Isopropyl-beta-D-thiogalactopyranoside
IRS1	Insulin Receptor Substrate 1
JNK	c-Jun N-Terminal Kinase
K ⁺	Potassium
K25	Control Salt solution with 25 mM K ⁺
K5	Control Salt Solution with 5 mM K ⁺
KCl	Potassium Chloride
kDa	kilo Dalton
KSR	Kinetic Scan Reader
Leu	Leucine
LC3	Microtubule-associated protein 1 Light Chain 3
LLVY.AMC	Succinyl-Leu-Leu-Val-Tyr-7-amino-4-methylcoumarin
LLVYase	Ability to process the fluorogenic substrate Leucine-Leucine-Valine-Tyrosine-7-amino-4-methyl-coumarin
Lys	Lysine
MAPK	Mitogen-Activated Protein Kinase Kinase
MCL1	Myeloid Cell Leukaemia Sequence-1
MDM	Mouse Double Minute -2
MEFs	Mouse Embryonic Fibroblast cells
MEM	Minimum Essential Medium
Mg	Magnesium
MG115	Z-Leu-Leu-Norvalinal
MG132	Cbz-Leu-Leu-Leucinal
MgCl ₂	Magnesium Chloride
MJD	Machado Joseph Disease

MK-801	(5S, 10R)-(+)-5-methyl-10, 11-dihydro-5H-dibenzo[a, d]cyclohepten-5, 10-imine hydrochloride maleate
mRNA	Messenger Ribonucleic Acid
MTT	3-(4, 5-Dimethylthiazol-2-yl)-2, 5-diphenyltetrazolium bromide
N-BAK	alternatively spliced form of BAK expressed in neuronal cells
NaCl	Sodium Chloride
NAD ⁺	Nicotinamide Adenine Dinucleotide (oxidised form)
NCI	National Cancer Institute
NCS	Newborn Calf Serum
NEDD	Neuronal Precursor Cell Expressed Developmentally Down Regulated Protein
NGF	Nerve Growth Factor
NK	Natural Killer cells
NMDA	N-methyl-D-aspartic Acid
nPIST	Novel Form of Protein Interacting Specifically with Tc10
OD	Optical Density
OMM	Outer Mitochondrial Membrane
OTU	Ovarian Tumour Proteases
P	Postnatal day
PAC	Proteasome Assembling Chaperone
PAGE	Polyacrylamide gel electrophoresis
PAN	Proteasome Activating Nucleotidases
PARP	Poly (ADP-ribose) Polymerase
PAS	Phagophore Assembly Site
PBS	Phosphate Buffered Saline
PCR	Polymerase Chain Reaction
PD	Parkinson's Disease
PE	Phosphatidylethanolamine
Phe	Phenylalanine
PI(3)K	Phosphatidylinositol 3-Kinase
Pro	Proline
PS	Phosphatidylserine
PS-341	Bortezomib/Velcade
PUMA	p53 Upregulated Modulator of Apoptosis
r	Recombinant
Rad23	Radiation Gene 23
Raptor	Regulatory Associated Protein of mTOR
Rheb	Ras Homologue Enriched in Brain
RING	Really Interesting New Gene
RIP	Receptor Interacting Protein
RIPA	Radio Immuno Precipitation Assay
RNA	Ribonucleic Acid
ROS	Reactive Oxygen Species
RP	Proteasome 19S Regulatory Particle
RPT	Regulatory Particle Triphosphatase
RT	Room temperature
S1	human homologue of proteasome subunit Rpn2
S2	human homologue of proteasome subunit Rpn1
S5a	human homologue of proteasome subunit Rpn10
S6	human homologue of proteasome subunit Rpt5
S6K1	Ribosomal S6 Kinase 1
<i>S. cerevisiae</i>	<i>Saccharomyces cerevisiae</i>
SDS	Sodium dodecyl sulphate
SEM	Standard Error of the Mean
Ser	Serine

siRNA	Small Interfering Ribonucleic Acid
SMAC	Second Mitochondrial-derived Activator of Apoptosis
SOD	Superoxide Dismutase
Strep-HRP	Streptavidin-biotinylated-HRP
SUMO	Small Ubiquitin Like Modifier
SVM	Support Vector Machine
SYTOX	SYTOX orange, nucleic acid stain
TBS-T	Tris-Buffered Saline +0.1% (v/v) Tween
Thr	Threonine
TNF	Tumour Necrosis Factor
TNT	Transcription/Translation System
(m)TOR(C)	(mammalian) Target of Rapamycin (Complex)
TRADD	TNF Receptor-associated DD protein
TRAF2	TNR Receptor-associated factor-2
TRAIL	TNF-related apoptosis-inducing ligand
TRIS	2-Amino-2-(hydroxymethyl)-1, 3-Propanediol
tRNA	Transfer Ribonucleic Acid
Trp	Tryptophan
TSA	Trichostatin A
TSC	Tuberous Sclerosis Complex
TWEEN™ 20	Polyoxyethylenesorbitan monolaurate
Tyr	Tyrosine
UV	Ultraviolet
UBA	Ubiquitin Associated Domain
Ubi	ubiquitin
UBL	Ubiquitin-Like domain
UCH	Ubiquitin C Terminal Hydrolases
ULK1/2	human homologues of Atg1
ULP	UBL Specific Proteases
UPR	Unfolded Protein Response
UPS	Ubiquitin Proteasome System
USP	Ubiquitin Specific Proteases
UVRAG	UV Irradiated Resistance Associated Tumour Suppressor Gene
Val	Valine
VC	Vehicle Control
VEID	N-acetyl-Val-Glu-Ile-Asp-7-amino-4-trifluoromethylcoumarin
VPA	Valproic Acid
Vps	Vacuolar Protein Sorting
v/v	Volume to Volume
w/v	Weight to Volume
WT	Wild-type
z-VAD.fmk	Benzyloxycarbonyl-Valine-Alanine-Aspartic acid-fluoromethylketone

Chapter 1

Introduction

1.0. Introduction

1.1. Apoptosis

The term 'apoptosis' was coined in the seminal paper by Currie and colleagues in 1972, in which they described a highly regulated, programmed form of cell death for the normal turnover of various cell types and tissues (Kerr *et al.*, 1972). This was an alternative to the 'violent' form of cell death – necrosis that resulted in the disruption of cellular homeostasis (Bras *et al.*, 2005). Apoptosis is involved in a number of important biological processes, including the development of the nervous system, the immune system, hormone dependent atrophy and cell death induced by chemical and environmental stressors such as UV (Nagata, 1997; Oppenheim, 1991). Furthermore, inappropriate apoptosis has been implicated in a number of human diseases including autoimmune diseases, several neurodegenerative diseases and many forms of cancer (reviewed in (Hanahan and Weinberg, 2000; Munoz *et al.*, 2008; Yuan and Yankner, 2000)).

Apoptosis is initiated by two main pathways: the extrinsic pathway, in which extracellular death ligands bind to transmembrane death receptors; and the intrinsic pathway that is stimulated in response to cell stress or damage (Taylor *et al.*, 2008). The extrinsic and intrinsic pathways will be discussed in further detail in section 1.1.4 and 1.1.5 respectively. Both extracellular and intracellular apoptotic signals converge at the activation of a group of cysteine proteases, the caspases, which are responsible for the majority of the characteristics of apoptotic cells and will be discussed in greater detail in section.1.1.3.

The understanding of the genetic basis of apoptosis was gained from studies into the development of the nematode *Caenorhabditis elegans* (*C. elegans*) (Degterev and Yuan, 2008; Ellis and Horvitz, 1986). The activation of programmed cell death in *C. elegans* is controlled by the genes *ced-3*, *ced-4*, *ced-9* and *egl-1* (Conradt and Horvitz, 1998; Hengartner and Horvitz, 1994; Yuan and Horvitz, 1992; Yuan *et al.*, 1993). Multiple mammalian homologues to the identified genes have since been discovered and it was found that the key players in the apoptotic pathway are highly conserved in mammals, *C. elegans* and the fruitfly *Drosophila melanogaster*. The proteins encoded by *ced-3* and *ced-9* are homologues of the mammalian proteins interleukin-1 β -converting enzyme (ICE, caspase-1(Yuan *et al.*, 1993)) and anti-apoptotic BCL2 (B-cell lymphoma 2) protein (Hengartner and Horvitz, 1994) respectively. Furthermore, the mammalian homolog of CED-4 is the adaptor protein APAF1 (apoptotic protease

activating factor 1 (Zou *et al.*, 1997)) and EGL-1 closely resembles the BCL2 homology-3 (BH3)-only proteins of the BCL2 family (Conradt and Horvitz, 1998).

1.1.2. Morphological and Biochemical features of Apoptosis

Apoptosis is a morphologically and biochemically distinct form of cell death (Bratton *et al.*, 2000). Hundreds of proteins undergo proteolysis during apoptosis and most of the features described for apoptotic cells are the result of protease cleavage. The most noticeable feature of apoptosis is the condensation and fragmentation of the nucleus. Nuclear fragmentation is induced in part by the proteolysis of lamin A, B and C by caspases, which is thought to facilitate nuclear breakdown (Rao *et al.*, 1996). In addition, the degradation of DNA is also the result of chromatin cleavage by caspase activated DNase (CAD) at internucleosomal sites. In healthy cells, CAD is associated with its inhibitor ICAD (inhibitor of CAD), however during apoptosis ICAD is cleaved by caspases and CAD is released (Enari *et al.*, 1998; Sakahira *et al.*, 1998). However, studies from cells expressing caspase-resistant ICAD or CAD deficient cells suggest that it is not indispensable for early-stage apoptotic DNA degradation, and that there are contributions from other factors such as acinus during apoptosis (Nagata *et al.*, 2003; Sahara *et al.*, 1999; Samejima *et al.*, 2001; Samejima *et al.*, 1998).

In the early stages of apoptosis, the rounding and retraction of the cell is observed. This is the result of caspase-mediated proteolysis of many of the cytoskeletal constituents, including gelsolin and spectrin (Kothakota *et al.*, 1997; Martin *et al.*, 1995). Plasma membrane blebbing is also thought to be the result of a weakened cytoskeleton. In addition, caspase activation is required for the exposure of phagocytic signals on the cell surface, including phosphatidylserine (PS) (Fadok *et al.*, 1992; Taylor *et al.*, 2008). The release of cytochrome c (cyt c) from the intermembrane space of the mitochondria is the result of the permeabilization of the outer mitochondrial membrane mediated by the BCL2 proteins, BAX (BCL2-associated X protein) or BAK (BCL-antagonist/killer-1) (Kluck *et al.*, 1997; Liu *et al.*, 1996; Yang *et al.*, 1997). In addition, the caspase-mediated dismantling of the electron transport chain and secondary release of cyt c is associated with the loss of the mitochondrial transmembrane potential, energy depletion and the subsequent production of reactive oxygen species (ROS) (Chen *et al.*, 2000; Ricci *et al.*, 2004).

1.1.3. The Caspase Family

In 1992, two independent studies simultaneously identified ICE as the human protease responsible for the activation of the precursor interleukin-1 β (Cerretti *et al.*, 1992;

Thornberry *et al.*, 1992). This protease is today referred to as caspase-1 and is a member of a family of cysteine proteases that have a preference for cleaving after an aspartic acid residue in their target proteins. Fourteen mammalian caspases have been identified including eleven in humans (Cohen, 1997; Fuentes-Prior and Salvesen, 2004). Seven caspases are thought to be involved in apoptosis. In addition, caspase-1, caspase-4, caspase-5, caspase-11 and caspase-12 are thought to be involved in the response to inflammation (reviewed in (Martinon and Tschopp, 2007)); caspase-14 may be involved in keratinocyte differentiation.

Caspases are synthesized as inactive zymogens or proenzymes, consisting of an N-terminal pro-domain followed by a large subunit of ~20 kDa and a small subunit of ~10 kDa joined by a small spacer (Figure 1.1.1). The caspase family are subdivided into two categories, the “initiator” caspases (including caspase-2, -8, -9, and -10) and the “effector” caspases (caspase-3, -6 and -7) (Shi, 2002).

1.1.3.1. The Initiator Caspases

The initiator caspases are characterised by long pro-domains of more than 90 amino acids, which allow them to interact with death effector domains (DEDs) or caspase-activation recruitment domains (CARDs) in specific adapter proteins (Bratton *et al.*, 2001). In contrast to the effector caspases, cleavage of the initiator caspases is not required nor is it sufficient for their activation (Stennicke *et al.*, 1999). The zymogens of the initiator caspases exist as inactive monomers in the absence of an apoptotic stimulus. They are recruited to multiprotein complexes via their respective N-terminal recruitment domains (CARD for caspase-9 and DED for caspase-8) (Boldin *et al.*, 1996; Li *et al.*, 1997; Muzio *et al.*, 1996). The increase in the local concentration of the monomers allows them to adopt a dimeric active conformation. The processing of the initiator caspases then occurs (Boatright *et al.*, 2003; Donepudi *et al.*, 2003). Once active, caspase-8 is capable of processing caspase-3, caspase-7 and caspase-9 (Muzio *et al.*, 1997; Srinivasula *et al.*, 1996a); caspase-9 activates caspase-3 and caspase-7 (Li *et al.*, 1997).

1.1.3.2. The Effector Caspases

Zymogens of the effector caspases exist as inactive heterodimers at physiological concentrations. The activation of effector caspases is carried out by initiator caspases through cleavage at specific internal aspartate residues between the large and small subunits (Boatright *et al.*, 2003). A secondary autocatalytic event removes the pro-domain. The structure of ICE was solved simultaneously by two independent groups

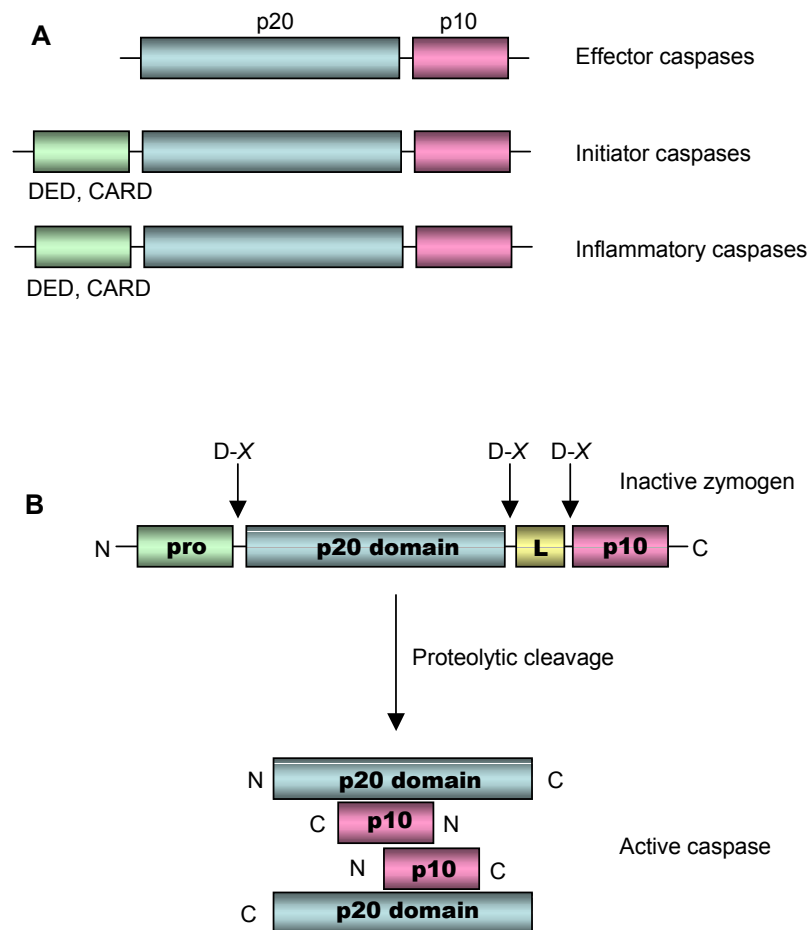


Figure 1.1.1. Schematic of caspase structure and maturation (Adapted from Degterev and Yuan, 2008; Twiddy, 2005). The inactive caspase zymogens have three main domains: a prodomain and large (p20) and small (p10) subunits. The prodomains of the initiator and inflammatory caspases contain protein-protein interaction domains that link them to apoptosis signalling complexes (CARD/DED) (**A**). These are proteolytically cleaved during activation after aspartate residues (D-X) to remove the prodomain and separate the p20 and p10 subunits. The large subunits contain the active site cysteine residue. Not all caspases contain the linker (L) domain (**B**).

and provided an insight into the mechanism of effector caspase activation (Walker *et al.*, 1994; Wilson *et al.*, 1994). It revealed that two cleaved caspase heterodimers, consisting of a large and small subunit combine to form an active heterotetramer containing the active site cysteine, a conserved residue in the active site of all caspases. The active site is formed by residue contributions from the p10 subunit of one heterodimer and the p20 subunit of the other; the active heterotetramer therefore contains two active sites. The studies also suggested that each heterodimer is proteolytically activated prior to the formation of the heterotetramer, allowing the structural rearrangements necessary for active site formation (Walker *et al.*, 1994; Wilson *et al.*, 1994). Once active, the effector caspases are able to cleave a broad array of structural and regulatory components of the cell, ultimately resulting in many of the apoptotic features already described.

Caspases recognise specific tetra- or pentapeptide motifs (P4-P3-P2-P1) in substrates, cleaving on the C-terminal side of P1, which is usually an aspartic acid residue. The optimal recognition motif for caspase-3 and -7 is DEXD. In comparison, caspase-6, -8 and -9 prefer the motif (L/V)EXD. Besides the near absolute requirement for Asp, N-terminal to the scissile bond at position P₁; a critical determinant of specificity has been shown to be position P₄. In general, the caspases also have a preference for Glu at position P₂, although this is not absolute (Thornberry *et al.*, 1997). At least for caspase-3 and -7, there does not seem to be a favourable specificity for amino acids at P₅ (Talanian *et al.*, 1997). Small amino acids such as Ser, Gly and Ala seem to be preferred at position P₁' (Stennicke *et al.*, 2000). The ability of caspases to recognise specific amino acid sequences results in a selective cascade of caspase activation, the motifs being present in many of the proforms of the inactive enzymes themselves.

1.1.4. The Extrinsic Pathway

The extrinsic pathway of apoptosis is responsible for the elimination of unwanted cells during immune system education, immunosurveillance and during development. It is triggered by the binding of a tumour necrosis factor (TNF) family member ligand (such as TNF, CD95L/FasL/APO-1L and TNF-related apoptosis-inducing ligand (TRAIL)) with their cognate receptors on the cell surface (Figure 1.1.2; reviewed in (Bratton *et al.*, 2000; MacFarlane, 2003)). The ligation of CD95L to the CD95 receptor induces receptor trimerization. This stimulates the recruitment of the adaptor protein FADD/Mort-1 (Fas-associated death domain) to the receptor's intracellular cytoplasmic domain known as the death domain (DD), forming the DISC (death-inducing signalling complex). FADD binds directly to the DD, through its own C-terminal DD (Boldin *et al.*,

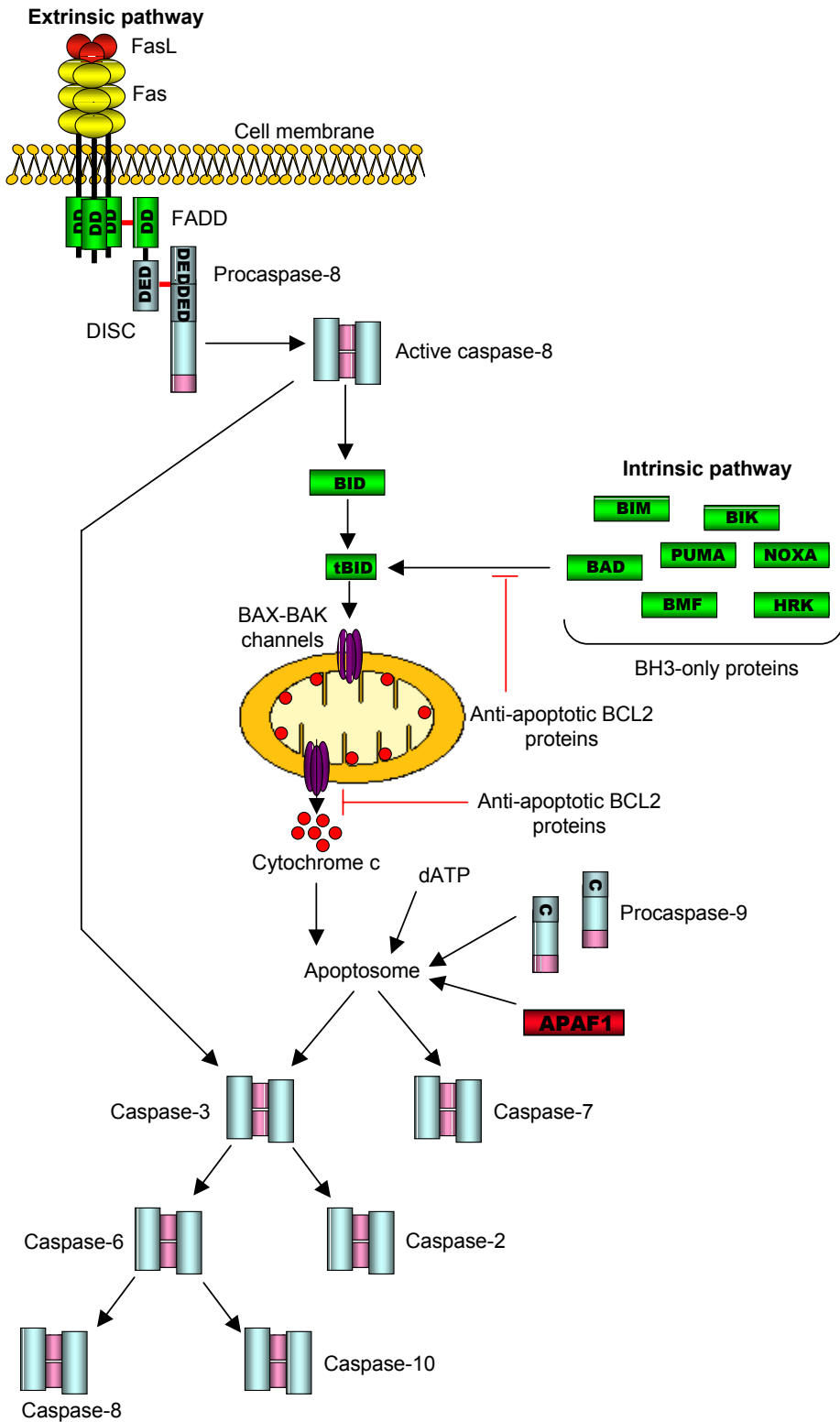


Figure 1.1.2. The Extrinsic and Intrinsic Pathways of Apoptosis (adapted from Hill *et al*, 2003). During the extrinsic pathway the binding of a death ligand to its cognate receptor, such as FasL, induces the recruitment and oligomerization of procaspase-8 via the adapter molecule FADD. Active caspase-8 processes and activates caspase-3, initiating a caspase cascade and substrate proteolysis. Active caspase-8 can also cleave the BCL2 family protein BID in certain cells, resulting in the activation of BAX/BAK, release of cyt *c* from the mitochondria and the formation of the apoptosome. Active caspase-9 can then process and activate caspase-3 and -7, and downstream caspase activation continues. The intrinsic pathway is initiated by BH3-only protein induction or post-translational activation that inactivate the pro-survival BCL2 proteins, leading to the activation of BAX/BAK as discussed above.

1995; Chinnaiyan *et al.*, 1995). The complete DISC is formed when FADD recruits procaspase-8, which binds to the death effector domain (DED) at the N-terminus of FADD through its own DED located in its prodomain (Boldin *et al.*, 1996; Medema *et al.*, 1997; Muzio *et al.*, 1996). Multiple monomeric procaspase-8 molecules are recruited via the dual adapter molecule FADD and the subsequent generation of active caspase-8 then occurs by dimerization followed by transcatolysis (Muzio *et al.*, 1998). Caspase-8 then activates a caspase cascade that results in the death of the cell (Muzio *et al.*, 1997; Srinivasula *et al.*, 1996a).

There are four TRAIL receptors that bind the ligand TRAIL. However, only TRAIL-R1 and TRAIL-R2 signal to apoptosis; TRAIL-R3 and -R4 do not have functional DDs. The TRAIL DISC also contains FADD and caspase-8 (Ashkenazi, 2002). In contrast to the TRAIL and Fas/CD95 DISCs, TNF-receptor 1 (TNF-R1) initially recruits a different adapter protein: TNF receptor-associated DD protein (TRADD) (Hsu *et al.*, 1995), which is then believed to associate with FADD. However, FADD and caspase-8 are not recruited to the DISC and are activated elsewhere in the cell (Harper *et al.*, 2003). In addition, TRADD acts as a platform for the interaction with other signalling molecules, including RIP (receptor-interacting protein) and TRAF2 (TNF receptor-associated factor 2), which signal to the JNK (c-Jun N-terminal kinase) and NF- κ B pathways respectively (Hsu *et al.*, 1996a; Hsu *et al.*, 1996b).

1.1.5. The Intrinsic Pathway of Apoptosis

The intrinsic pathway is triggered in response to various stress stimuli such as chemotherapeutic agents, ionising radiation and growth factor withdrawal (reviewed in (Bratton *et al.*, 2000; Cain *et al.*, 2002; Hengartner, 2000). The co-ordinated release of several proteins from the mitochondrial intermembrane space into the cytosol is a key event in the intrinsic apoptotic pathway (Figure 1.1.2). The release of cytochrome c in particular is important for the subsequent activation of caspases. Cytochrome c associates with APAF1 in the cytoplasm, possibly via the WD-40 repeats at the C-terminus of APAF1. This results in the unfolding of APAF1 and exposes its central nucleotide domain, which facilitates the binding and hydrolysis of dATP/ATP causing APAF1 oligomerisation and exposure of the APAF1 CARD domain (Hu *et al.*, 1998; Jiang and Wang, 2000; Li *et al.*, 1997; Saleh *et al.*, 1999). Multiple monomeric molecules of procaspase-9 are recruited through the interaction of the CARD regions on both proteins. The APAF1: cyt c: caspase-9 multimeric complex is known as the apoptosome. The molecules of multimeric caspase-9 dimerize and undergo autocatalysis to generate active caspase-9 (Srinivasula *et al.*, 1998). Caspase-9 then

recruits and activates caspase-3/-7 at the apoptosome (Bratton *et al.*, 2001). Caspase-3 processes and activates caspase-6 (Srinivasula *et al.*, 1996b), followed by activation of caspase-8 and 10. Caspase-3 also feeds back on caspase-9 and produces a differentially processed form of caspase-9 (p37) (Slee *et al.*, 1999; Srinivasula *et al.*, 1996b).

There is also crosstalk between the intrinsic and extrinsic signalling pathways. The BCL2 family member, BID (BH3-interacting domain death agonist), is processed by caspase-8, initiating its translocation to the mitochondria, where it induces the release of cytochrome c and the assembly of the apoptosome (Li *et al.*, 1998; Sun *et al.*, 1999).

Endogenous controls exist to delay cell death mediated by the apoptosome. Apoptosis can be suppressed by the direct inhibition of caspases by the inhibitor of apoptosis proteins (IAPs) (Bratton *et al.*, 2001; Deveraux *et al.*, 1998; Twiddy *et al.*, 2006). However, the anti-apoptotic activity of the IAPs can be neutralized by the mammalian IAP inhibitor SMAC (second mitochondria-derived activator of caspases)/DIABLO (direct IAP-binding protein with low PI), which is released from the mitochondria at the same time as cytochrome c (Du *et al.*, 2000; Srinivasula *et al.*, 2001; Verhagen *et al.*, 2000) or as a secondary event in a caspase-dependent manner (Adrain *et al.*, 2001).

1.1.6. The BCL2 family

The intrinsic pathway of apoptosis is strictly controlled by the actions of the BCL2 family proteins (Figure 1.1.2; reviewed in (Desagher and Martinou, 2000; Walensky, 2006; Youle and Strasser, 2008)). The BCL2 family is divided into three groups based on their structure and function (Figure 1.1.3). One class contains the anti-apoptotic BCL2 family members, BCL2, BCLxL, BCLW (BCL2-like-2), MCL1 (myeloid cell leukaemia sequence-1), BCLB/BCL2L10 and A1/BCL2A1 (BCL2-related protein A1) which share three to four conserved BCL2-homology domains (BH1-4). In contrast, the second group are anti-survival and include BAX, BAK and BOK/MTD. These are essential inducers of the permeabilization of the outer mitochondrial membrane (OMM) and the release of cytochrome c and share three conserved domains (BH1-3). The BH3-only proteins make up the third class. This includes BAD (BCL2-antagonist of cell death), BIK/BLK/NBK (BCL2-interacting killer), BID, HRK (harakiri)/DP5 (death protein-5), BIM/BOD (BCL2-like-11), BMF, NOXA and PUMA/BBC3 (BCL2-binding component-3). They all contain a BH3 domain, which binds to the anti-apoptotic BCL2 members to promote apoptosis. In addition, most anti-apoptotic BCL2 proteins contain

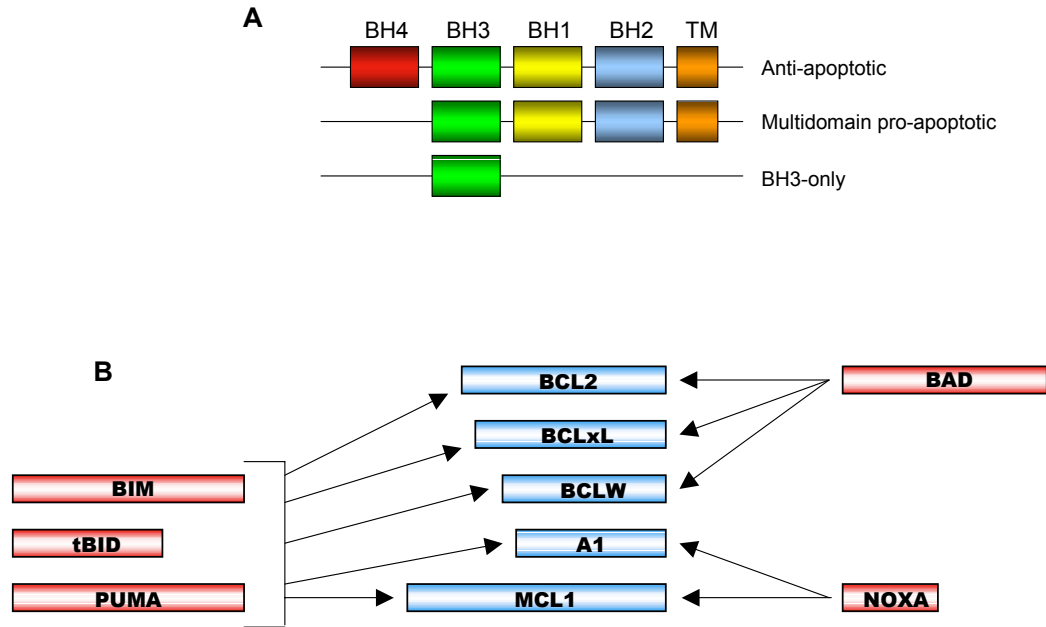


Figure 1.1.3. Schematic of BCL2 family structure and the BH3-only protein binding specificity (Adapted from Youle and Strasser, 2008; Degterev and Yuan, 2008). The BCL2 family is subdivided into three subclasses: Anti-apoptotic (BCL2, BCLxL, BCLW, A1 and MCL1), Multidomain pro-apoptotic (BAX and BAK) and BH3-only (BIM, tBID, PUMA, BAD and NOXA). BH1/BH2/BH3/BH4, BCL2 homology-1/2/3/4 domains; TM, transmembrane domain (**A**). The BH3-only proteins, BIM and PUMA bind to all five anti-apoptotic BCL2 proteins, tBID binds to BCLxL, BCLW, A1 and MCL1, but only weakly to BCL2. NOXA selectively binds to MCL1 and A1; BAD only binds to BCL2, BCLxL and BCLW (**B**).

a C-terminal membrane-targeting hydrophobic domain and are typically found associated with membranes (Goping *et al.*, 1998).

BAX exists as a monomer and is mainly localised in the cytosol in healthy cells. Upon the induction of apoptosis, BAX translocates to the mitochondria and undergoes an N-terminal conformational change to reveal a hidden N-terminal epitope, which is coupled to its oligomerization and insertion in the mitochondrial membrane (Goping *et al.*, 1998; Hsu and Youle, 1998; Nechushtan *et al.*, 1999; Wolter *et al.*, 1997). In contrast, BAK resides on the OMM bound to BCLxL and MCL1, however it also undergoes a conformational change and oligomerises during apoptosis stimulation (Griffiths *et al.*, 1999; Willis *et al.*, 2005).

BAX and BAK activation is inhibited by the anti-apoptotic BCL2 family proteins. Several models have been proposed for the derepression of BAX and BAK. The indirect model of BAX/BAK activation was recently demonstrated, in which the BH3-only proteins bind and inhibit the BCL2 anti-apoptotic proteins, and in doing so relieve their constraints on BAX and BAK (Willis *et al.*, 2007). In contrast, an alternative model proposes the direct activation of BAX and BAK by the BH3-only proteins tBID and BIM, while the other BH3-only proteins act as sensitizers, displacing the activators (BIM, tBID) from the pro-survival proteins (Certo *et al.*, 2006; Kuwana *et al.*, 2005; Letai *et al.*, 2002). However, apoptosis is still induced in BID/BIM^{-/-} mice, suggesting that the indirect mechanism is correct (Willis *et al.*, 2007). The protein binding specificity of the BH3-only proteins is shown in Figure 1.1.3.

1.1.7. The Calpain Family

The calpain family are a heterogenous family of calcium-activated cysteine proteases, also implicated in the cell death process (reviewed in (Goll *et al.*, 2003; Huang and Wang, 2001; Saez *et al.*, 2006)). There are multiple isoforms that are both ubiquitous and tissue specific. The two 'classical' calpains are calpain 1 and 2, which are activated by low and high micromolar concentrations of free calcium (Ca²⁺) respectively; these are the most abundant and well studied members of the calpain family. They exist as heterodimers consisting of a large 78-80 kDa catalytic subunit and a small 29 kDa regulatory subunit. The binding of Ca²⁺ to calpain 1 and 2 induces a conformational change to form the active site. In addition, a short N-terminal prodomain in the large subunit is removed (Hosfield *et al.*, 1999; Strobl *et al.*, 2000). Calpain 1 and 2 also have the ability to interact with membrane phospholipids via an alternative domain in their structure. At normal intracellular levels of Ca²⁺ calpain is involved the modulation

of Ca^{2+} -regulated events such as cell cycle progression, cell proliferation, differentiation, platelet activation and apoptosis. The activation of calpain under pathological concentrations of Ca^{2+} is associated with excitotoxicity, metastasis and neuronal degeneration (Bano *et al.*, 2005; Huttenlocher *et al.*, 1997; Saito *et al.*, 1993).

Calpain cleavage of substrates is generally an action to modify rather than terminate the action of their substrates and occurs in a limited manner. The identification of cleavage motifs for calpain 1 is complex. The preferred residues of the ubiquitous calpains – μ - and m-calpain at position P_2 are Leu, Val or Thr; Arg or Lys (and to a lesser extent Tyr) are often found at position P_1 . There is also a preference for the amino acids at positions P_3 (Phe, Trp, Leu, Val or Pro) and at position P_1' (Arg, Lys, Leu or Pro) but these are weaker than those stated for P_2 and P_1 (Sasaki *et al.*, 1984; Stabach *et al.*, 1997; Tompa *et al.*, 2004). Amino acid preferences seem to extend over 11 residues around the scissile bond (Tompa *et al.*, 2004). The secondary structure of a substrate is also an important determinant of calpain cleavage. In general, proteases cleave in sterically accessible and flexible regions; the majority of calpain recognition sites are in disordered and unstructured regions of proteins (Tompa *et al.*, 2004).

1.1.8. Neuronal Apoptosis

Excessive numbers of neurons are produced during development in order to compete to establish contacts with their target partners, with subsequent refinements during their life span. Neuronal differentiation and death are therefore tightly controlled and regulated in postmitotic systems to achieve and preserve a functional nervous system. This is accomplished by the activation of several signalling pathways, one of which is apoptosis (Buss *et al.*, 2006; Oppenheim, 1991; Pettmann and Henderson, 1998). The basic apoptotic programme is shared by neurons with all other cell types. The specificity of regulation is provided by the expression of different neurotrophic factors, BCL2 family members and caspase family members in different types of neurons and at different stages of development. .

The importance of apoptosis in the developing brain is exemplified by mice with a targeted deletion of caspase-3, caspase-9 or APAF1. These animals displayed gross brain abnormalities, the result of reduced progenitor cell death and increased embryo lethality (Kuida *et al.*, 1998; Kuida *et al.*, 1996; Yoshida *et al.*, 1998). However, subsequent studies demonstrated that there may be a strain-dependent redundancy for the action of caspase-3 (Houde *et al.*, 2004; Leonard *et al.*, 2002). In addition,

excessive cell death was observed in the dorsal root ganglia and spinal cord of the BCLxL^{-/-} mice (Motoyama *et al.*, 1995).

Classically, the form of cell death associated with ischemia is necrosis, however, morphological and biochemical features of apoptosis have been documented in experimental animals. Moreover, caspase-3 activity has been demonstrated in ischemic brain, hypothesised to be the result of activation by caspase-11 (Kang *et al.*, 2000; Namura *et al.*, 1998). Neurodegenerative diseases in the adult are often caused by protein aggregation for example by the expression of expanded polyglutamine tracts, which cause neuronal death in specific neuronal populations. There is some evidence that the expression of expanded polyglutamine tracts in primary cerebellar, striatal and cortical neurons, results in protein aggregates that induce apoptosis (Sanchez *et al.*, 1999). In addition, caspase-mediated proteolysis of proteins with expanded polyglutamine tracts may result in the generation of highly toxic fragments (Graham *et al.*, 2006). In mutant superoxide dismutase (SOD-1) transgenic mice, a model for amyotrophic lateral sclerosis (ALS), active caspase-1 and caspase-3 were observed. In addition, a delay in disease progression in the transgenic mouse model was demonstrated by the inhibition of caspase-1. It is thought that caspase-1 predisposes neurons to cell death by directly activating caspase-3 and by increasing the levels of IL-1 β , a pro-inflammatory cytokine (Li *et al.*, 2000; Yuan and Yankner, 2000).

1.2. Protein and Organelle Degradation

The intracellular concentration of proteins in a cell is determined by the balance between their rate of synthesis and degradation. There are two predominant, highly regulated degradative pathways for short and long-lived protein and organelle turnover in the cell. These are the ubiquitin proteasome system and autophagy. These pathways are critical for maintaining cell growth and development by controlling the balance between anabolism and catabolism. Furthermore, they have essential roles in aging, cell death, differentiation, starvation and also in the prevention of several types of cancer (Ciechanover, 1994; Ciechanover *et al.*, 1978; Reggiori and Klionsky, 2002; Schwartz and Ciechanover, 1999; Wilkinson, 2004).

The lysosome was initially thought to be the site for most protein degradation, due to the organelle's high concentration of lysosomal proteases and its ability to degrade endocytosed proteins. The existence of nonlysosomal proteases and the almost total depression of protein degradation by inhibitors of energy production indicated that

there is a simultaneous process (Ciechanover, 2005). In 1978, Ciechanover *et al* reported the first molecular dissection of the proteasomal system (Ciechanover *et al.*, 1978). Since then much has been discovered regarding the proteolysis of intracellular proteins and its importance in biological systems.

The demonstration of a non-lysosomal, ATP-dependent system in cell free extracts was carried out by Etlinger and colleagues in 1977 (Etlinger and Goldberg, 1977). This protein degradation system was shown to be composed of a small heat stable protein (ATP-dependent proteolysis factor – APF-1). This was devoid of proteolytic activity until it was combined with two further components, which contained complementary activity, one of which interacted directly with ATP (Ciechanover *et al.*, 1978; Hershko *et al.*, 1980; Hershko *et al.*, 1979). APF-1 was later identified as ubiquitin, a ubiquitous protein initially identified from bovine thymus (Goldstein *et al.*, 1975; Wilkinson *et al.*, 1980).

1.2.1. The Ubiquitin-Proteasome System

The ubiquitin-proteasome system (UPS) enforces protein quality control and regulates many cellular processes in the cytosol and nucleus of eukaryotic cells, by its degradation of intracellular proteins (Tanaka *et al.*, 2004; Wolf and Hilt, 2004). It controls the levels of many regulatory proteins involved in fundamental biological reactions, such as cell-cycle progression, DNA repair, transcription, metabolism, signal transduction, development and apoptosis. In addition, it plays a role in the stress response. Defects in the UPS have been implicated in several human diseases such as cancers, neurological disorders and inflammation (reviewed in (Glickman and Ciechanover, 2002)). The degradation of proteins via the UPS begins with the attachment of an ubiquitin tag to the substrate in a multi-step process. The substrates are then targeted to the 26S proteasome, where the degradation takes place.

1.2.1.1. The Ubiquitin Conjugation Pathway

Ubiquitin is a 76 amino acid, heat stable, evolutionally conserved peptide. Ubiquitin molecules can be conjugated to one another to form extended polymers on a protein substrate (Chau *et al.*, 1989). A specific amide (isopeptide) linkage is formed between the ϵ -amino group of a lysine residue in one ubiquitin (or the protein substrate) and the C-terminal carboxyl group (glycine 76, G76) of the next ubiquitin in the chain (Goldknopf and Busch, 1977). In ubiquitin there are seven potential lysine residues for ubiquitin chain synthesis. The attachment of four or more ubiquitin moieties to lysine-48 (K48) targets the protein substrate for degradation by the 26S proteasome (Cook *et al.*, 1994; Thrower *et al.*, 2000). Tetraubiquitin chains are the shortest polymer that binds

efficiently to proteasomes. It appears that chains of four or more ubiquitin molecules are recognised differently to those with just one (Thrower *et al.*, 2000).

The process of polyubiquitination involves the sequential action of three enzymes: an ubiquitin-activating enzyme (E1), ubiquitin-conjugating enzyme (E2) and ubiquitin-protein ligase (E3) (Figure 1.2.1; reviewed in (Glickman and Ciechanover, 2002; Pickart, 2001)). In most organisms a single E1 activates ubiquitin for the subsequent conjugating reactions; in yeast the enzyme is UBA1 (McGrath *et al.*, 1991). The human orthologue was identified as UBE1 (Ciechanover *et al.*, 1984; Finley *et al.*, 1984; Handley *et al.*, 1991). However, this was recently challenged by the identification of a novel tissue specific E1, UBE1L2, which is highly expressed in the testis (Pelzer *et al.*, 2007) and the identification of a divergent E1 in vertebrates, UBA6 (Jin *et al.*, 2007).

The 'activation' of ubiquitin begins when the E1 binds Mg^{2+} -ATP and ubiquitin (Ciechanover *et al.*, 1982) and catalyses the adenylation of glycine-76 (G76) at the C-terminus of ubiquitin (Hershko *et al.*, 1981), which extends away from the core ubiquitin molecule (Cook *et al.*, 1992). The ubiquitin-adenylate is attacked by the E1's catalytic cysteine, forming a covalent thioester linkage between the C-terminus of ubiquitin and the active site cysteine of the E1. A second molecule of ubiquitin then noncovalently binds to the E1 via its C-terminal G76 at the adenylation active site (Haas *et al.*, 1982). Thus, during the activation cycle two molecules of ubiquitin are bound to the E1 at two of the E1's three distinct domains: the adenylation domain (ATP and ubiquitin) and the catalytic cysteine domain; the acyl carrier for ubiquitin (Walden *et al.*, 2003).

E1s bind their E2 substrates with high affinity when they are doubly loaded (Hershko *et al.*, 1983; Pickart and Rose, 1985a). The third E1 domain, the C-terminal ubiquitin-fold domain, which is required to recruit specific E2's (Huang *et al.*, 2007; Huang *et al.*, 2005; Walden *et al.*, 2003), is unmasked by a conformational change in the doubly-loaded E1 (Huang *et al.*, 2007; Lee and Schindelin, 2008). The thioester-linked ubiquitin is released from the E1 and transferred to the E2's conserved catalytic cysteine in a transthiolation reaction and the E1 reverts back to its singly-loaded conformation. In addition, this is necessary for the subsequent binding of the E2s to E3s as there is a structural overlap of the E2 binding sites for E1 and E3s (Eletr *et al.*, 2005; Huang *et al.*, 2005). The activation cycle continues, with the E1 cycling between its doubly and singly loaded forms as it binds and releases ubiquitin. The E2-ubiquitin thioester then associates with the E3.

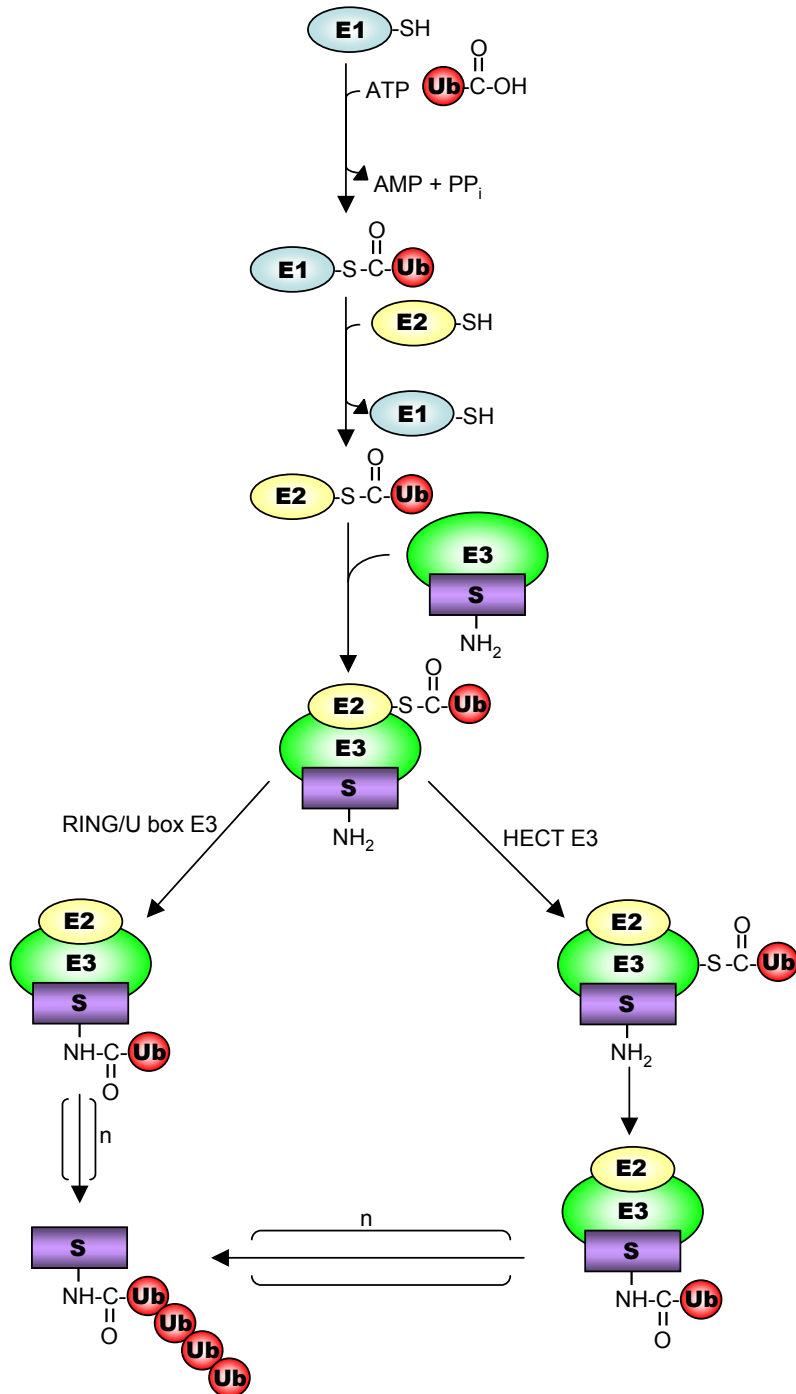


Figure 1.2.1. The Ubiquitination Pathway (adapted from Weissman, 2001). The covalent attachment of ubiquitin (Ub) to the substrate protein (S) occurs through the sequential actions of ubiquitin-activating enzyme (E1), ubiquitin-conjugating enzyme (E2) and ubiquitin-ligase (E3). For HECT domain E3s, the ubiquitin is transferred to the active site cysteine of the E3, then transferred to the substrate protein. For RING domain and U box E3s, ubiquitin is directly transferred to the substrate protein. After sequential rounds of ubiquitination (n), a polyubiquitin chain is attached to the protein and the protein is targeted to the proteasome and/or induce downstream signalling pathways.

The E3s catalyse the transfer of ubiquitin from the E2 to the ϵ -amino group of a lysine residue (K48 for proteasomal degradation (Chau *et al.*, 1989)) in the substrate target to generate a covalent isopeptide bond. Three main families of E3s have been identified, which contain conserved protein domains. The best-characterised member of the HECT (Homologous to E6-AP C Terminus) domain E3s is E6-AP (E6-Associated Protein), which targets the tumour-suppressor protein, p53 for ubiquitin-dependent proteolysis (Huibregtse *et al.*, 1995; Huibregtse *et al.*, 1991; Huibregtse *et al.*, 1993). HECT domain E3s have a conserved domain of ~350 amino acids at their C-terminus, which harbours the essential active site cysteine through which the E3s form the thioester with ubiquitin and interact with the E2s (Huibregtse *et al.*, 1995; Huibregtse *et al.*, 1991; Huibregtse *et al.*, 1993; Scheffner *et al.*, 1995). The N-terminal regions are variable and are thought to have an involvement in the recognition of the protein substrate. Following its association with the charged E2, the HECT domain E3 forms a thioester linkage between its active site cysteine and the C-terminal glycine of ubiquitin. Two models have been proposed for the subsequent transfer of the thioester ubiquitin to the protein target. The first of which involves the direct transfer via an isopeptide bond of ubiquitin to the protein substrate; successive addition of ubiquitin molecules to the previously transferred ubiquitin elongates the ubiquitin chain. In contrast, the second model involves the sequential addition of noncovalently bound ubiquitin molecules to the E3, the ubiquitin chain is elongated at the E3 prior to transfer onto the target protein (Verdecia *et al.*, 2003; Wang and Pickart, 2005). The mechanisms employed by the HECT domain E3s for the synthesis of polyubiquitin chains are distinct between enzymes (Wang and Pickart, 2005).

The globular E2-binding domain of the RING (Really Interesting New Gene) domain E3s are stabilised by the coordination of two zinc ions by multiple cysteine (Cys) and histidine (His) residues. RING E3s do not form covalent linkages with ubiquitin, instead they act as scaffolds that position and orientate the E2-thioester ubiquitin conjugate and target proteins for ubiquitin transfer (Zheng *et al.*, 2002; Zheng *et al.*, 2000). From mechanistic studies using the cullin-RING ligase SCF^{Cdc4} (Kkp1-Cdc53-F Box), it is thought that both the E2-thioester ubiquitin and the target protein bind to separate domains on the E3 and the lysine residue (K48) of the protein substrate attacks the C-terminal G76 ubiquitin. The ubiquitin molecule is then transferred to the target protein. The rapid successive addition of ubiquitin molecules to the substrate protein elongates the ubiquitin chain (Petroski and Deshaies, 2005). Well-characterised members of the RING-ligase E3 family include c-Cbl proto-oncogene (Joazeiro *et al.*, 1999), the IAP (Inhibitor of Apoptosis Proteins) family of anti-apoptotic proteins (Huang *et al.*, 2000),

the proto-oncogene MDM2 (Mouse Double Minute-2) (Fang *et al.*, 2000) and the multi-subunit SCF and anaphase-promoting complex (APC) cell cycle regulatory complexes (Cardozo and Pagano, 2007). It is thought that the E3s determine the specific lysine residue in the target protein for ubiquitination during chain assembly (Wang *et al.*, 2006).

The third family of E3s is the U box E3s. Their three dimensional structure is similar to that of the RING domain E3s. In contrast to the HECT domain E3s, the U box E3s do not form thioester intermediates with ubiquitin, it is directly transferred to the target protein (Hatakeyama and Nakayama, 2003).

Several E3 ligases have been demonstrated to be associated with the proteasome and may directly transfer polyubiquitinated proteins via their ubiquitin-like (UBL) domains. This includes the RING E3, Parkin (Sakata *et al.*, 2003) and the HECT domain-containing E3-ligase Hul5 (Leggett *et al.*, 2002). In addition, Rad23 (radiation gene 23), Dsk2 (Elsasser *et al.*, 2002; Rosenzweig *et al.*, 2008; Saeki *et al.*, 2002; Schmidt *et al.*, 2005), Ddi 1 (Schmidt *et al.*, 2005), and Shp1/p47 in complex with cdc48/p97 have also been proposed to mediate the transfer of polyubiquitinated proteins. In addition to their UBL domains, these proteins contain polyubiquitin-interacting ubiquitin-associated domains (UBA) domains, which bind polyubiquitin chains. The UBL domains interact with the proteasome, delivering the substrates for degradation (Welchman *et al.*, 2005).

1.2.1.1.1. Variations on Ubiquitination

Polyubiquitin chains can also be assembled on other lysine residues in ubiquitin to regulate a number of cellular processes (reviewed in (Haglund and Dikic, 2005; Weissman, 2001)). All seven lysine residues (K6, K11, K27, K29, K33, K48 and K63) in ubiquitin are involved in cell signalling. The attachment of ubiquitin chains to K63, in particular, is a well characterised alternative to conjugation at K48. Ubiquitination at alternative lysine residues has also been demonstrated to be important for ribosomal function (Spence *et al.*, 2000), post replication DNA repair (Spence *et al.*, 1995), the initiation of the inflammatory response (Deng *et al.*, 2000) and the function of certain transcription factors (Kaiser *et al.*, 2000).

1.2.1.1.2. Ubiquitin-like (UBL) proteins

Many ubiquitin-like modifiers (UBLs) have been identified (reviewed in (Hochstrasser, 2000; Welchman *et al.*, 2005)). The basic set of ubiquitinylation enzymological reactions is used for their conjugation to target substrates, a requirement for their

function, in a wide range of cellular processes. The best characterised UBLs include NEDD8 (neuronal-precursor-cell-expressed developmentally downregulated protein-8), which is involved in the regulation of E3s such as cullins and MDM2 (Hori *et al.*, 1999; Xirodimas *et al.*, 2004) and SUMO (small ubiquitin-like modifier) -1, -2, -3 that have been implicated in nuclear localisation, transcriptional regulation, the antagonism of ubiquitination and mitosis (Azuma *et al.*, 2003; Eaton and Sealy, 2003; Gill, 2004). In addition, the autophagy-related proteins (Atg), Atg8 and Atg12 are involved in the elongation of the autophagic vesicle and in the cytoplasm-to-vacuole- targeting (Cvt) pathway (discussed in further detail in section 1.2.2.2.6).

1.2.1.2. Deubiquitinating enzymes

Deubiquitinating enzymes (DUBs) and UBL-specific proteases (ULPs) serve to deconjugate the UBL/ubiquitin modified proteins and counteract the actions of ubiquitin- or UBL-ligases (reviewed in (Chung and Baek, 1999; Love *et al.*, 2007; Nijman *et al.*, 2005)). The function of deubiquitination is to recycle ubiquitin (which is transcribed at low levels), to rescue substrates from proteasomal degradation or to control trafficking (Millard and Wood, 2006). There are five subclasses of DUB, in which specific structural diversity exists: ubiquitin C-terminal hydrolases (UCHs), ubiquitin-specific proteases (USPs), ovarian tumour proteases (OTUs), Machado Joseph disease protein domain proteases (MJDs) and JAMM motif (zinc metallo) proteases.

1.2.1.3. The 26S Proteasome

The eukaryotic proteasome is a 26S, ATP-dependent, multisubunit protease that controls the degradation of polyubiquitinated proteins involved in numerous intracellular processes (reviewed in (Pickart and Cohen, 2004; Wolf and Hilt, 2004)). It is composed of two subcomplexes – the 20S core particle (CP) is responsible for the catalytic activity, and one or two 19S regulatory particles (RP; PA700), which are attached to one or both ends of the CP (DeMartino and Slaughter, 1999).

1.2.1.3.1. The 20S Core Particle

The CP is a barrel-like structure, with the catalytic active sites residing on the inside of the cylinder. It is composed of four heptameric rings stacked axially (Groll *et al.*, 1997; Lowe *et al.*, 1995). The two distal rings contain seven highly homologous α -subunits (α 1-7) and seven highly homologous β -subunits (β 1-7) form the two central rings. Proteolysis is catalysed in the central chamber by the N-terminal threonine residues of the β -subunits, β 5, β 2 and β 1. The proteasome has three distinct hydrolysing abilities,

namely chymotrypsin-like, trypsin-like and peptidyl-glutamyl, enzymatic activities respectively (Groll *et al.*, 1997; Groll *et al.*, 1999); the latter also being referred to as caspase-like (Kisselev *et al.*, 1999). However, the 20S-CP requires the binding of the regulatory complex to become fully active (Kohler *et al.*, 2001).

Eukaryote and prokaryote β subunits of the 20S are expressed in precursor form with an N-terminal propeptide sequence. Proteasome assembly is initiated by the formation of the α -subunit ring. Subsequently, half proteasomes are formed composed of one seven membered α -subunit ring and one unprocessed β -subunit ring. A prehaloproteasome is formed by the association of two half proteasomes and the processing of the β -subunits results in the mature haloproteasome ($\alpha_7\beta_7\beta_7\alpha_7$) (Chen and Hochstrasser, 1996; Seemuller *et al.*, 1996; Sharon *et al.*, 2007). The removal of the propeptide sequence exposes the N-terminal threonine, ensuring that the formation of the active sites occur upon completion of 20S assembly (Zuhl *et al.*, 1997). In addition, the chaperones, proteasome assembling chaperone-1 (PAC1) and PAC2 are proposed to facilitate the assembly of the precursor proteasomes, by providing a scaffold for α -ring formation (Hirano *et al.*, 2005).

The immunoproteasome is induced by the major immunomodulatory cytokine, interferon- γ (IFN γ) and is responsible for antigen presentation. The β -subunits, β_1 , β_2 and β_5 are replaced by the catalytically active $i\beta_1$ (LMP2), $i\beta_2$ (MECL-1) and $i\beta_5$ (LMP7) in the immunoproteasome (Kloetzel and Ossendorp, 2004).

1.2.1.3.2. The 19S Regulatory Particle

The 19S-RP is composed of at least eighteen individual subunits and is split into two subcomplexes: the lid and the base. The base contains six AAA-ATPases (Regulatory Particle Triphosphatase (Rpt) 1-6) that are adjacent to the 20S α -subunits (Glickman *et al.*, 1998). In addition, three further non-ATPase subunits (Regulatory Particle Non-ATPase 1 (Rpn1), Rpn2 and Rpn10) are also assigned to the base. The remaining subunits make up the lid subcomplex, which sits above the base and is linked by Rpn10. The lid subcomplex is required for ubiquitin-dependent proteolysis. The 19S performs a set of important functions including recognition of the polyubiquitin chain (Lam *et al.*, 2002; Young *et al.*, 1998), selective binding and unfolding of substrates tagged for degradation, degradation-coupled deubiquitination (Verma *et al.*, 2002; Yao and Cohen, 2002) and opening of the pore into the 20S-CP (da Fonseca and Morris, 2008; Smith *et al.*, 2007; Whitby *et al.*, 2000). In addition, they provide the force to drive the substrates into the proteolytic chamber (Kohler *et al.*, 2001). In archaea, the six

identical subunits that make up the proteasome-regulatory complex, PAN, are close homologues of the 19S ATPases (Zwickl *et al.*, 1999). The subunit composition of the *S.cerevisiae* regulatory particle and the corresponding nomenclature for the human homologues are shown in Table 1.2.1. (Finley *et al.*, 1998).

Table 1.2.1. The Unified Nomenclature of the *S.cerevisiae* Regulatory Particle and the Corresponding Human Forms (adapted from (Finley *et al.*, 1998)).

<i>S.cerevisiae</i>	Human homologues
Rpn1	S2
Rpn2	S1
Rpn3	S3
Rpn4	
Rpt1	S7
Rpt2	S4
Rpt3	S6
Rpt4	S10b
Rpt5	S6'
Rpn5	
Rpn6	S9
Rpn7	S10
Rpt6	S8
Rpn8	S12
Rpn9	
Rpn10	S5a
Rpn11	Poh1
Rpn12	S14

When the CP and RP are not associated, the N-termini of the α -subunits occlude the centrally located channel into the catalytic core (Groll *et al.*, 2000; Smith *et al.*, 2007). The association of the putative AAA-ATPase subunits of the 19S-RP, with the adjacent α -ring of the 20S-CP seems to involve the interaction of α_5 , α_6 and the interface between α_7 and α_1 with the C-terminus of Rpt2, Rpt5 and possibly Rpt1 (da Fonseca and Morris, 2008; Smith *et al.*, 2007; Whitby *et al.*, 2000). This is proposed to initiate gate opening and proteasome activation. Furthermore, the attachment of the 19S-RP subunits with the α -subunits induces a radial movement in each of the α -subunits and

in the β -subunits. This converts the relatively narrow inner chamber into a wider accessible channel for unfolded protein substrates. This is proposed to be required for the translocation of the target protein into the proteasomal core, after it has been recognised and unfolded by the 19S and may contribute to enhanced proteolytic activity (da Fonseca and Morris, 2008). ATP binding and hydrolysis play distinct roles in 26S proteasome function. The assembly of the 19S with the 20S requires ATP binding, but not hydrolysis; ATP removal promotes disassembly and inactivation of the 26S proteasome. ATP binding is also required for gate opening. ATP hydrolysis couples mechanisms for degradation including substrate unfolding. The translocation of unfolded substrates into the chamber can occur through the ATPase by facilitated diffusion (Liu *et al.*, 2006; Smith *et al.*, 2005).

An additional regulator of the 20S, induced by IFN- γ , the 11S regulator (PA28), binds to the 20S-CP and activates proteolysis, in an ubiquitin and ATP-dependent manner. 11S regulators may form hybrids, capping the 20S at one end, with a 19S at the other (da Fonseca and Morris, 2008; Hendil *et al.*, 1998; Kloetzel and Ossendorp, 2004).

1.2.1.4. Inhibitors of Proteasomal Activity

Proteasome inhibitors are commonly used tools in the laboratory for the rapid analysis of protein degradation. Inhibitors of the proteasome include the peptide aldehydes, which are reversible transition state substrate analogue inhibitors that primarily target the proteasomal chymotrypsin-like activity. This group includes Cbz-leu-leu-leucinal (MG132), Cbz-leu-leu-norvalinal (MG115) and acetyl-leu-leu-norleucinal (ALLN). However, the peptide aldehydes may also inhibit calpains and lysosomal hydrolases. In contrast, lactacystin (and its derivative *clasto*-lactacystin β -lactone) and peptides containing a C-terminal vinyl sulfone moiety are more specific (Lee and Goldberg, 1998). These inhibitors covalently modify the active site threonine of the β -subunits. The boronic dipeptides, MG262 and bortezomib (Velcade™, formerly PS-341 (Adams *et al.*, 1998; Adams *et al.*, 1999)) form stable, reversible tetrahedral intermediates with the N-terminal threonine residues of the β -subunits active site, exhibiting high selectivity for the inhibition of the chymotrypsin-like activity of the proteasome. Bortezomib was shown to have potent anticancer activity in a National Cancer Institute (NCI) screen of 60 cancer cell lines derived from multiple human tumours (Adams *et al.*, 1999). Bortezomib has U. S. Food and Drug Administration (FDA) and European Medicines Agency (EMA) approval for its use in the treatment of patients with multiple myeloma and clinical trials are ongoing for its use in solid and haematological malignancies (Zavrski *et al.*, 2005).

1.2.1.5. The Proteasome and Apoptosis

It was revealed in the early 1990's that the proteasome plays a specific role in the regulation of apoptosis. Through the identification of ubiquitinated substrates, it appears that ubiquitination regulates the function and levels of several apoptosis-related proteins (Shinohara *et al.*, 1996; Yang and Yu, 2003).

One such protein is the tumour suppressor and nuclear transcription factor, p53, which is activated by DNA damage, oncogene activation, and cellular stress (Culmsee and Mattson, 2005). The level of p53 is regulated post-transcriptionally by MDM2 (murine double minute-2 (human homologue – HDM2)), a RING domain E3 that binds p53 in the nucleus, and mediates its transportation into the cytosol, where it is ubiquitinated and undergoes proteasomal degradation. In addition, MDM2 mediates its own ubiquitination and degradation (Culmsee and Mattson, 2005; Fang *et al.*, 2000; Kubbutat *et al.*, 1997)

Other apoptosis-related proteins known to be targets of the ubiquitin-proteasome pathway include the IAPs. Several IAP family members act as RING domain E3 ubiquitin-ligases, targeting caspase-3, caspase-7 and Smac/DIABLO for degradation (Huang *et al.*, 2000; MacFarlane *et al.*, 2002). The BCL2 family members such as BIM, BID, BIK and MCL1 have also been demonstrated to be substrates of the UPS, thought to be important for the regulation of the apoptotic threshold (Fennell *et al.*, 2008).

1.2.2. The Autophagy Pathway

The alternative site for protein degradation in eukaryotic cells takes place at the lysosomes. These contain a range of acidic hydrolases, which are capable of rapid and efficient degradation of all cellular constituents. The process of autophagy takes place at these sites and is exclusively responsible for the turnover of organelles and long-lived proteins (Juhász and Neufeld, 2006; Reggiori and Klionsky, 2002). Autophagy (derived from the Greek terms; “auto” oneself, “phagy” to eat or “self-eating”) is evolutionarily conserved among animal, plant and yeast cells. Three main forms of autophagy have been identified: chaperone-mediated autophagy, macroautophagy and microautophagy (Levine and Kroemer, 2008; Xie and Klionsky, 2007). Microautophagy, which is not well characterised in higher eukaryotes, involves the uptake of the cytoplasm at the lysosome surface by invagination. This is in contrast to macroautophagy, in which the sequestering membrane is distinct from the lysosome (Rubinsztein *et al.*, 2007). Chaperone-mediated autophagy is regarded as a secondary response to starvation; it is induced under conditions of prolonged nutrient inadequacy.

During this process misfolded proteins are translocated directly across the lysosomal membrane (Dice, 2007; Majeski and Dice, 2004). The primary response to nutrient limitation is macroautophagy; this is the major lysosome-dependent mechanism for degradation and will be referred to as autophagy in the rest of this thesis.

While autophagy is generally thought of as being relatively non-selective, several types of selective autophagy have been described (van der Vaart *et al.*, 2008). These include the well-characterised biosynthetic cytoplasm-to-vacuole targeting (Cvt) pathway in yeast, necessary for the transport of the vacuolar protease aminopeptidase I (Ape I) and ER-phagy in which autophagy participates in the degradation of excessive ER during the unfolded protein response (UPR) (Bernales *et al.*, 2006). In addition, mitophagy refers to the selective elimination of non-functional mitochondria by autophagy, a process that can prevent aging (van der Vaart *et al.*, 2008) and is hypothesised to occur upon treatment with an apoptotic stimulus in the presence of caspase inhibitors (Xue *et al.*, 2001). Pexophagy refers to the selective degradation of the peroxisomes. There is an overlap in the autophagic machinery that is required for the functioning of the selective autophagy processes and the non-selective 'bulk' autophagy (discussed below). The key difference is the signal for membrane biogenesis, which is a result of the direct activation of the autophagic machinery for non-selective autophagy, whereas it comes from the cellular component targeted for degradation in selective autophagy (Kundu and Thompson, 2008).

Low basal levels of autophagy occur in virtually all cells. When cells need to generate energy and intracellular nutrients, for example during growth factor withdrawal (Lum *et al.*, 2005), starvation (Kang *et al.*, 2007; Kuma *et al.*, 2004), or to meet high bioenergetic demands, autophagy is rapidly upregulated (Levine and Kroemer, 2008). The autophagic response is also enhanced as a defence mechanism during infection (Orvedahl and Levine, 2008), oxidative stress (Scherz-Shouval *et al.*, 2007) and protein aggregate accumulation (Hara *et al.*, 2006; Komatsu *et al.*, 2006; Pandey *et al.*, 2007). Furthermore, autophagy is thought to contribute to the clearance of dead cells during embryonic development (Qu *et al.*, 2007).

1.2.2.1 Morphological features

The morphology of autophagic cells was initially described in the 1960's from studies using electron microscopy (EM) (Ashford and Porter, 1962). The induction of autophagy is characterised by the presence of a fold of membrane, known as the isolation membrane (IM) or phagophore in mammals, which enwraps part of the

cytoplasm. Sealing the edges of the IM sequesters the cytoplasmic constituents into a double-membrane cytosolic vesicle, known as an autophagosome. This then fuses with the lysosome and the inner vesicle of the autophagosome is released into the lysosomal lumen. This so called 'autophagic body' is degraded by hydrolases along with the cytoplasmic load (Juhász and Neufeld, 2006; Reggiori and Klionsky, 2002). Lysosomal membrane permeases then release the resulting macromolecules for recycling (Xie and Klionsky, 2007). The number of autophagic vacuoles observed in dying cells is far greater than that associated with the cytoplasmic turnover in normal cells (Clarke, 1990).

1.2.2.2. The Autophagic Process

The molecular control of the autophagic process was discovered by independent genetic screens in the yeast *Saccharomyces cerevisiae* (*S. cerevisiae*) (Thumm *et al.*, 1994; Tsukada and Ohsumi, 1993). These were referred to as the *APG* genes (AutoPhaGy, (Tsukada and Ohsumi, 1993)) or the *AUG* genes (AUTophagocytosis, (Thumm *et al.*, 1994)). To date at least thirty genes have been identified and demonstrated to be involved in starvation-induced autophagy, the Cvt pathway and pexophagy. Many known orthologues of the genes have been described in higher eukaryotes. The large number of names associated with the autophagy-related genes led to the adoption of a unified gene and protein nomenclature. The new gene and protein names - *ATG* and Atg (AuTophagY-related) respectively were employed and are used below in the description of the pathway (Klionsky *et al.*, 2003). Among the *ATG* genes, a subset is required for autophagosome formation in all subtypes, the products of which are known as the 'core' autophagic machinery. These can be organised by function into three main groups, which include (1) the cycling system of Atg9, the Atg1 kinase complex, Atg2 and Atg18; (2) the phosphatidylinositol 3-OH kinase (PI(3)K) complex; (3) the ubiquitin-like protein (UBL) system (Reggiori and Klionsky, 2002; Xie and Klionsky, 2007).

1.2.2.2.1. The Phagophore Assembly Site

The basic mechanism of the autophagic process occurs in four discrete steps: induction and cargo packaging, formation and completion of the autophagosome, docking and fusion with the lysosome and the breakdown and release of the contents. The induction of vesicle formation during autophagy is stimulated by cellular signals as discussed above and is proposed to take place at the phagophore assembly site (PAS) (Kim *et al.*, 2002; Suzuki *et al.*, 2001). It is here in which the phagophore undergoes expansion and evolves into the autophagosome by the concerted actions of the core

machinery. Most of the core machinery proteins are excluded from the completed autophagosome and relocated to peripheral sites; the exception being Atg8. The co-localisation of the phagosome with components of the core machinery has previously been demonstrated in both mammalian and yeast cells (Kirisako *et al.*, 1999; Mizushima *et al.*, 2001).

1.2.2.2.2. The Target of Rapamycin (TOR)-dependent and independent induction of autophagy

Autophagy is negatively regulated by the actions of the target of rapamycin (TOR; in mammals, referred to as the mammalian target of rapamycin (mTOR)). TOR, a serine/threonine phosphatidylinositol kinase-related kinase, is maintained in an active conformation in response to amino acids and growth factors, where it is responsible for coordinating many aspects of cell growth. (Noda and Ohsumi, 1998).

In mammals mTOR resides in a complex (mTOR complex 1; mTORC1) that is composed of the mTOR catalytic subunit, regulatory associated protein of mTOR (raptor) and mLST8 (GβL). Analogous complexes are also found in yeast (Pattingre *et al.*, 2008). The key negative regulator of mTORC1 is the tuberous sclerosis 1 (TSC1) and TSC2 tumour suppressor complex. TSC1 and TSC2 form a heterodimer, which is a GTPase activating protein for Rheb (Ras homologue enriched in brain). Rheb is a small GTP-binding protein that binds and activates the kinase domain of mTOR (Saucedo *et al.*, 2003; Stocker *et al.*, 2003). Multiple stimuli such as DNA damage, energy depletion, hypoxia and insulin signal to TSC1-TSC2 through the regulation of several kinases that directly phosphorylate TSC2. The downstream targets of mTORC1 include the regulators of translation, 4EBP1 (eukaryotic translation initiation factor 4E binding protein 1) and S6K1 (ribosomal S6 kinase 1). S6K1 is an important regulator of cell growth and in conditions of high mTORC1 activity, its direct phosphorylation of the insulin receptor substrate 1 (IRS1) via a feedback loop is responsible for the inhibition of Akt (Harrington *et al.*, 2004). In addition, rapamycin, a macrolide antifungal agent, in complex with its intracellular receptor FKBP12 directly binds to mTORC1, suppressing the phosphorylation of S6K1 and 4EBP1 and stimulates autophagy (Sabatini, 2006). Inhibition of the TOR pathway is required for the Atg1 kinase-dependent regulation of autophagosome formation (Kamada *et al.*, 2000). Furthermore, suppressing TOR activity increases the transcription of *ATG8* (Abeliovich *et al.*, 2000).

mTOR-independent routes have also been described for the induction of autophagy. Lithium was proposed to increase the clearance of aggregates by autophagy induced

in response to the reduced intracellular levels of myo-inositol-1, 4, 5-triphosphate (IP₃). In addition, the mood stabilisers carbamazepine and valproic acid (VPA) were shown to have the same effect (Sarkar *et al.*, 2005). Furthermore, the disaccharide Trehalose was demonstrated to induce autophagy independently of mTOR and increase the clearance of aggregates in cell lines transfected with EGFP-tagged huntingtin exon 1 with 74 polyglutamine repeats (EGFP-HDQ74) (Sarkar *et al.*, 2007). In addition, many other molecules that have been demonstrated to regulate autophagy include calcium, the eukaryotic initiation factor 2 α (eIF2 α), the pro-survival BCL2 family proteins, reactive oxygen species (ROS) and calpain 1 and 2 (Demarchi *et al.*, 2006; Hoyer-Hansen *et al.*, 2007; Kuroku *et al.*, 2007; Pattingre *et al.*, 2005; Shimizu *et al.*, 2004).

1.2.2.2.3. Atg1 Kinase Complex

In yeast the activity of Atg1 (mammalian homologues, ULK1 and ULK2 (Chan *et al.*, 2007; Yan *et al.*, 1998; Yan *et al.*, 1999), a serine/threonine kinase is modulated by the phosphorylation state of Atg13. Autophagy is repressed in nutrient rich conditions when Atg13 is hyperphosphorylated by TOR, and its affinity for Atg1 kinase is low (Figure 1.2.2). In contrast, the rapid dephosphorylation of Atg13 and its interaction with Atg1 kinase during starvation for example, enhances the activity of autophagy (Abeliovich *et al.*, 2000; Kamada *et al.*, 2000). An additional regulator of Atg1 is Atg17, which binds to the Atg1 kinase-Atg13 complex in an Atg13-dependent manner. In addition, the interaction of Atg13 with Atg17 is required by Atg1 for its kinase activity (Kabeya *et al.*, 2005). The Atg1-Atg13-Atg17 complex is essential for the localisation of the subsequent Atg proteins to the PAS and is proposed to facilitate the assembly of the autophagosome. However, the kinase activity of Atg1 is not required for this purpose; it is more likely to be important for the dissociation of the Atg proteins from the completed vesicle or for the disassembly of the PAS (Cheong *et al.*, 2008). While the majority of the autophagy pathway has been characterised in yeast, mammalian homologues of the Atg proteins display high homology with their yeast counterparts. In addition, most of the core autophagic machinery are considered critical for autophagosome formation, the autophagic process being inhibited in their absence. However, a mammalian orthologue of the yeast protein Atg13 has not been identified. Interestingly, a novel mammalian autophagy factor, FIP200 has been described, which functions with ULK1 in autophagy (Hara *et al.*, 2008)

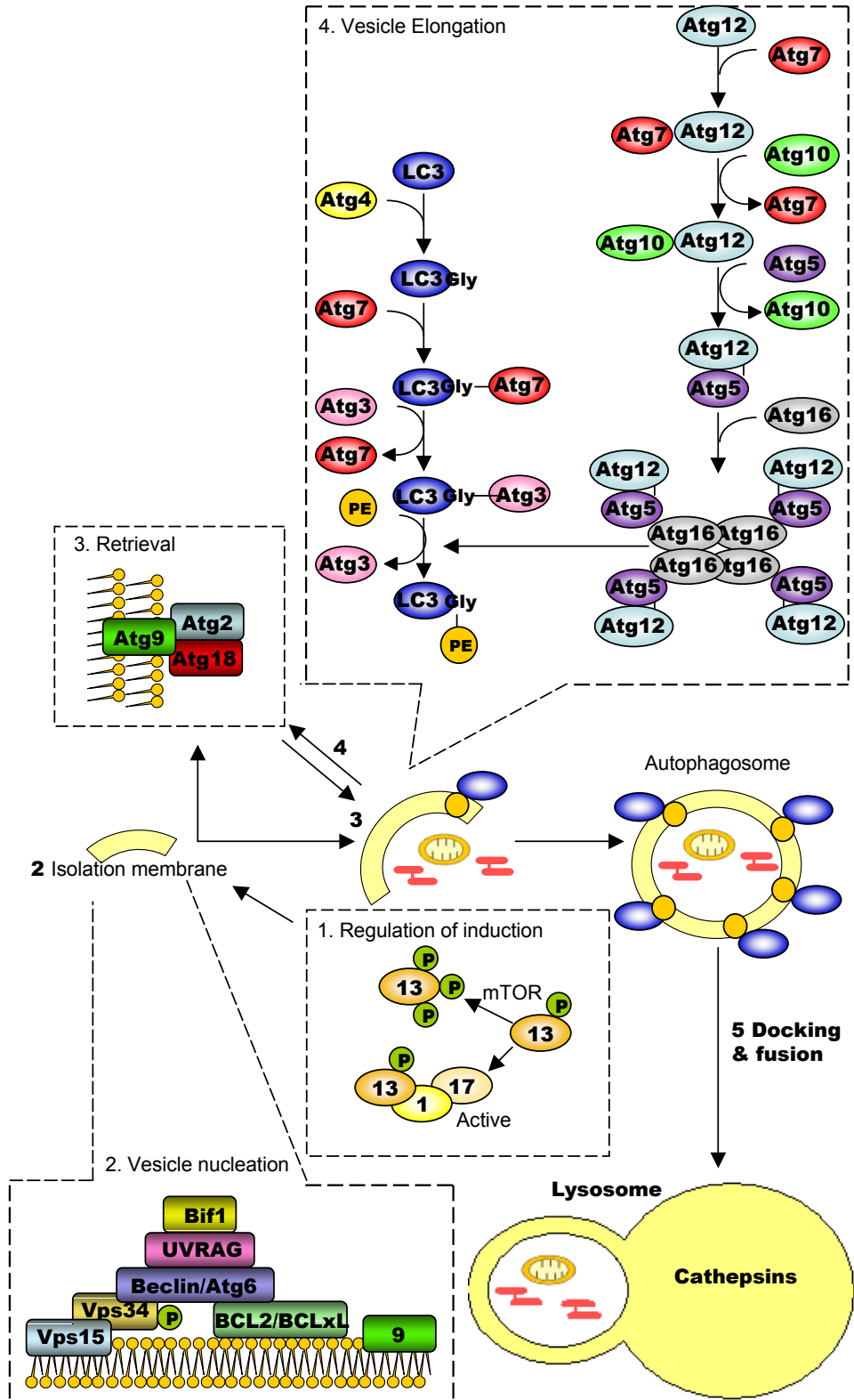


Figure 1.2.2. The Autophagy Pathway (adapted from Maiuri *et al*, 2007; Yorimitsu and Klionsky, 2005). Autophagy begins with the engulfment of cytoplasmic material, such as intracellular proteins or organelles, by the isolation membrane. The material is eventually sequestered in a double-membraned vesicle, known as the autophagosome. The induction of autophagy is regulated in many cellular settings by mTOR, which phosphorylates Atg13 (13), leading to its dissociation from the Atg1 kinase complex, which also contains Atg17 (17). The re-association of dephosphorylated Atg13 with Atg1 stimulates autophagy when mTOR is inhibited (1). The initial steps of vesicle nucleation involves the activation of Vps34, which requires the formation of a multiprotein complex, involving Atg8 (Beclin 1 in mammalian cells) and Vps15 (p150 in mammals). In mammals the complex also includes UVRAG and Bif-1, and is regulated by the interaction of Beclin 1 with BCL2/BCLxL; in yeast the complex contains Atg14 in addition to the core proteins. The activation of Vps34 generates PtdIns3P, which may recruit PtdIns3P-binding proteins such as Atg18 (2). Atg9 is recruited to the PAS by the Atg1kinase complex and interacts with Atg2 and 18. Exit of Atg9 from the PAS involves Atg1, Atg2 and Atg18. It is thought that Atg9 may contribute to the delivery of the membrane to the PAS (3). The two UBL conjugation systems that are essential for vesicle elongation (4) involves the conjugation of Atg12 to Atg5, catalysed by Atg7 (E1-like) and Atg10 (E2-like). In addition, LC3/Atg8 is cleaved by Atg4 to expose the C-terminal glycine residue, which is conjugated to PE by the actions of Atg7 and Atg3 (E2-like). This then becomes associated with the phagophore membrane, in a process that requires the Atg12:Atg5:Atg16 complex. Autophagosomes fuse with lysosomes (5), and the inner vesicle of the autophagosome and the constituents are released into the lumen of the lysosome and are degraded by hydrolases.

1.2.2.2.4. Atg9, Atg2 and Atg18

Atg9 is a multi-spanning membrane protein with both termini residing in the cytoplasm. It is localised on the juxta-nuclear Trans Golgi membrane, and peripherally on late endosomes in mammalian cells (Young *et al.*, 2006). In yeast, it seems to shuttle between the mitochondria and PAS. The role of Atg9 in autophagy is not well-characterised, but it has been proposed that it may contribute towards the delivery of the membrane to the PAS (Figure 1.2.2) (Reggiori *et al.*, 2005). The suggested process of Atg9 recruitment to the PAS begins with the individual recruitment of Atg9 and the Atg1 kinase complex. Atg2 and Atg18 are then recruited and the Atg1 kinase complex mediates their interaction with Atg9. The final step involves the exit of Atg9 from the PAS, a step that requires the Atg1 kinase complex and Atg2:Atg18 (Reggiori *et al.*, 2004). It is unknown whether Atg9 cycles continuously during autophagosome formation or cycles only once. Two mammalian homologues of yeast Atg9 have been identified; Atg9L1 (autophagy-related protein 9-like 1; Atg9A) is ubiquitously expressed, in contrast Atg9L2 (Atg9B) is mainly expressed in the placenta and pituitary gland (Yamada *et al.*, 2005).

1.2.2.2.5. The Phosphatidylinositol 3-Kinase Complex

The initiation of vesicle nucleation involves the activation of the class III phosphatidylinositol 3-kinase (PI3K), vacuolar protein sorting (Vps) 34. In yeast, Vps34 forms two discrete PI3K complexes: complex I contains Vps34, Vps15 (p150 in humans), a myristylated kinase required for the membrane association and activation of Vps34 (Stack *et al.*, 1993); Vps30/Atg6 and Atg14. It is complex I that localises to the PAS and functions in autophagy (Kihara *et al.*, 2001). The activation of Vps34 generates phosphatidylinositol-3-phosphate (PtdIns3P) (Petiot *et al.*, 2000). It is thought that the role of the PI3K complex at the PAS is to recruit PtdIns3P binding proteins, including Atg18. The localisation of Atg2:Atg18 is dependent on the interaction of Atg18 with PtdIns3P and is essential for full autophagic activity (Obara *et al.*, 2008). In mammalian cells, Vps34 is similar to yeast Vps34 and it depends upon the formation of the multi-protein complex with Beclin 1 (the mammalian homologue of Atg6 (Furuya *et al.*, 2005)), UVRAG (UV irradiation resistance-associated tumour suppressor gene (Liang *et al.*, 2006)), Bif-1 (Endophilin B1 (Takahashi *et al.*, 2007)) and Vps15 for activation (Figure 1.2.2). However, in contrast to Atg6, there is no proposed role for Beclin 1 in endocytosis or in the delivery of proteins to the lysosome. Beclin 1 primarily functions in autophagy (Zeng *et al.*, 2006). In addition, no mammalian homologue of Atg14 has been described. In mammals, Beclin 1 was demonstrated to be an essential component of autophagy. Furthermore, Beclin 1^{-/-} mice die early in

embryogenesis and there is an increased incidence of Beclin 1^{+/-} mice with spontaneous tumours. Beclin 1 was therefore established as a haploinsufficient tumour suppressor gene (Yue *et al.*, 2003). In the nervous system, Beclin 1 has also been demonstrated in complex with the glutamate receptor $\delta 2$ (Yue *et al.*, 2002) and Ambra1 during the development of the nervous system (Fimia *et al.*, 2007).

1.2.2.2.6. The Ubiquitin-like Protein Conjugation Systems

Two ubiquitin-like (UBL) conjugation systems are essential for the biogenesis and expansion of the vesicle (Figure 1.2.2) (Ichimura *et al.*, 2000; Mizushima *et al.*, 1998). While the UBL proteins, Atg8 and Atg12, are structurally similar to ubiquitin, there is no clear homology. The initial steps of expansion involve the activation of Atg12 by the formation of a high energy thioester bond between the C-terminal glycine of Atg12 and the active site cysteine (Cys-507 in yeast) of Atg7, in an ATP-dependent manner (Figure 1.2.4). Atg7 is a homologue of the E1 ubiquitin-activating enzyme UBA1 (Kim *et al.*, 1999; Mizushima *et al.*, 1998; Tanida *et al.*, 1999). Atg12 is then transferred to the active site cysteine of the E2-like ubiquitin-conjugating enzyme, Atg10, forming a new thioester bond (Mizushima *et al.*, 1998; Nemoto *et al.*, 2003). The covalent linkage of Atg12 to lysine-149 (K149) of Atg5 is the final step in the sequence of reactions (Mizushima *et al.*, 1998). The two domains at the N- and C-terminus of Atg5 then associate with Atg16, to form the trimeric complex: Atg12:Atg5:Atg16. The interaction site of Atg5 with Atg16 is on the opposite side to its association with Atg12 (Matsushita *et al.*, 2007). This complex is then capable of undergoing oligomerization via the self-interaction of Atg16, while Atg5 mediates the association with the membrane (Kuma *et al.*, 2002; Mizushima *et al.*, 1999). Multiple isoforms of Atg16 (Atg16L) are generated in mammals by alternative splicing events (Mizushima *et al.*, 2003).

The second UBL system involves the initial cleavage of newly synthesised Atg8 by Atg4, a cysteine protease. This removes the C-terminal arginine residue of Atg8, resulting in the exposure of the glycine residue (Figure 1.2.4), which is required for subsequent conjugation reactions (Kirisako *et al.*, 2000). Atg8 is then activated by the formation of a thioester bond between the C-terminal glycine and the active site cysteine of the E1-like Atg7. Atg8 is transferred and forms a new thioester bond with Atg3 (at Cys-234), an E2-like enzyme (Ichimura *et al.*, 2000). In the final reaction, Atg8 is covalently conjugated with a phosphatidylethanolamine (PE) molecule and becomes strongly associated with the membrane of the phagophore. The two UBL conjugation systems proceed independently with only a dual requirement for Atg7. However, while the Atg12:Atg5 complex with Atg16 forms in the absence of the Atg8 pathway, the

Atg12 system is essential for Atg8:PE conjugation (Mizushima *et al.*, 2001). It has been proposed the Atg12:Atg5:Atg16L complex localises to an as yet undetermined membrane, in a step that requires Atg16L. The high energy Atg3:Atg8 conjugate is then recruited via the interaction of Atg3 with Atg12, hypothesised to display E3-like activity. In this way, Atg8 is brought into the vicinity of PE in the membrane, resulting in its lipidation; the Atg12:Atg5:Atg16L complex acts as a scaffold for the conjugation of Atg8 with PE (Fujita *et al.*, 2008a; Hanada *et al.*, 2007).

The Atg12:Atg5:Atg16 complex is associated with the outer leaflet of the phagophore during its expansion; upon completion the complex is released (Mizushima *et al.*, 2003; Mizushima *et al.*, 2001). Atg8:PE localises to the entire preautophagosome membrane. The amide bond linking Atg8 to PE is cleaved by Atg4 when the autophagosome is completed and the pool of Atg8 on the outer leaflet of the membrane dissociates (Kirisako *et al.*, 2000). Atg8 that is trapped in the autophagosome, together with the autophagic body is degraded in the lumen.

The core autophagic machinery is mostly conserved in mammalian cells. There are three mammalian homologues of yeast Atg8: microtubule-associated protein 1 light chain 3 (LC3), which is directly implicated in autophagy, Golgi associated ATPase enhancer of 16 kDa (GATE-16) and GABA_A receptor associated protein (GABARAP) (Kabeya *et al.*, 2000; Paz *et al.*, 2000). There are also four mammalian homologues of the yeast Atg4: Atg4B/autophagin-1, Atg4A/autophagin-2, Atg4C/autophagin-3 and Atg4D/autophagin-4 (Marino *et al.*, 2003). The mammalian Atg4 homologues differ in their tissue distribution and in their substrate efficiencies. Atg4B is capable of removing the C-terminal amino acids to expose the conserved glycine residue in all three mammalian Atg8 homologues for subsequent conjugation. In addition, it delipidates LC3 and GABARAP (Tanida *et al.*, 2004b); Atg4A cleaves GATE-16 (Scherz-Shouval *et al.*, 2003).

1.2.2.2.7. Maturation of the Autophagosome and Fusion with the Lysosome

The mechanisms of the progression of late autophagosomes into degradative autolysosomes are not well characterised. The machinery for autophagosome formation and the trafficking of endosomes, and the fusion of both with lysosomes may overlap (Levine and Klionsky, 2004; Liang *et al.*, 2008). A role for the small GTP binding protein, Rab7 in the maturation of late autophagosomes and their fusion with lysosomes has been described in mammalian cells (Gutierrez *et al.*, 2004; Jager *et al.*, 2004; Kimura *et al.*, 2007). Furthermore, it seems that UVRAG, a component of the

PI3K complex through its interaction with Beclin 1 (Liang *et al.*, 2006), also promotes late autophagosome maturation, endocytic trafficking and fusion with endosomes/lysosomes. This is mediated by its association with the class C Vps (C-Vps) proteins and was demonstrated to be independent from its interaction with Beclin 1 and its upstream autophagic role (Liang *et al.*, 2008). After the formation of the autolysosome the luminal contents are degraded by acidic lysosomal hydrolases such as cathepsin B, D and L (Tanida *et al.*, 2005).

1.2.2.3. Autophagy and Apoptosis

Aged, damaged and superfluous cells or organelles are eliminated by apoptosis or autophagy. A complex functional relationship exists between the induction of autophagy and apoptosis. In some cellular settings autophagy is induced as a survival mechanism to avoid cell death; in others, morphological features of autophagy are observed in dying cells and the cell death is termed autophagic cell death (or type II cell death) (Clarke, 1990). In addition, the simultaneous induction of both autophagy and apoptosis is obvious upon the treatment of cells with several cell death stimuli. However, other stimuli predominantly induce one form of cell death over the other, suggesting that the development of the processes may be controlled by a cellular 'decision' (Maiuri *et al.*, 2007b).

Several overlapping processes that link apoptosis and autophagy have been described. The most widely studied is the interaction of the members of the antiapoptotic BCL2 family with Beclin 1 (Erlich *et al.*, 2007; Liang *et al.*, 2006; Liang *et al.*, 1998; Maiuri *et al.*, 2007a; Oberstein *et al.*, 2007; Pattingre *et al.*, 2005; Shimizu *et al.*, 2004; Wei *et al.*, 2008). BCL2 was demonstrated to be important for the regulation of the autophagic threshold induced by starvation (Pattingre *et al.*, 2005). Furthermore, the regulation of the ability of BCL2 to regulate Beclin 1 function was shown to involve multisite phosphorylation of BCL2 by JNK1 (Wei *et al.*, 2008).

The caspase-8-mediated proteolysis of RIP has also been implicated in the regulation of Beclin 1/Atg7-dependent autophagy (Lin *et al.*, 1999). The induction of autophagy in response to inhibition of caspase-8 by zVAD was shown to require the simultaneous blockage of a calpain-like protease (Madden *et al.*, 2007). In contrast, calpain 1 and 2 were hypothesised to be required for the promotion of autophagy in mammalian cells. The point at which calpain played a role in the autophagic process was not identified, but it was suggested that it may play a part in the delivery of the membrane to the

autophagosome or modulate the action of one of the components of the pathway (Demarchi *et al.*, 2006).

The critical autophagic factor, Atg5 has been implicated in both the autophagic and apoptotic response to stimuli. It was shown in complex with FADD in resting cells and during the simultaneous induction of autophagy and apoptosis by interferon- γ (Pyo *et al.*, 2005). The cleavage of Atg5 by calpain 1 and 2 was detected in a variety of cell types undergoing both intrinsic and extrinsic apoptosis. The truncation of Atg5 was proposed to be a critical pro-apoptotic event for some forms of apoptosis, but had no effect on the autophagic response (Yousefi *et al.*, 2006). The Atg proteins, particularly those of the UBL-conjugation pathways are essential for the process of autophagy. This is demonstrated by the early neonatal death of the *ATG5* and *ATG7* conditional knockout mice (Komatsu *et al.*, 2005; Kuma *et al.*, 2004). It is therefore likely that there are multiple levels of regulation, which remain uncharacterised. It is essential to investigate these points of control to further our understanding of the autophagic process.

While autophagy is primarily a survival response, in conditions of defective apoptosis or when autophagy is excessively induced; self-destruction may be initiated by the autophagic machinery. The mechanism for this cellular decision remains unclear (Levine and Yuan, 2005).

1.2.2.4. Degradation in the Nervous System

During neuronal development axonal guidance is required for axons to locate the appropriate target. At the outer end of the developing axon, a growth cone resides, which determines axonal branching. The UPS induce rapid local changes in protein levels to regulate growth cone behaviour (Campbell and Holt, 2001). In addition, local protein synthesis and degradation are involved in the regeneration of the axon after axotomy (Verma *et al.*, 2005) and in degeneration during axonal pruning in *Drosophila* (Watts *et al.*, 2003). The regulation of several neuronal proteins such as neurotransmitter receptors by the UPS is thought to be essential for the control of synaptic strength and transmission. Taken together, this suggests that a fully functioning UPS during development and in fully differentiated neurons is highly important for the efficient operation of these processes (van Tijn *et al.*, 2008).

The loss of UPS function is directly linked to the accumulation of ubiquitinated aggregates in several neurological conditions such as Parkinson's disease (PD),

Alzheimer's disease (AD) and an array of polyglutamine diseases including Huntington's disease (HD) and ALS (Ciechanover and Brundin, 2003). In addition, genetic mutations in several UPS related genes have been described in forms of familial variants of PD (Kitada *et al.*, 1998).

It has been proposed that aggregates formed when UPS function is diminished can be transported to aggresomes, perinuclear aggregates of protein at the microtubule-organising centre, where they become encapsulated by vimentin (Johnson *et al.*, 1998). Aggresomes are thought to develop when a threshold of misfolded protein has been exceeded and may be the cell's way of concentrating the protein aggregates in one location to sequester them from the cytosol (Kopito, 2000; Taylor *et al.*, 2003a).

Evidence for the importance of autophagy in the nervous system is highlighted in studies using conditional knockout mutant mice. The specific ablation of *ATG7* in cerebellar Purkinje cells demonstrated that it is essential for axonal homeostasis and in the prevention of axonal degeneration (Komatsu *et al.*, 2007). In addition, progressive neurodegeneration and massive neuronal death, associated with the accumulation of polyubiquitinated aggregates was evident in neural cell specific *ATG5* and *ATG7* deficient mice (Hara *et al.*, 2006; Komatsu *et al.*, 2006). It was therefore suggested that the clearance of cytosolic proteins by autophagy is critical for the prevention of neurodegeneration.

In *Drosophila* it was demonstrated that autophagy is induced as a compensatory degradation system when there is an impairment in the UPS. In addition histone deacetylase 6 (HDAC6) was shown to be an essential mechanistic link between the UPS and autophagy system (Pandey *et al.*, 2007). HDAC6, a microtubule associated deacetylase (Hubbert *et al.*, 2002) has previously been demonstrated to regulate the formation of aggresomes and their subsequent removal by autophagy in mammalian cells (Iwata *et al.*, 2005; Kawaguchi *et al.*, 2003).

1.3. The HDAC Family

Chromatin is a highly dynamic complex of DNA, histones and non-histone proteins. The basic unit of chromatin is formed by nucleosomes, which consists of DNA wrapped around histone octomers (Luger *et al.*, 1997). Higher-order nucleosome structure can be altered by post-translational methylation, phosphorylation and acetylation of the histone tails. Nucleosome structure is regulated by the opposing actions of histone acetylases (HATs) and histone deacetylases (HDACs). HATs acetylate the ϵ -NH₂

group on lysine residues in the histone tails, inducing an open chromatin conformation and active gene transcription in the open regions. In contrast HDACs function by catalysing the deacetylation of the histone tails and chromatin condensation, resulting in transcription repression (Bolden *et al.*, 2006; Johnstone, 2002).

In humans, eighteen HDACs have been identified and are subdivided into four classes according to their homology to yeast HDACs, their enzyme activities and their subcellular localisation (Bolden *et al.*, 2006). The class I HDACs (1, 2, 3 and 8) are expressed ubiquitously in human cell lines and tissues and generally have a nuclear localisation. Class II HDACs (4, 5, 6, 7, 9 and 10) shuttle between the nucleus and the cytoplasm and their expression is cell-type specific. In contrast to the other HDACs, HDAC6 and HDAC10 contain an additional deacetylase domain (de Ruijter *et al.*, 2003). HDAC6 also has unique substrate specificities for α -tubulin (Hubbert *et al.*, 2002; Matsushita *et al.*, 2007) and heat shock protein 90 (HSP90) (Bali *et al.*, 2005; Kovacs *et al.*, 2005) and has the ability to bind ubiquitinated proteins (Boyault *et al.*, 2006). Class III HDACs (SIRT1-7), homologues of the yeast protein Sir2, require NAD⁺ to regulate the cellular redox status. The sole member of the class IV HDACs, is the novel HDAC11 (Gao *et al.*, 2002).

Many HDAC inhibitors (HDACi) have been developed to inhibit the class I, II and IV HDACs. In our laboratory the use of HDACi as sensitizers for TRAIL-induced apoptosis was demonstrated (Inoue *et al.*, 2004; Inoue *et al.*, 2006a; Inoue *et al.*, 2006b) and clinical trials for their use in various types of cancer are ongoing. In addition, the use of HDACi for the treatment of HD is currently being investigated (Butler and Bates, 2006).

1.4. Aims

In our laboratory it was shown for the first time that the proteasomal subunits S1, S6' and S5a are cleaved by caspase-3 during apoptosis. The initial aim of this project was therefore to investigate the cleavage in a physiological model of neuronal cell death and to determine the functional significance in the cleavage of proteasomal subunits. For this purpose, a model of cell death induced by the withdrawal of potassium (K^+) in murine CGNs was employed. K^+ withdrawal-induced cell death is a well-characterised model for neuronal cell death and is thought to mimic the first afferent stimulation of the granule neurons *in vivo*.

In addition, there are multiple levels of regulation for the autophagic pathway that remain uncharacterised. Therefore, the second aim of this project was to investigate the potential regulation of the autophagic response during apoptosis. An *in vitro* cleavage assay would be used to investigate the cleavage of several autophagy-related proteins by cell death proteases *in vitro*.

Furthermore, neuroprotection mediated by HDACi has been demonstrated in several neuronal models. However, the definitive mechanism of HDACi-induced survival is not yet known. The aims of this work were to compare the effects of the HDACi, TSA, in immature and mature CGNs and to explore the possible mechanisms of its neuroprotective action.

Chapter 2

Materials and Methods

2.0. Materials and Methods

All chemicals were of the highest quality and were purchased from Sigma-Aldrich or Fisher Scientific unless otherwise stated.

2.1. Primary Culture of Mouse Cerebellar Granule Neurons

Balb/c mice were obtained from the Division of Biomedical Services at the University of Leicester. Cerebellar Granule Neurons (CGNs) were isolated from 6-8 day-old pathogen free Balb/c mice as previously described (Leist *et al.*, 1997). Freshly dissected cerebella were dissociated briefly by mechanical disruption, and enzymatic digestion at 37 °C for 12 min in 1% trypsin. Dissociated neurons were plated on poly-L-lysine (100 µg/ml for plastic, 250 µg/ml for glass) coated dishes (Greiner) at a density of $\sim 4 \times 10^5$ per well (24-well plate), $\sim 9 \times 10^5$ per well (12-well plate) and $\sim 2.4 \times 10^6$ per well (6-well plate). CGNs were cultured in Eagle's Basal Medium (2 x containing L-glutamine and without phenol red; Invitrogen) supplemented with 10% (v/v) heat-inactivated fetal bovine serum (FBS; Invitrogen), 25 mM KCl and 1% penicillin-streptomycin (Invitrogen) at 37 °C in an atmosphere of 5% CO₂. Cytosine arabinoside (10 µM) was added to prevent the proliferation of nonneuronal cells such as fibroblasts and glial cells, 48 h after plating. There were no further medium changes until neurons were used at 7 days *in vitro* (DIV). In general, the frequency of granule cells in CGN cultures is thought to be >95% (Berliocchi *et al.*, 2005). However, while the level of astrocytes was found to be approximately 2% in this study at DIV7, levels of other glial cells such as microglia and oligodendrocytes were not assessed.

2.2. Potassium (K⁺) withdrawal-induced apoptosis

Under normal conditions CGNs are grown in a depolarising concentration of KCl (25 mM). At DIV7 apoptosis can be stimulated through the withdrawal of K⁺. CGNs were first incubated with MK-801 (2 µM) and MgCl₂ (2 mM) to prevent NMDA receptor activation and excitotoxic neurodegeneration (Leist *et al.*, 1998). CGNs were then washed in control salt solution (CSS buffer; 120 mM NaCl, 25 mM KCl, 1.8 mM CaCl₂, 25 mM HEPES, 15 mM glucose, 2 mM MgCl₂, pH 7.4) and switched to CSS-5 buffer (CSS with 5 mM KCl; K5) containing 2 µM MK-801 and 2 mM MgCl₂. Control CGNs were treated as above but maintained in CSS buffer (K25).

To determine the extent of involvement of proteases implicated in the cell death pathway, CGNs were incubated with the poly-caspase inhibitor z-VAD(OMe).fmk (Enzyme Systems), the caspase-3/7 inhibitor DEVD(OMe).fmk (Bachem) and the

calpain-specific inhibitor calpeptin (Merck) for 1 h prior to the withdrawal of K^+ . The inhibitors were then added to the maintenance CSS-5 buffer as indicated.

For experiments in which the proteasome inhibitors MG132 (Calbiochem) or PS-341 (Millenium Pharmaceuticals) were used the inhibitors were added simultaneously with the withdrawal of K^+ (CSS-5).

2.3. Treatment with inhibitors of histone deacetylases (HDACi)

CGNs were treated with TSA (100-500 nM), MC1568 (1-10 μ M; a kind gift from Prof. A. Mai) or the necessary vehicle control (Dimethyl sulfoxide; DMSO) at the indicated times.

2.4. Assessment of neuronal viability

Nuclear condensation and shrinkage, morphological changes that occur during apoptosis, can be assessed through the use of nuclear stains. Hoechst 33342 (H33342) is a membrane permeant nucleic acid stain that emits a blue fluorescence when bound to double-stranded DNA. It also allows the distinction between live cells (diffuse blue nuclei) and those undergoing apoptosis (condensed highly fluorescent blue nuclei). SYTOX Orange (SYTOX) emits a green fluorescence when it interacts with nucleic acids in cells with compromised membranes. These two fluorescent chromatin-binding dyes were used to measure CGN viability by distinguishing live, apoptotic and necrotic cells.

CGNs were incubated with a combination of H33342 (0.5 μ g/ml) and SYTOX (0.5 μ M; both Molecular Probes) for 10 min at 37 °C. Nuclear morphology was then analysed by fluorescent microscopy (objective 40x). Each treatment was performed in duplicate with three different fields scored per well from three independent cultures unless otherwise indicated.

In addition, the 3-(4, 5-Dimethylthiazol-2-yl)-2, 5-diphenyltetrazolium bromide (MTT) assay was employed to assess cellular viability. In functional intact mitochondria, active mitochondrial dehydrogenases reduce the water soluble MTT salt (yellow solution) to insoluble purple formazan. This conversion measures the functionality of the mitochondria and can be directly related to the number of viable cells in a given sample; therefore it is used as a measure of cytotoxicity.

MTT (0.5 mg/ml) was added to the treatment medium and incubated at 37 °C, 5 % CO₂ for 1 h. The capacity of the neurons to reduce the MTT to formazan was then quantified by removal of the reaction media, and solubilisation in MTT lysis buffer (5 % (v/v) formic acid, 95 % (v/v) isopropanol). The absorbance of the formazan product was measured at 550 nm using a Tecan Genios Fluorescence, Absorbance and Luminescence Reader. Results were analysed in Excel after being imported by the Magellan program. The viability of treated neurons was expressed as a percentage of its corresponding control.

2.5. Preparation of CGN whole cell extracts for immunoblot

As described previously (Berliocchi *et al.*, 2005). CGNs were lysed in Radio Immuno Precipitation Assay (RIPA) buffer (150 mM NaCl, 50 mM Tris, pH 7.4, 1% (v/v) Nonidet-P40 (NP-40), 0.25% (w/v) sodium deoxycholate, 1 mM EGTA, supplemented with complete protease inhibitors without EDTA (1 tablet/10 ml; Roche). Cell debris were removed by high speed centrifugation at 16060 x g, and the protein content of the lysate determined by the Bradford assay.

For experiments in which CGN lysates were incubated with recombinant enzymes, the CGNs were lysed in caspase lysis buffer (section 2.11).

2.6. Preparation of isolated cerebella for immunoblot

Cerebella were isolated from postnatal Balb/c mice at the indicated times, frozen on dry ice and stored at -80 °C until all samples were collected. Tissue was lysed in 1% SDS on ice for 30 min, sonicated for five cycles (5 sec on, 5 sec off) and boiled for 5 min. The protein content of the lysate was determined by the Bradford Assay. Lysates (50 µg) were then loaded onto SDS polyacrylamide gels for immunoblot.

2.7. Bradford Assay

The protein content of the CGN lysates was established using the Bradford Protein Assay. This assay is based upon the absorbance shift that occurs when Coomassie Brilliant Blue dye binds to proteins on arginine and hydrophobic residues (Bradford, 1976).

BioRad Protein Assay Concentrate was diluted according to the manufacturers instructions (1:5 with deionised water) and 1 ml was added to 1 cm path length polystyrene cuvettes. The appropriate dilution of lysate was added and the cuvette inverted several times. The absorbance of the sample was then measured at a

wavelength of 595 nm on a Perkin Elmer Lambda 2S UV/VIS spectrophotometer. BSA standards (1-8 µg/ml) were used to produce a standard curve of protein concentration vs. OD₅₉₅ and the protein concentration of the lysate was quantified by comparing its absorbance against the reference BSA curve in Excel.

2.8. SDS-Polyacrylamide Gel Electrophoresis (SDS-PAGE)

In a given sample, unknown/known proteins can be separated on the basis of their molecular weight by SDS-PAGE.

CGN lysates (5-50 µg protein) were equally loaded onto 7, 10, 12, 13 or 15% SDS-polyacrylamide gels (Protean III mini SDS-PAGE Kits; BioRad), and the proteins were separated by SDS-polyacrylamide gel electrophoresis against a molecular marker (See Blue; Invitrogen). Gels were then either electroblotted to nitrocellulose for western blot analysis (Hybond-C Extra, Amersham) or stained with Coomassie Blue.

2.9. Coomassie Blue Staining

After SDS-PAGE electrophoresis the gels were incubated for 1 h in Coomassie Blue Stain (0.25% Coomassie brilliant blue, 45% (v/v) methanol, 10% (v/v) acetic acid) and destained (10% (v/v) acetic acid, 40% (v/v) methanol) until clear.

2.10. Western blotting

Immunodetection of the protein of interest was essentially carried out as described previously (MacFarlane *et al.*, 1997). Membranes were blocked in 5% milk in Tris-buffered Saline Tween-20 (TBST; 20 mM Tris, 137 mM NaCl, 0.1% (v/v) Tween 20, pH 7.6) in the presence of 0.5% BSA and incubated in primary antibody at room temperature (RT) for 1 h unless indicated otherwise (Table 2.10.1). After incubation with the appropriate horseradish peroxidase (HRP)-conjugated secondary antibody (1 h, RT; Table 2.10.2), enhanced chemiluminescence (ECL; Amersham) was used to detect the HRP activity on X-ray film.

Table 2.10.1.

Antibody	Host	Source	Concentration
Fodrin	Mouse	Chemicon	1/500
S1	Mouse	BIOMOL (formerly Affiniti)	1/2000
S6 ^r	Mouse	BIOMOL (formerly Affiniti)	1/2000
S5a	Rabbit	AG Scientific	1/500

Antibody	Host	Source	Concentration
S5a	Mouse	Novus	1/500
S2	Rabbit	Abcam	1/2000
Caspase-3	Rabbit	In house, XMSR894	1/2000
Active caspase-3	Rabbit	Cell Signalling	1/500 o/n at 4 °C
GAPDH	Mouse	Abcam	1/5000
LC3	Mouse	Nanotools (5F10)	1/20
BID (human)	Rabbit	Gift from Xiao-Dong Wang	1/1000
FLAG (M2)	Mouse	Sigma	1/2500
myc	Mouse	Cell Signaling	1/1000 o/n at 4 °C
Beclin 1	Rabbit	Cell Signaling	1/1000 o/n at 4 °C
GFP	Rabbit	Clontech	1/400
HDAC1	Rabbit	Cyclex	1/1000 o/n at 4 °C
HDAC2	Rabbit	Cyclex	1/1000 o/n at 4 °C
HDAC3	Rabbit	Bethyl Labs	1/5000 o/n at 4 °C
HDAC4	Mouse	Abcam	1/2000 o/n at 4 °C
HDAC5	Rabbit	Cell Signalling	1/1000 o/n at 4 °C
HDAC6	Rabbit	Cell Signalling	1/1000 o/n at 4 °C
HDAC7	Rabbit	Cell Signalling	1/1000 o/n at 4 °C
HDAC8	Mouse	Sigma	1/600 o/n at 4 °C
Ac-H3	Rabbit	Upstate	1/2000
Ac-Tub	Mouse	Sigma	1/2000
Ac-Tub	Mouse	Abcam	1/2000
Tubulin	Mouse	Oncogene	1/2000
Caspase-9	Mouse	MBL	1/1000
Caspase-7	Rabbit	In house, XMSR151	1/1000
BCL2	Rabbit	Cell Signalling	1/1000 o/n at 4 °C
BCLxL	Mouse	Santa Cruz	1/250 o/n at 4 °C
MCL1	Rabbit	Rocklands	1/2000 o/n at 4 °C
BIM	Rabbit	Chemicon	1/1000 o/n at 4 °C
PUMA	Rabbit	Proscience	1/500 o/n at 4 °C
BID	Mouse	BD Biosciences	1/1000 o/n at 4 °C
BAX	Rabbit	Upstate	1/500
BAK	Rabbit	Santa Cruz	1/500 o/n at 4 °C
BAD	Mouse	BD Biosciences	1/500 o/n at 4 °C

Table 2.10.2.

Antibody	Host	Source	Concentration
Anti-mouse	Goat	Sigma	1/2000 (for Fodrin, 1/1000)
Anti-rabbit	Goat	Dako	1/2000

In some experiments, the membranes were re-probed with primary antibody after stripping in stripping buffer (62.5 mM Tris, 0.5% SDS, pH 6.8, 10 mM β -mercaptoethanol) at 55 °C for 30 min.

2.11. Assay of Caspase-3/7 Activity

Caspase-3 and caspase-7 preferentially cleave substrates after the recognition site DEVD. This is also a well characterised caspase-3/7 cleavage motif in PARP (Nicholson *et al.*, 1995). Based on this observation and using results from positional scanning substrate combinatorial libraries, the fluorogenic substrate Ac-DEVD.AFC was developed for assay of caspase-3/7 activity (Stennicke *et al.*, 2000; Thornberry *et al.*, 1997). The cleavage to the C-terminus of the tetrapeptide releases 7-amino-4-trifluoromethylcoumarin (AFC), which can be measured using U.V. spectrofluorometry.

DEVDase activity (Ac-DEVD.AFC cleavage) was measured as described previously (Berliocchi *et al.*, 2005). CGNs were lysed in ice-cold lysis buffer (25 mM HEPES, 5 mM MgCl₂, 1 mM EGTA, 0.5% (v/v) Triton X-100, pH 7.5, and 1 mM PEFA Block, supplemented with one protease inhibitor tablet without EDTA/10 ml (Roche), and subjected to high-speed centrifugation at 16060 x g for 30 min at 4 °C. 50 μ g of protein was incubated in assay buffer (50 mM HEPES, 10 mM DTT, 1% (w/v) sucrose, 0.1% (w/v) CHAPS) in 96-well plates at 37 °C for 15 min. Ac-DEVD.AFC (40 μ M final concentration in assay buffer; Enzyme Systems) was added and assayed for 10 cycles ($\lambda_{\text{ex}}/\lambda_{\text{em}}=400\text{-}505$ nm) on a Wallac Victor² 1420 multilabel counter at 37 °C. Cleavage rates were determined by linear regression and expressed as activity in pmol/min/mg protein.

For experiments in which the DEVDase activity of recombinant pro/active caspase-3 was measured, recombinant enzyme and the substrate Ac-DEVD.AFC were diluted in assay buffer (100 mM HEPES, 10% (w/v) sucrose, 0.1% (w/v) CHAPS, pH 7, 10 mM DTT) and Ac-DEVD.AFC was used at a final concentration of 20 μ M.

The activities of the recombinant caspases-6, -7 and -8 were assayed as above using the substrates VEID.AFC, DEVD.AFC and IETD.AFC (all Enzyme Systems) respectively, at a final concentration of 40 μ M.

2.12. Assay of the Chymotrypsin-like Activity of the 20S Proteasome

The measurement of the chymotrypsin-like activity of the 20S proteasome was carried out by monitoring the release of 7-amino-4-methylcoumarin (AMC) after cleavage to the C-terminus of the tetrapeptide LLVY of Suc-LLVY.AMC. This was based on the method described previously (Beyette *et al.*, 1998). CGNs were lysed in ice-cold buffer (20 mM Tris/HCl, pH 7.2, 0.1 mM EDTA, 1 mM 2-mercaptoethanol, 5 mM ATP, 20% (v/v) glycerol, 0.4% (v/v) NP-40), and subjected to centrifugation at 16060 x g at 4 °C for 30 min. 10 μ g of protein lysate was incubated at 37 °C in reaction buffer (50 mM HEPES, pH 8.0, 5 mM EGTA) for 15 min in 96-well plates. Suc-LLVY.AMC (80 μ M final concentration) in reaction buffer; BIOMOL) was added, and assayed for 30 cycles ($\lambda_{\text{ex}}/\lambda_{\text{em}}=380\text{-}460$ nm) on a Wallac Victor² 1420 multilabel counter at 37°C. Cleavage rates were determined by linear regression and expressed as activity in pmol/min/mg protein or as a percentage of the corresponding control.

2.13. Production and Purification of Recombinant Caspase-3

As described previously (Stennicke and Salvesen, 1999), BL21 cells (DE3; Novagen) were transformed with a pET-21b plasmid containing the gene for His₆-tagged procaspase-3. Colonies were grown in terrific broth, 1% (w/v) glucose and the antibiotic ampicillin (100 μ g/ml; Melford laboratories) for selection. Isopropyl β -D-1-thiogalactopyranoside (IPTG (1 mM); Melford laboratories) was added when the culture density reached an OD₆₀₀ of 0.6, and incubated at 30 °C for 3 h. The bacteria were then pelleted and lysed in lysis buffer (20 mM HEPES, 100 mM NaCl, 10 mM imidazole, 1 protease inhibitor tablet – EDTA/10 ml, pH 8.0) and 8 cycles of sonication on ice (15 sec on, 45 sec off). The His₆-tagged protein was then incubated with Ni-NTA Agarose beads (QIAGEN) for 2 h at 4 °C on a daisy wheel. The beads were washed in wash buffer (20 mM HEPES, 500 mM NaCl, 20 mM imidazole, pH 8.0), the His₆-tagged protein was eluted (20 mM HEPES, 5% (w/v) sucrose, 0.1% (w/v) CHAPS, 0.5 mM DTT, 250 mM imidazole, pH 8.0) and its purity determined by Coomassie staining after SDS-PAGE (section 2.9 and 2.8 respectively). The purification profile of recombinant active caspase-3 is shown in Figure 2.13.1.

The total concentration of the recombinant active caspase-3 was determined by active site titration with unmethylated z-VAD.fmk (Enzyme Systems). The recombinant

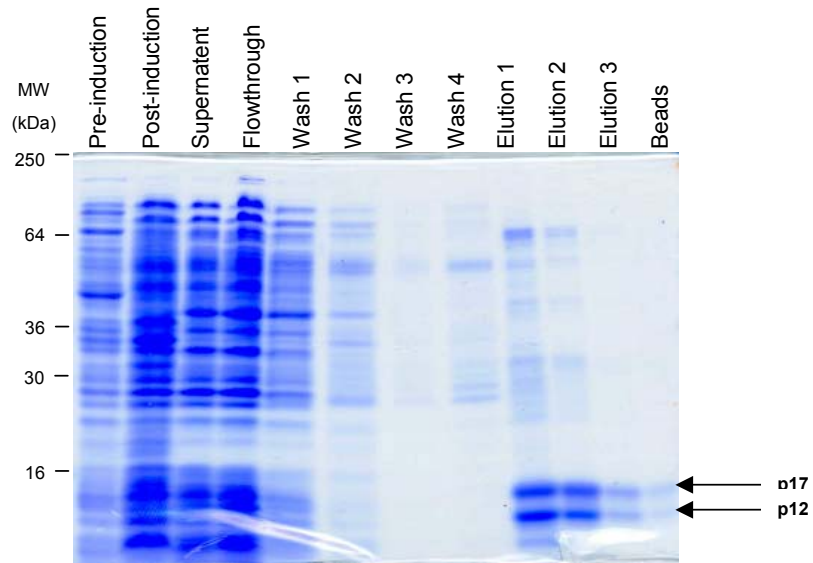


Figure 2.13.1. Purification profile of recombinant His₆-Caspase-3 using Ni-NTA beads

enzyme was incubated with varying concentrations of the inhibitor for 30 min at 37 °C and then assayed with Ac-DEVD.AFC on the Wallac fluorimeter. The total concentration of the enzyme was determined from the intercept with the X axis when the linear rate of hydrolysis was plotted against the inhibitor concentration (Stennicke and Salvesen, 1999). Recombinant active caspase-3 was stored at – 80 °C in 10% glycerol.

Recombinant caspases-6, -7 and -8 were prepared as above by Dr. X. M. Sun and assayed using their corresponding substrates as described in section 2.11 for their active site titration.

2.14. Construction of 26S Proteasome Sensor

This was essentially carried out as described in Stack *et al*, 2000. A schematic of the process can be found in Figure 2.14.1 (Stack *et al.*, 2000).

The full length wild type (WT) ubiquitin gene was amplified by Pfx Polymerase (Invitrogen) in a two-step PCR reaction from the mammalian expression vector pHis₆-ubiquitin (gratefully received from Dr. R Hays) using oligonucleotides to introduce a 5' BglII site and a 3' BamHI site. The upstream primer also contained an ATG start site, a Kozak consensus sequence, which was required to target protein synthesis to the correct ATG start site and a mutation for an internal BglII site that was found in the ubiquitin sequence.

Ubiquitin was then excised (Gel Extraction Kit, QIAgen) and ligated using T4 DNA ligase (Promega) into the BamHI restriction site of pcDNA3.1 + (HYGRO) (Invitrogen). All restriction enzymes were purchased from Invitrogen and the reactions were carried out at 37 °C for 1-2 h. By exploiting the compatible ends of BglII and BamHI, the 5' BamHI site in the vector was destroyed, and the 3' lower BamHI site was free for the sequential additions of ubiquitin/fusion protein. Ligation reactions were transformed into Library Efficient DH5α cells (Promega) and DNA from the resulting clones was purified using a DNA Miniprep Kit according to the manufacturers instructions (QIAgen). All manipulations of the DNA were verified by sequencing either in the 5' or 3' direction or both.

Further amplification and addition of ubiquitin to the vector was carried out in a similar manner using the same oligonucleotides without the Kozak sequence in the upstream

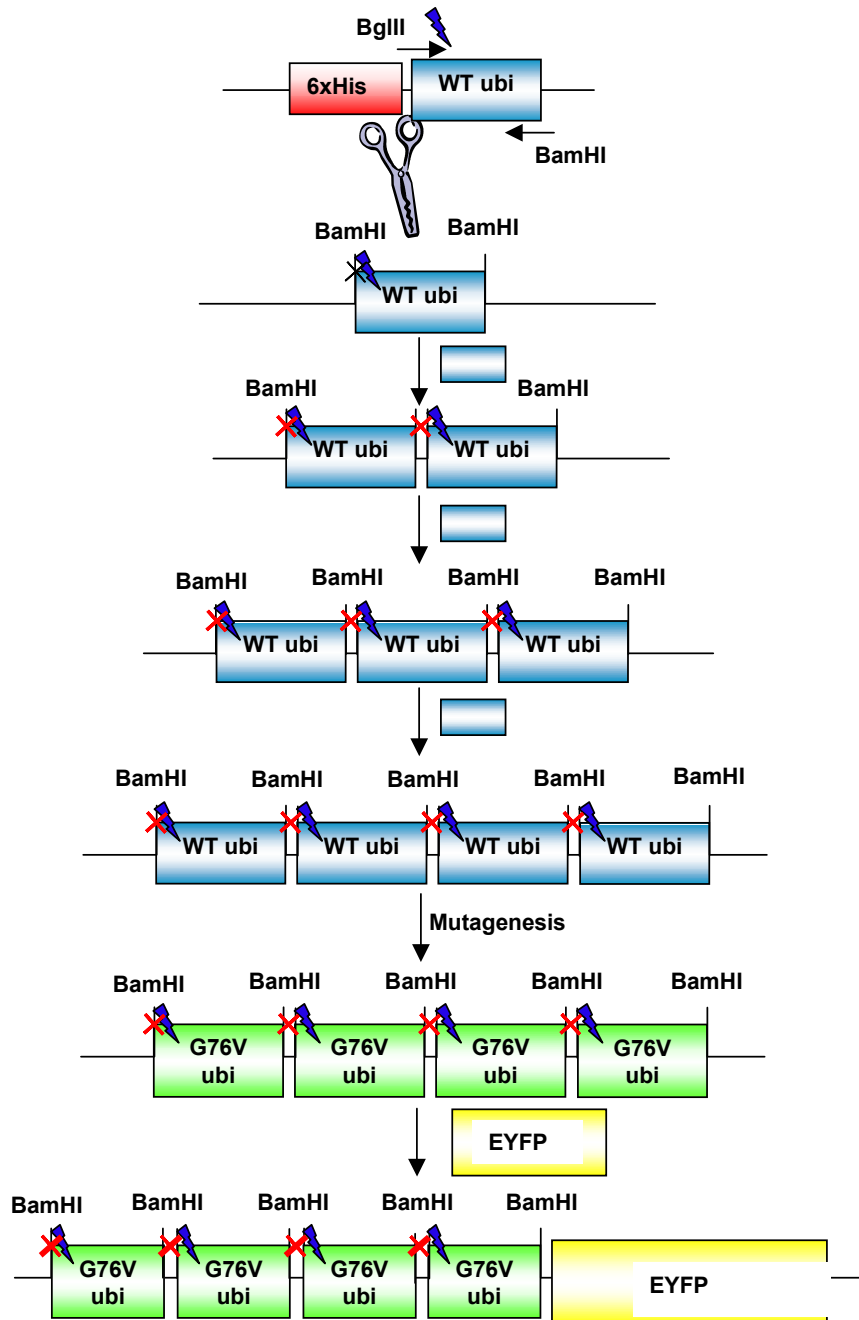


Figure 2.14.1. Schematic of the construction of the proteasome sensor – p4xubi(G76V)-EYFP. Process described in section 2.16. ‘Lightening’ signs indicates the BglIII restriction site in the wild type ubiquitin sequence that was mutated as part of the amplification primer.

primer. This was carried out until there were four sequential ubiquitin sequences in the vector (Stack *et al.*, 2000).

In order to prepare ubiquitin that resists cleavage by ubiquitin C-terminal hydrolases, it was necessary to mutate the final amino acid in the ubiquitin sequence. The QuikChange® Multi Site-Directed Mutagenesis Kit (Stratagene) was used according to the manufacturers instructions to introduce a glycine to valine mutation at amino acid 76 (G76V) in all ubiquitin sequences.

The gene for enhanced yellow fluorescent protein (EYFP; CLONTECH) was then amplified from pEYFP-Bid-ECFP (a kind gift from Dr. K. Taira and modified to pECFP-Bid-EYFP by Dr Davina Twiddy) using oligonucleotides to introduce a 5' BamHI site and a 3' XbaI site. EYFP was then excised and ligated into the p(1-4x)G76V-ubi vectors/2xWT-ubi vector at the BamHI/XbaI restriction sites. For use as a negative control EYFP was also ligated into the same sites of pcDNA3.1 + (HYGRO) containing no ubiquitin sequences. A Kozak consensus sequence was then introduced using the QuikChange® Site-Directed Mutagenesis Kit (Stratagene) according to the manufacturers instructions.

2.15. Extraction of RNA from HeLa cells

HeLa cervical adenocarcinoma cells (European Collection of Animal Cell Cultures (ECACC)) were grown in Dulbecco's Modified Eagle Medium (high glucose, without pyruvate DMEM, Invitrogen) supplemented with 10% FBS at 5% CO₂, 37 °C. RNA was extracted from approximately 5 x 10⁶ cells in 150 µl RNase-free water using the RNeasy Kit according to the manufacturers instructions (QIAGEN). RNA was stored at -80 °C until further use.

2.16. Reverse Transcription-PCR

cDNA was prepared from 1 µg RNA using the Omniscript Reverse Transcription Kit (QIAGEN) according to the manufacturers instructions. Oligo-dT primers (Promega) that specifically hybridise to the poly-A-tail of mRNAs were used at a final concentration of 1 µM.

2.17. Construction of plasmids for hAtg3, 4A, 4B, 4C, 4D, 5, Beclin 1, 7, LC3, GABARAP, 9, 10 and 12

Expression vectors containing the cDNA sequences of the human forms of Atg3 (hAtg3), 4A, 4B, 4C, 4D, 7, 9 (Atg9A), 10 and 12 were constructed as follows, a

schematic of which is shown in Figure 2.17.1. The sequences for the hAtg proteins were acquired from NCBI and oligonucleotides were designed against the 5' and 3' ends of the mRNA sequence. In addition oligonucleotides to incorporate the coding sequence for an epitope tag to the 5' and 3' ends of the construct were designed.

Multiple rounds of PCR was used to amplify desired sequences from HeLa cDNA, followed by the addition of an epitope tag to the 5' end of the sequence. The resulting amplified PCR products were then excised and purified using the QIAgen PCR Purification Kit as per manufacturers instructions. The tagged cDNA sequence was excised using the 5'/3' restriction sites introduced and ligated into pcDNA6/myc-His B (Invitrogen) 5' to the myc-His epitope tag sequence. The ligated vectors were transformed with DH5 α library efficient cells and a PCR screen was performed to identify positive clones; which were purified and sequenced in both the 5' and 3' direction. Sequences also underwent a NCBI BLAST search to confirm sequence integrity.

The constructs for pAtg5, pFLAG-Beclin 1, pYFP-3xmyc-GABARAP and pEGFP-LC3 were gratefully received from Profs. A. Tolkovsky, N. Mizushima and T. Yoshimori respectively. The DNA for each was amplified by PCR (Pfx Polymerase) using oligonucleotides to introduce restriction sites for the restriction enzymes Nhe I, Bam HI, Xba I and Kpn I. The amplified DNA was then excised and cloned into the same restriction sites of pcDNA3.1 (+) (HYGRO). Schematics of the subcloned constructs given as gifts and those prepared from HeLa cDNA are shown in Figure 2.17.2.

2.18. *In Vitro* Translation (TNT Reaction)

For the *in vitro* translation of the constructs prepared in sections 2.14 and 2.17 the TNT™ Coupled Reticulocyte Lysate System (Promega) for *in vitro* translation was used. The reactions were prepared according to the manufacturers instructions with the addition of Transcend™ tRNA (Promega). During translation, Transcend™ tRNA incorporates biotinylated lysine residues into nascent proteins that can be detected using Streptavidin conjugates, eliminating the need for radioactivity.

1 μ l (2 μ l for experiments with pcDNA3.1-YFP, pEGFP-LC3, pFLAG-Atg9, pFLAG-Atg12-myc/His) of Transcend™ tRNA was added to the reaction mixture and the reaction was allowed to proceed for 60 min at 30 °C. 3 μ l of the TNT reaction was then added to 15 μ l of 2xSDS sample buffer and heated to 99 °C for 5 min. 15 μ l was then loaded onto an SDS-polyacrylamide gels and electroblotted to nitrocellulose. Detection

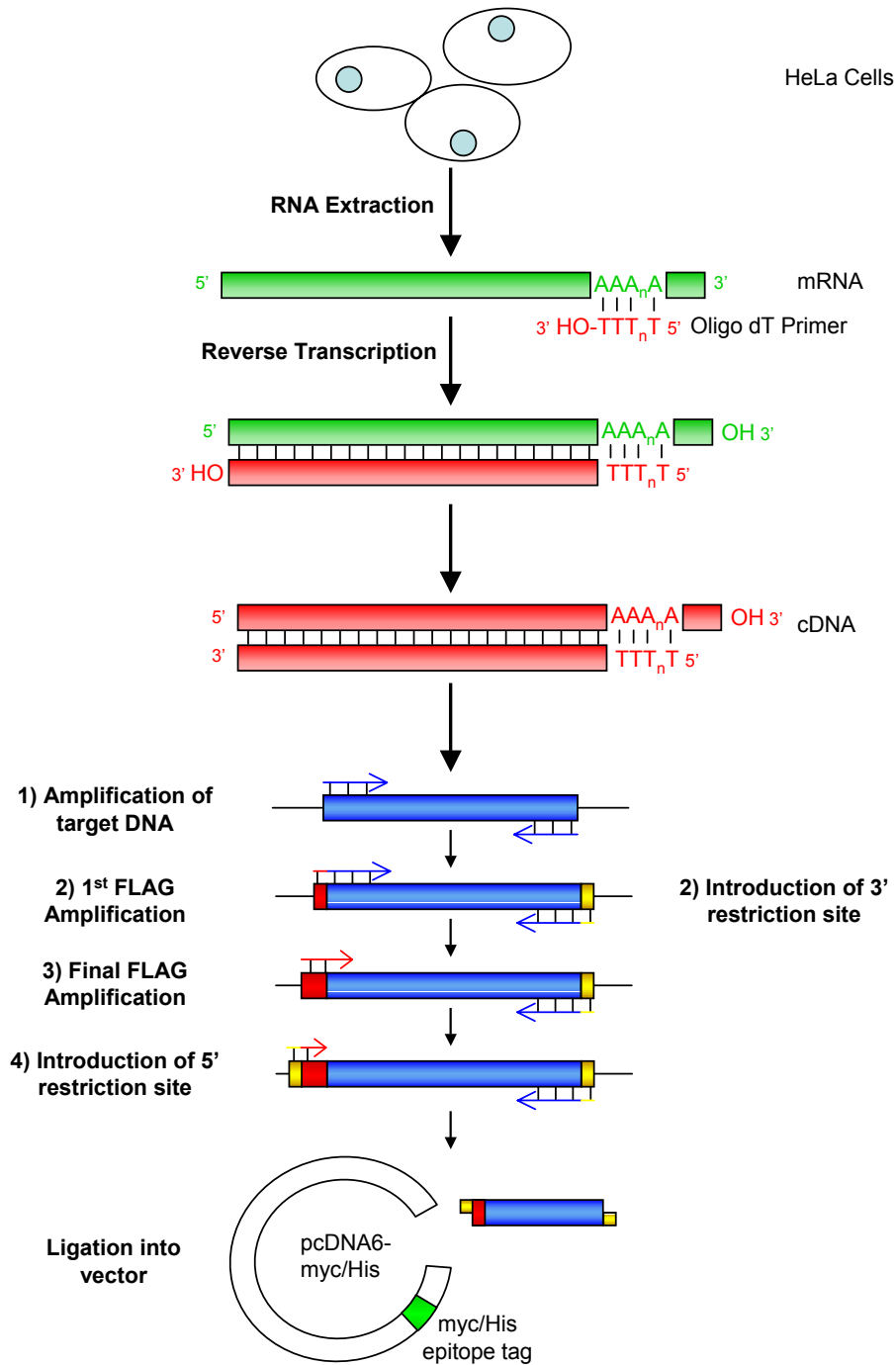


Figure 2.17.1. Schematic of the construction of the hAtg plasmids for *in vitro* expression.

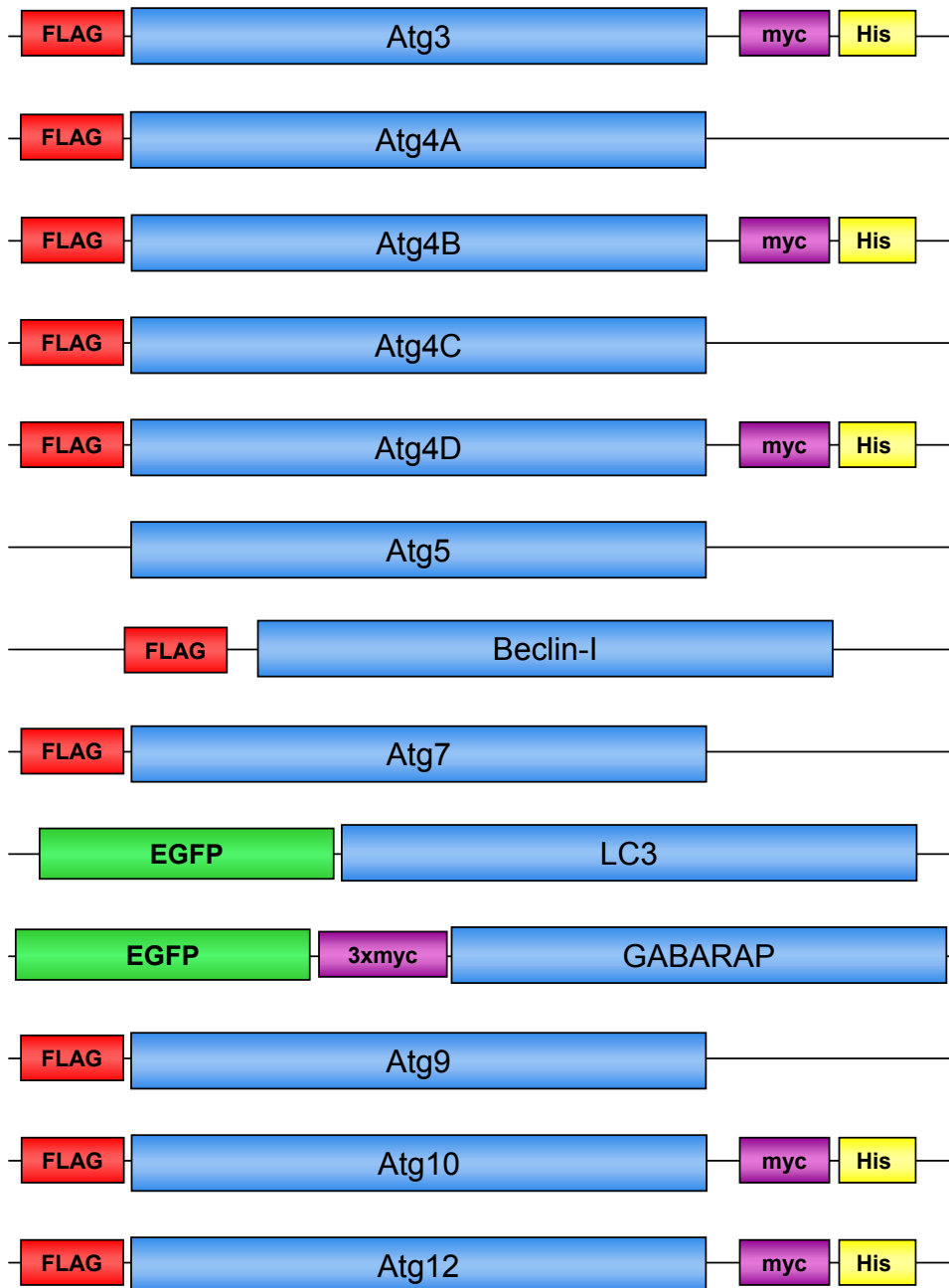


Figure 2.17.2. Schematics of the hAtg constructs

of the TNT reaction was carried out by incubation with Streptavidin-biotinylated-HRP complex (Strep-HRP; Amersham Biosciences; 1:5000 in TBST) and exposure to x-ray film following ECL.

2.19. *In Vitro* Protease Cleavage Assays

The *in vitro* cleavage by recombinant calpain 1 (rCalpain 1) was performed essentially as described by Bano *et al.*, 2005. TNT reactions (prepared in the presence of Transcend™ tRNA as described in section 2.20) were incubated in calpain buffer (50 mM NaCl, 10 mM EGTA, 0.1% (v/v) Triton, 100 mM HEPES, pH 7.5) with recombinant calpain 1 (Calbiochem). Reactions were carried out in the presence of CaCl₂ at a final concentration of 20 mM for 1 h at 37 °C (Bano *et al.*, 2005; Munarriz *et al.*, 2005). Similarly for the *in vitro* assay of recombinant caspase cleavage, TNT reactions (prepared in the presence of Transcend™ tRNA were incubated in caspase assay buffer (100 mM HEPES, 10% (w/v) sucrose, 0.1% (w/v) CHAPS, pH 7.0, 10 mM DTT) at 37 °C for 60 min. The reactions were stopped by the boiling the reaction in 2xSDS sample buffer and then run on SDS PAGE and immunoblotted as described previously (sections 2.8 and 2.10 respectively).

2.20. SH-SY5Y Cell Culture

Human neuroblastoma cells (SH-SY5Y; American Type Culture Collection (ATCC)) were cultured in Minimum Essential Medium (MEM; Invitrogen) supplemented with 5% (v/v) FCS, 5% (v/v) Newborn Calf Serum (NCS), 1% glutamax and 1% penicillin-streptomycin at 5% CO₂, 37 °C. Cells were passaged every 3-4 days at 7.5x10⁵/ml. Cells were seeded at 7x10⁵/well (6 well plate, Nunc) at least 16 h prior to treatment.

For experiments in which SH-SY5Y cells were used for immunoblot, cells were lysed as described previously in RIPA buffer (section 2.5). SH-SY5Y cells were lysed in LLVYase lysis buffer for assay of the chymotrypsin-like activity (section 2.12).

2.21. Transfection of SH-SY5Y cells

SH-SY5Y cells were seeded at 4 x 10⁵ and 7.5 x 10⁴/well in 6 well and 12 well plates respectively. 5 µl Lipofectamine™ 2000 Reagent (Invitrogen) and 2 µg DNA were incubated with 400 µl Optimem (Invitrogen) for 30 min at RT. The transfection mix was then added to each well of a 6 well plate. For 12 well plates 2.5 µl Lipofectamine™ 2000 reagent, 1 µg DNA in 200 µl Optimem was used.

2.22. FACS Analysis for the measurement of YFP expression

Treatment of SH-SY5Y cells was carried out at least 16 h after transfection. Inhibitors used to characterise the 26S Proteasome sensor in transfected SH-SY5Y cells were PS-341, MG132, z-VAD.fmk, Calpeptin and Bafilomycin A1 (Calbiochem) as indicated.

At the indicated times, SH-SY5Y cells were harvested in trypsin/EDTA and resuspended in media. They were then pelleted in a FACS tube (Becton Dickinson) and resuspended in PBS. The tubes were gently vortexed and YFP expression was measured on a FACS Calibur Flow Cytometer (Becton Dickinson).

2.23. Mouse Embryonic Fibroblast Cell Culture

Mouse Embryonic Fibroblast cells (MEFs; a kind gift from Dr C. Borner) were grown in Dulbecco's Modified Eagle Medium (high glucose, without pyruvate DMEM, Invitrogen) supplemented with 10% FCS at 5% CO₂, 37 °C. Cells were seeded at 3 x 10⁵/ml and passaged every 3-4 days.

2.24. Treatment of MEFs with HDACi

Cells were seeded at 7.5 x 10⁴/well (12-well plate), 16 h prior to treatment. MEFs were then treated with the indicated HDACi for 4 h, and lysed on ice in RIPA buffer as described previously. MS-275 was purchased from Calbiochem.

2.25. HDAC4 activity following immunoprecipitation

As described by Inoue *et al.*, 2006. CGNs (approximately 14 x 10⁶ cells per treatment) were lysed on ice for 20 min in lysis buffer (20 mM Tris/HCl pH 8.0, 150 mM NaCl, 10% (v/v) glycerol, 0.5% (v/v) NP-40). After high speed centrifugation (16060 x g, 30 min), 900 µg lysate was incubated with 10 µg mouse IgG or anti-HDAC4 (Sigma) o/n at 4 °C. Protein Sepharose A beads (50 µl; Amersham) were then added to the cell lysate for 3 h at 4 °C, after which beads were washed with PBS and resuspended in 50 µl HDAC assay buffer (20 mM Tris/HCl pH 8.0, 120 mM NaCl, 1% (v/v) glycerol) (Inoue *et al.*, 2006a). HDAC4 activity was then measured using the HDAC Fluorimetric Activity Assay (*Fluor de Lys* kit, BIOMOL) according to the manufacturers instructions. HeLa nuclear extract (3 µg; provided by the manufacturer) was used as a positive control. For experiments in which the HDAC activity was measured directly in CGN lysates, 50 µg of the lysates was used and the assay was carried out as above.

2.26. Statistical Analysis

All comparative tests were carried out using Student's t. test. Unless otherwise indicated these were one-tailed based on the *a priori* explicit expectation that

experimental treatments would produce an expected increase or decrease in the direction as stated in the text. Appropriate Bonferroni correction was applied to the p-value dependent on the number of comparisons made with the control (Strassburger and Bretz, 2008).

Chapter 3

S1 and S6' are Cleaved in CGNs during K⁺ Withdrawal-induced Cell Death

3.1. Introduction

The 26S proteasome regulates cellular processes and enforces protein quality control in the cytosol and nucleus of eukaryotic cells through its degradation of intracellular proteins (Rechsteiner and Hill, 2005). Degradation by the UPS begins with the attachment of ubiquitin to the protein substrate. This is followed by the sequential addition of further ubiquitin moieties forming a polyubiquitin chain, which is recognised by the 19S regulatory particle of the 26S proteasome. The tagged protein is then threaded into the 20S core where degradation takes place.

The proteasome plays an important role in the control of apoptosis by regulating the function and level of several apoptosis related proteins. As a consequence, the use of proteasome inhibitors such as PS-341 (also known as Bortezomib or Velcade) either alone or in combination with other therapeutics are promising agents for the treatment of various cancers. Investigations into the mechanisms of cell death by proteasome inhibitors indicate that different points in the apoptotic pathway are stabilised by proteasome inhibition depending on the cell type studied (Almond and Cohen, 2002).

An early role for the proteasome during cell death was proposed by Canu *et al.*, 2000 in CGNs undergoing apoptosis through the withdrawal of K⁺. They demonstrated a rapid increase in proteasomal activity early in the apoptotic process, followed by a progressive decline past that of the constitutive resting level, accompanied by an accumulation of ubiquitinated proteins. The reduction in proteasomal activity was hypothesised to be downstream of caspase activation (Canu *et al.*, 2000).

In our laboratory the regulation of proteasomal function by caspase-3 was recently demonstrated for the first time. The proteasomal subunits S1 (Rpn2 in yeast), S6' (Rpt5) and S5a (Rpn10), components of the 19S regulatory particle of the proteasome, were cleaved by caspase-3 during apoptosis induced by both extrinsic and intrinsic apoptotic stimuli in a variety of cells, resulting in loss of proteasome function (Sun *et al.*, 2004). Furthermore, in an independent study, the same subunits plus the 11S activator, PA28 γ , were found to be caspase substrates in Jurkat cells (Adrain *et al.*, 2004)

The aim of this investigation is to observe the potential caspase-dependent inactivation of the proteasomal subunits in a primary neuronal system and to determine the functional significance of the cleavages. For this purpose, the well-characterised model

of K⁺ withdrawal-induced apoptosis in CGNs was utilised, the death of which by this stimulus is thought to mimic the *in vivo* elimination of granule neurons during cerebellar development (Yan *et al.*, 1994).

3.2. Results

3.2.1. The caspase-3 cleavage sites in S1 and S6' are conserved in the mouse.

To investigate the potential cleavage of the proteasome subunits S1, S5a and S6' in the K⁺ withdrawal model of cell death in cerebellar granule neurons from mouse, it was first necessary to confirm the presence of the previously identified cleavage sites by Sun *et al*, 2004. The caspase-3 cleavage sites in S1 at Asp-857 and S6' at Asp-27 were confirmed through the alignment of the human with mouse protein sequences from NCBI as shown (Figure 3.2.1, A-B). The S5a cleavage sites are yet to be determined therefore were not verified in the mouse. Based on the best alignment of the protein sequences for S5a, there was an estimated 97% conservation between the two species (Figure 3.2.1, B).

3.2.2 The proteasomal subunits S1 and S6' are cleaved by recombinant caspase-3 in CGN lysates *in vitro*.

To initially observe caspase-3 cleavage *in vitro*, it was decided to assess the ability of recombinant caspase-3 to cleave the proteasomal subunits in lysates prepared from untreated CGNs. His-tagged recombinant active human caspase-3 was therefore prepared from *E-coli* and its concentration determined by active site titration.

The activity of active caspase-3/7 can be measured by following its cleavage of the highly specific fluorogenic substrate Ac-DEVD-AFC. In order to confirm the activity of the recombinant active caspase-3, its activity was compared with that of the 'inactive' recombinant procaspase-3 using the DEVDase assay.

The activity of the recombinant active caspase-3 was significantly higher than that of the recombinant procaspase-3, which exhibited no activity when measured with the DEVDase assay (Figure 3.2.2 A). In agreement, the immunoblot demonstrated the cleavage of recombinant active caspase-3 to its p17 fragment, thought to be the mature active form of caspase-3 (Han *et al.*, 1997) that was absent from the recombinant procaspase-3 (Figure 3.2.2 B).

To further confirm that the recombinant active caspase-3 cleaves substrates under the experimental conditions, the ability of recombinant active caspase-3 to cleave α -fodrin in CGN lysates was assessed. α -Fodrin (non-erythroid α -spectrin) is an



Figure 3.2.1. Sequence alignment of the human S1, S6' and S5a proteins with those from the mouse. The protein sequences of human and mouse S1 (A), S6' (B) and S5a (C) were obtained from NCBI and sequence alignment was assessed. The regions surrounding the identified caspase-3 cleavage sites in S1 and S6' are shown in black. NCBI Accession Numbers: S1 - NP_002798 (human), NP_081633 (mouse); S6' - NP_002795 (human), NP_032974 (mouse); S5a - NP_002801 (human), NP_032977 (mouse).

C – S5a

HUMAN	1	MVLESTMVCVDNSEYMRNGDFLPTRLQAQQDAVNI	35
MOUSE	1	MVLESTMVCVDNSEYMRNGDFLPTRLQAQQDAVNI	35
	36	VCHSKTRSNPENNVGLITLANDCEVLTTLTPDTGR	70
	36	VCHSKTRSNPENNVGLITLANDCEVLTTLTPDTGR	70
	71	ILSKLHTVQPKGKITFCTGIRVAHLALKHRQGKNH	105
	71	ILSKLHTVQPKGKITFCTGIRVAHLALKHRQGKNH	105
	106	KMRIIAFVGSPVEDNEKDLVKLAKRLKKEKVNVDI	140
	106	KMRIIAFVGSPVEDNEKDLVKLAKRLKKEKVNVDI	140
	141	INFGEEEVNTEKLTAFVNTLNGKDGTSGLVTVPP	175
	141	INFGEEEVNTEKLTAFVNTLNGKDGTSGLVTVPP	175
	176	GPSLADALISSPILAGEGGAMLGLGASDFEFGVDP	210
	176	GPSLADALISSPILAGEGGAMLGLGASDFEFGVDP	210
	211	SADPELALALRVSMEEQRQRQEEEARAAAASAAE	245
	211	SADPELALALRVSMEEQRQRQEEEARAAAASAAE	245
	246	AGIATTGTEDSDDALLKMTISQQEFGRTGLPDLSS	280
	246	AGIATPGTEDSDDALLKMTINQQEFGRPGLPDLSS	280
	281	MTEEEQIAYAMQMSLQGAEFGQAESADIDASSAMD	315
	281	MTEEEQIAYAMQMSLQGTEFSQ-ESADMDASSAMD	314
	316	TSEPAKEEDDYDVMQDPEFLQSVLENLPGVDPNNE	350
	315	TSDPVKEEDDYDVMQDPEFLQSVLENLPGVDPNNA	349
	351	AIRNAMGLASQATKDGKKDKKKEEDKK	377
	350	AIRSVMGALASQATKDGKNDKKEEEKK	376

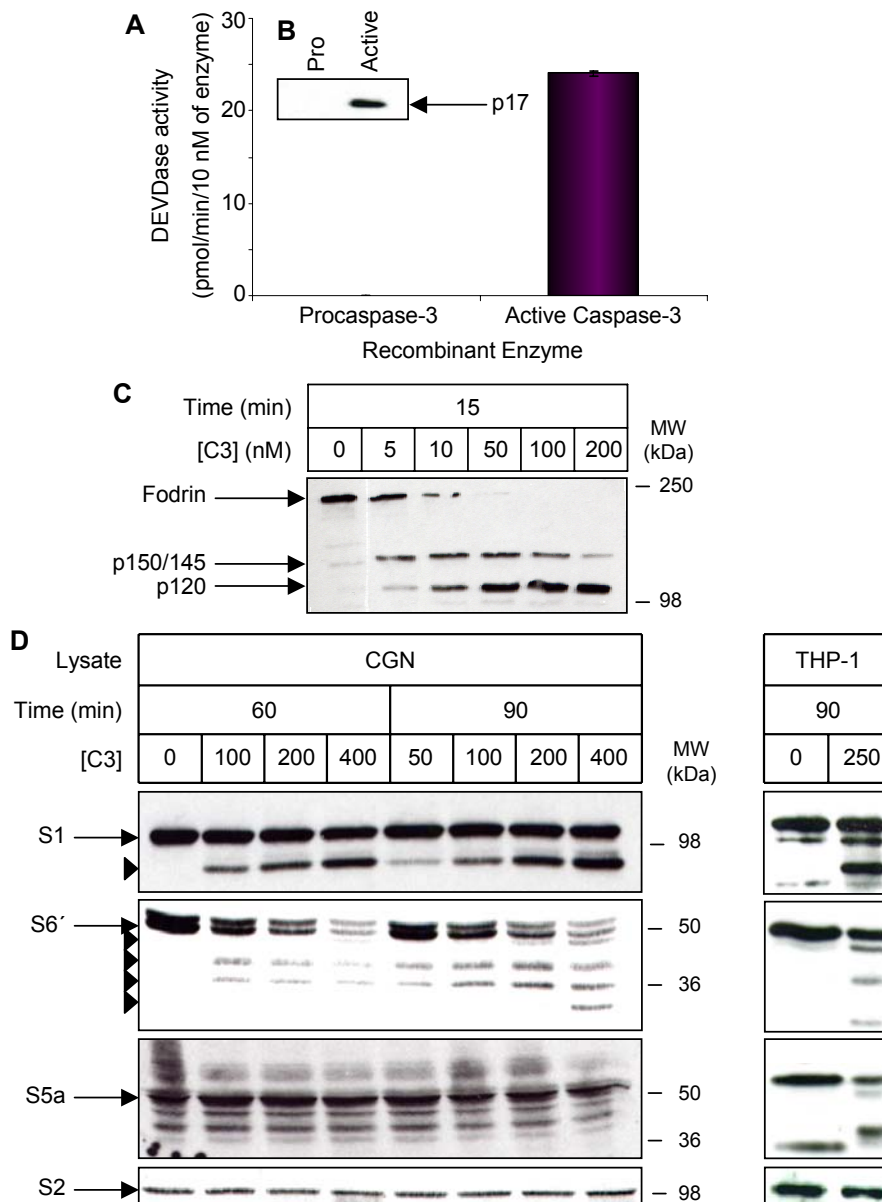


Figure 3.2.2. Active rCaspase-3 is able to cleave S1 and S6' in mouse CGN lysates. Recombinant active caspase-3 was prepared and its DEVDase activity was compared against that of procaspase-3 (A). An aliquot was taken from each sample and immunoblotted for active (p17) caspase-3 (B). CGN lysates (50 μ g) were incubated with recombinant active caspase-3, separated by SDS PAGE and immunoblotted for α -fodrin (C), S1, S6', S5a and S2 (D). The incubation of THP-1 cell lysates with recombinant active caspase-3 was used as a positive control. Arrowheads indicate possible cleaved forms of the proteins.

abundant membrane-associated cytoskeletal protein. It lines the cortical cytoplasm of neurons, having binding sites for actin, calmodulin and microtubules (Jänicke *et al.*, 1998; Siman *et al.*, 1984). α -Fodrin is cleaved during apoptosis induced by both extrinsic and intrinsic apoptotic stimuli, disruption of which is thought to be at least partly responsible for the membrane blebbing seen during apoptosis (Martin *et al.*, 1995). Full length α -fodrin contains two potential caspase-3 cleavage sites, resulting in cleavage fragments of 150 and 120 kDa. The calcium-dependant proteases, calpains are also able to cleave full-length α -fodrin. Active calpains cleave to produce a doublet at 150/145 kDa. Due to the overlapping cleavage pattern by caspase-3 and calpains, the 120 kDa caspase-3 cleavage fragment in particular is used to illustrate caspase-3 activation (Nath *et al.*, 1996; Siman *et al.*, 1984)

The cleavage of α -fodrin was observed at all recombinant caspase-3 concentrations (Figure 3.2.2 C). The complete loss of full length α -fodrin was evident at the higher caspase-3 concentrations, in concurrence with the increase in the 120 kDa cleavage of α -fodrin. Interestingly the observed 150 kDa cleavage fragment was evident at the lowest caspase-3 concentration and declined in a concentration-dependent manner, again in association with the enhanced level of the 120 kDa fragment. It was therefore concluded that the recombinant caspase-3 was able to recognise and cleave substrates in a manner analogous to that of endogenous caspase-3.

To investigate the *in vitro* cleavage of the proteasomal subunits – S1, S5a and S6' by caspase-3 as shown by Sun *et al.*, 2004, CGN lysates were incubated with recombinant active caspase-3. THP-1 cell lysates were used as a positive control. Active caspase-3 cleaved S1 in a concentration- and time-dependent manner in CGN lysates (Figure 3.2.2 D). This cleavage fragment was analogous to that observed upon caspase-3 cleavage of the S1 protein in THP-1 cell lysates at approximately 90 kDa. There was little loss in the full length S1 protein, however this seemed to have reached saturation on the immunoblot, and therefore no discernible difference within the detection limit of the immunoblot would be observed.

In contrast to that seen with the full length S1 protein; full length S6' was lost in a time and concentration-dependent manner (Figure 3.2.2 D). The cleavage pattern by active caspase-3 was similar to that observed in THP-1 cell lysates, although there was evidence of further cleavage in the CGN lysates as shown by the additional cleavage fragments at the higher concentrations (~32-40 kDa). The primary cleavage fragment identified by Sun *et al.*, 2004 (at Asp-27, producing a cleavage fragment of

approximately 49 kDa) did not seem to be the initial cleavage fragment in the CGN lysates as this was only apparent at higher concentrations and at later time points. In contrast, the other cleavage fragments were observed relatively earlier. This suggests alternate *in vitro* cleavage sites in the mouse S6' protein for active caspase-3. However, this may also have been the result of using recombinant human caspase-3 rather than that from the mouse. The higher molecular weight form of full length S6', which also declined in a time and concentration-dependent manner, was thought represent the post-translational modification of S6' such as phosphorylation. The phosphorylation of another proteasomal ATPase, S6, was described previously and was thought to be involved in the regulation of its ATPase activity (Mason *et al.*, 1998).

The loss of full length S5a was used to indicate caspase mediated cleavage of the protein by Sun *et al.*, 2004 rather than the observation of cleavage fragments. This was due to antibody problems and in subsequent studies the group were able to detect the fragments resulting from cleavage by caspases-3 using an alternative antibody. The same problems were experienced in detection of S5a in CGNs and only the loss of full length protein was assessed. There was no evidence of loss of full length S5a protein at any time or concentration of active caspase-3 added to the lysates (Figure 3.2.2 D), suggesting that in this *in vitro* system, the proteasome subunit S5a is not cleaved.

The inclusion of S2, a further component of the 19 S proteasome was to serve as a negative control. As expected there was no loss of full length S2 protein and cleavage fragments were absent until the highest concentration of active caspase-3 (400 nM; Figure 3.2.2 D), upon which there was an indication of cleavage on higher immunoblot exposure. Similarly, in TRAIL-treated MCF-7 cells overexpressing caspase-3, there was some evidence of S2 cleavage (Sun *et al.*, 2004). Taken with the very small amount of cleavage observed at high recombinant caspase-3 concentrations in CGN lysates this supports the observation of a minimal level of S2 cleavage upon overexpression of caspase-3.

3.2.3. The loss of CGN viability correlates with the activation of caspase-3/7.

The largest homogenous population of neurons in the mammalian brain are granule neurons from the deepest layer of the trilaminar cerebellar cortex. Cerebellar granule neurons largely undergo postnatal neurogenesis, enabling the *in vitro* culture of primary neurons from explanted cerebella isolated from neonatal mice and rats. The primary

culture of CGNs is well established and useful for the study of neurobiology (Contestabile, 2002).

The *in vivo* differentiation and migration of post mitotic granule cells through the Purkinje layer to their final destination in the internal granule layer, occurs during early postnatal life (days 4-10). It is here that they receive their first synaptic input from the glutaminergic mossy fibres (D'Mello *et al.*, 1993; Gallo *et al.*, 1987; Hack *et al.*, 1993; Yan *et al.*, 1994). The *in vitro* survival of cerebellar granule neurons requires the presence of a depolarising concentration of K⁺ in the culture medium (Lasher and Zagon, 1972). Depolarising concentrations of K⁺ are thought to mimic the physiological innervations of the post migratory granule cells by the mossy fibres. This is mediated by depolarisation-induced Ca²⁺ entry through voltage sensitive Ca²⁺ channels and the activation of a Ca²⁺/calmodulin-dependent protein kinase (Gallo *et al.*, 1987; Hack *et al.*, 1993). The reduction of K⁺ to a more physiological concentration of 5 mM results in the degeneration and death of differentiated CGNs in culture. The ensuing apoptosis is extremely well characterised, making it an ideal model in which to study neuronal cell death (D'Mello *et al.*, 1993; Yan *et al.*, 1994).

In order to assess the time course of viability in CGNs undergoing apoptosis through the withdrawal of K⁺, CGNs were cultured in medium containing 25 mM K⁺ and in the presence of serum for 7 days. At DIV 7, neuronal viability was reduced through the simultaneous lowering of the K⁺ concentration to 5 mM and the removal of serum. Cell death was determined by means of a combination of double nuclear staining with H33342 and SYTOX and the MTT assay. Control CGNs were maintained in 25 mM K⁺ by the addition of CSS25 (K25) as described in section 2.2, however the K25 neurons were also subjected to the removal of serum.

There was a time-dependent decline in the viability of neurons as shown by the mitochondrial reduction of MTT in the CGNs in low K⁺ (K5; Figure 3.2.3 A). This was evident from the first time point at 6 h in K5 when there was already more than a 15% loss of MTT reduction. The ability of the mitochondria to reduce MTT further declined to 12 h. Following this initial rapid loss, the fall in the reduction of MTT by the mitochondria progressed at a steady state to 27% (± 2%) by 48 h in K5 (Figure 3.2.3 A). The loss of MTT reduction by the mitochondria in the CGNs in high K⁺ (K25) closely paralleled the time-dependent loss in the K5 neurons, but to a lesser extent. It is possible that the mitochondrial function is reduced in the K25 neurons due to the

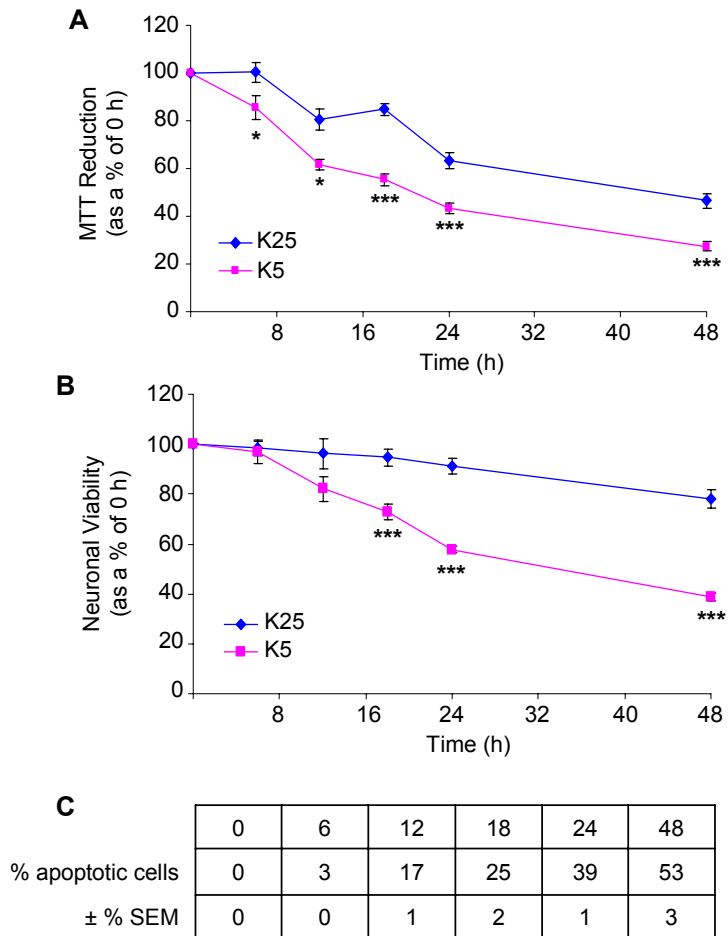


Figure 3.2.3. The time course of K⁺ withdrawal in CGNs . At DIV 7 CGNs were switched to K5 buffer and viability was assessed over time by the MTT assay (**A**) and H33342/SYTOX staining (**B**) at the indicated time, and expressed as a % of 0h. The percentage of apoptotic cells was also quantified from the H33342/SYTOX counts (**C**). Data expressed as mean ± % SEM from three independent cultures (n=3). * $p \leq 0.05$, ** $p \leq 0.01$, *** $p \leq 0.001$. The K⁺ withdrawal-induction of cell death is also a serum withdrawal challenge.

simultaneous withdrawal of serum from the cultures when the treatment medium (CSS25) was added.

There are some problems associated with the use of the MTT assay as a measure of viability. In addition to its reduction by mitochondrial enzymes, MTT has also been shown to be reduced by cytosolic and microsomal enzymes, which may give an enhanced view of the function of the mitochondria and the viability of the cells (Gonzalez and Tarloff, 2001). This does not seem to be a problem in this investigation as there was a decrease in the level of MTT reduction rather than an increase as would be expected if the cytosolic enzymes were contributing to the reduction. In addition, the reduction of MTT in the K25 and K5 neurons was significantly different at all time points (Figure 3.2.3 A). This indicates that the mitochondrial function in the K25 neurons was greater than that of the K5 neurons throughout the K⁺ withdrawal time course.

The nuclear features of apoptosis were not observed at 6 h in K5. The initial loss of viability in the K5 neurons was demonstrated by the nuclear stains H33342/SYTOX between 6 and 12 h (Figure 3.2.3 B). This was followed by a period of progressive decline in the viability of the neurons in K5. The loss of viability in the K25 neurons estimated by H33342/SYTOX was extremely small over the 48 h period and the difference in viability observed between the K5 and the K25 neurons was highly significant after 18 h (Figure 3.2.3 B). Furthermore there was a corresponding increase in the number of apoptotic cells as estimated using H33342/SYTOX staining (Figure 3.2.3 C). These results are consistent with those demonstrated by D'Mello *et al*, 1993.

The H33342/SYTOX measurements of neuronal viability were consistent with that observed by the MTT assay. However, the loss in viability of the CGNs assessed by H33342/SYTOX was observed at a later time point than that measured by the MTT assay. This is not surprising given that the mitochondrial role during the intrinsic pathway of apoptosis is upstream of apoptosome formation and activation of the effector caspases -3, -7 and -6. These enzymes are the executioners of the nuclear changes assessed using the nuclear stains H33342/SYTOX. The nuclear changes would therefore be observed at a later stage in the apoptotic process in comparison to the effects on the mitochondria as assessed using the MTT assay.

In order to investigate the possible caspase-3 mediated cleavage of the proteasomal subunits – S1, S6' and S5a during K⁺ withdrawal-induced cell death in CGNs it was first necessary to assess the activity of caspase-3/7. CGN lysates were prepared from

neurons at the indicated times of K⁺ withdrawal and the lysates were assayed for DEVDase activity. Due to the assay being repeated only twice, the results can only be considered a trend and were not statistically verified. The range of the results was therefore included to provide some indication of the variance.

The DEVDase activity of the K25 and K5 CGN lysates overlapped at 8 h of K⁺ deprivation (Figure 3.2.4, mean of 11 pmol/min/mg vs. 12 pmol/min/mg respectively), indicating low caspase-3/7 cleavage of the fluorogenic substrate, Ac-DEVD.AFC. There was a peak in the DEVDase activity of the K5 lysates at 16 h, and while the range of variance was large at this time, there was no observed overlap with that of the K25 lysates, suggesting that this time period is one of maximal caspase-3/7 activity. This is consistent with the significant loss of viability described in the K5 neurons when compared to those in K25 (Figure 3.2.3 B). A decrease in DEVDase activity was observed at 20 h, before further declining by 24 h in low K⁺ (Figure 3.2.4). The range in the activities between the K5 and K25 lysates at 20 h and 24 h again overlapped. The large range of variance observed for the DEVDase assay was the result of a delay in the repetition of the experiment. This resulted in the use of different aliquots of Ac-DEVD.AFC, and the lower overall enzymatic activity in both the K5 and K25 lysates when the experiment was performed for the second time.

Collectively these data indicate the initial activation of caspase-3 is between 6 h and 16 h in low K⁺ at which point active caspase-3 cleaves its substrates; mitochondrial effects occur prior to the activation of caspase-3 in K5 neurons.

3.2.4. The detection of the cleavage fragments of S1 and S6' correlate with the peak in caspase-3/7 activity.

In order to investigate the possibility of caspase-3-mediated cleavage of the proteasomal subunits – S1, S5a and S6', their processing by caspase-3 in this model was analysed. CGN lysates were prepared from neurons at the indicated times of K⁺ withdrawal and proteins resolved using Western blot analysis.

The processed form of caspase-3, detected using the antibody to the p17 cleaved from caspase-3 was evident by 8 h in low K⁺ (Figure 3.2.5, Lane 4), in agreement with the enzyme assay and immunofluorescence data. The cleaved (p17) form of caspase-3 was also observed at a very low level in the negative control CGN lysates (K25, 8 h, Lane 1), consistent with the slight increase in DEVDase activity (Figure 3.2.4). Further

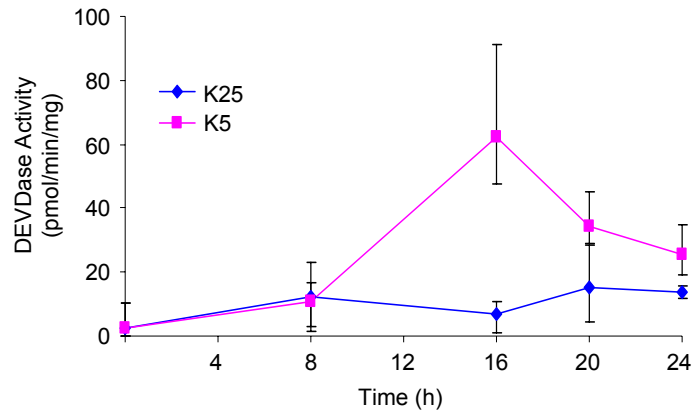


Figure 3.2.4. Caspase-3/7 activity peaks at 16 h in CGNs in low K⁺. CGNs were incubated in K5 for the indicated times and lysates prepared for DEVDase assay. Data expressed as mean in pmol/min/mg from two independent cultures \pm the range of variance.

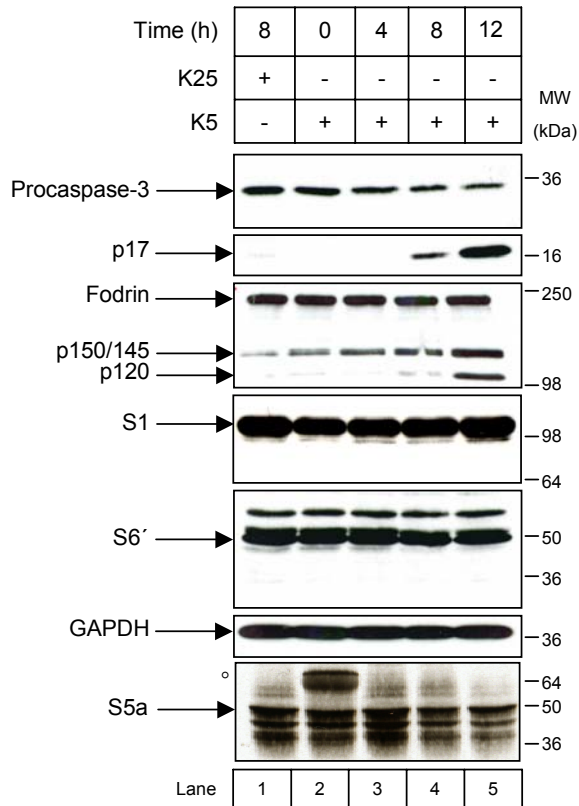


Figure 3.2.5. Active caspase-3 is evident at 8 h in low K⁺. CGNs (DIV7) were treated with K5, and lysed for immunoblot at the indicated times for procaspase-3, active caspase-3 (p17), α -fodrin, S1, S6', GAPDH and S5a. \circ denotes possible modified form of S5a as described in the text.

processing of caspase-3 was apparent at 12 h with the accumulation of the p17 form of the active enzyme (Lane 5). In addition, the initial processing of caspase-3 was shown by the reduction in the proform of caspase-3 by 4 h in low K⁺ compared with that of the CGN lysates at 0 h and negative control lysates (Figure 3.2.5, Lanes 3-5).

In order to evaluate whether the processing of caspase-3 resulted in an activated, functional enzyme that was itself capable of cleaving at recognised cleavage motifs, its ability to cleave α -fodrin was investigated. The 120 kDa caspase-3 cleavage fragment was evident in the CGN lysate at 8 h in low K⁺, with a progressive build-up of this degradation fragment at 12 h (Figure 3.2.5, Lanes 4-5). The same cleavage fragment was largely absent in the negative control lysate (K25, 8 h, Lane 1), and at the earlier time points (Lanes 2-3). The 150 kDa fragment gradually increased over time, indicating a build up of protein, probably due to caspase-3 cleavage. There was also some residual p150/145 in all CGN lysates, however, these sites in the protein are highly sensitive to protease cleavage (Nath *et al.*, 1996).

The proteasomal subunits S1, S6' and S5a identified by Sun *et al.*, 2004 as caspase-3 substrates, were unchanged in CGN lysates between 0 –12 h in low K⁺ when compared to the negative control CGN lysate (K25, 8 h). There were no changes in full-length protein and cleavage fragments were not detected at any time. Interestingly a band at approximately 70 kDa was consistently observed in the CGN lysates at 0 h, which was lost upon the incubation with K5 and K25. This has previously been suggested to be a post-translational modified form of S5a (Ram *et al.*, 2003). It is also important to note that the immunoblot for S5a in Figure 3.2.5 is representative of S5a during K⁺ withdrawal-induced cell death in CGNs but is not from the same experiment as the other immunoblots in the figure. A commercially available antibody was only recently developed for detection of S5a in murine cells.

Overall, these data indicate that the fragments are not observably cleaved by 12 h in CGN lysates; the subunits at later time points were therefore investigated. CGNs were exposed to K5 and lysates prepared at the indicated times for SDS-PAGE and immunoblot. The caspase-3 mediated cleaved form of S1 was observed at 16 h in K5 when compared to 0 h (Figure 3.2.6 A), correlating with the peak in caspase-3/7 activity demonstrated by the DEVDase activity assay. The cleaved form was also observed at 20 h in K5, but at 24 h the fragment was absent. In addition, the cleaved form of S6' was observed by 16 h in K5, however its detection was limited to overexposed immunoblots. The cleavage fragment observed for S6' seemed to correspond to that

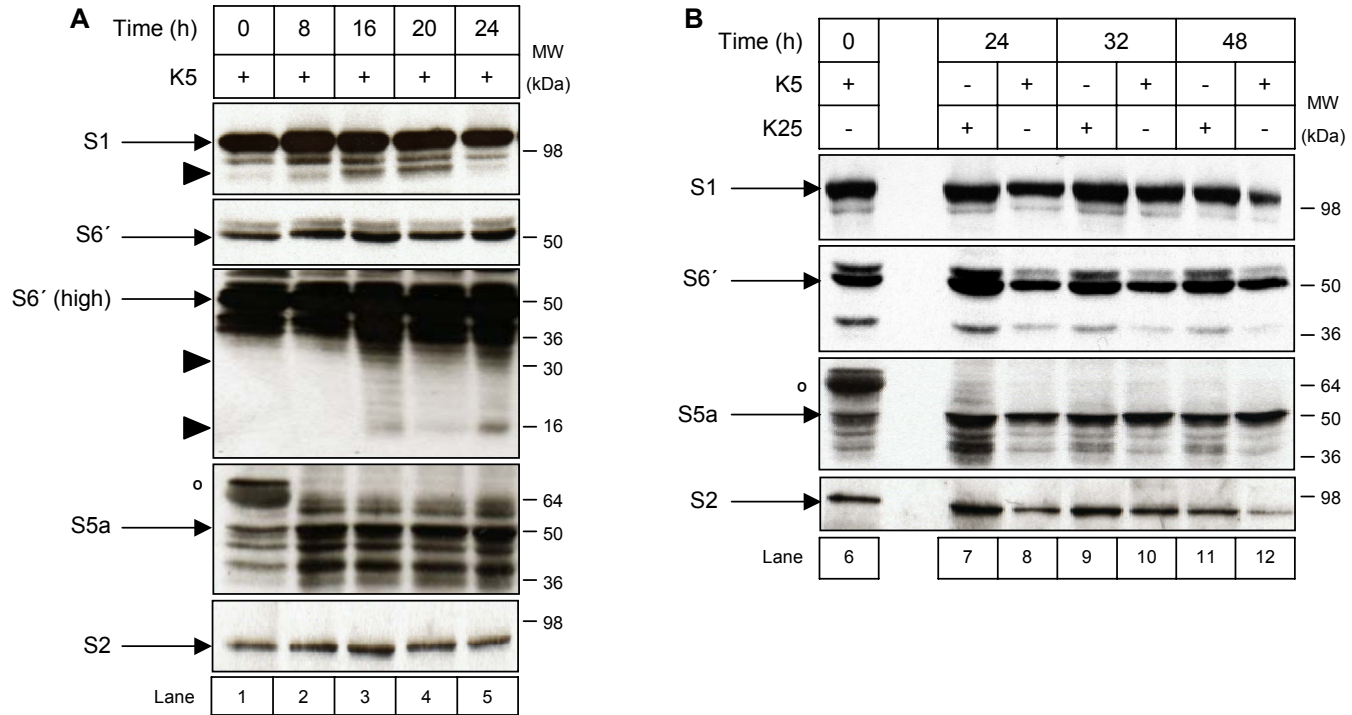


Figure 3.2.6. S1 and S6' are cleaved by 16 h in low K⁺. CGNs (DIV7) were treated with K5, and lysed for immunoblot for S1, S6', S5a and S2 at 0-24 h (A) or 0-48 h (B). ° denotes possible modified form of S5a. S1 (high) and S6' (high) indicate immunoblots that were exposed for more than 1 h. Arrowheads denote the cleavage fragments.

produced at 200-400 nM rCaspase-3 for 90 min in the *in vitro* cleavage assay (~32 kDa, Figure 3.2.2 D). In addition a possible cleavage fragment at approximately 16 kDa was also identified upon overexposure. There did not appear to be any cleavage of S5a. The 'modified' form of S5a was evident at 0 h and was again lost upon withdrawal of K⁺. Interestingly in the absence of the modified form of S5a, the full length form increased (compare Lanes 2-5 with 1, Figure 3.2.6 A), suggesting the reversal of modification upon exposure to the cell death stimulus. This was also evident in lysates prepared from K25 lysates (Figure 3.2.6 B, Lanes 7, 9 and 11), indicating that it is not a specific response to the cell death process.

In comparison with 0 h and their corresponding time controls (K25), there was a decrease in the full length forms of S1 and S6' at 24 h, 32 h and 48 h in K5 (Figure 3.2.6 B). In addition, the full length form of S2 also declined during this period, a trend not observed at the earlier time points (Figure 3.2.6 A). In contrast there was little change in the full length form of S5a after 0 h with the exception of the increase already discussed above. There were no cleavage fragments observed at any time point for any of the proteasomal subunits assessed.

Collectively these data suggest that the proteasomal subunits S1 and S6' are cleaved during K⁺ withdrawal-induced cell death in CGNs at a point when caspase-3/7 is at its most active.

3.2.5. The loss of 20S proteasomal activity is restored by caspase inhibitors.

Having established that the proteasomal subunits S1 and S6' are cleaved during cell death in CGNs, it was necessary to evaluate its consequence for proteasomal degradation. For this purpose CGNs were deprived of K⁺ and lysates were prepared for assay of the chymotrypsin-like activity of the 20S proteasome (LLVYase assay). As with the DEVDase assay, the results could not be verified by statistical analysis because the experiment had only been performed twice. The range in the activities was therefore included to provide an indication of the variance in the results.

There was an early peak in the LLVYase activity of the lysates from CGNs in K5 compared to CGNs in K25 at the same time point (Figure 3.2.7 A). This is consistent with the findings of Canu *et al*, 2000, in which an initial surge in LLVYase activity was demonstrated during K⁺ withdrawal-induced cell death (Canu *et al.*, 2000). It is possible that the preliminary increase in LLVYase activity is a response to the apoptotic signal to

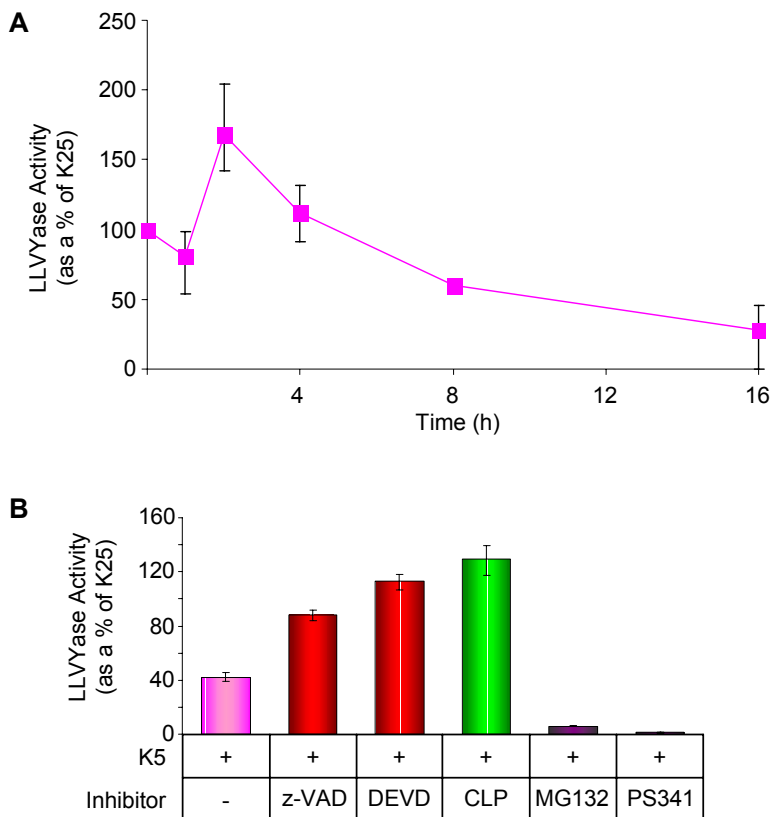


Figure 3.2.7. Protease inhibitors restore proteasomal activity lost after 8 h in low K⁺. CGNs (DIV7) were treated with K5 for the indicated times and lysed for LLVYase assay (as a % of K25 neurons at the same time) (A). Data is expressed as the mean from two independent cultures \pm the range of variance. CGNs were incubated with z-VAD.fmk (100 μ M), DEVD.fmk (50 μ M) or calpeptin (5 μ M; CLP) for 1 h prior to the withdrawal of K⁺. MG132 (5 μ M) and PS-341 (1 μ M) were added at the same time as K5. At 8 h, lysates were prepared and assayed for LLVYase activity (as a % of K25 neurons) (B). Data is expressed as the mean of the assay performed in triplicate from one CGN culture \pm the range of variance.

mediate the degradation of anti-apoptotic proteins, ensuring an unrestricted cell death. Alternatively, the rapid increase in proteasomal activity may be a defence against the early induction of reactive oxygen species (ROS) (Valencia and Moran, 2001); a corresponding upregulation in the proteasomal-regulated antioxidant activity has previously been described at 3 h in low K⁺ (Atlante *et al.*, 2003). This was followed by a progressive decline in activity between 4 and 16 h. In fact by 8 h in low K⁺ the activity of the CGN lysates had fallen below that of the resting constitutive activity of the 20S proteasome. The low range of variance observed indicates that the trend described above was consistent between the two cultures.

In an attempt to clarify whether the caspase-3 mediated cleavage of the proteasomal subunits S1 and S6' was responsible for the loss in 20S proteasomal activity, CGNs were incubated with z-VAD.fmk, DEVD.fmk and calpeptin for 1 h prior to the withdrawal of K⁺. Lysates were then prepared after 8 h in low K⁺ and assayed for LLVYase activity.

The loss of LLVYase activity demonstrated by the neurons in K5 was restored by z-VAD.fmk, a pan caspase inhibitor and DEVD.fmk, a proposed caspase-3/-7 inhibitor (Figure 3.2.7 B). Interestingly, calpeptin, a highly specific calpain inhibitor (Lee *et al.*, 2000) also enhanced the LLVYase activity lost during low K⁺ induced apoptosis. The complete loss of LLVYase activity was evident in K5 CGNs co-incubated with the proteasome inhibitors MG132 and PS-341 verifying the activity being measured was in fact proteasomal rather than that of another protease in the lysates. However, the data presented here is the mean of the assay performed in triplicate from only one CGN culture and therefore cannot be verified by statistical analysis. While the experiment was repeated with other CGN cultures and the caspase inhibitors, z-VAD.fmk and DEVD.fmk abrogated the loss of proteasome activity, problems with the control CGNs prevented their inclusion here. The range in the LLVYase activities was included to demonstrate the deviation in the results. There was little variation in the activities; however this was expected as the lysates were prepared from the same CGN culture. It is therefore essential to repeat this experiment with healthy CGN cultures to enable accurate conclusions to be made.

These data propose that proteasomal degradation has an early role in K⁺ withdrawal-induced apoptosis in CGNs, which is lost at a point when caspase-3 becomes active. There is also a suggestion that caspase inhibitors can restore the proteasomal LLVYase activity. It is therefore possible that that caspase-3/7 are responsible for the loss of activity at this time. However, as demonstrated previously, the subunit cleavage

fragments were not observed until 16 h (Figure 3.2.6 A). In previous experiments, the cleavage of S1 was detected at ~12 h when a pre-lysis centrifugation step was introduced to the lysis procedure, to assess the apoptotic cells that had detached from the wells during the cell death process (data not shown). This still suggests that the loss of proteasomal activity is upstream of the subunit cleavage, but that caspases contribute at least in part to the decline in function.

To confirm that the cleavage of the proteasomal subunits S1 and S6' during K⁺ withdrawal-induced cell death is caspase-dependent, CGNs were pre incubated with the above inhibitors and deprived of K⁺. Lysates were then prepared after 16 h for immunoblot. The loss of procaspase-3 was evident in the K5 CGNs alone and in combination with calpeptin when compared to the negative control (K25, Figure 3.2.8 compare Lanes 1 with 2 and 5). Both z-VAD.fmk and DEVD.fmk inhibited the cleavage of caspase-3 to its p17 active form as seen in the K5 CGN lysates and the lysates from CGNs incubated with K5 and calpeptin. Interestingly MG132 also seemed to partially protect against the loss of procaspase-3 and the p17 active form of caspase-3 when compared to the K5 lysates (Figure 3.2.8, Lanes 1 and 6).

Consistent with this, the cleavage of α -fodrin to its p120 form was detected in the lysates from K5 CGNs alone and in combination with calpeptin (Figure 3.2.8, Lanes 2 and 5). The p150 form was also present in the CGN lysates from CGNs treated with K5 and calpeptin, probably the result of caspase-3 cleavage, the p145 cleaved form being absent, verifying the inhibition of calpain by calpeptin. The caspase inhibitors zVAD and DEVD both prevented the cleavage of α -fodrin to the p120; the p150 form was also reduced by these inhibitors (Figure 3.2.8, Lanes 3 and 4), confirming caspase-3 was not active in these lysates. Interestingly, although there was some α -fodrin cleavage (p120) in the lysates prepared from CGNs exposed to a combination of low K⁺ and MG132, it was greatly reduced in comparison with those from CGNs in K5 alone. Furthermore the p145 cleaved form was also absent from these lysates (Figure 3.2.8, Lane 6 vs. 2).

S1 cleavage was clearly apparent in K5 alone CGN lysates (Figure 3.2.8, Lane 2). The cleavage fragment was also evident in lysates from CGNs treated with a combination of K5 and calpeptin and to a lesser extent MG132; detection in these lysates required overexposure of the film. Furthermore, overexposure of the film revealed the same cleavage fragment in lysates from K25 CGNs. This is not surprising given the low level of caspase-3 activation in K25 CGNs at this time point, shown by the active p17 form of

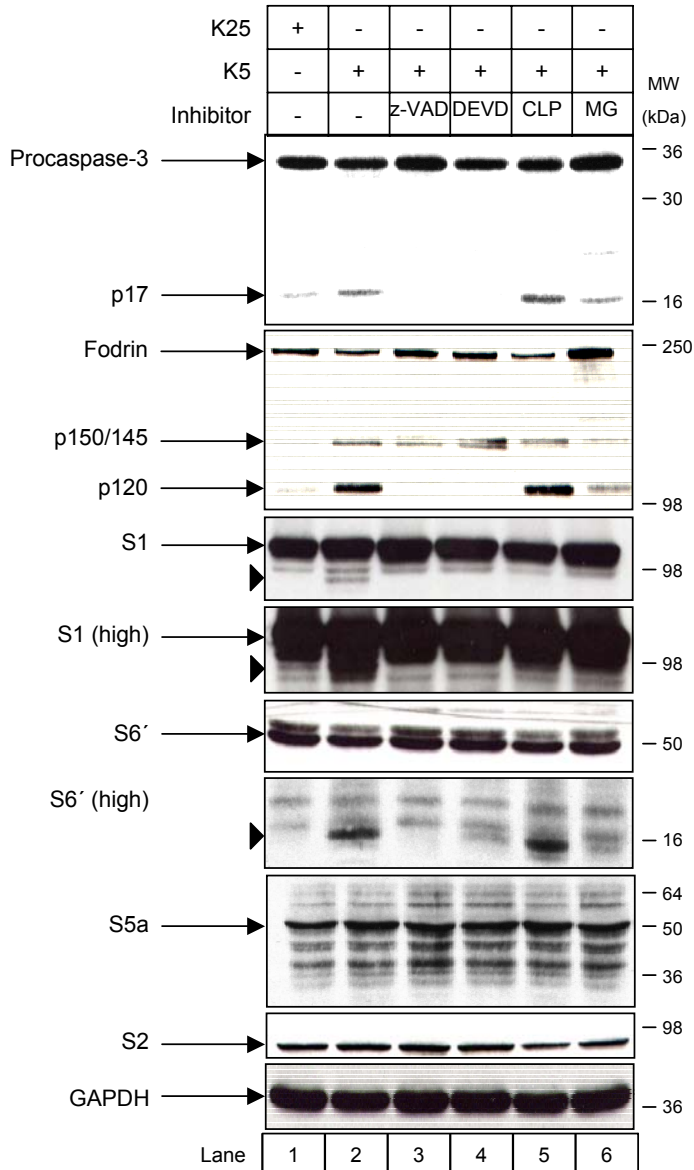


Figure 3.2.8. The S1/S6' cleavage fragments are lost in the presence of caspase inhibitors. CGNs (DIV7) were preincubated for 1 h with z-VAD.fmk (100 μ M), DEVD.fmk (50 μ M) or calpeptin (5 μ M; CLP), treated with K5 for 16 h, and lysates prepared for procaspase-3, α -fodrin, S1, S6', S5a, S2 and GAPDH immunoblots. MG132 (5 μ M; MG) was added at the same time as K5. S1 (high) and S6' (high) indicate immunoblots that were exposed for more than 1 h. Arrowheads denote the cleavage fragments.

caspase-3 and the small amount of p120 (α -fodrin) detected. The caspase inhibitors z-VAD.fmk and DEVD.fmk completely inhibited the cleavage of S1. The cleavage fragment of S6' at ~16 kDa, previously identified (Figure 3.2.6 A, Lanes 3-5) was the only fragment detected in Figure 3.2.8. This was evident in lysates prepared from K5 CGNs alone and in combination with calpeptin. There also seemed to be a slight loss in the full length form of S6' in the presence of these treatments. S5a and S2 remained unchanged after all treatments.

Collectively, these data support the suggestion that the cleavage of the proteasomal subunits in CGNs during K⁺ withdrawal-induced cell death is mediated by caspases.

3.2.6. The proteasome inhibitor MG132 delays the cell death stimulated by withdrawal of K⁺ in CGNs.

Having established that the pan caspase inhibitor z-VAD.fmk and the specific caspase-3/7 inhibitor, DEVD.fmk, prevented the cleavage of the proteasomal subunits S1 and S6', it was necessary to investigate the functional significance of the cleavage. CGNs were therefore incubated with the protease inhibitors prior to the withdrawal of K⁺ and cell death was assessed using the nuclear stains H33342/SYTOX and the MTT assay.

The caspase inhibitors z-VAD.fmk and DEVD.fmk slightly enhanced ability of the mitochondria to reduce MTT when compared with the CGNs in K5 alone. MG132 also offered partial protection against the loss of MTT reduction in response to withdrawal of K⁺, whereas another proteasome inhibitor, PS-341 had no effect (Figure 3.2.9 A). This is consistent with the immunoblots showing reduced levels of caspase-3 activation and subsequent α -fodrin and proteasomal subunit cleavage in K5 CGNs in the presence of MG132 (Figure 3.2.8, Lane 6). Statistical analysis was performed on the data in Figure 3.2.9 A, however the *p* values were greater than 0.05, and were therefore not considered significant.

In agreement, the simultaneous induction of apoptosis by the withdrawal of K⁺ and inhibition of the proteasome in CGNs has previously been demonstrated to reduce the normal levels of apoptotic cell death by low K⁺ in CGNs (Atlante *et al.*, 2003; Bobba *et al.*, 2002; Butts *et al.*, 2005; Canu *et al.*, 2000). This was hypothesised to be upstream of caspase-3 activation (Canu *et al.*, 2000) and prior to cytochrome c release from the mitochondria (Atlante *et al.*, 2003; Bobba *et al.*, 2002). It was later hypothesised that the stabilisation of MEF2 transcription factors by proteasome inhibitors accounted for

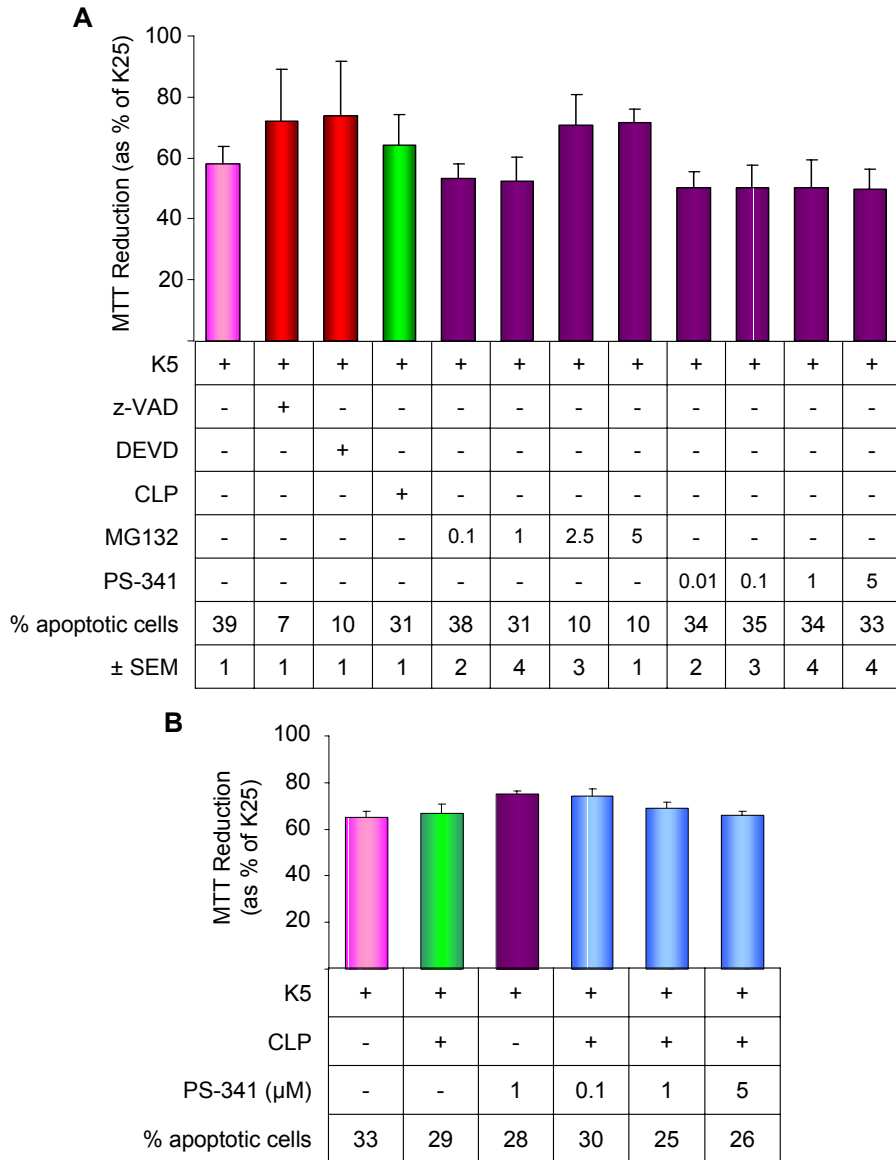


Figure 3.2.9. MG132 delays low K⁺ induced cell death in CGNs. CGNs (DIV7) were incubated with z-VAD.fmk (100 µM), DEVD.fmk (50 µM) and calpeptin (5 µM; CLP) for 1 h prior to treatment with K5 for 16 h. MG132 and PS-341 were simultaneously added with K5. Viability was assessed by the MTT assay (as a % of K25) and H33342/SYTOX (A). Data expressed as mean ± % SEM from three independent cultures. CGNs were incubated with calpeptin (5 µM, 1 h; CLP) prior to the withdrawal of K⁺. PS-341 was simultaneously added with K5 (B). The MTT assay was used to assess viability at 16 h (as a % of K25). Data expressed as mean ± % SEM from three independent cultures.

their pro-survival effects in K⁺ withdrawal-induced apoptosis in CGNs (Butts *et al.*, 2005). However, PS-341, a highly specific dipeptide boronic inhibitor of the proteasome (Adams *et al.*, 1998; Adams *et al.*, 1999) did not offer any protection against the loss of viability, indicating the effects of the two proteasome inhibitors are quite different in low K⁺ induced cell death. In agreement, the proteasome inhibitor, lactacystin, had no effect on the loss of viability observed in the K5 neurons at 24 h (data not shown). It was therefore necessary to establish the target of MG132 inhibition.

The p145 calpain mediated cleavage fragment of α -fodrin was greatly reduced upon treatment of CGNs with a combination of K5 and MG132 (Figure 3.2.8). In addition, MG132 was previously reported to inhibit calpains at high concentrations (Lee and Goldberg, 1998). Therefore, it was possible that the partial protection by MG132 was through inhibition of calpains. However, calpeptin had little effect on the ability of the mitochondria to reduce MTT. It was therefore proposed that the combined actions of a proteasome and calpain inhibitor may be responsible for the effects seen.

To assess this, CGNs were pre-incubated with calpeptin (where indicated), and cell death was induced by the withdrawal of K⁺. PS-341 was also simultaneously added to the K5 buffer. Viability and mode of cell death were measured at 16 h (Figure 3.2.9 B). The loss of the mitochondria's ability to reduce MTT did not alter in the K5 treated CGNs compared to K5 neurons with either calpeptin or PS-341 or both. Apoptotic cell levels also remained largely constant between treatments. It was therefore concluded that the partial protection from cell death was not due to the combined actions of MG132 on the proteasome and calpain systems.

Taken together these data suggest that by 24 h, inhibition of the cleavage of the proteasomal subunits does not greatly reduce the level of cell death induced through the withdrawal of K⁺ in CGNs. Furthermore, the delay in cell death through the actions of MG132 is an effect additional to its role as a proteasome and calpain inhibitor.

3.2.7. The induction of autophagy is an early event in K⁺ withdrawal in CGNs.

The proliferation of the autophagosomal-lysosomal compartments prior to the activation of caspases following serum and K⁺ deprivation in CGNs was previously demonstrated by Canu *et al.*, 2005. The induction of the autophagic process was also reported by Kaasik *et al.* in the same year. The potential induction of autophagy by the simultaneous withdrawal of K⁺ and serum in CGNs is unsurprising given the numerous

reports regarding autophagy as a survival mechanism particularly in times of nutrient deprivation (Boya *et al.*, 2005; Kang *et al.*, 2007; Kuma *et al.*, 2004; Lum *et al.*, 2005). Furthermore, autophagy was also shown to be activated in response to apoptotic signals including nerve growth factor (NGF) withdrawal, in isolated cultured sympathetic neurons (SCGs). The formation of autophagosomes was demonstrated upstream of the morphological features of apoptosis and the autophagy inhibitor 3-MA blocked apoptotic cell death of the SCG neurons (Xue *et al.*, 1999).

To assess the induction of autophagy in CGNs after the deprivation of K⁺/serum, lysates from neurons that had been subjected to K5 in the presence of protease inhibitors were run on immunoblot and probed with an antibody for anti-LC3. The conversion of LC3-I (the active cytosolic form, with the exposed Gly) to LC3-II (membrane associated, lipidated form) can be assessed using SDS-PAGE. Immunoblotting of LC3 gives two bands representing LC3-I at ~18 kDa and LC3-II at ~16 kDa (Bampton *et al.*, 2005; Kabeya *et al.*, 2000; Mizushima, 2004).

LC3-II was demonstrated in the lysates from K5 CGNs in the presence of the caspase inhibitors z-VAD.fmk and DEVD.fmk (Figure 3.2.10 A). This is consistent with that demonstrated by Xue *et al.*, 1999 who reported high levels of autophagic activity in newly isolated SCG neurons grown in the absence of NGF with BAF, a pan-caspase inhibitor, which was accompanied by the widespread elimination of mitochondria (Xue *et al.*, 1999; Xue *et al.*, 2001). Furthermore, at an earlier point in the cell death process LC3-II was further enhanced upon addition of Bafilomycin A1 (Figure 3.2.10 B), an inhibitor of the vacuolar-type H(+)-ATPase, which prevents the acidification of the lysosomes (Yamamoto *et al.*, 1998; Yoshimori *et al.*, 1991).

Collectively these data further indicate the possible induction of autophagy during the initial stages of K⁺/serum withdrawal induced cell death in CGNs consistent with that previously reported (Canu *et al.*, 2005; Kaasik *et al.*, 2005). This requires further confirmation as the increase in LC3-II in the presence of caspase inhibitors may be the result of a reduction its degradation in the lysosomes by z-VAD-inhibited cathepsins. However, taken with the failure of the caspase inhibitors to prevent the cell death induced by K⁺/serum withdrawal, it suggests that the autophagic response may contribute to the death of the neurons when the activation of caspases is inhibited.

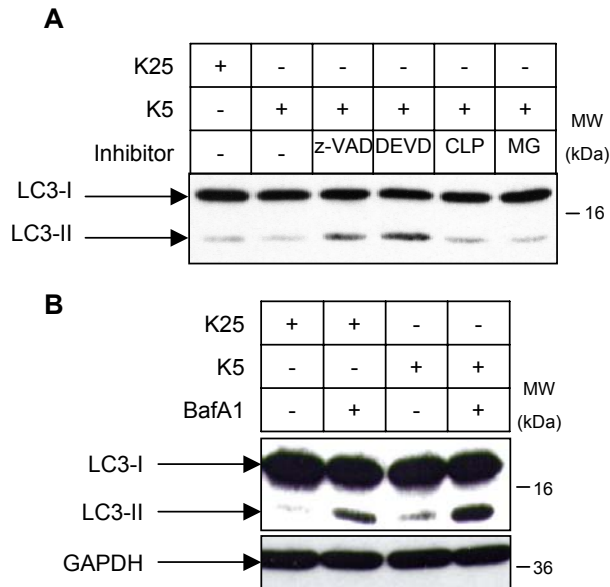


Figure 3.2.10. There is evidence of autophagy during the early stages of K⁺ withdrawal cell death in CGNs. CGNs (DIV7) were preincubated for 1 h with z-VAD.fmk (100 μ M), DEVD.fmk (50 μ M) or calpeptin (5 μ M; CLP), treated with K5 for 16 h, and lysates prepared for LC3 immunoblots (**A**). MG132 (5 μ M; MG) was added at the same time as K5. CGNs (DIV7) were treated with K5 (or K25) in the presence of Bafilomycin A1 (100 nM; BafA1) for 4 h. Lysates were prepared and immunoblotted for LC3 and GAPDH (**B**).

3.2.8. The construction of a proteasome sensor for single cell analysis of proteasomal degradation and its *in vitro* characterisation.

Earlier in this chapter the partial caspase-dependent loss of proteasome activity was demonstrated. To overcome the problems experienced with the LLVYase assay and to ascertain the contribution of the active caspases to the loss of proteasome activity on a single cell level, a proteasome sensor was constructed to detect changes for real time analysis.

Fluorescent probes, developed over the past few years by various groups can behave as substrates for the UPS under steady state conditions (Neefjes and Dantuma, 2004). The sequential attachment of ubiquitin moieties to internal lysine residues in the protein structure by ubiquitination enzymes act as degradation signals. These are then recognised by the 26S proteasome and the protein substrates tagged for degradation are unfolded and threaded into the 20S core (Hol *et al.*, 2006). Many of the fluorescent probes for assessment of proteasomal activity are based on ubiquitin-fusion degradation signals (Johnson *et al.*, 1995). An N-terminal ubiquitin moiety that is fused to green fluorescent protein (GFP) for example, acts as an acceptor for the sequential addition of further ubiquitin molecules, forming a polyubiquitin chain (Neefjes and Dantuma, 2004). The construction of sensors with multiple copies of ubiquitin further accelerate the turnover of the protein (Stack *et al.*, 2000; Zhu *et al.*, 2005).

The proteasome sensor was achieved by fusing tandem copies of mutant ubiquitin (G76V) that limit cleavage by ubiquitin hydrolases (deubiquitinating enzymes) (Luker *et al.*, 2003) to the N-terminus of EYFP, a derivative of GFP. The EYFP sensor can be used to image the proteasomal activity in the cell. GFP and its variants are very stable proteins in their native conformation and the formation of their chromophore does not require additional proteins or cofactors, making them ideal proteins for monitoring proteasomal activity (Menendez-Benito *et al.*, 2005). In addition, for characterisation purposes a construct was prepared that possessed multiple copies of wild type ubiquitin. A schematic representation of all constructs used for the *in vitro* characterisation of the proteasome sensor is shown in Figure 3.2.11.

Initially it was required to assess the ability of the constructs to undergo further ubiquitination and proteasomal degradation. The constructs were therefore expressed in a nonradioactive transcription-translation (TNT) system in rabbit reticulocyte lysates. The components of both the ubiquitination process and degradation by the proteasome

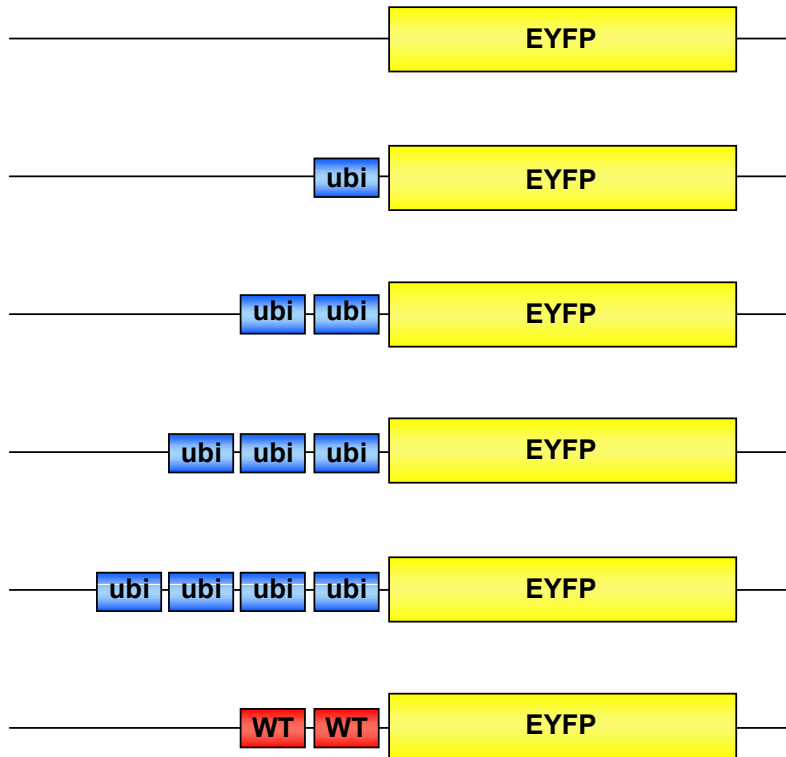


Figure 3.2.11. Schematic representation of the multi-ubiquitinated sensors prepared. ubi=G76V ubiquitin, WT=WT ubiquitin.

were collectively discovered and described in rabbit reticulocyte lysates (Ciechanover *et al.*, 1980; Etlinger and Goldberg, 1977; Hershko *et al.*, 1979). This is therefore an ideal system in which to characterise proteasomal substrates *in vitro*. For this purpose TNT reaction reactions were prepared in the presence of Transcend tRNA, immunoblotted and detected using Strep-HRP.

The expression of EYFP alone in the *in vitro* system produced a single band that resolved at the predicted molecular weight from the protein sequence of EYFP (Figure 3.2.12 A). The sensor with the addition of one G76V ubiquitin moiety resolved at a slightly higher molecular weight (compared to EYFP alone). Interestingly the multi-ubiquitinated EYFP sensors demonstrated several species of higher molecular weight on immunoblot, in a manner reminiscent of substrates in various degrees of ubiquitination, consistent with that demonstrated by Stack *et al.*, 2000. In fact, only higher order ubiquitinated complexes were evident on immunoblot when p4xubi(G76V)-EYFP was expressed in the TNT system. The number of ubiquitin moieties that are linked to the substrate is thought to be an effective determinant of efficiency for degradation by the proteasome, with four ubiquitin moieties being optimal (Thrower *et al.*, 2000). The expression of the multi-ubiquitinated constructs in this manner is thought to represent the constitutive process of ubiquitination and proteasomal degradation in the rabbit reticulocyte lysates. In accordance, the addition of the proteasome inhibitor MG132 to the TNT reaction for p4xubi(G76V)-EYFP prevented the degradation of multiple species on the immunoblot that were consistent with 1xubi(G76V)-EYFP, 2xubi(G76V)-EYFP and 3xubi(G76V)-EYFP (Figure 3.2.12 B).

Based on its predicted molecular weight, the resolution of p2xubi(WT)-EYFP should have been analogous with p2xubi(G76V)-EYFP. It resolved at the same point as EYFP however, without evidence of further ubiquitination (Figure 3.2.12 A). This is consistent with removal of the ubiquitin moieties from the sensor by deubiquitinating enzymes already present in the rabbit reticulocyte lysates (Hershko *et al.*, 1980; Pickart and Rose, 1985b). To further demonstrate that the mutation G76V in ubiquitin prevents cleavage by deubiquitinating enzymes, the TNT reactions for p2xubi(G76V)-EYFP and p2xubi(WT)-EYFP were prepared in the presence of ubiquitin aldehyde, a DUBs inhibitor (Hershko and Rose, 1987). Samples were then run on an immunoblot.

p2xubi(G76V)-EYFP resolved on the immunoblot at a point as shown previously (Figure 3.2.12 C and A respectively), with a higher molecular weight species above the full length form, representative of the tri-ubiquitinated protein. The presence of ubiquitin

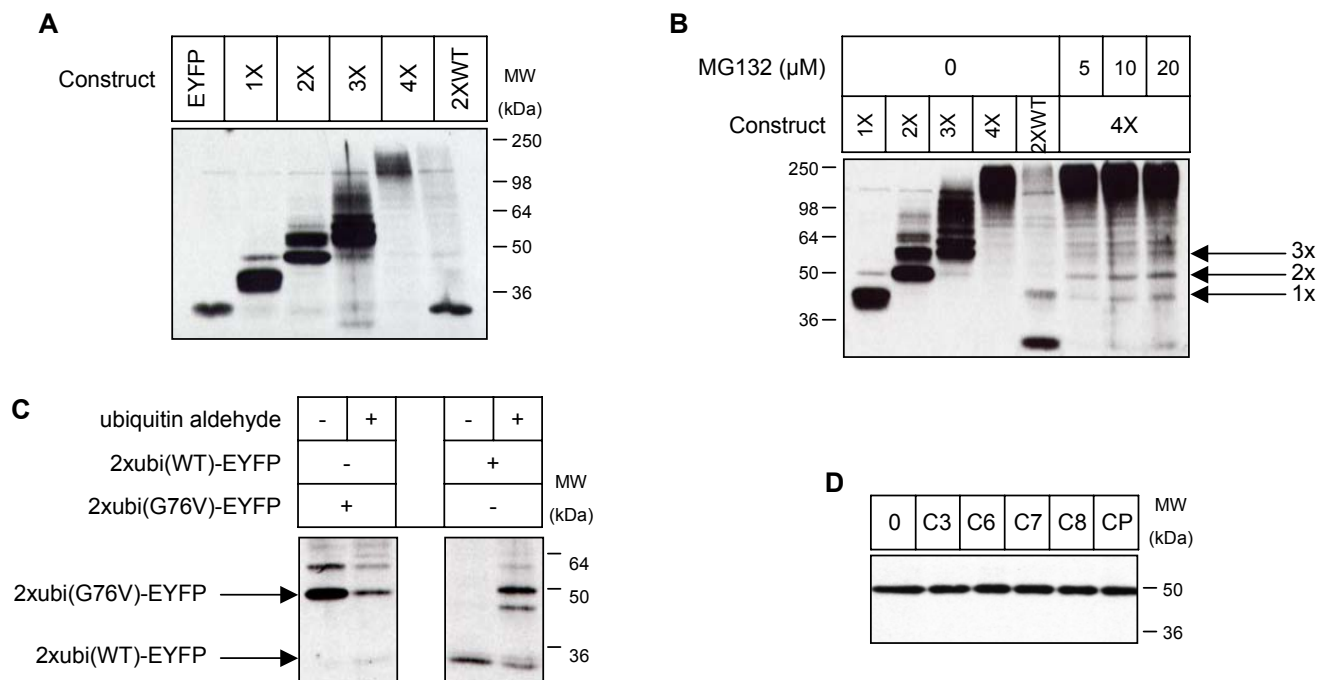


Figure 3.2.12. The *in vitro* characterisation of constructed proteasome sensors. pEYFP (EYFP), p1xubi(G76V)-EYFP (1X), p2xubi(G76V)-EYFP (2X), p3xubi(G76V)-EYFP (3X), p4xubi(G76V)-EYFP (4X) or p2xubi(WT)-EYFP (2XWT) were expressed in the *in vitro* TNT system in the presence of Transcend™ tRNA at 30 °C for 60 min, after which samples were taken and immunoblotted using Strep-HRP (**A**). The TNT reactions were repeated with p4xubi(G76V)-EYFP expressed in the presence of MG132 (5-20 μ M; **B**). p2xubi(G76V)-EYFP and p2xubi(WT)-EYFP were expressed as described previously in the presence of ubiquitin aldehyde (5 μ M). Aliquots were run on immunoblot and detected with Strep-HRP (**C**). Samples of the p2xubi(G76V)-EYFP TNT reaction were incubated with recombinant active caspase-3 (C3), -6 (C6), -7 (C7), -8 (C8) and calpain-1 (CP; in the presence of 20 mM Ca^{2+}) for 60 min at 37 °C. Aliquots were then immunoblotted using Strep-HRP.

aldehyde had no effect on the resolution of the expressed construct. In contrast, p2xubi(WT)-EYFP resolved at a lower molecular weight equivalent to that of EYFP alone. The addition of ubiquitin aldehyde to the TNT reaction almost completely reversed the cleavage by the DUBs; the resultant protein being comparable in molecular weight to that of p2xubi(G76V)-EYFP.

Given that the proteasome sensor would be required to be expressed in CGNs during K⁺ withdrawal-induced cell death, it was necessary to ensure that cell death proteases would not cleave the sensor and contribute to its accumulation. The TNT reaction for p2xubi(G76V)-EYFP was therefore incubated with recombinant caspase-3, -6, -7, -8 and calpain 1 (in the presence of Ca²⁺) for 1 h at 37 °C. p2xubi(G76V)-EYFP was completely untouched by all the recombinant proteases (Figure 3.2.12 D) Taken together, these data verify the use of the constructs as proteasome sensors and their ability to be used in cell death settings.

3.2.9. The characterisation of the proteasome sensor constructs in SH-SY5Y cells.

Prior to the use of the proteasome sensors in CGNs it was necessary to characterise their expression in a cell culture model. For this purpose the neuroblastoma cell line, SH-SY5Y was used. To ensure that the constructs were able to be expressed in mammalian cells, SH-SY5Y cells were transiently transfected with each construct; lysates were prepared and resolved on immunoblot. Detection was performed using an anti-GFP antibody. The expression of the constructs and their resolution was consistent with that demonstrated in the rabbit reticulocyte lysates during the *in vitro* characterisation (Figure 3.2.13 A). pEYFP and p2xubi(WT)-EYFP were comparable in molecular weight indicating that DUBs were actively removing the ubiquitin moieties, resulting in EYFP alone. The molecular weight of the G76V ubiquitin sensors sequentially increased according to the number of ubiquitin moieties. The expression of p4xubi(G76V)-EYFP was below the level of detection by immunoblot due to its low overall transfection efficiency and probably its degradation by the proteasome.

To demonstrate the degradation of the constructs in cultured cells, SH-SY5Y cells were transiently transfected with each construct. The protein synthesis inhibitor cycloheximide was then added to the culture medium for the indicated times, and EYFP expression was measured using FACS analysis.

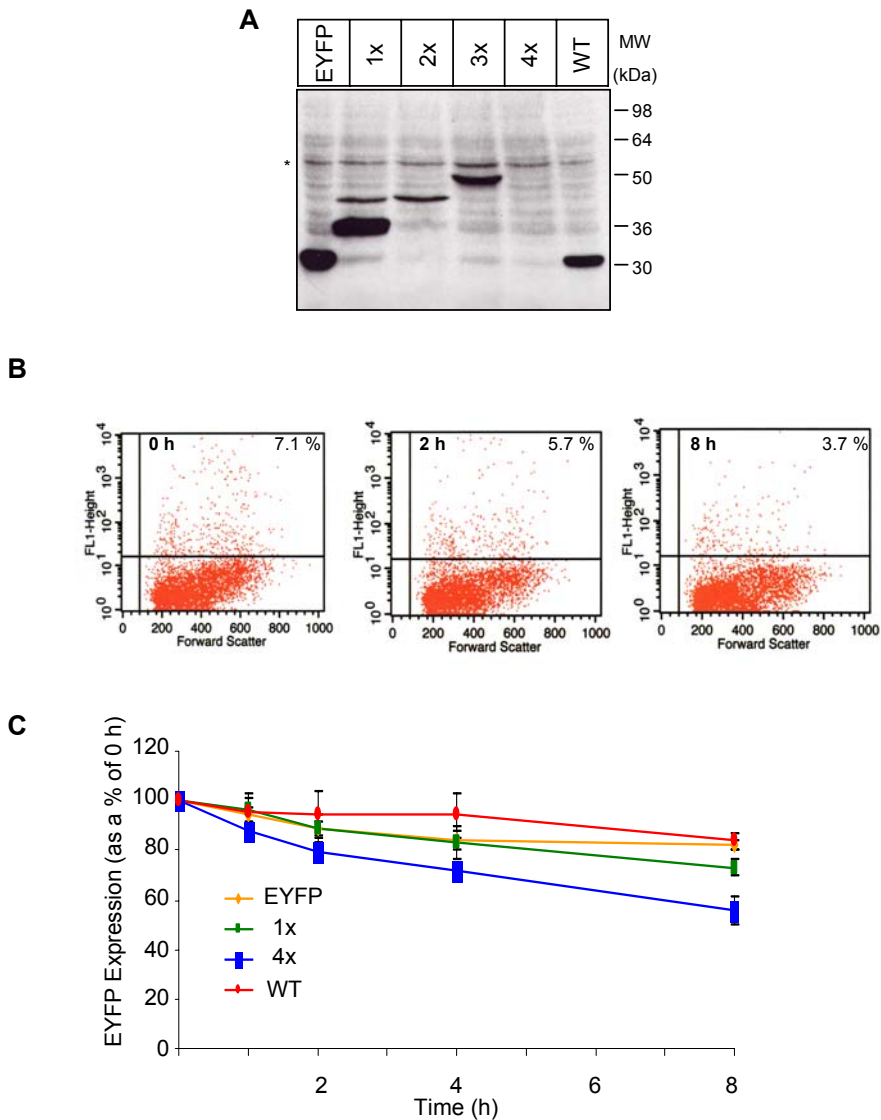


Figure 3.2.13. The characterisation of the proteasome sensors in SH-SY5Y cells. SH-SY5Y cells were transfected with pEYFP, p1xubi(G76V)-EYFP, p2xubi(G76V)-EYFP, p3xubi(G76V)-EYFP, p4xubi(G76V)-EYFP or p2xubi(WT)-EYFP. After 16 h, (A) cells were lysed and immunoblotted for GFP or (C) treated with cycloheximide (10 μ M) for the indicated times. EYFP expression (as a % of 0 h) was assessed using FACS analysis (representative panels for 4xubi(G76V)-EYFP (B)). Data expressed as mean \pm % SEM (n=3). * indicates a non-specific band

There was minimal change in the level of EYFP expression in the SH-SY5Y transfected with pEYFP and p2xubi(WT)-EYFP over the 8 h time period (Figure 3.2.13 C). Similarly the change in EYFP expression was low for p1xubi(G76V)-EYFP until 4 h in the presence of cycloheximide, when there was a slightly greater loss in EYFP expression (compared to pEYFP/p2xubi(WT)-EYFP, Figure 3.2.13 B and C). There was a much greater loss in the expression of EYFP in the SH-SY5Y cells transfected with p4xubi(G76V)-EYFP.

If the sensor was a *bona fide* proteasome sensor, an increase in the level of EYFP would be expected in the presence of proteasomal inhibition. Therefore, SH-SY5Y cells were transiently transfected with each construct and treated with the proteasome inhibitor PS-341 for 8 h. EYFP expression was quantified using FACS analysis. The inhibition of the proteasome by PS-341 was initially ensured by treating untransfected SH-SY5Y cells with PS-341 for 8 h and preparing lysates for an LLVYase assay. The complete inhibition of the 20 S proteasome in SH-SY5Y cells was observed at all concentrations (Figure 3.2.14 A). Treatment of the SH-SY5Y cells transfected with pEYFP and p2xubi(WT)-EYFP with PS-341 had no effect on the EYFP expression (Figure 3.2.14 B). There was a marked increase in the level of EYFP at all concentrations of PS-341 in the SH-SY5Ys expressing p1xubi(G76V)-EYFP and p4xubi(G76V)-EYFP (compared to 0 nM PS-341). This was not dependent on the concentration of PS-341 for p4xubi(G76V)-EYFP as it seemed to reach maximal EYFP expression at 10 nM PS-341, the lowest concentration of the inhibitor used in the study.

To demonstrate that the enhanced EYFP expression is the result of the specific inhibition of the proteasome, inhibitors of cell death proteases and an autophagy inhibitor Bafilomycin A1 (BafA1) were introduced. After transient transfection of SH-SY5Y cells with p4xubi(G76V)-EYFP, the indicated inhibitors were added to the culture medium for 8 h, and EYFP expression was analysed. Consistently PS-341 and the additional, less specific proteasome inhibitor MG132 markedly enhanced the expression of EYFP compared to vehicle control SH-SY5Y (Figure 3.2.14 C). In contrast, inhibitors of caspases, calpain and autophagy had no effect. Furthermore, the simultaneous treatment of SH-SY5Y cells expressing p4xubi(G76V)-EYFP with PS-341 and each of the additional inhibitors increased the level of EYFP.

The purpose for the design of the proteasome sensor was to overexpress in CGNs and assess the proteasomal activity during K⁺ withdrawal-induced cell death on a single cell

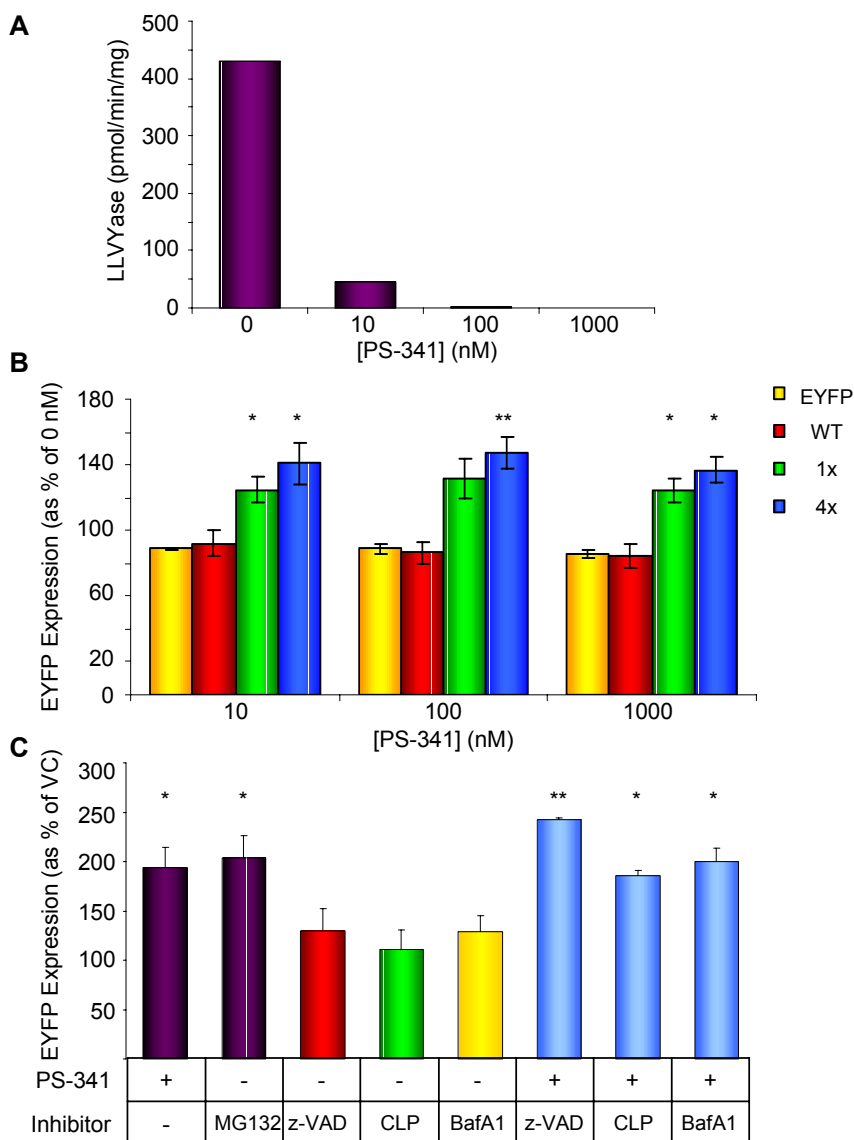


Figure 3.2.14. Proteasome inhibitors cause the accumulation of EYFP in SH-SY5Y cells, confirming their use as a proteasome sensor. SH-SY5Y cells were treated with PS-341 for 8 h. Lysates were then prepared for LLVYase activity (pmol/min/mg) (A). SH-SY5Y cells were transfected with pEYFP, p1xubi(G76V)-EYFP, p2xubi(G76V)-EYFP, p3xubi(G76V)-EYFP, p4xubi(G76V)-EYFP or p2xubi(WT)-EYFP. (B) After 16 h, cells were treated with PS-341 for 8 h, and prepared for FACS analysis (EYFP expression as a % of 0 nM). Data expressed as mean \pm SEM (n=3). * $p \leq 0.05$, ** $p \leq 0.01$. (C) After 16 h, cells were treated with PS-341 (10 nM), MG132 (5 μ M), z-VAD.fmk (100 μ M), calpeptin (5 μ M; CLP), Bafilomycin A1 (100 nM; BafA1) or a combination for 8 h. EYFP expression (as a % of 0 nM) was assessed using FACS analysis. Data expressed as mean \pm % SEM (n=3). * $p \leq 0.05$, ** $p \leq 0.01$.

level. Unfortunately, the transfection efficiency of pEYFP in CGNs was extremely low at approximately 8% and was completely undetectable for p4xubi(G76V)-EYFP.

3.3. Discussion

The induction of apoptosis by K⁺ withdrawal in CGNs is an extensively studied model of neuronal cell death. It is likely that regulation of the cell death process involves multiple biochemically distinct factors that are simultaneously activated and are functionally cooperative (O'Hare *et al.*, 2000). Low K⁺ induced cell death in CGNs is dependent on *de novo* RNA and protein synthesis, caspases and reactive oxygen species (D'Mello *et al.*, 1993; Schulz *et al.*, 1996; Taylor *et al.*, 1997).

The apoptotic pathway also has an absolute requirement for the activation of Bax as shown by the studies in CGNs from Bax^{-/-} mice (Miller *et al.*, 1997). It has been proposed that Bax is activated by GSK-3 β by phosphorylation at Ser-163. This results in its conformational change and translocation to the mitochondria, where it mediates the release of cytochrome c (Brewster *et al.*, 2006; Linseman *et al.*, 2004; McGinnis *et al.*, 1999), formation of the apoptosome and caspase-9 activation (Gerhardt *et al.*, 2001). Caspase-9 is then capable of activating the effector caspases, of which caspase-3 is particularly relevant to this investigation.

In addition, the release of cytochrome c also seems to require the upregulation of the BH3-only protein Bim (and Dp5/Hrk); for which there appears to be multiple pathways for its induction during K⁺ withdrawal apoptosis in CGNs (Desagher *et al.*, 2005; Linseman *et al.*, 2002; Putcha *et al.*, 2002; Shi *et al.*, 2005). The mitogen-activated protein kinase (MAPK) kinase induced activation of JNK2/3 and /or Egr-1, and the proceeding activation of c-jun is in part responsible for the induction of Bim/Dp5 (Coffey *et al.*, 2002; Levkovitz and Baraban, 2001; Trotter *et al.*, 2002; Watson *et al.*, 1998). The forkhead transcription factor FKHRL1 may play an additional role in the induction of Bim; its upregulation may also be an outcome of the release of the transcription factor E2F-1 (O'Hare *et al.*, 2000; Padmanabhan *et al.*, 1999; Zhao *et al.*, 2005).

In this investigation, the activation of caspase-3 (p17 processed, mature form) was initially evident at approximately 8 h in low K⁺. Maximal DEVDase activity was noted at 16 h after K⁺ withdrawal, which corresponded to further processing of caspase-3 and increased accumulation of the p17 fragment. It is widely acknowledged that effector caspases share overlapping substrate specificity enabling the substitution of one for another in systems where there is a redundancy (Talanian *et al.*, 1997); the DEVDase assay is an example of this, being additionally cleaved by caspase-7 during apoptosis.

However, the cleavage of α -fodrin to its apoptotic p120 fragment is specific for caspase-3 (Slee *et al.*, 2001). The ability of active caspase-3 to cleave its substrates in CGNs was therefore confirmed by the related cleavage of α -fodrin, resulting in the caspase-3 mediated 120 KDa fragment accumulating as apoptosis progressed. In combination with the DEVDase assay data, the activity of caspase-3 in CGNs after K⁺-withdrawal induced apoptosis was confirmed.

The observed cleavage of the proteasomal subunits, S1 and S6' corresponded with the peak in caspase-3 activity at 16 h in low K⁺. The presence of the non-selective caspase inhibitor z-VAD.fmk and the caspase-3/7 inhibitor, DEVD.fmk abrogated the cleavage fragments detected by immunoblot. Cleavage of the additional proteasome subunits, S5a and S2 was not apparent at any time.

As described previously in the Introduction, the 26S proteasome is composed of two subcomplexes – the 20S core particle and the 19S regulatory particle. S1 and S6' (and S5a/S2) are components of the 19S complex. S1 (also known as Rpn2) and S2 (Rpn1) were previously demonstrated to interact with the adapter proteins, Rad23 and Dsk2 via their ubiquitin-like domains during the delivery of polyubiquitinated substrates for degradation in *Saccharomyces cerevisiae* (Saeki *et al.*, 2002), leading to the suggestion that S1 and S2 form a receptor for ubiquitin-like proteins. Furthermore, in HEK293T cells S1 was shown to interact with Adrm1, which recruits the deubiquitinating enzyme UCH37 and was found partially responsible for the deubiquitinating activity of the proteasome (Hamazaki *et al.*, 2006). Recently in *Saccharomyces cerevisiae*, S1 was demonstrated to attach directly to the outer α -ring surface of the 20S core particle with S2 placed distally to S1. The six ATPases (including Rpt5a or S6') were demonstrated in a peripheral position, forming a ring around the inner S1-S2 stack. In this model S1 and S2 were hypothesised to facilitate the entry of small substrates into the 20S core, by regulating the channel gating. In addition, Rad23 was recruited to the proteasome by S2 rather than the previously identified S1 (Rosenzweig *et al.*, 2008).

In addition to its role as an ATPase, S6' (Rpt5) has been implicated in the regulation of the gate opening into the 20S core of the proteasome (Smith *et al.*, 2007). S6' has also specifically been shown to play a role in the recognition of the polyubiquitin chain that tag the substrate for degradation (Lam *et al.*, 2002), although other groups favour the hypothesis that S6' gathers substrates that are delivered to the proteasome by other recognition pathways (such as Rpn10 (S5a) or Rad23). Its function here would be to

position the substrates for unfolding and deubiquitination prior to entry into the catalytic chamber (Verma *et al.*, 2004). The interaction of S6' with the E3 ligase, RNF2 has also been described, binding of which is linked to enhanced ATP hydrolysis of the proteasome (Lee *et al.*, 2005).

It would seem that S1 would be inaccessible to cleavage by caspase-3 if the structural studies described by Rosenzweig *et al.*, 2008 are to be accepted. However, the authors do not exclude the possibility that S1 may have regions that are exposed beyond the ATPase ring (Rosenzweig *et al.*, 2008). Upon ATP hydrolysis the carboxy termini of S6' becomes buried in pockets formed by the outer α -ring of the 20S core. This stimulates the opening of the gate that limits substrate entry into the channel (Smith *et al.*, 2007). The caspase-3 cleavage site identified by Sun *et al.*, 2004 after Asp-27 however would be exposed and accessible for cleavage by caspase-3 (Sun *et al.*, 2004).

From the evidence detailed above, it would seem that cleavage of the proteasome subunits by caspase-3 would be predicted to have deleterious effects on the ability of the 26S proteasome to mediate ubiquitin-dependent protein degradation. The loss of the LLVYase activity associated with the proteasome was markedly reduced at a time when active caspase-3 was first detected. The addition of caspase inhibitors negated the loss of proteasomal activity; however, as previously discussed, conclusions cannot be drawn from this as the experiment requires repetition, although this result was also demonstrated by Canu *et al.*, 2000 (Canu *et al.*, 2000). In addition, the LLVYase assay is not only a measure of 20S proteasome activity, it is also used for the measurement of calpain activity (Giguere and Schnellmann, 2008; Seidah *et al.*, 2003), and proved problematic in this study. Furthermore, the other proteasome activities were not assayed; therefore conclusions cannot be made regarding the overall proteasome function. The multiubiquitinated fluorescent sensor – p4xubi(G76V)-EYFP would have provided a more accurate method for the assessment of proteasome activity. It is possible that caspases contribute at least in part to the loss of proteasome function.

The cleavage pattern of S6', demonstrated for caspase-3 cleavage by Sun *et al.*, 2004 was markedly different from that observed in CGNs during K⁺ withdrawal-induced cell death. In fact the cleavage of S6' produced during cell death in CGNs was also different to that observed during the *in vitro* cleavage by recombinant active caspase-3. It is possible that an alternate caspase cleaves S6' rather than caspase-3 when the CGNs are undergoing cell death, particularly if the initial cleavage site is occluded by,

for example proteasome associated proteins. Caspase-8 is a possible candidate, given that Sun and colleagues previously described its additional cleavage of S6' (Sun *et al.*, 2004). The K⁺ withdrawal-induced model of cell death in CGNs follows the intrinsic pathway of apoptosis; caspase-3 may therefore be responsible for the cleavage and activation of caspase-8 (Gerhardt *et al.*, 2001). It would still ultimately be accountable for the loss of proteasomal function. The cleavage of S6' by caspase-8 may be of particular importance during receptor-mediated apoptosis, because it would occur early in the apoptotic pathway as opposed to 'past the point of no return' as with caspase-3. It is also possible that the inconsistent cleavage of S6' is due to the use of human recombinant caspase-3 in murine CGN lysates. Species differences are known to exist for certain caspases, such as the role of caspase-12 in inflammation and ER stress-induced apoptosis in humans and mice respectively, however information regarding caspase-3 is limited.

K⁺ withdrawal-induced cell death in CGNs can be delayed by insulin-like growth factor (IGF-I) (D'Mello *et al.*, 1993; Galli *et al.*, 1995), cAMP (D'Mello *et al.*, 1993; Moran *et al.*, 1999) and forskolin (Galli *et al.*, 1995; Moran *et al.*, 1999). Cell death was also delayed by the proteasome inhibitor MG132 in this investigation as previously demonstrated (Bobba *et al.*, 2002; Butts *et al.*, 2005; Canu *et al.*, 2000). In contrast, PS-341, a dipeptide boronic inhibitor that targets an identical site to MG132 in the 20S core of the proteasome, had no effect on the cell death induced. The inhibition of calpains by MG132 has also been reported (Lee and Goldberg, 1998), however there was no change in the level of cell death when CGNs were co-treated with a combination of calpeptin and PS-341. It was concluded that MG132 targets another stage of the apoptotic pathway other than calpains and the proteasome.

Canu *et al.*, 2005 and Kaasik *et al.*, 2005 both highlighted the importance of cathepsin B and L respectively in the early autophagic pathway in CGNs induced to undergo apoptosis by the withdrawal of K⁺ (and serum), although some of their data seem to contradict each other. It is possible that MG132 was acting as a cathepsin inhibitor (Lee and Goldberg, 1998) in addition to its inhibition of calpains and the proteasome. The early induction of an autophagic response was further implied in this investigation, and is possibly responsible for the cell death observed in the presence of caspase inhibitors and the slow caspase-independent cell death described in Bax^{-/-} CGNs (Miller *et al.*, 1997). The coordination of the distinct autophagic and apoptotic pathways to elicit cell death is likely to be tightly regulated and requires further investigation.

We have demonstrated the cleavage of the proteasomal subunits S1 and S6' in CGNs during K⁺ withdrawal-induced cell death. This is probably a consequence of caspase-3 activation and may contribute to the loss of 20S proteasomal function. It is possible that cleavage of the proteasome is a mechanism to ensure cell death continues. By disabling the proteasome the stability of many pro-apoptotic proteins is enhanced, allowing them to mediate the cell death process.

Chapter 4

The *In Vitro* Cleavage of the hAtg Proteins by Cell Death Proteases.

4.1. Introduction

Having established that the autophagic response may be induced in the serum/K⁺ withdrawal model of cell death in CGNs, I then investigated the potential relationship between autophagy and apoptotic cell death.

Morphological features of autophagy such as excessive levels of autophagic vacuoles have been described in dying cells, leading to its designation as Type 2 cell death (Clarke, 1990). It is however primarily an adaptive survival response. In many cells, constitutive basal levels of autophagy control the cell's normal homeostasis. Autophagy may be implicated in the cell death process when apoptosis is defective or when it becomes excessive (Kang *et al.*, 2007; Levine, 2007; Lum *et al.*, 2005). It is likely that cell death is an integrated mechanism whereby the components of the cell death processes – apoptosis and autophagy (and necrosis) are coordinated and regulate each other (Thorburn, 2008).

Many groups have described overlapping components involved in both apoptosis and autophagy to date. One of the most widely studied is the interaction of the members of the antiapoptotic BCL2 family with Beclin 1 (Erich *et al.*, 2007; Liang *et al.*, 2006; Liang *et al.*, 1998; Maiuri *et al.*, 2007a; Oberstein *et al.*, 2007; Pattingre *et al.*, 2005; Shimizu *et al.*, 2004), which was first identified while investigating the protective mechanism of BCL2 during apoptosis induced by the Sindbis virus in mouse neurons (Liang *et al.*, 1998). The association of Beclin 1 and BCL2 has since been shown to be important in the regulation of starvation-induced autophagy, possibly by antagonising the function of Beclin 1 upstream of its complex with Vps34 (Pattingre *et al.*, 2005).

The induction of Beclin 1/autophagy-related protein 7 (Atg7) dependent autophagy has also been demonstrated in response to the simultaneous inhibition of caspase-8 and a calpain-like protease (Lin *et al.*, 1999; Madden *et al.*, 2007). In addition, Atg5 has been implicated in both the autophagic and apoptotic response in complex with FADD (Pyo *et al.*, 2005) and through its truncation by calpain 1 and 2 during apoptosis (Yousefi *et al.*, 2006). Furthermore, calpain 1 and 2 have been hypothesised to have an additional role in the promotion of autophagy in mammalian cells (Demarchi *et al.*, 2006).

Although many attempts have been made to elucidate the molecular mechanisms involved in the regulation of the autophagic and apoptotic pathways and control of the 'switch' between the two, it seems that there may be multiple points of control. To

investigate the regulation further, I examined the potential modulation of the human autophagy-related (hAtg) proteins by proteases that are implicated in both pathways. Although commercial antibodies for the detection of some of the Atg proteins are available, previous experience has indicated that many are not adequately specific in order to assess the cleavage of proteins. It was therefore necessary to construct plasmids encoding the Atg proteins for enforced expression and epitope-tagged for immunodetection in apoptotic cells. An *in vitro* cleavage assay was employed to identify the proteases involved in the potential cleavage of the hAtg proteins. Detection of the cleaved fragments using the epitope tags then aided in the prediction of the protease cleavage sites. This information would then enable the design of uncleavable mutants for further assessment of their functional significance when transfected into cells.

4.2. Results

4.2.1. The hAtg plasmids are expressed in an *in vitro* transcription-translation system.

In order to assess the *in vitro* cleavage of hAtg proteins by proteases that are implicated in the cell death process, it was first necessary to ensure that the hAtg constructs were translated in an *in vitro* transcription-translation system. TNT reactions were carried out using Transcend™ tRNA and then subjected to SDS-PAGE and immunoblotted using Strepavidin-biotinylated-HRP (Strep-HRP; Figure 4.2.1).

The majority of the hAtg constructs resolved at the approximate molecular weight predicted from their DNA sequence plus that of the epitope tags. Low expression of EGFP-LC3 and hAtg12 was detected using Strep-HRP (Figure 4.2.1, Lanes 9 and 13 respectively) with hAtg9 undetectable. The *in vitro* translation of these constructs was therefore repeated using a higher amount of Transcend™ tRNA, which enhanced their detection on immunoblot (as shown later, see Figure 4.2.3).

hAtg4D resolved at a lower molecular weight (~42 kDa) than predicted from its protein sequence (52 kDa; Figure 4.2.1, Lane 5). Re-examination of the protein sequence revealed that pFLAG-hAtg4D-myc/His has a deletion in its nucleotide sequence, which resulted in a truncated form of the protein.

4.2.2. The recombinant enzymes for *in vitro* characterisation are active.

In order to ensure the activity of the recombinant enzymes for the *in vitro* characterisation, it was necessary to measure their ability to cleave well-characterised substrates.

Active recombinant caspase-3 (rCaspase-3) was shown in the previous chapter (Figure 3.2.2) to cleave four potential substrates; α -Fodrin, the proteasome subunits S1 and S6' in CGN lysates and after the tetrapeptide DEVD to release AFC in the DEVDase assay. To evaluate the activities of active rCaspase-6, -7 and -8, enzymatic assays using the substrates VEID.AFC, DEVD.AFC and IETD.AFC respectively were performed. The activity of the recombinant enzymes was demonstrated in a concentration dependent manner, with rCaspase-7 being the most active, and rCaspase-6, the least, against their preferred substrates (Figure 4.2.2 A). However, to

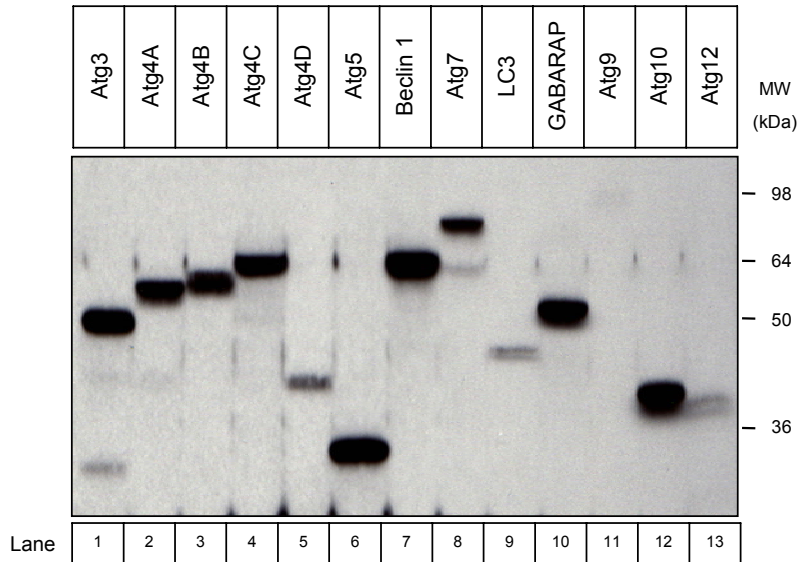


Figure 4.2.1 The prepared Atg constructs are expressed in an *in vitro* transcription-translation system. TNT reactions were prepared for each construct in the presence of Transcend™ tRNA. Samples were then taken and immunoblotted using Strep-HRP.

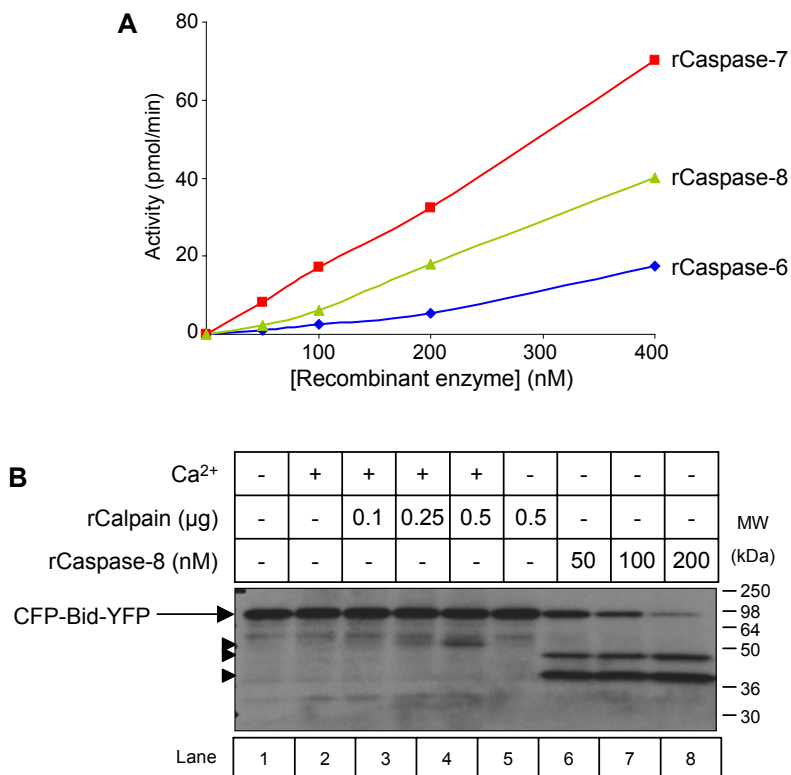


Figure. 4.2.2. The recombinant proteases cleave substrates in a concentration-dependent manner. The activity of active recombinant caspase-6, -7, and -8 was assessed using the substrates VEID.AFC, DEVD.AFC and IETD.AFC respectively (40 μ M), and expressed in pmol/min (**A**). The TNT reaction for pCFP-Bid-YFP was prepared in the presence of Transcend™ tRNA and incubated with rCalpain 1 (+ 20 mM Ca²⁺) or rCaspase-8. Cleavage was assessed by immunoblotting and detection using Strep-HRP. Arrowheads indicate cleavage fragments.

give a clearer understanding of the difference in activity between the recombinant enzymes, the activity of rCaspase-3 should have been demonstrated in the same experiment as that of rCaspase-6, -7 and -8. In addition, the overlapping substrate specificities of the recombinant caspases should have been assessed.

The activity of rCalpain 1 was evaluated by its ability to cleave BID compared to rCaspase-8. Calpain 1 cleaves BID at an alternative, downstream site (Gly70) to that recognised by caspase-8 (Asp60 (Chen *et al.*, 2001)). The TNT product of BID-FRET (CFP-BID-YFP (Onuki *et al.*, 2002)) was incubated with rCalpain 1 (in the presence and absence of Ca²⁺) and rCaspase-8, and its cleavage was detected using the anti-human BID antibody. Both rCalpain 1 and rCaspase-8 were able to cleave BID-FRET in a concentration dependent manner (Figure 4.2.2 C). The obligatory activation of rCalpain 1 was clearly observed when the cleavage fragment was eliminated in the absence of calcium. In addition, there was a marked loss of full-length BID-FRET upon the addition of rCaspase-8, with the observation of two cleavage fragments at ~43 and 36 kDa. These correspond to YFP + Bid (C-terminus) and CFP + Bid (N-terminus) respectively, consistent with that shown by Onuki *et al.*, 2002.

Collectively these data confirm that the recombinant proteases are active and able to cleave their respective substrates *in vitro*, and therefore are suitable for use in the *in vitro* cleavage assays of hAtgs.

4.2.3. Recombinant caspases and calpain 1 cleave numerous hAtg proteins *in vitro*.

In order to identify the proteases that are able to cleave the hAtg proteins *in vitro*, one concentration of each recombinant enzyme was incubated with each TNT product. The reactions were then resolved by SDS-PAGE immunoblotted and detected using Strep-HRP (Figure 4.2.3).

All the hAtg proteins were cleaved by rCalpain 1 (Figure 4.2.3 A-C, Lane 6). For the majority of the hAtg proteins, the cleavage by rCalpain 1 resulted in their complete degradation. Cleavage fragments were only observed for hAtg9 at ~60 and 54 kDa, and GABARAP, just below that of the full length form. The cleavage of Atg5 by rCalpain 1 is consistent with that previously described by Yousefi *et al.*, 2006, although the cleavage fragment was not observed in this study (Yousefi *et al.*, 2006),

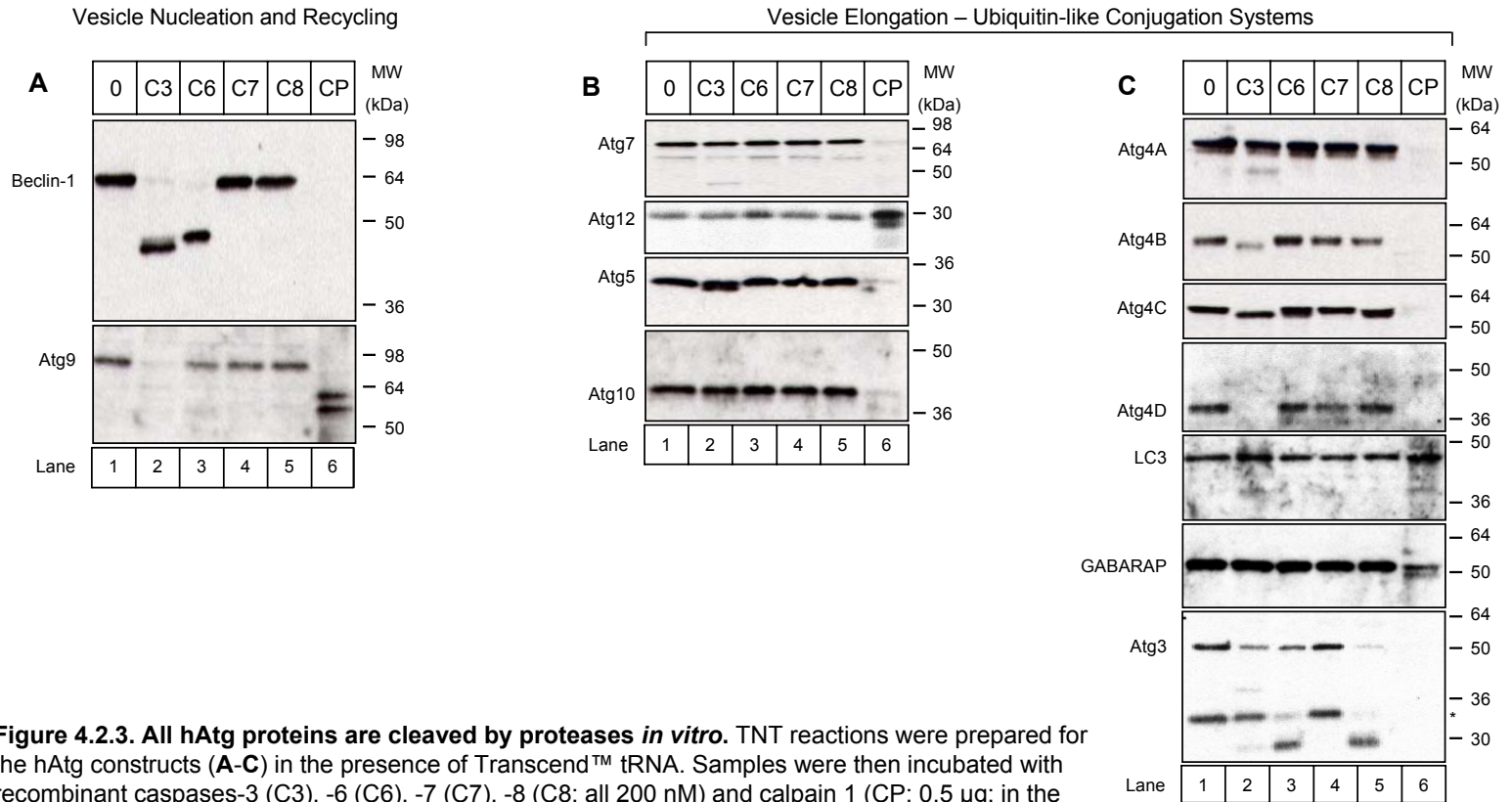


Figure 4.2.3. All hAtg proteins are cleaved by proteases *in vitro*. TNT reactions were prepared for the hAtg constructs (A-C) in the presence of Transcend™ tRNA. Samples were then incubated with recombinant caspases-3 (C3), -6 (C6), -7 (C7), -8 (C8; all 200 nM) and calpain 1 (CP; 0.5 µg; in the presence of 20 mM Ca²⁺). After 60 min at 37 °C, the reaction was stopped with 2xSDS sample buffer, run on SDS-PAGE and immunoblotted using Strep-HRP. * indicates the possible alternative form of hAtg3 as discussed in the text. Immunoblots are ordered according to the roles of the Atgs in the autophagic pathway.

rCaspase-3 cleaved Beclin 1, hAtg9, hAtg7 and the hAtg4 homologues (Figure 4.2.3 A-C, Lane 2). Furthermore, in contrast to that previously reported by Yousefi *et al*, 2006, rCaspase-3 also cleaved hAtg5 resulting in a cleavage fragment just below that of full length hAtg5 (Figure 4.2.3 B, Lane 2 (Yousefi *et al.*, 2006)). The cleavage fragments of Beclin 1, hAtg7 and hAtg3 were observed at ~46, 40 and 43 kDa respectively. In addition, the cleavage of hAtg4A, 4B and 4C resulted in a slight downward shift in molecular weight, indicating that the cleavage is near to the N- or C-terminus. The caspase-3 cleavage of hAtg4D at the canonical cleavage site DEVD was previously reported (He and Orvedahl, 2007). There was also a slight loss of hAtg4D upon incubation with rCaspase-7 (Figure 4.2.3 C, Lane 3), which probably occurs at the same DEVD site, though is less efficiently processed. As a truncated form of pFLAG-hAtg4D-myc/His was produced and caspase-3 cleavage of hAtg4D was previously reported, no further work was carried out using this construct.

rCaspase-6 and rCaspase-8 cleaved hAtg3, resulting in cleavage fragments of ~29 kDa (Figure 4.2.3 C, Lanes 3 and 5). However, there also appeared to be a lower molecular weight species that was detected by the Strep-HRP, which seemed to be cleaved by the same proteases and was detected using an antibody for the epitope tag, FLAG (see later, Figure 4.2.13 A). This indicates that the construct contained two forms of hAtg3, a full length form and a truncated version, both of which were expressed in the TNT reaction. Beclin 1 was cleaved by rCaspase-6 producing a fragment at ~47 kDa (Figure 4.2.3 A, Lane 3), and the cleavage of hAtg4C by rCaspase-8 resulted in a small downward shift in the molecular weight of the protein (Figure 4.2.3 C, Lane 5).

The cleavage of LC3 by the recombinant enzymes was unclear on the immunoblot. There appeared to be a cleavage fragment at approximately 40 kDa upon rCaspase-3 and rCalpain-1 treatment, however there was no loss in the full-length form of LC3. The potential cleavage of LC3 was not further investigated in this study, and it is difficult to predict the site at which the recombinant enzymes cleaved the protein. The EGFP tag was not utilised to identify whether the possible cleavage occurred at the N- or C-terminus of the protein, therefore the sites could fall within either the EGFP tag or in the middle of LC3. Further work is required to examine the possible cleavage of LC3 to ensure that the protein is actually cleaved rather than the cleavage fragments observed being the result of a 'dirty' immunoblot.

These data indicate that the hAtg proteins are cleaved *in vitro* by a number of proteases involved in the cell death process, some of which are the targets of multiple proteases. rCalpain 1 seems promiscuous with respect to cleavage of the proteins involved in the autophagic pathway, potentially highlighting the importance of this protease for autophagy and the 'switch' between autophagy and apoptosis.

4.2.4. The cleavage of the hAtg constructs are further confirmed; and the potential cleavage sites identified.

Having established that all the hAtg proteins were cleaved by recombinant calpain 1, caspase-3, -6 and -8 *in vitro*, it was necessary to further confirm the actions of these proteases and attempt to map the sites of their actions. TNT reactions were prepared for each hAtg construct, incubated with increasing concentrations of recombinant protease and immunoblotted using Strep-HRP or an antibody to the appropriate epitope tag.

4.2.4.1. Beclin 1 is cleaved at its N-terminus by rCaspase-3 and -6, and in the middle of the protein by rCalpain 1.

rCaspase-3 cleaved Beclin 1 in a concentration dependent manner (Figure 4.2.4 A, Lanes 2-4), with a doublet of cleavage fragments detected at ~43 and 40 kDa. The smaller fragment appeared to be a secondary cleavage as it increased upon incubation with higher concentrations of the protease. Higher exposures of the film revealed additional cleavage fragments at ~23, 19 and 17 kDa, the 17 kDa fragment again increasing in a concentration-dependent manner. rCaspase-6 cleaved Beclin 1 to produce fragments at 43 and 19 kDa (Figure 4.2.4 A, Lanes 5-7), which increased with higher concentrations of rCaspase-6.

Beclin 1 was cleaved in a concentration-dependent manner by Ca²⁺-activated rCalpain 1 (Figure 4.2.4 A, Lanes 10-12). The complete loss of Beclin 1 by rCalpain 1 at the highest concentration was fully blocked by the removal of Ca²⁺ from the reaction (Figure 4.2.4 A, Lanes 13-14), and by the addition of the specific calpain 1 inhibitor calpeptin (Lane 14). There appeared to be a cleavage fragment just below the full length form of Beclin 1 upon incubation with 0.25 µg Ca²⁺-activated rCalpain 1 (Lane 11). However, additional cleavage fragments were observed after the addition of Ca²⁺ alone to the reaction (Lane 9). This suggests that there is some activation of

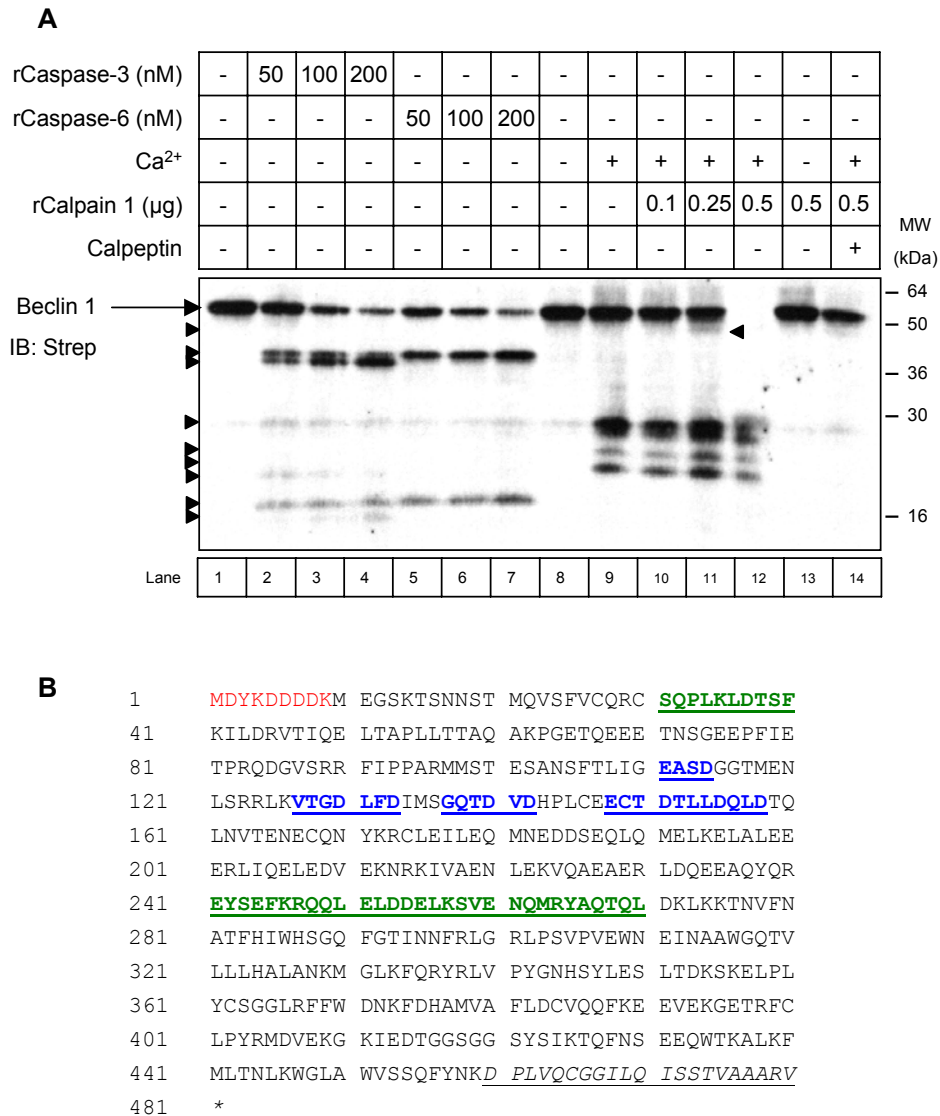


Figure 4.2.4. Beclin 1 is cleaved by rCaspase-3, -6 and rCalpain 1. TNT reactions were prepared for pFLAG-Beclin 1 in the presence of Transcend™ tRNA. Samples were then incubated with recombinant caspases-3, -6 and calpain 1 (in the presence of absence of 20 mM Ca²⁺ or calpeptin (10 μM)). After 60 min at 37 °C, the reaction was stopped with 2xSDS sample buffer, run on SDS-PAGE and immunoblotted using Strep-HRP (A). Arrows denote full length forms; arrowheads indicate cleavage fragments. The protein sequence of pFLAG-Beclin 1, showing the predicted caspase (blue, underlined residues) and calpain (green, underlined residues) cleavage sites (B). The N-terminal FLAG epitope tag is in red and the 3' vector sequence is underlined and in italics.

endogenous Ca^{2+} -dependent proteases, such as calpains already present in the rabbit reticulocyte lysates.

The construct for Beclin 1 also contained an N-terminal FLAG tag and therefore the membranes were stripped and re-probed using anti-FLAG M2 antibody to detect any N-terminal cleavage fragments. The ~43 and 40 kDa fragments generated by the actions of rCaspase-3 and -6, and those produced by rCalpain 1 (~49 kDa and 20-30 kDa) were not detected using the anti-FLAG antibody, suggesting N-terminal cleavage of Beclin 1 by these proteases. However, fragments at ~30 kDa (rCalpain 1) indicate that the cleavage sites are near to the middle of the protein.

Given the extensive research that has already been applied in determining the nature of specific domains in Beclin 1, the predicted cleavage sites estimated from the data were able to be mapped to various sites in the Beclin 1 primary protein sequence. Whilst there are various guidelines with respect to identifying cleavage sites for the caspases and calpains (as discussed in the introduction) these are not absolute.

Therefore all potential cleavage sites that correspond with the predicted molecular weight of the fragments from the immunoblot within a particular region have been highlighted (Figure 4.2.4 B). In addition, caspase cleavage sites were verified using a web-server for predicting caspase cleavage using support vector machine (SVM) algorithms (Wee *et al.*, 2006).

The potential cleavage sites of caspase-3/6 responsible for the fragments at ~43 and 40 kDa were mapped to a region that has previously been shown to be the minimal requirement for interaction with the anti-apoptotic BCL2 family members (amino acids 97-159; Figure 4.2.4 B (Liang *et al.*, 1998)). The precise interaction domain has been further refined to a putative Beclin 1 BH3 domain comprising the amino acids 117-136 (Figure 4.2.4 B) that binds in the hydrophobic groove of BCL2/xL (Maiuri *et al.*, 2007a; Oberstein *et al.*, 2007). In fact, four of the potential cleavage sites were identified in the BH3 domain of Beclin 1. Other domains of interest within human Beclin 1 include the coiled-coil (residues 153-278 in Figure 4.2.4 B (Liang *et al.*, 1998)) that has been shown to interact with nPIST (Yue *et al.*, 2002) and UVRAG (Liang *et al.*, 2006). In addition Beclin 1 contains an evolutionary conserved domain (ECD) spanning amino acids 252-356 (Figure 4.2.4 B), which interacts with Vps34 (Furuya *et al.*, 2005).

Interestingly, the potential rCalpain 1 cleavage site identified at the N-terminus of the protein did not fall within any of the identified domains that are important for the function of Beclin 1 (Figure 4.2.4 B); however, the potential cleavage sites near the middle of the protein could potentially interfere with Beclin 1's interaction with nPIST, UVRAG and Vps34.

4.2.4.2. hAtg9 was weakly expressed, despite efforts to increase its expression.

Despite increasing the amount of Transcend™ tRNA for this construct, hAtg9 was weakly expressed (Figure 4.2.5 A, Lane 1). The loss of full length hAtg9 could be observed in a concentration dependent manner upon rCaspase-3 incubation (Lane 2-3). The loss of hAtg9 was complete upon the incubation with rCalpain 1 (Lanes 5-7). With higher exposure there was evidence of rCaspase-3 mediated cleavage fragments at ~23 and 19 kDa (data not shown).

Although the hAtg9 plasmid contained a FLAG tag, the anti-FLAG antibody could not be used for detection, as the expression of hAtg9 in the TNT system was low. However, from the size of the cleavage fragment generated by rCalpain 1 (Figure 4.2.3 A, Lane 6; ~60 kDa) it could be predicted that the cleavage site would fall near to the middle of the protein (Figure 4.2.5 B). The caspase-3 cleavage sites would be predicted to be close to the end of the protein. The 23 kDa fragment could be produced by cleavage at either the N- or C-terminus (TELD/SGVD). The 19 kDa fragment could only result from C-terminal cleavage (RESD/SAPD) as an appropriate site at the N-terminus could not be identified.

4.2.4.3. rCaspase-3 and rCalpain 1 cleave in the middle of hAtg7.

Although there was little loss in full length hAtg7 by rCaspase-3 cleavage (Figure 4.2.6 A), the concentration-dependent increase in cleavage fragment at ~42 kDa was consistent with that previously demonstrated (Figure 4.2.3 B). Although the cleavage fragment was observed using the anti-FLAG antibody (lower panel), the molecular weight suggested that the cleavage site was in the middle of the protein. The loss of hAtg7 was evident upon incubation rCalpain 1, with a cleavage fragment detected at ~36 kDa (Figure 4.2.6 A Lanes 5-7), suggests that the cleavage site falls in the middle of the protein.

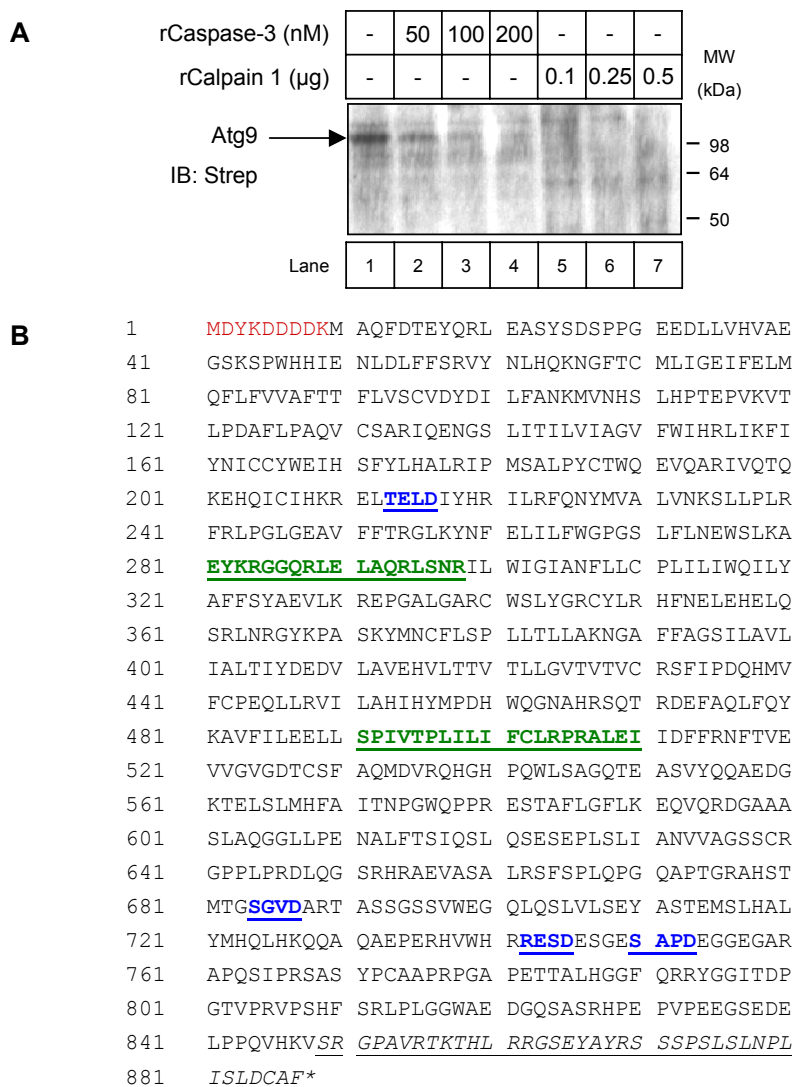


Figure 4.2.5. The expression of hAtg9 is weak in the TNT reaction. TNT reactions were prepared for the pFLAG-Atg9 in the presence of Transcend™ tRNA. Samples were then incubated with recombinant caspase-3 and calpain 1 (in the presence of 20 mM Ca²⁺). After 60 min at 37 °C, the reaction was stopped with 2xSDS sample buffer, run on SDS-PAGE and immunoblotted using Strep-HRP (**A**). Arrows denote full length form; arrowheads indicate cleavage fragments. The protein sequence of pFLAG-Atg9, showing the predicted caspase (blue, underlined residues) and calpain (green, underlined residues) cleavage sites (**B**). The N-terminal FLAG epitope tag is in red and the 3' vector sequence is underlined and in italics.

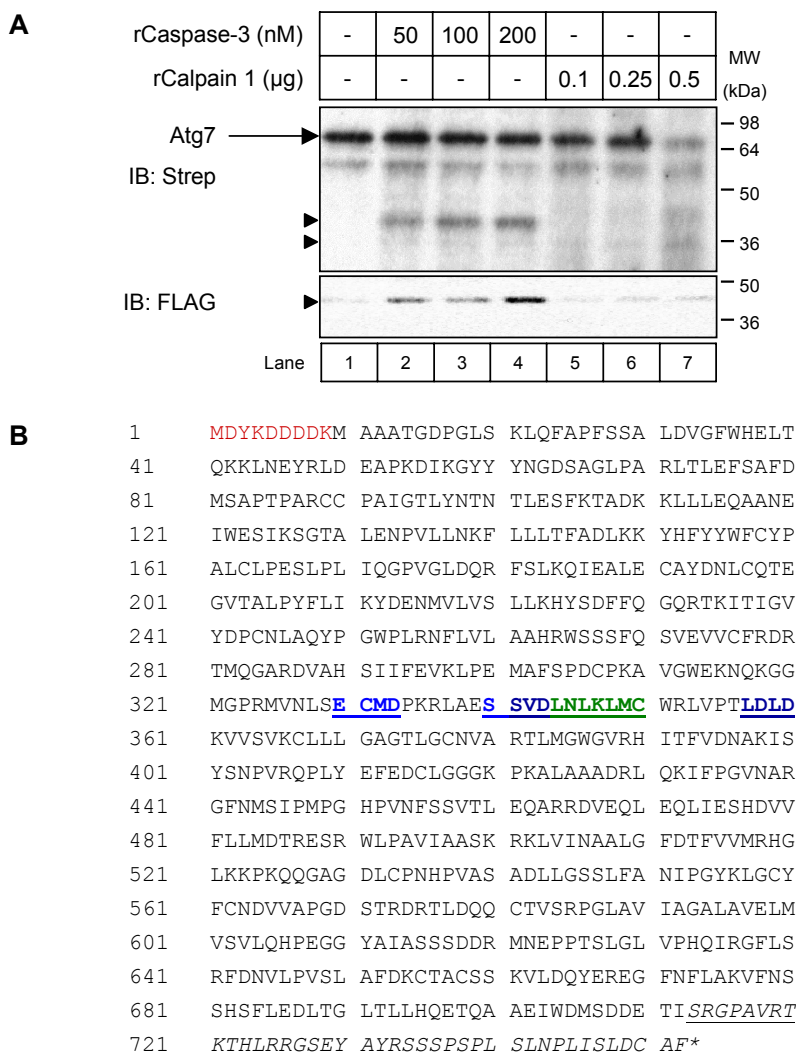


Figure 4.2.6. hAtg7 is cleaved by rCaspase-3 and rCalpain 1. TNT reactions were prepared for the pFLAG-Atg7 in the presence of Transcend™ tRNA. Samples were then incubated with recombinant caspase-3 and calpain 1 (in the presence of 20 mM Ca²⁺). After 60 min at 37 °C, the reaction was stopped with 2xSDS sample buffer, run on SDS-PAGE and immunoblotted using Strep-HRP and anti-FLAG (**A**). Arrows denote full length form; arrowheads indicate cleavage fragments. The protein sequence of pFLAG-Atg7, showing the predicted caspase (blue, underlined residues) and calpain (green, underlined residues) cleavage sites (**B**). The N-terminal FLAG epitope tag is in red and the 3' vector sequence is underlined and in italics.

Based on the predicted molecular weights of the cleavage fragments, the potential cleavage sites of caspase-3 and calpain within the middle of the protein were identified (Figure 4.2.6 B). However, given the current knowledge about hAtg7, cleavage of the protein at these sites would not be predicted to directly interfere with the function of hAtg7 in the autophagic pathway (Komatsu *et al.*, 2001).

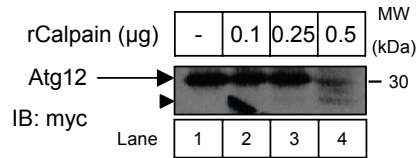
4.2.4.4. hAtg12 is cleaved by rCalpain 1 at its N-terminus; the cleavage of hAtg5 is predicted to fall in its hAtg16-interacting domains.

hAtg12 was only detected using the anti-myc antibody against the 3' myc epitope tag as it was undetectable using Strep-HRP. This detected the loss of full length hAtg12 with rCalpain 1 (Figure 4.2.7 A). A potential cleavage fragment of hAtg12 was evident at ~25 kDa indicating that the cleavage site was N-terminal. Cleavage spanning the amino acids 40-50 would correspond to a cleavage fragment of ~24-25 kDa (Figure 4.2.7 B).

The cleavage of hAtg5 by rCaspase-3 resulted in a cleavage fragment directly below that of the full length form at all concentrations of rCaspase-3 tested (Figure 4.2.7 C, Lanes 2-4), as previously observed in Figure 4.2.3. However, it was extremely difficult to differentiate full length hAtg5 from the cleaved form as both bands were highly saturated on the immunoblot. The size of the fragment suggested that the cleavage was very close to either the N- or C-terminus of the protein. Three potential cleavage sites were identified; two N-terminal, one C-terminal. Interestingly, all three motifs fell within the domains that would interact with hAtg16L, in fact one of the cleavage sites included an amino acid (leucine-8) that interacts directly with hydrophobic residues in hAtg16 (Figure 4.2.7 D) (Matsushita *et al.*, 2007). Cleavage of hAtg5 could therefore potentially disrupt the essential interaction of hAtg5 with hAtg16L during autophagic vesicle expansion (Matsushita *et al.*, 2007).

4.2.4.5. rCalpain 1 cleaves hAtg10 at its N-terminus.

The rCalpain 1 cleavage of hAtg10 is evidenced by the loss of full length and the appearance of a cleavage fragment (~36 kDa), when detected with both Strep-HRP and the anti-myc antibody (Figure 4.2.8 A). The cleavage fragment however also decreased at high rCalpain concentrations, suggesting that there are two rCalpain 1 mediated cleavages of hAtg10, primarily at the N-terminus followed by cleavage at the C-terminus (Figure 4.2.8 B). The C-terminal cleavage mapped to a region in the protein

A**B**

1 MDYKDDDDKM TSREHQVSLC NCVPLLRRL

31 CDAPWRKARP LHALSRYFRS RVSPSKMAEE

61 PQSVLQLPTS IAAGGGLTD VSPETTTPEP

91 PSSAAVSPGT EEPAGDTKKK IDILLKAVGD

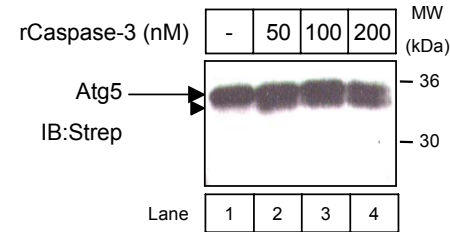
121 TPIMKTKKWA VERTRTIQGL IDFIKKFLKL

151 VASEQLFIYV NQSFAPSPDQ EVGTLYEFCG

181 SDGKLVLYHC KSQAWGGSTS PVWWSADIQ

211 HSGGRSSLEG PRFEQKLISE EDLNMHTGHH

241 HHHH*

C**D**

1 MTDDKDVLRD VWFGRIPTCF TLYQDEITER

31 EAEPYYLLLP RVSYLTLVTD KVKKHFQKVM

61 RQEDVSEIWF EYEGTPLKWH YPIGLLFDLL

91 ASSSALPWNI TVHFKSFPEK DLLHCPSKDA

121 VEAHFMSCMK EADALKHKSQ VINEMQKQKH

151 KQLWMGLQND RFDQFWAINR KLMEYPPPEEN

181 GFRYIPFRIY QTTERPFIQ KLFPRVAADG

211 QLHTLGDLLR EVCPSA VAPE DGEKRSQVMI

241 HGIEPMLETP LQWLXEHLSY PDNFLHISIV

271 PQPTD*

Figure 4.2.7. The cleavage of hAtg12 by rCalpain 1 and hAtg5 by rCaspase-3 . TNT reactions were prepared for the pFLAG-Atg12-myc/His and pAtg5 in the presence of Transcend™ tRNA. Samples were then incubated with recombinant calpain 1 in the presence of 20 mM Ca²⁺ or caspase-3. After 60 min at 37 °C, the reaction was stopped with 2xSDS sample buffer, run on SDS-PAGE and immunoblotted using anti-myc (for Atg12; **A**) or Strep-HRP (for Atg5; **C**). Arrows denote full length forms; arrowheads indicate cleavage fragments. The protein sequence of pFLAG-Atg12 (**B**) and pAtg5 (**D**) showing the predicted calpain (green, underlined residues) and caspase (blue, underlined residues) cleavage sites. The N-terminal FLAG epitope tag is in red and the 3' vector sequence the C-terminal myc/His tags in pFLAG-Atg12-myc/His are underlined and in italics. The downward pointing arrow indicates the calpain cleavage site, previously described (Yousefi *et al.*, 2006)

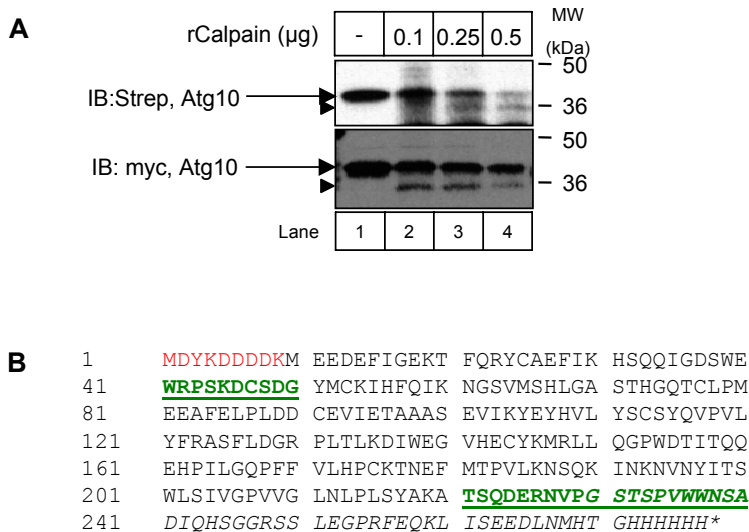


Figure 4.2.8. hAtg10 is cleaved by rCalpain 1 at its N-terminus. TNT reactions were prepared for the pFLAG-Atg10-myc/His in the presence of Transcend™ tRNA. Samples were then incubated with recombinant calpain 1 (in the presence of 20 mM Ca^{2+}). After 60 min at 37 °C, the reaction was stopped with 2xSDS sample buffer, run on SDS-PAGE and immunoblotted using Strep-HRP and anti-myc (**A**). Arrows denote full length form; arrowheads indicate cleavage fragments. The protein sequence of pFLAG-Atg10-myc/His, showing the predicted calpain (green, underlined residues) cleavage sites (**B**). The N-terminal FLAG epitope tag is in red and the 3' vector sequence and C-terminal myc/His tags are underlined and in italics.

at either the very end of hAtg10 or in the vector sequence prior to the myc/His epitope tags.

4.2.4.5. hAtg4A is cleaved at its N-terminus by rCalpain 1 and rCaspase-3 cleaves its C-terminus.

The loss of full length hAtg4A was minimal when the TNT reaction was incubated with rCaspase-3 (Figure 4.2.9 A, Lanes 1-4). In contrast, the cleavage fragment at ~50 kDa, appeared to be concentration-dependent and was also detected using the anti-FLAG antibody (lower panel), indicating the cleavage was C-terminal. Upon incubation with rCalpain 1 there was a slight loss of full length hAtg4A and a cleavage fragment just below the full length form was detected (~54 kDa), which was also observed using the anti-FLAG antibody, again indicating C-terminal cleavage. Furthermore, there appeared to be a rCalpain 1 mediated cleavage fragment at ~50 kDa that was not detected by the anti-FLAG antibody, suggestive of cleavage at the N-terminal (Lanes 5-7, lower panel). The anti-FLAG antibody also recognised a high molecular weight, non-specific protein in the rabbit reticulocyte lysates that also seemed to be cleaved by the proteases (Figure 4.2.9 and later in 4.2.10 as shown by the asterisk).

The C-terminal cleavage of hAtg4A by rCaspase-3 was mapped to two sites that were situated very close to the end of hAtg4A and were next to each other in the primary sequence (Figure 4.2.9 B). C-terminal cleavage of hAtg4A by rCalpain 1 to produce a fragment at ~54 kDa was either at the C-terminus or in the vector sequence and could not be identified. The additional cleavage site for rCalpain 1 to produce the ~50 kDa fragment was downstream of the N-terminus (shown in Figure 4.2.9 B).

4.2.4.6. hAtg4B is cleaved at the N-terminus by rCaspase-3; rCalpain 1 cleaves at the C-terminus.

rCaspase-3 cleaved hAtg4B at all concentrations and resulted in a slight downward shift in hAtg4B, consistent with that shown previously in Figure 4.2.3 C (Figure 4.2.10 A, Lanes 2-4). Detection of hAtg4B using the N-terminal FLAG epitope tag demonstrated the loss of full length hAtg4B in a concentration dependent manner, without the detection of the cleavage fragment slightly below this (centre panel). Consistent with this result, the C-terminal myc tag permitted the detection of the cleavage fragment (lower panel). Collectively this indicates that the rCaspase-3 cleavage of hAtg4B is at the N-terminal end of the protein. In contrast, the cleavage by

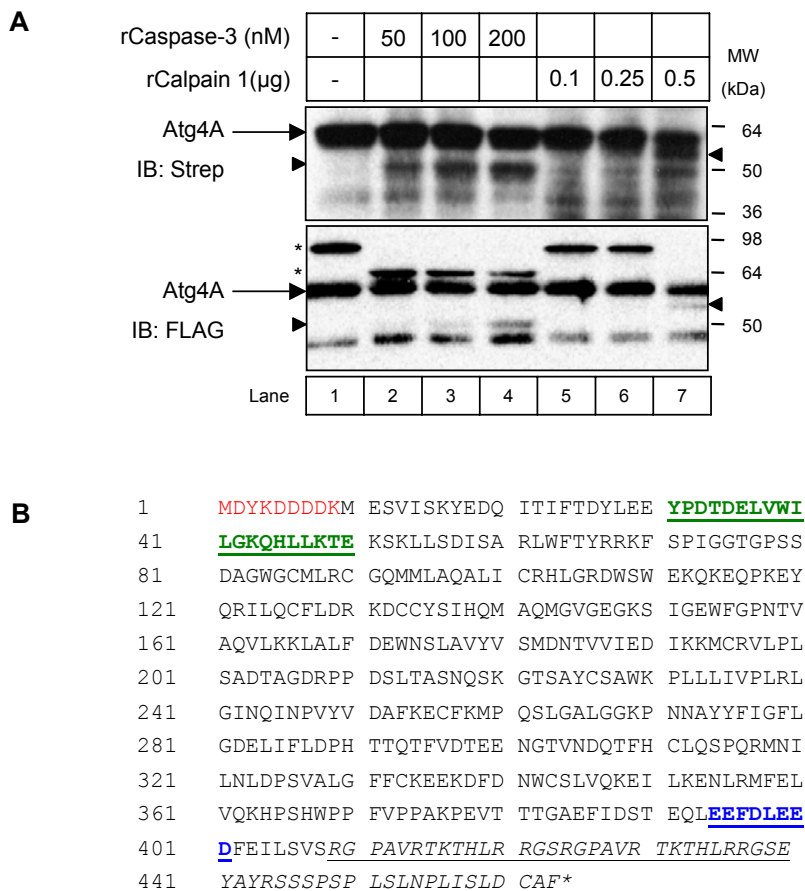


Figure 4.2.9. hAtg4A is cleaved by rCaspase-3 and rCalpain 1. TNT reactions were prepared for the pFLAG-Atg4A in the presence of Transcend™ tRNA. Samples were then incubated with recombinant caspase-3 and calpain 1 (in the presence of 20 mM Ca²⁺). After 60 min at 37 °C, the reaction was stopped with 2xSDS sample buffer, run on SDS-PAGE and immunoblotted using Strep-HRP and anti-FLAG (A). Arrows denote full length form; arrowheads indicate cleavage fragments. * indicates non-specific protein in the rabbit reticulocyte lysate detected by the anti-FLAG antibody. The protein sequence of pFLAG-Atg4A, showing the predicted caspase (blue, underlined residues) and calpain (green, underlined residues) cleavage sites (B). The N-terminal FLAG epitope tag is in red and the 3' vector sequence is underlined and in italics.

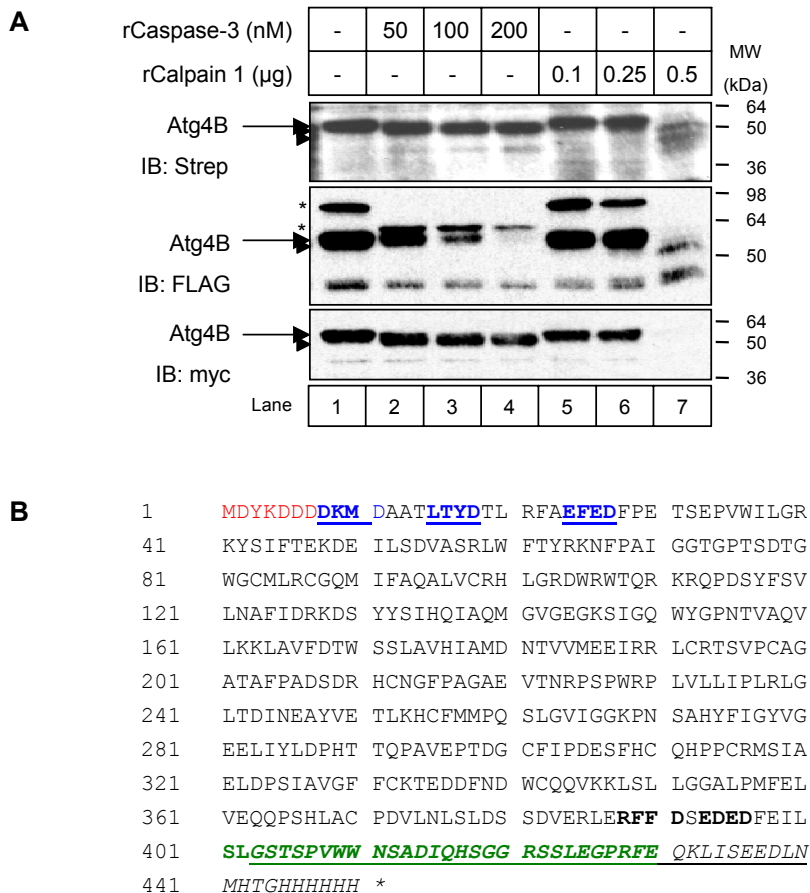


Figure 4.2.10. The cleavage of hAtg4B by rCalpain 1 may fall in the vector sequence. TNT reactions were prepared for the pFLAG-Atg4B-myc/His in the presence of Transcend™ tRNA. Samples were then incubated with recombinant caspase-3 and calpain 1 (in the presence of 20 mM Ca²⁺). After 60 min at 37 °C, the reaction was stopped with 2xSDS sample buffer, run on SDS-PAGE and immunoblotted using Strep-HRP, anti-FLAG and anti-myc (**A**). Arrows denote full length form; arrowheads indicate cleavage fragments. * indicates non-specific protein in the rabbit reticulocyte lysate detected by the anti-FLAG antibody. The protein sequence of pFLAG-Atg4B-myc/His, showing the predicted caspase (blue, underlined residues) cleavage sites (**B**). The N-terminal FLAG epitope tag is in red and the 3' vector sequence and C-terminal myc/His tags are underlined and in italics.

rCalpain 1 resulted in a loss of full length hAtg4B (Figure 4.2.10 A, Lanes 5-7) and the production of a cleavage fragment, just below that of the full length protein. This fragment was also evident when using the anti-FLAG antibody, suggesting that the cleavage is at the C-terminus (centre panel). The absence of the cleavage fragment upon incubation with the anti-myc antibody confirmed this result (lower panel).

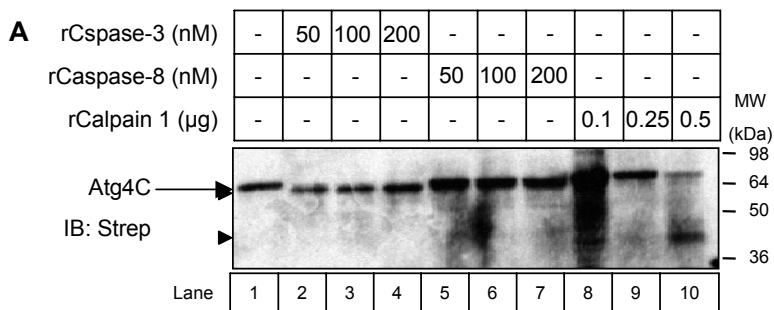
Three potential N-terminal rCaspase-3 cleavage sites were identified in hAtg4B (Figure 4.2.10 B), however one site was only present in the protein sequence as part of the FLAG tag and therefore would not occur in the endogenous protein. rCaspase-3 cleavage at the alternative N-terminal sites would not interfere with the critical residues for the autophagic function of hAtg4B. This includes those involved in substrate recognition (Lys146, Trp151, Gly153, Pro154, Figure 4.2.10 B) or residues that are part of the inhibitory loop (amino acids 266-272), which masks the active site of the enzyme (Sugawara *et al.*, 2005). It is also possible that the rCalpain 1 mediated cleavage, resulting in a fragment just below that of the full length protein, is due to cleavage by rCalpain 1 in the vector sequence.

4.2.4.7. rCaspase-3 cleaves hAtg4C at its canonical N-terminal DEVD site; rCalpain 1 cleavage occurs in the middle of hAtg4C.

hAtg4C was cleaved by rCaspase-3 to produce a cleavage fragment that was just smaller than the full length form (Figure 4.2.11 A). In contrast to that shown previously (Figure 4.2.3), the effect of rCaspase-8 on hAtg4C is not evident (Figure 4.2.11 A, Lanes 5-7). The cleavage of hAtg4C was almost complete upon incubation with rCalpain 1; the detection of a cleavage fragment being at ~38 kDa (Lane 10). The rCaspase-3 cleavage site was predicted to be canonical site DEVD at the N-terminus of the protein, similar to that observed with hAtg4D (He and Orvedahl, 2007). The potential cleavage sites of rCalpain 1 were mapped to two sites near to the middle of the primary sequence of hAtg4C (Figure 4.2.11 B).

4.2.4.8. GABARAP is cleaved at the C-terminus by rCalpain 1.

The cleavage of GABARAP by rCalpain 1 occurred at all concentrations and resulted in a cleavage fragment that was situated below the full length protein (Figure 4.2.12 A, Lanes 2-4). As the YFP and myc tags were N-terminal to GABARAP (YFP: amino acids 1-239, myc: amino acids 252-261, 264-273, 276-285, Figure 4.2.12 B), the recognition



B

1 MDYKDDDDKM EATGTDEVDK LKTKFISAWN NMKYSWVLKT

41 KTYFSRNSPV LLLGKCYHFK YEDEDKTLPA ESGCTIEDHV

81 IAGNVEEFRK DFISRIWLTY REEFQIEGS ALTTDCGWGC

121 TLRTGQMLLA QGLILHFLGR AWTWPDALNI ENSDSESWTS

161 HTVKKFTASF EASLSGEREF KTPTISLKET IGKYSDDHEM

201 RNEVYHRKII SWFGDSPLAL FGLHQLIEYG KKS~~G~~KAGDW

241 YGPAVVAHIL RKAVEEARHP DLQGITIYVA QDCTVYNSDV

281 IDKQSASMTS DNADDKAVII LVPVRLGGER TNTDYLEFVK

321 GILSLEYCVG IIGGKPKQSY YFAGFQDDSL IYMDPHYCQS

361 FVDVSIKDFP LETFHCPSPK KMSFRKMDPS CTIGFYCRNV

401 QDFKRASEEI TKMLKFSSKE KYPLFTFVNG HSRDYDFTST

441 TTNEEDLFSE DEKKQLKRFS TEEFVLLLES RGPAVRTKTH

481 LRRGSEYAYR SSSPSPLSLN PLISLDCAF*

Figure 4.2.11. hAtg4C is cleaved by rCaspase-3 and rCalpain 1. TNT reactions were prepared for the pFLAG-Atg4C in the presence of Transcend™ tRNA. Samples were then incubated with recombinant caspase-3, -8 and calpain 1 (in the presence of 20 mM Ca^{2+}). After 60 min at 37 °C, the reaction was stopped with 2xSDS sample buffer, run on SDS-PAGE and immunoblotted using Strep-HRP (A). Arrows denote full length form; arrowheads indicate cleavage fragments. The protein sequence of pFLAG-Atg4C, showing the predicted caspase (blue, underlined residues) and calpain (green, underlined residues) cleavage sites (B). The N-terminal FLAG epitope tag is in red and the 3' vector sequence are underlined and in italics.

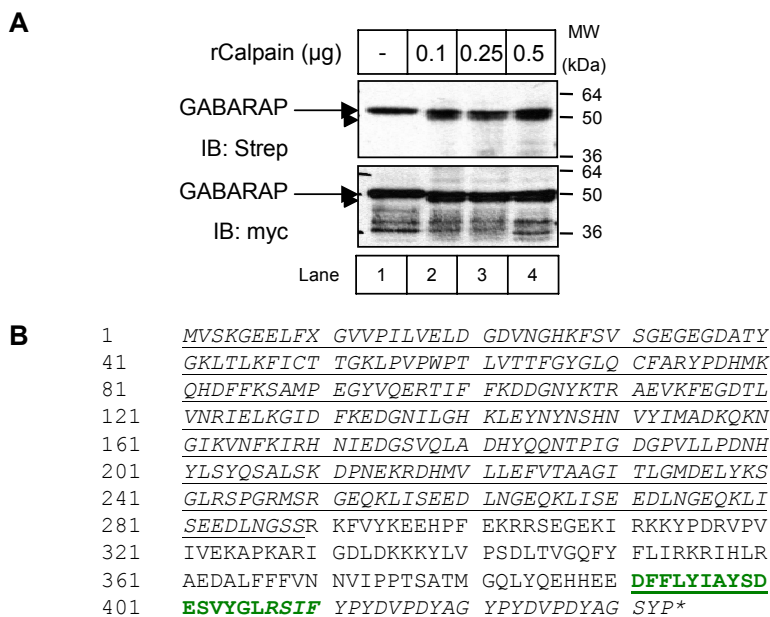


Figure 4.2.12. GABARAP is cleaved by rCalpain 1. TNT reactions were prepared for the pYFP-3xmyc-GABARAP in the presence of Transcend™ tRNA. Samples were then incubated with recombinant calpain 1 (in the presence of 20 mM Ca²⁺). After 60 min at 37 °C, the reaction was stopped with 2xSDS sample buffer, run on SDS-PAGE and immunoblotted using Strep-HRP and anti-myc (**A**). Arrows denote full length form; arrowheads indicate cleavage fragments. The protein sequence of pYFP-3xmyc-GABARAP, showing the predicted calpain (green, underlined residues) cleavage site (**B**). The 5' vector sequence (including the YFP and 3xmyc tags) and the 3' vector sequence are underlined and in italics.

of the rCalpain 1 mediated cleavage fragment with the anti-myc antibody suggests that the cleavage was C-terminal.

The rCalpain 1 cleavage site was predicted to occur at the C-terminal end of GABARAP in the domain required for autophagosome formation (Gly405; Figure 4.2.12 B) (Sugawara *et al.*, 2004). However it cannot be ruled out that the recognition motif for rCalpain 1 involves some of the vector sequence.

4.2.4.9. rAtg3 cleavage by rCaspase-3, -6 and -8, and rCalpain 1 occurs in the middle of the protein.

The concentration dependent loss of hAtg3 was observed upon incubation with rCaspase-3, rCaspase-6, rCaspase-8 and rCalpain 1 (Figure 4.2.13 A, upper panel). In fact the effect of rCaspase-8 was almost complete at its highest concentration of 200 nM. The cleavage fragments produced after incubation with rCaspase-3 were identified at ~36 kDa and at higher exposures, at ~26 kDa (Figure 4.2.13 A, Lanes 2-4). The cleavage fragment at ~26 kDa was also apparent after incubation with rCaspase-6 and rCaspase-8 (Figure 4.2.13 A, Lanes 5-10). The anti-myc antibody also detected the rCaspase-dependent cleavage fragments (Lanes 2-10, lower panel) suggesting N-terminal cleavage. The loss in the full length form of hAtg3 by rCalpain 1 was detected by the anti-myc antibody, which also recognised a novel fragment at ~22 kDa as a result of rCalpain 1 treatment (Figure 4.2.13 A, Lanes 11-13). These data suggest that protease cleavage of hAtg3 is within the middle region of the protein.

hAtg3 has a unique hammer-like structure; consisting of a 'head' and a 'handle'. In addition there is an inserted region named the flexible region, which is essential for the interaction of hAtg3 with hAtg7 in autophagy (Yamada *et al.*, 2007) The caspase cleavage sites were predicted to fall in this domain (Figure 4.2.13 B). In contrast, cleavage mediated by rCalpain 1 was thought to occur in the region separating the flexible and the handle regions (Figure 4.2.13 B).

The cleavage of hAtg proteins by recombinant proteases in an *in vitro* assay has been further established here. These data can be used as a basis to identify the regions in which cleavage sites may exist and aid in the determination of potential significance in the autophagic pathway.

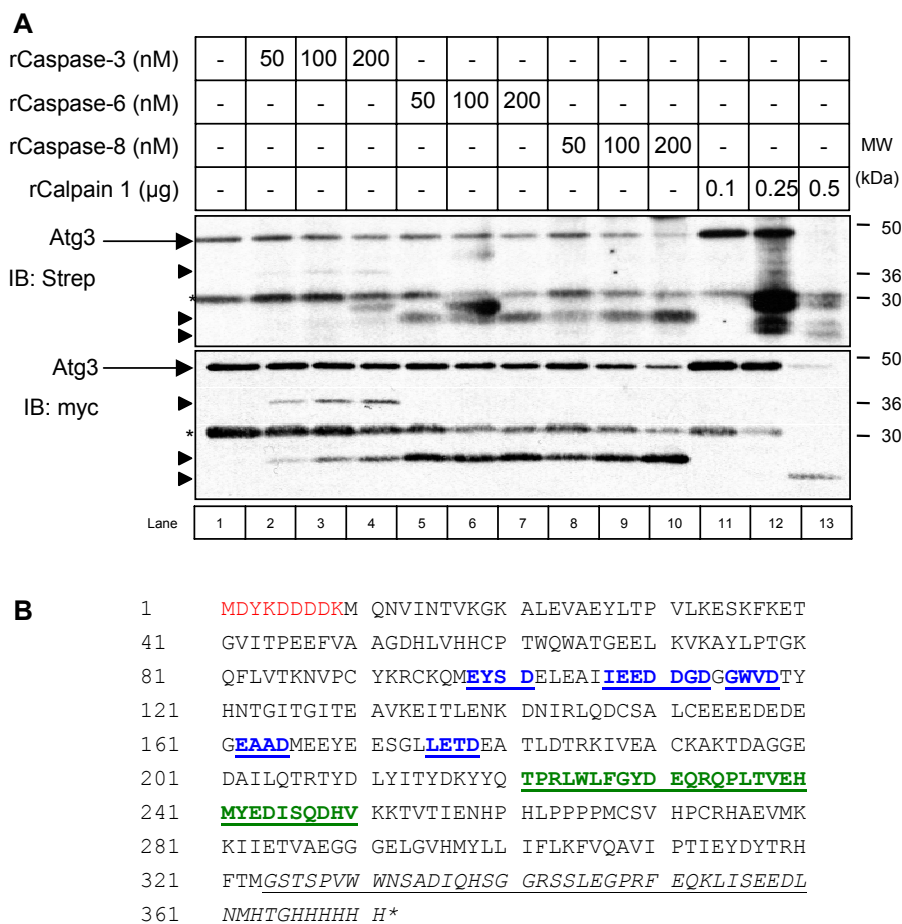


Figure 4.2.13. hAtg3 is cleaved by rCaspase-3, -6, -8 and rCalpain 1. TNT reactions were prepared for the pFLAG-Atg3-myc/His in the presence of Transcend™ tRNA. Samples were then incubated with recombinant caspase-3,-6,-8 and calpain 1 (in the presence of 20 mM Ca²⁺). After 60 min at 37 °C, the reaction was stopped with 2xSDS sample buffer, run on SDS-PAGE and immunoblotted using Strep-HRP and anti-myc (**A**). Arrows denote full length form; arrowheads indicate cleavage fragments. * indicates the possible alternate form of hAtg3 as discussed in the text. The protein sequence of pFLAG-Atg3-myc/His, showing the predicted caspase (blue, underlined residues) and calpain (green, underlined residues) cleavage sites (**B**). The N-terminal FLAG epitope tag is in red and the 3' vector sequence and C-terminal myc/His tags are underlined and in italics.

4.2.5. A minor amount of Beclin 1 is cleaved during K⁺ withdrawal-induced cell death in CGNs

In order to confirm the significance of the cleavage of the hAtg proteins, it was necessary to assess their cleavage in a cell culture model under apoptotic conditions. Beclin 1 is a key regulator of the autophagic response and its interaction with the BCL2 proteins suggest that it may play a role in both autophagy and apoptotic cell death. For this reason, the cleavage of Beclin 1 was evaluated during K⁺ withdrawal-induced cell death in CGNs. The CGN lysates that were prepared from CGNs in K5 in the presence of the caspase inhibitors z-VAD.fmk and DEVD.fmk as used in the previous chapter (Figure 3.2.8 & 3.2.10), were separated by SDS-PAGE and immunoblotted for Beclin 1.

The cleavage of Beclin 1 was evident in the lysates prepared from the apoptotic K5 CGNs (Figure 4.2.14). The cleavage fragments (~48 and 50 kDa) were consistent with that previously demonstrated in the *in vitro* cleavage of Beclin 1 by rCaspase-3 (Figure 4.2.4 A). The addition of DEVD.fmk to the K5 CGNs did not inhibit Beclin 1 cleavage (Lane 5). The remaining cleavage was possibly due to caspases activated during the cell death process that are not inhibited by DEVD.fmk, such as caspase-6 (Allsopp *et al.*, 2000; Canu *et al.*, 2005; Rouaux *et al.*, 2003). In contrast, z-VAD.fmk partially abrogated the cleavage of Beclin 1 (Figure 4.2.14, Lane 4). Whilst z-VAD.fmk was previously demonstrated to inhibit caspase-3 in these lysates (Figure 3.2.9), other caspases implicated in this pathway were not investigated and their activation may account for the incomplete inhibition of Beclin 1 cleavage by z-VAD.fmk. However, there was no loss of full length Beclin 1 in the lysates prepared from apoptotic CGNs, and in contrast to the full length form, the amount of cleavage was minimal. This suggests that the majority of Beclin 1 in CGNs during K⁺ withdrawal-induced cell death remains uncleaved. Furthermore, this experiment was only carried out once and therefore requires further investigation to conclude whether the caspase processing of Beclin 1 occurs.

These data suggest that there is a minor amount of Beclin 1 cleavage during K⁺ withdrawal-induced cell death in CGNs, verifying the *in vitro* findings. The *in vitro* cleavage of the hAtg proteins by the cell death proteases, rCaspase-3, -6, -8 and rCalpain 1 suggest that the autophagic process is regulated by multiple uncharacterised mechanisms. The finding that several of the potential cleavage sites fall in domains that are critical for the induction of the autophagic response is of particular interest.

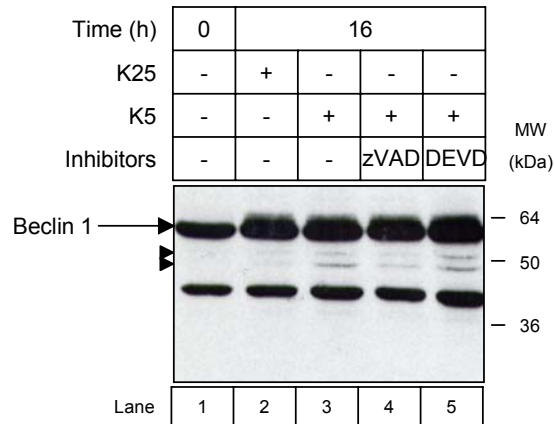


Figure 4.2.14. Beclin 1 is cleaved in CGNs undergoing cell death through K⁺ withdrawal. CGNs (DIV7) were preincubated for 1 h with zVAD.fmk (100 μ M) or DEVD.fmk (50 μ M), treated with K5 for 16 h, and lysates prepared for Beclin 1 immunoblot. Arrowheads indicate cleavage fragments.

4.3. Discussion

The regulation of the autophagic and apoptotic response has previously been shown to require components that are involved in both processes. These include the anti-apoptotic BCL2 family and their interaction with Beclin 1 (Maiuri *et al.*, 2007a; Pattingre *et al.*, 2005; Shimizu *et al.*, 2004), the interaction of Atg5 with FADD (Pyo *et al.*, 2005), the truncation of Atg5 by calpain 1 and 2 (Yousefi *et al.*, 2006) and control of the pathways by caspase-8 (Yu *et al.*, 2004) and calpain 1 and 2 (Demarchi *et al.*, 2006; Madden *et al.*, 2007).

Here I have demonstrated for the first time the *in vitro* cleavage of a large number of the hAtg proteins by rCaspase-3, rCaspase-6, rCaspase-8 and rCalpain 1. An *in vitro* approach was employed for preliminary studies in an attempt to identify initial targets for further investigation and for easier identification of the regions involved, using epitope tags. Furthermore, due to the lack of specific antibodies for the Atg proteins, epitope tagged constructs would be required to detect overexpression in cell culture models. Importantly, the cleavage of Beclin 1 was also shown in lysates from apoptotic CGNs.

The *in vitro* cleavage of Beclin 1 by rCaspase-3, -6 and rCalpain 1 was demonstrated at sites that are conserved in the mouse and rat. The caspase cleavage sites were predicted to fall in the region that is thought to interact with the BCL2 anti-apoptotic family members – BCL2, BCLxL, BCLW (Erllich *et al.*, 2007); with several of the sites specifically located in the BH3 domain of Beclin 1 (Maiuri *et al.*, 2007a; Oberstein *et al.*, 2007). This would suggest that the tight regulation of Beclin 1 by the BCL2 family members would be abolished during apoptosis (Pattingre *et al.*, 2005), while the other domains in Beclin 1 (those capable of interacting with nPIST, UVRAG and Vps34) would remain intact (Furuya *et al.*, 2005; Liang *et al.*, 2006; Yue *et al.*, 2002). Following cleavage, Beclin 1 may then be considered a pro-autophagic factor, being capable of initiating a sustained autophagic response in the absence of its regulation by the BCL2 family proteins (Figure 4.3.1). This is in direct contrast to the pro-apoptotic truncation of Atg5 by calpain 1 and 2 (Yousefi *et al.*, 2006).

The 'doublet' of cleavage fragments observed upon incubation of Beclin 1 with rCaspase-3 was also demonstrated during K⁺ withdrawal-induced cell death in CGNs. The caspase cleavage of Beclin 1 was partially negated in the presence of z-VAD.fmk.

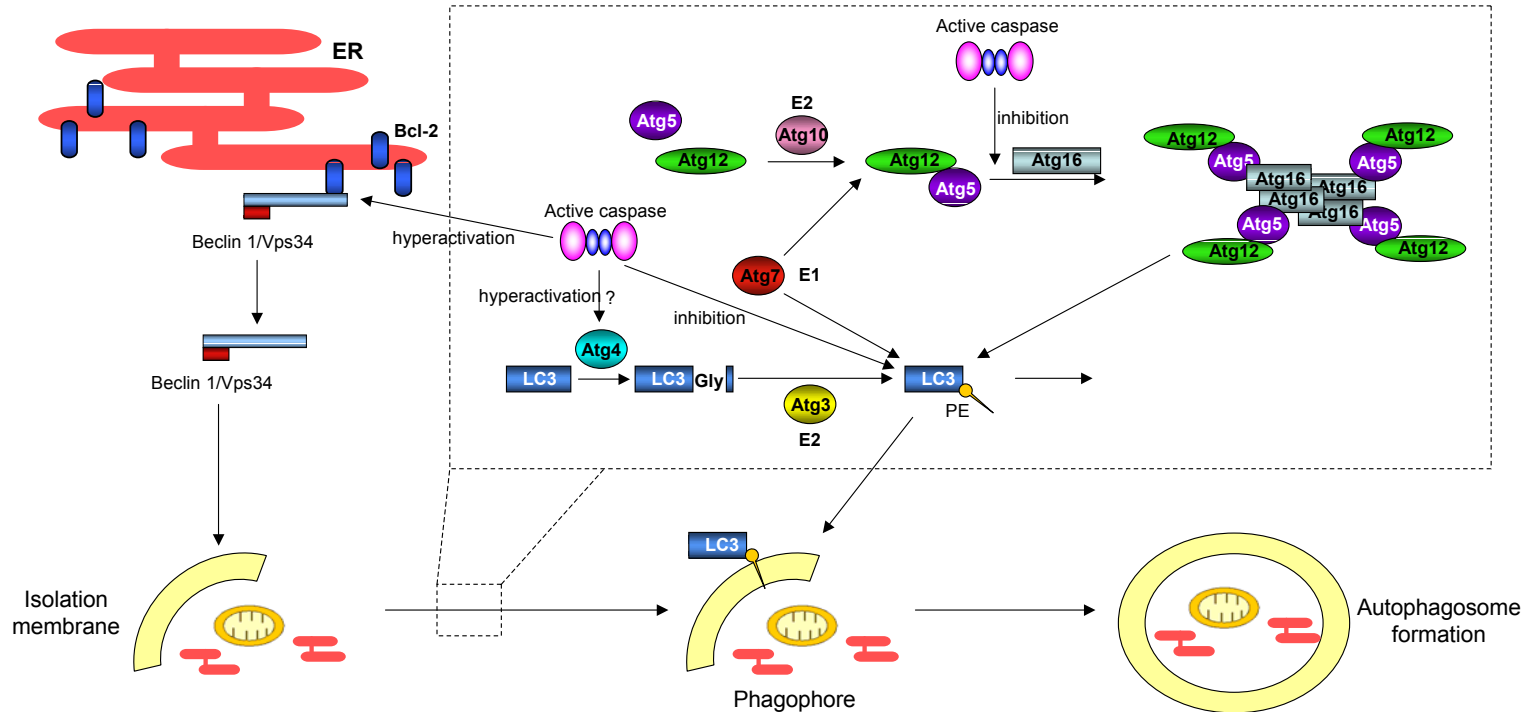


Figure 4.2.15. The cleavage of the hAtg proteins by active caspases. The formation of the multiprotein complex of Beclin-1, Vps34 (shown above), UVRAG and Vps15 in humans activates Vps34, one of the initial steps of vesicle nucleation for autophagosome formation. The elongation and shape of the autophagosome is determined by two sequential protein conjugation pathways, which result in the lipidation of LC3 with phosphatidylethanolamine (PE) and its specific recruitment to autophagosomes. Upon the simultaneous induction of the apoptotic pathway for example with staurosporine, the activation of caspases may result in the inhibition of autophagy through cleavage of several hAtg proteins, or their hyperactivation as shown, resulting in a sustained autophagic response.

However, the inhibition of other caspases activated during K⁺ withdrawal, by z-VAD.fmk was not investigated and therefore cannot be ruled out. The addition of the caspase inhibitor DEVD.fmk had no effect on the production of Beclin 1 cleavage fragments. This suggests that a caspase that is not inhibited by DEVD.fmk is cleaving Beclin 1 in this system. A candidate for this may be caspase-6, whose activation has previously been proposed to be upstream that of caspase-3 in CGNs undergoing apoptosis through the withdrawal of K⁺ (Allsopp *et al.*, 2000; Canu *et al.*, 2005; Rouaux *et al.*, 2003). Although caspase-3 activity predominates in CGN apoptosis, caspase-6 activity was elevated within 1 h of the withdrawal of K⁺ and was constant throughout the apoptotic process (Allsopp *et al.*, 2000; Canu *et al.*, 2005; Rouaux *et al.*, 2003). Interestingly a role for caspase-6 has also been proposed in Huntington's disease, by the specific caspase-6 cleavage of huntingtin leading to the dysfunction and degeneration of neurons (Graham *et al.*, 2006). These data suggest an upstream role for caspase-6, independent of apoptosis.

The early features of autophagy during K⁺ withdrawal-induced cell death have been demonstrated in Chapter 3, with the level of autophagy enhanced in the presence of the caspase inhibitors (Figure 3.2.10) and in other studies (Xue *et al.*, 1999). In the absence of caspase activation, uncleaved Beclin 1 would be able to induce autophagy, as the necessary domains are intact. However, it is probable that the cleavage of Beclin 1 would have a negligible impact on its function in autophagy and apoptosis in CGNs during K⁺ withdrawal-induced cell death, as the amount of cleavage observed in comparison with the full-length form of Beclin 1 was minor.

While calpains have been implicated in apoptosis and are thought to be essential in necrotic cell death, their functions are not wholly limited to that of a cell death protease. Calpains have also been implicated in processes such as cell cycle progression and cell mobility (Huttenlocher *et al.*, 1997; Santella *et al.*, 1998). A role for calpain has also been proposed in autophagy. Defective autophagy induction, autophagosome formation and long-lived protein degradation was demonstrated in MEFs derived from mice containing a targeted knockout of the regulatory subunit of calpain (CAPNS1^{-/-}) (Demarchi *et al.*, 2006). They proposed that calpain may modulate the actions of one or more of the components of the autophagic pathway. This is consistent with the findings in this study, where I have shown calpain 1 cleaves several of the hAtg proteins in this.

The cleavage of Beclin 1 by rCalpain 1 resulted in several cleavage fragments. The cleavage site of one did not fall within any of the identified domains of interest within Beclin 1 and therefore the effect on the action of Beclin 1 cannot be predicted. Alternative cleavage sites were predicted within the domains that have been demonstrated to interact with the proteins nPIST, UVRAG or Vps34. The interaction of a nPIST with Beclin 1 provides a physical link between the Glutamate receptor $\delta 2$ (GluR $\delta 2$) and the induction of autophagy. It was suggested that nPIST modulates the ability of Beclin 1 to induce autophagy (Yue *et al.*, 2002). This is of particular importance in the heterozygous *lurcher* mutant mice, a model of neurodegeneration, in which the constitutive activation of the GluR $\delta 2^{Lc}$ causes an inward current and 'autophagic' cell death of cerebellar Purkinje cells (Yue *et al.*, 2002). In response to GluR $\delta 2^{Lc}$, Beclin 1 alone, or Beclin 1 and nPIST are released from the complex and activate autophagy in Purkinje cells (Yue *et al.*, 2002). It is possible that the cleavage of the coiled-coil domain of Beclin 1 by calpain 1 is responsible for the induction of autophagy in these cells. In contrast however, cleavage of the coiled-coil domain or the ECD, which interact with UVRAG and Vps34 respectively, would be predicted to inactivate an autophagic response (Figure 4.3.2, (Furuya *et al.*, 2005; Liang *et al.*, 2006)).

hAtg4D was cleaved by caspase-3 (and to a lesser extent by caspase-7) in this *in vitro* analysis. The caspase-3 mediated cleavage of hAtg4D at a canonical caspase cleavage site DEVD was previously reported (He and Orvedahl, 2007). In this study they demonstrated cleavage of hAtg4D by caspase-3 enhanced the cleavage of GATE-16 and GABARAP, a step that is required for their lipidation and autophagosome membrane formation. Overexpression of a cleaved form of hAtg4D (hAtg4d-63) significantly increased cell death (He and Orvedahl, 2007). The authors suggested that the cleavage of hAtg4D by caspase-3 is an activation event that coordinates autophagy with cell death induction (He and Orvedahl, 2007). In addition, the canonical DEVD cleavage site previously identified was conserved in hAtg4C, which was also found to be an *in vitro* substrate of caspase-3.

hAtg4A and hAtg4B were shown to be equally cleaved by caspase-3. Sequence alignment of the amino acid sequences of the four human homologues of Atg4 revealed that the sequence prior to and including the canonical DEVD motif is absent from the primary sequences of hAtg4A and hAtg4B (Marino *et al.*, 2003). It is possible that hAtg4A and hAtg4B do not require this N-terminal cleavage by caspase-3 for their activation, being already present in their 'active' form and able to effectively mediate

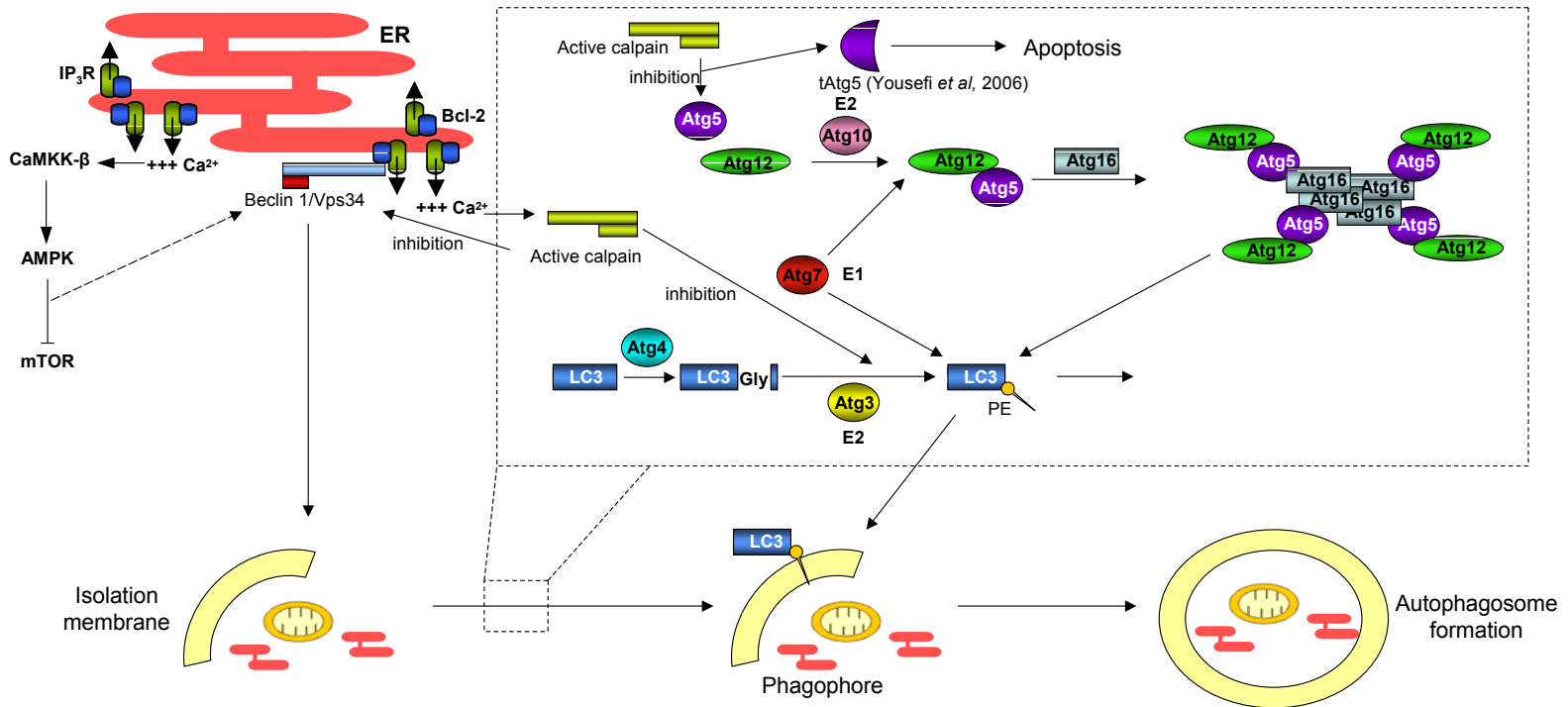


Figure 4.2.16. The cleavage of the hAtg proteins by calpain 1. Høyer-Hansen *et al*, 2007 described the activation of CaMKK-β in response to release of Ca²⁺ from ER stores by thapsigargin for example. It then phosphorylates and activates AMPK, which inhibits mTOR kinase activity, inducing autophagy. The activation of calpain 1 by the local increase in cytosolic concentration of Ca²⁺ may inhibit the autophagic response through the cleavage of several hAtg proteins. Bcl-2 modulates the release of Ca²⁺ from the ER.

the exposure of the essential Gly residue of LC3, GABARAP and GATE-16 required for lipidation (Scherz-Shouval *et al.*, 2003; Tanida *et al.*, 2004a). Given that autophagy is able to proceed in the absence of apoptosis, it is reasonable to suggest that under normal autophagy-inducing conditions, hAtg4A and hAtg4B are able to mediate the efficient cleavage of LC3, GABARAP and GATE-16. In apoptotic conditions the caspase-3 mediated hyperactivation of all hAtg4 homologues would cause excessive autophagy and cell death. This hypothesis is consistent with the findings of López-Otín and colleagues, who demonstrated that Atg4C is only required for a proper autophagic response under stressful conditions (Marino *et al.*, 2007).

The cleavage of Atg5 by caspase-3 at either its N- or C-terminal was predicted to interfere with its interaction with Atg16 with all sites being conserved in the mouse. The formation of the Atg12-Atg5-Atg16 multimeric complex; Atg16 directly interacting with Atg5, is an essential part of the protein conjugation system required for autophagy (Kuma *et al.*, 2002; Matsushita *et al.*, 2007; Mizushima *et al.*, 1999). The crucial nature of the Atg5-Atg16 interaction is also evidenced from the early death of *ATG5*^{-/-} mice due to a loss of autophagy (Kuma *et al.*, 2004). The consequence therefore of the disruption of the Atg5-Atg16 complex would be the inactivation of the autophagic response (Figure 4.3.1). Equally, the cleavage sites of caspase-3, -6 or -8 in Atg3 are predicted to fall in the region that is required for its interaction with Atg7 (Yamada *et al.*, 2007) and are conserved in the mouse and rat. As previously described, Atg7 and Atg3 are the E1 and E2 enzymes respectively that catalyse the lipidation of Atg8 (LC3, GATE-16 or GABARAP) (Ichimura *et al.*, 2000; Tanida *et al.*, 2003; Tanida *et al.*, 2002). Therefore, disruption of this association would inhibit the autophagic response (Figure 4.3.1). This interaction is particularly important in neuronal systems, given that Atg7 is essential for autophagy associated with axonal homeostasis and in the prevention of neuronal degeneration in *Drosophila* (Juhász *et al.*, 2007; Komatsu *et al.*, 2007). Interestingly, caspase-8 has previously been proposed to play a role in the regulation of Beclin 1/Atg7-dependent autophagy and cell death (Madden *et al.*, 2007; Yu *et al.*, 2004). It is possible that the enhanced level of autophagy observed during K⁺ withdrawal-induced cell death in CGNs in the presence of z-VAD.fmk is the result of the inhibition of caspase-mediated disruption of the interactions between Atg5 with Atg16 and Atg3 with Atg7. Autophagy will then predominate as demonstrated. Furthermore the cleavage of Atg3 by calpain 1 in the region separating the domains that interact with Atg7 and Atg8 may result in uncoordinated conjugate formation and inefficient autophagy induction (Yamada *et al.*, 2007). This site is also conserved in the mouse and rat.

The C-terminus of Atg7 has been proposed to be essential for its E1 activity for Atg12 and Atg8 and its E1-E2 complex formation with Atg3 (Komatsu *et al.*, 2001).

Interestingly, none of the predicted caspase-3 or calpain 1 cleavage sites were predicted to fall within this region, therefore a minimal effect on autophagy would be predicted following hAtg7 cleavage. In addition, given that the C-terminal of Atg12 is essential for the conjugate formation catalysed by the E2-like enzyme Atg10 and the assembly of the Atg12-Atg5-Atg16 complex (Hanada and Ohsumi, 2005), it is unlikely that calpain 1 cleavage at the N-terminus of hAtg12 will have a profound impact on its autophagic role.

The potential calpain-cleavage site in GABARAP was mapped to its C-terminus. This region is involved in its conjugation with phosphatidylethanolamine (PE) during autophagy; it is likely therefore that modulation of GABARAP by calpain will affect its role in autophagy. However, the importance of GABARAP in the autophagic pathway remains to be determined. Similarly, the function of Atg9 is yet to be fully characterised. During starvation-induced autophagy in HEK-293 cells, Atg9 only partially localised with LC3, suggesting that it may have an additional role (Young *et al.*, 2006). Until further functions have been identified it is difficult to comment on the significance of cleavage by proteases in addition to those already presented here.

While further work in cell lines is required to identify the particular protease cleavages that predominate under autophagic and apoptotic conditions; this study has provided the foundations for future characterisation of the potential regulation of the cell death pathways by proteases. Figure 4.3.1 and 4.3.2 illustrate the potential cleavages of the hAtg proteins identified in this *in vitro* assay by active caspases and calpain during cell death and the possible regulation of the autophagic process.

Chapter 5

The Modulation of the BCL2 Family Proteins by HDACi in CGNs

5.1. Introduction

The induction of autophagy in models of neurodegenerative diseases is thought to be a compensatory defence against the accumulation of ubiquitinated proteins due to the loss of proteasomal activity. The histone deacetylase, HDAC6 is proposed to mediate the transport of polyubiquitinated proteins to aggresomes and the subsequent induction of autophagy in cell lines and in *Drosophila* (Iwata *et al.*, 2005; Kawaguchi *et al.*, 2003; Pandey *et al.*, 2007).

Interestingly, histone deacetylase inhibitors (HDACi) have been demonstrated to protect against oxidative stress-induced death in cortical neurons (Langley *et al.*, 2008), lipopolysaccharide-induced neurotoxicity in mesencephalic neuron-glia cultures (Chen *et al.*, 2007), and glutamate-induced excitotoxicity in CGNs, alone (Leng and Chuang, 2006) and in combination with lithium (Leng *et al.*, 2008). In addition they have been reported to arrest degeneration in the N171-82Q transgenic mouse model of Huntington's disease (HD) (Gardian *et al.*, 2005) and in *Drosophila* expressing the polyglutamine-containing domain of huntingtin (Htt) (Steffan *et al.*, 2001). Furthermore, they provided protection in several models of ischemia (Kim *et al.*, 2007; Ren *et al.*, 2004) and enhanced memory and learning in mice (Fischer *et al.*, 2007; Vecsey *et al.*, 2007).

Dysfunction of gene transcription is an early feature in cell culture and animal models of polyglutamine diseases such as HD (Cha *et al.*, 1998). The opposing activities of histone acetyltransferases (HATs) and histone deacetylases (HDACs) tightly regulate gene transcription by controlling the acetylation and deacetylation of histones. The opening of the chromatin structure by the transfer of acetyl groups to N-terminal lysines in histones is catalysed by HAT's and allows regulatory proteins increased accessibility to the DNA. In contrast, HDACs remove acetyl groups from histones, resulting in chromatin condensation and gene repression (Bolden *et al.*, 2006; Butler and Bates, 2006). Reductions in the level of acetyltransferase activity, particularly that of cAMP response element binding protein (CREB)-binding protein (CBP), due to its interaction with proteins containing expanded polyglutamine domains has been reported in patient tissues, cell culture models (McCampbell *et al.*, 2000), animal models (Steffan *et al.*, 2000), *Drosophila* (Steffan *et al.*, 2001; Taylor *et al.*, 2003b) and *C. elegans* (Bates *et al.*, 2006). HDACi enhance gene transcription by inhibiting the deacetylation of histones by HDACs; favouring acetylation by HATs.

HDACi have been investigated for their use as cancer therapeutics for a number of years and Phase I/II clinical trials are currently underway for their treatment of patients (Minucci and Pelicci, 2006). In addition, the HDACi phenylbutyrate has been used to treat patients with cystic fibrosis, sickle cell anaemia, thalassemia and urea cycle disorders (Gardian *et al.*, 2005) and valproic acid (VPA) is commonly used as an anticonvulsant and mood-stabiliser (Jeong *et al.*, 2003). Taken together, HDACi seem promising agents for the treatment of neurodegenerative conditions.

The aim of this study is to investigate the consequences of HDAC inhibition in CGNs to fully understand their actions in the absence of other cell death stimuli. This will potentially allow the identification of further targets for therapy and aid in the understanding of off-target effects. In order to highlight potential modulations by HDACi, CGNs were treated with the broad spectrum HDACi, Trichostatin A (TSA), (Furumai *et al.*, 2001), and its effect at different developmental stages of CGN cultures was determined.

5.2. Results

5.2.1. Multiple HDACs are expressed in CGNs.

Human HDACs are divided into four classes based on their similarity to yeast HDACs, their enzyme activities and subcellular localisation (Bolden *et al.*, 2006). The class I HDACs – HDAC1, 2, 3 and 8 are expressed in most cell types and are found almost exclusively in the nucleus. The expression of HDAC4, 5, 6, 7, 9 and 10 (the class II HDACs) is more tissue specific. Class II HDACs seem to shuttle between the nucleus and the cytoplasm in response to certain cellular signals (de Ruijter *et al.*, 2003). The sole member of class IV is the novel HDAC11 (Gao *et al.*, 2002). In addition, homologues of the yeast protein Sir2 (SIRT1-7) are members of the class III HDACs; these fall outside of the scope of this study (Bolden *et al.*, 2006).

To fully investigate the effects of HDACi in CGNs, lysates were prepared from CGNs at DIV7 and the expression of a panel of class I and class II HDACs were compared with those from Mouse Embryonic Fibroblasts (MEFs) and human SH-SY5Y cells. All cells expressed the class I HDACs, HDAC 1, HDAC2 and HDAC3 and the Class II HDACs, HDAC4 and HDAC6 (Figure 5.2.1). The level of HDAC7 was barely detectable in all cells and HDAC5 was observed as a doublet in CGNs, consistent with its reported phosphorylation by calcium/calmodulin-dependent kinases (CaMK) in CGNs (Linseman *et al.*, 2003). The phosphorylation of HDAC4 and HDAC5 in CGNs results in their docking to cytoplasmic 14-3-3 proteins and their nuclear exclusion. This is proposed to be important for the activity of myocyte enhancer factor-2 (MEF2) transcription factors in mediating CGN survival (Bolger and Yao, 2005; Linseman *et al.*, 2003). HDAC8 was detected in the lysates from CGNs and MEFs. Antibodies for the detection of HDAC9 and 10 were not available for this study.

5.2.2. The HDACi, TSA, induces rapid cell death in CGNs treated at DIV1, yet survival is maintained when treated at DIV7.

By 7 days *in vitro* (DIV7), CGNs have acquired many features of mature neurons (Contestabile, 2002). Although the neuroprotective mechanisms of HDACi has been well documented in differentiated, 'mature' neurons their effects on undeveloped neurons is lacking. With this in mind and in an attempt to fully understand the effects of HDACi, CGNs (DIV1) were treated with TSA, which inhibits both class I and class II HDACs (Furumai *et al.*, 2001). At the indicated times CGNs were fixed for imaging, cell

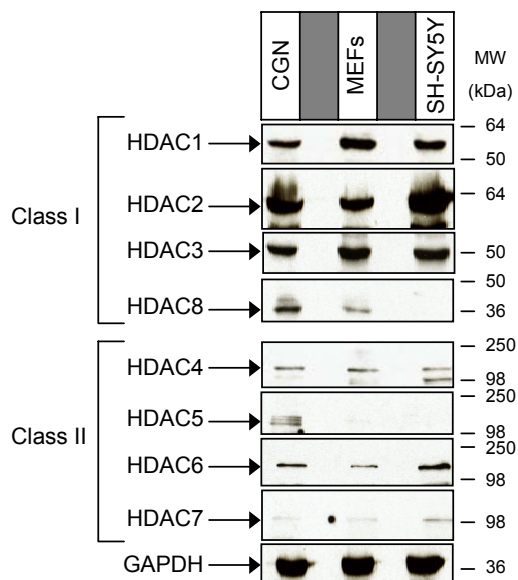


Figure 5.2.1. HDAC protein expression in CGNs, MEFs and SH-SY5Y cells. CGN (DIV7), MEFs and SH-SY5Y cell lysates (50 μ g) were separated by SDS-PAGE and immunoblotted for HDAC1-8 and GAPDH.

viability was assessed using H33342/SYTOX nuclear staining and the MTT assay, and lysates were prepared for immunoblot. A loss of MTT reduction would be expected if TSA was causing a loss of neuronal viability.

TSA induced the death of CGNs after treatment for 24 h in contrast with the CGNs treated with the vehicle control DMSO (Figure 5.2.2 A). This was evidenced by the absence of neurite growth in the TSA treated CGNs. The loss in the mitochondria's ability to reduce MTT was observed in a time dependent manner at all concentrations of TSA (Figure 5.2.2 B). Furthermore, the time dependent increase in apoptotic cells was also demonstrated. Apoptotic cells in the vehicle control neurons was 4% at 8 h, $4\% \pm 1\%$ at 16 h and $5\% \pm 1\%$ at 24 h (data not shown)

The ability of TSA to inhibit HDACs was confirmed by the accumulation of acetylated histone-3 (ACh3), a well characterised substrate of HDACs (Figure 5.2.3). This was apparent by 8 h and the level of ACh3 increased further at 16 and 24 h. Caspase-9 is autoprocessed at the apoptosome to its p35 form (Li *et al.*, 1997). However, mouse caspase-9 is larger and this corresponds to the p39 fragment that was initially observed, 8 h after treatment with TSA and additionally accumulated by 16 and 24 h (Figure 5.2.3). In addition, once caspase-9 has processed caspase-3 at Asp175, caspase-3 feeds back on caspase-9, resulting in the p37 form, which seemed to be the p42 caspase-9 fragment in the mouse. Therefore, while the active p17 form of caspase-3 was demonstrated at 8 h using the cleaved caspase-3 (p17) antibody, processing of caspase-9 to the p42 form was not observed until 16 h of TSA treatment, when the level of p17 caspase-3 was enhanced (Srinivasula *et al.*, 2001). The cleavage of caspase-7 was also obvious at 16-24 h as demonstrated by the cleavage to its p32, p22 and p19 forms (Denault and Salveson, 2003).

In contrast to the rapid apoptotic cell death induced by the treatment of CGNs with TSA at DIV1, in CGNs treated at DIV7, the ability of the mitochondria to reduce MTT was not affected until 48 h (Figure 5.2.4 A). Even at this time, the loss in MTT reduction was minimal. By 72 h of TSA treatment, the ability to reduce MTT had significantly declined. The levels of apoptotic cells were also elevated at 72 h in the CGNs treated with 250 nM and 500 nM TSA. The levels of apoptotic cells in the time control neurons remained at 1% throughout the experiment (data not shown).

The autoprocessed form of caspase-9 (p39) was apparent in CGNs (DIV7) treated with TSA for 24 h (Figure 5.2.4 B; Lanes 2-4). At 48 h and 72 h the p39 fragment of

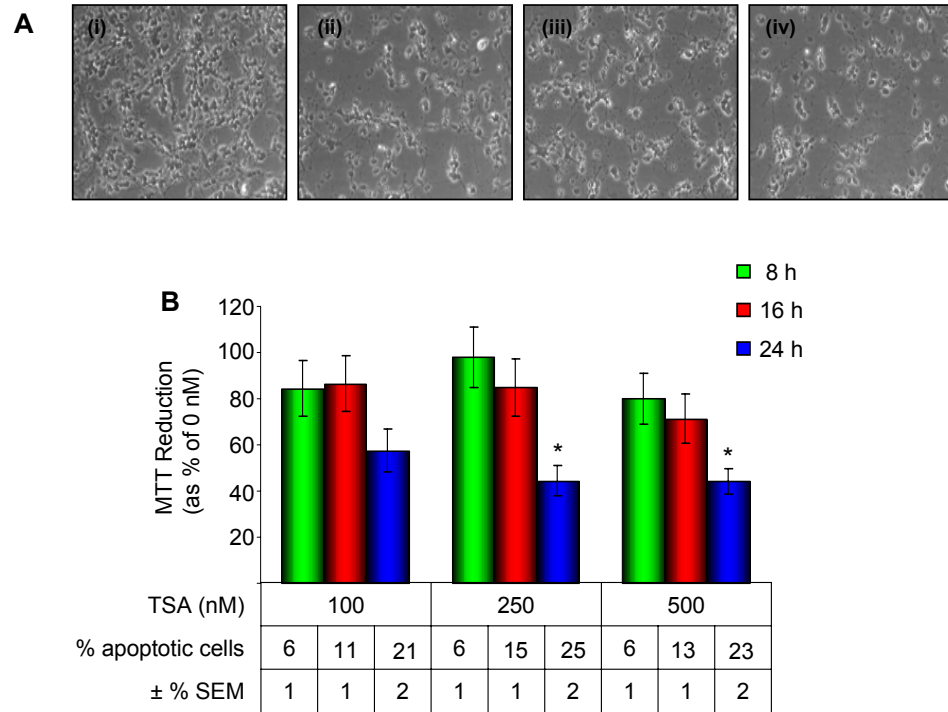


Figure 5.2.2. TSA induces apoptosis at DIV1. CGNs (18-24 h after plating) were treated with either (i) vehicle control or increasing concentrations of TSA (ii) 100 nM, (iii) 250 nM, (iv) 500 nM and fixed for phase contrast imaging at 24 h (**A**) or cell viability was assessed using the MTT assay and H33342/SYTOX nuclear staining at 8-24 h (**B**). * $p \leq 0.05$

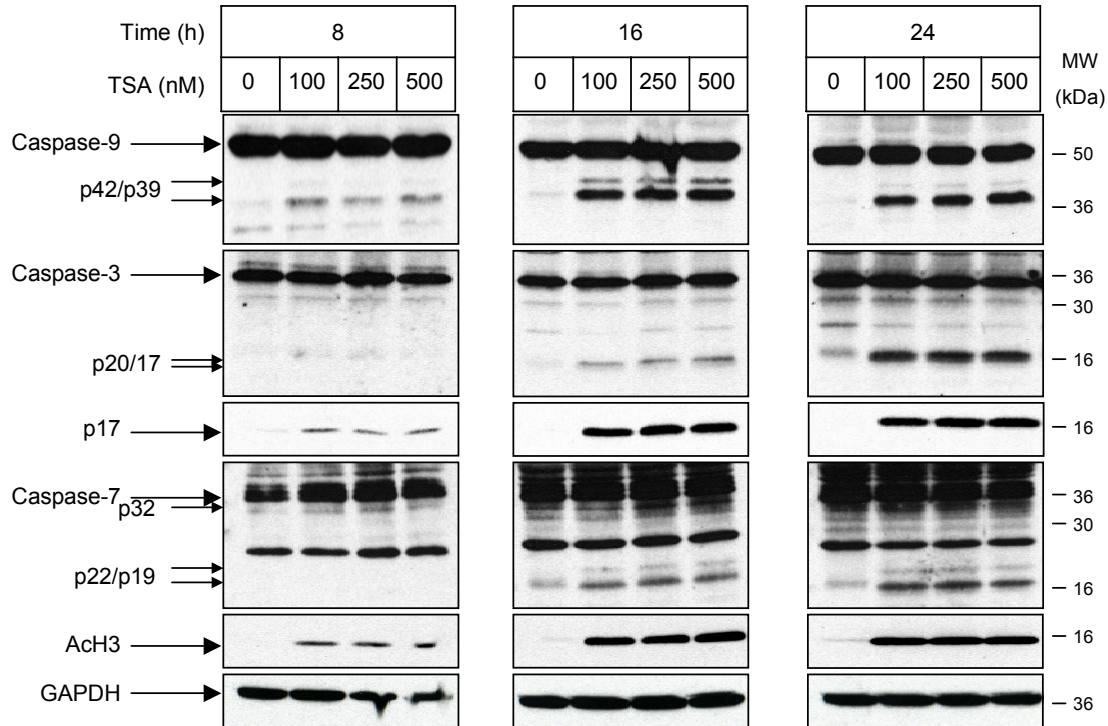


Figure 5.2.3. TSA induces caspase cleavage in immature CGNs. CGNs (18-24 h after plating) were treated with TSA for 8-24 h. Lysates were separated by SDS-PAGE and immunoblotted for caspase-9, -3, -7, cleaved caspase-3 (p17), AcH3 and GAPDH.

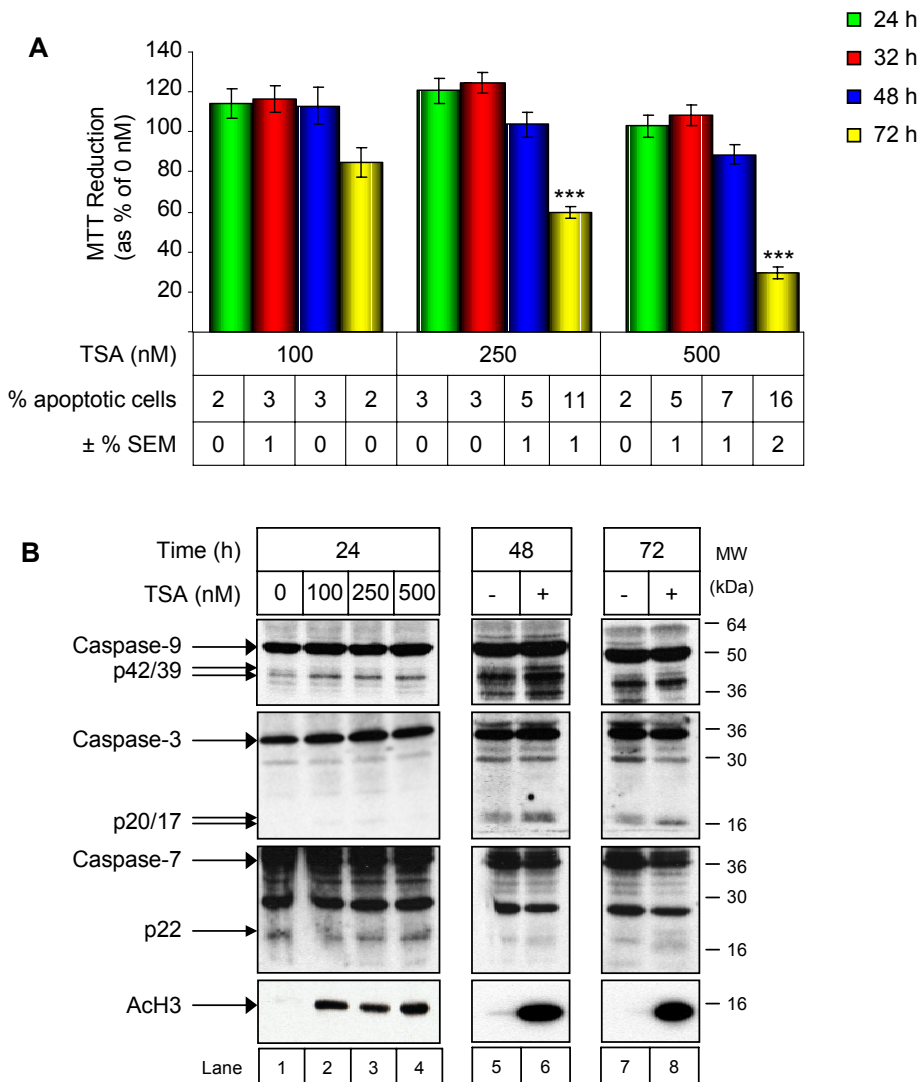


Figure 5.2.4. The survival of mature CGNs (DIV7) is maintained up to 72 h after TSA treatment. CGNs were treated with TSA (100-500 nM) and cell viability was assessed using the MTT assay and nuclear staining with H33342/SYTOX after 24-72 h (A). Data expressed as mean ± % SEM from three independent cultures. *** $p \leq 0.001$ At these times lysates were also prepared, separated by SDS-PAGE and immunoblotted for caspase-9, -3, -7 and ACh3 (B).

caspase-9 was markedly enhanced when compared to that at 24 h (compare Lanes 6 and 8 with 2-4). However, the p39 form of caspase-9 was also observed at 48 h and 72 h in the vehicle control CGNs (VC; Lanes 5 and 7). This indicates that control CGNs were also undergoing apoptosis at these times. The p42 form of caspase-9 was observed in CGNs at 48 h of TSA treatment, suggesting that caspase-3 was active in these lysates (Lane 6). There was no cleavage of caspase-3 and caspase-7 in CGNs (DIV7) treated with TSA for 24 h (Lanes 2-4). The p20/17 fragments of caspase-3 were observed at 48 h and 72 h of TSA treatment, corresponding with its cleavage of caspase-9 (p42). However, the p20 form of caspase-3 was also present in the lysates from the corresponding time controls as shown for caspase-9 (Lanes 5 and 7). The p22 form of caspase-7 was detected at a very low level after 72 h of TSA treatment (Lane 8). From observation of the CGN cultures under the light microscope, there appeared to be some neurite degeneration in both the VC CGNs and those treated with TSA at 72 h. Taken together this suggests that there may be age-related degeneration of the CGN cultures; however this requires further confirmation with experimental data.

These data suggest that undifferentiated neurons respond to HDAC inhibition by inducing apoptosis. In contrast, the survival of mature neurons is maintained even in the presence of HDAC inhibition.

5.2.3. The 'switch' between the induction of cell death or the continued survival of CGNs after 24 h treatment with TSA is at approximately DIV4

Previous studies have proposed that the developmental stage of the neuron is an important factor that determines whether a single agent will induce apoptosis or promote survival (D'Mello *et al.*, 1994; Levick *et al.*, 1995). To identify the time in culture at which TSA mediates the 'switch' from cell death induction to having little effect on the CGNs and to explore the possible mechanisms of this action, CGNs at DIV1, 3, 5, 7 and 9 were treated with TSA for 24 h. Their viability was then assessed using the MTT assay and the nuclear stains H33342/SYTOX.

The treatment of CGNs at DIV1 and DIV3 with TSA for 24 h induced apoptotic cell death in a concentration dependent manner. This was demonstrated by the highly significant loss in the ability to reduce MTT by the mitochondria and the elevated levels of apoptotic cells (Figure 5.2.5 A). By DIV5, the loss of MTT reduction was markedly reduced and did not greatly differ from the corresponding vehicle control. This trend was further observed in CGNs at DIV7 and DIV9.

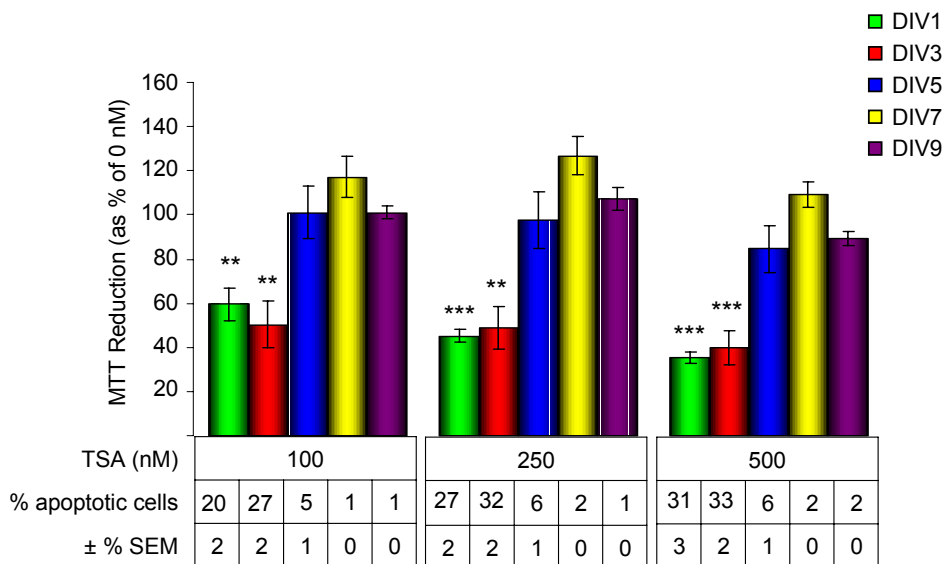


Figure 5.2.5. The ‘switch’ in the differential response of CGNs to TSA occurs around DIV4. CGNs were treated with TSA (100-500 nM) for 24 h at the indicated time in culture and cell viability was assessed using the MTT assay and H33342/SYTOX nuclear staining. Data expressed as mean \pm % SEM from three independent cultures. ** $p \leq 0.01$, *** $p \leq 0.001$.

During the development of the nervous system and throughout adult life, the BCL2 family are critical for the maintenance of neurons. Although BCL2 knockout mice did not display gross phenotypic abnormalities in the CNS (Veis *et al.*, 1993); massive cell death was observed in the brain, dorsal root ganglia and spinal cord of BCLxL^{-/-} mice (Motoyama *et al.*, 1995). The differential expression of the BCL2 family proteins during the development of CGNs in culture was therefore investigated in an attempt to identify possible candidates for the continuation of CGN survival at DIV7. For this purpose, CGNs were lysed at DIV1, 3, 5 and 7 and immunoblotted for various BCL2 family proteins. Whilst densitometry was performed to quantify the level of protein expression of the BCL2 family, some of the immunoblots were highly saturated. Thus, the estimation of protein levels was not highly accurate. In addition, the experiment was repeated in three independent cultures, however due to the reduced viability of the third, only the results for two of the cultures are presented here.

The expression of the anti-apoptotic proteins, BCLxL and MCL1 were greatly reduced in CGNs over time in culture, particularly by DIV5 and DIV7 (Figure 5.2.6 A and B). Interestingly, both BCLxL and MCL1 migrated as doublets on SDS-PAGE. The upper form of BCLxL is probably the deamidated form of the protein, whereas the lower band represents the transamidated form of BCLxL (Aritomi *et al.*, 1997). MCL1 migrates as a doublet on SDS-PAGE as the full length protein and probably a modified form of the protein (lower and upper bands respectively); both bands were reduced in MEFs upon treatment with siRNA for MCL1 (data not shown, experiment performed by Dr. S. Inoue). A decrease in the expression of BAX, BID and the alternatively spliced forms of BIM - BIM_{EL} and BIM_L (O'Connor *et al.*, 1998) was also demonstrated. The reduction in BIM_{EL/L} is consistent with its transcriptional regulation in many cell types (Putcha *et al.*, 2001). The expression of BCL2 and BAD was inconsistent over time. The expression of the α and β forms of PUMA were greatly increased in CGN cultures between DIV3 and DIV7 when compared against their expression at DIV1.

Interestingly, the expression of the alternatively spliced form of BAK (N-BAK) at ~16 kDa (Sun *et al.*, 2003; Sun *et al.*, 2001; Uo *et al.*, 2005) was elevated at DIV5 and 7 (Figure 5.2.6 A and B). Upon overexpression in noneuronal cells, N-BAK was shown to be a proapoptotic BH3-only protein, while it was neuroprotective in neuronal cells (Sun *et al.*, 2003; Sun *et al.*, 2001). In contrast however, a subsequent study in cortical, hippocampal and cerebellar granule neurons demonstrated that N-BAK functions as a BAX-dependent proapoptotic BH3-only protein by interacting with BCLxL and promoting BAX translocation to the mitochondria (Uo *et al.*, 2005). The role of

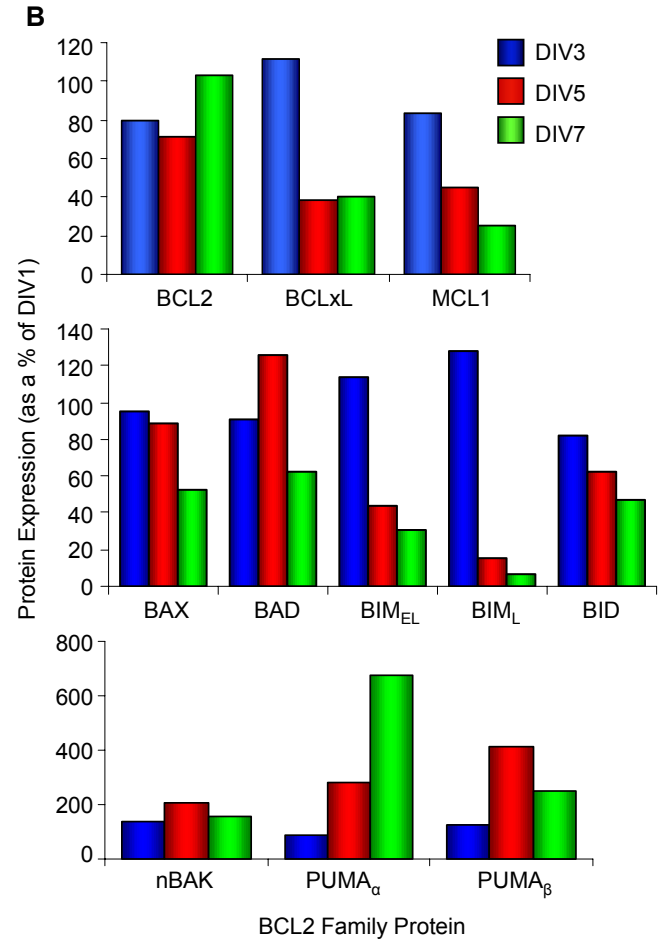
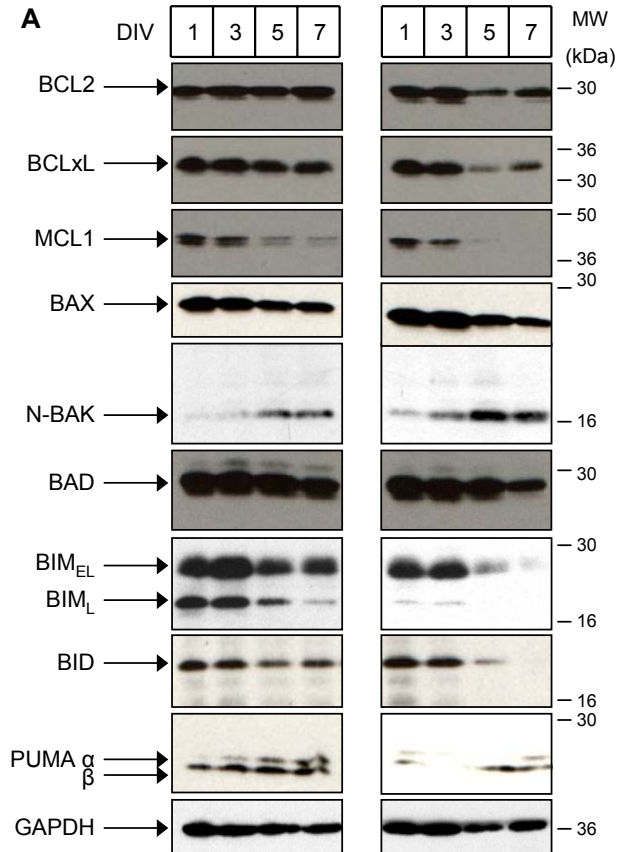


Figure 5.2.6. The BCL2 family proteins are differentially expressed between DIV1-7. Two independent cultures of CGNs were lysed at DIV1, 3, 5 and 7, separated on SDS-PAGE and immunoblotted for BCL2, BCLxL, MCL1, BAX, BAK, BAD, BIM, BID, PUMA and GAPDH (**A**). Densitometry was then performed, the protein expression was normalised against GAPDH, and expressed as a percentage of that at DIV1 (**B**). Data is the mean of the protein expression from the two independent cultures.

N-BAK in cell death in CGNs therefore requires further examination; however this was not investigated further in this study.

These data suggest that the expression of certain apoptotic proteins, namely the BCL2 family proteins may be responsible for the different response to TSA over time in CGNs. It is unlikely that the reduced expression of the anti-apoptotic proteins BCLxL and MCL1 at DIV5 and DIV7 are responsible for the protection from the TSA-induced cell death observed at DIV1 and DIV3. The decrease in the expression of the pro-apoptotic proteins BAX and the BH3-only proteins BIM_{EL} and BID is more probable.

5.2.4. TSA modulates the protein level of MCL1, BIM_{EL}, BID and BAX in CGNs at DIV7

Having established that the differential protein expression of the BCL2 family proteins in CGNs correlates with TSA induced cell death at DIV1, or the survival of CGNs in the presence of TSA at DIV7, their involvement in these processes was examined. CGNs were therefore treated with TSA on DIV1 and DIV7 and lysates were prepared for immunoblot.

TSA induced an increase in the protein expression of BIM_{EL}, BID and BAX in CGNs at DIV7 (Figure 5.2.7 A). The HDACi mediated increase in BIM_{EL} is consistent with that previously described by Inoue *et al*, 2007 (Inoue *et al.*, 2007). However, an increase in the level of BH3-only proteins, such as BIM_{EL} and BID, and that of BAX does not correspond with the continued survival of the neurons as suggested by their loss of protein expression in CGN cultures. The protein expression of BCLxL declined upon treatment with TSA, whereas the level of BCL2 remained unchanged. Interestingly, there was an additional TSA-induced elevation in the protein level of MCL1, consistent with that previously demonstrated by Inoue *et al*, 2008 (Inoue *et al.*, 2008).

In addition to the differential expression of the BCL2 family proteins during the development of neuronal cultures, the protein expression of APAF1 has also been shown to be reduced as neurons mature, resulting in the reduction of apoptosome activity (Wright *et al.*, 2004; Wright *et al.*, 2007; Yakovlev *et al.*, 2001). Furthermore, the treatment of immature sympathetic neurons with TSA, resulted in the upregulation of APAF1 expression, however, its upregulation in mature neurons required simultaneous transcriptional activation by E2F-1, and chromatin derepression by TSA (Wright *et al.*, 2007). The protein expression of APAF1 in CGNs at DIV7 in the presence of TSA was

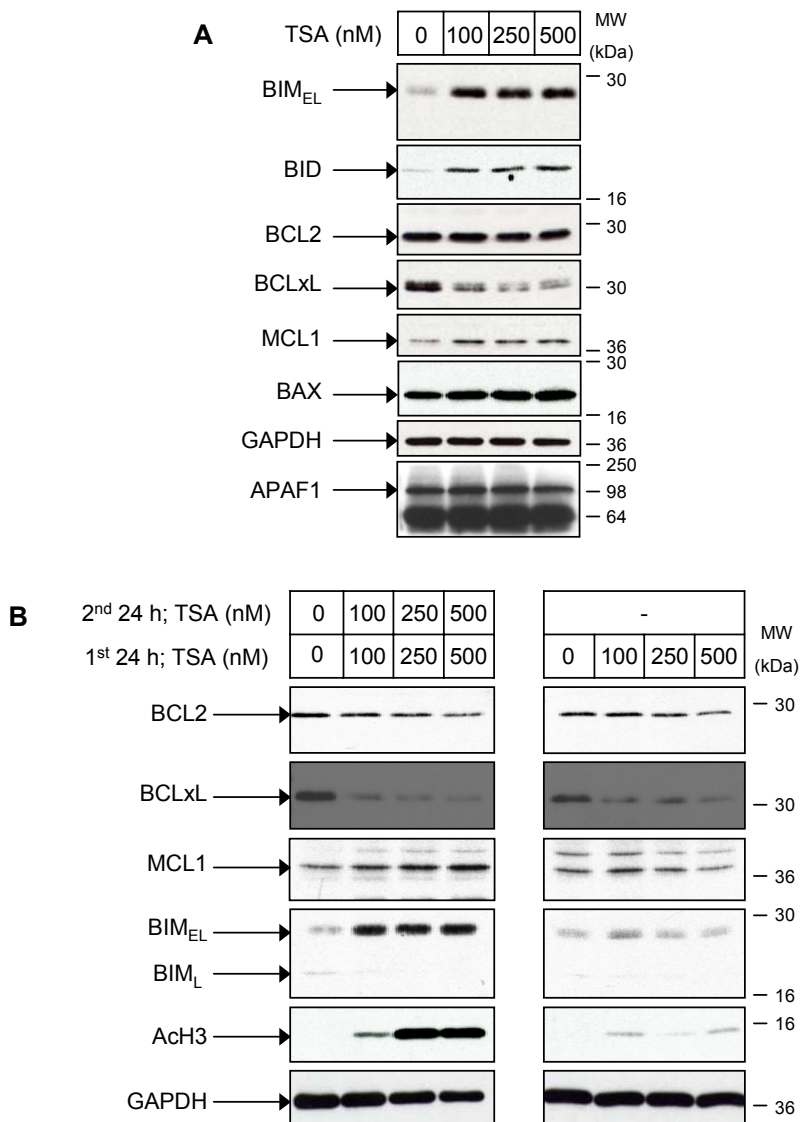


Figure 5.2.7. MCL1, BIM_{EL}, BID and BAX are modulated by TSA in CGNs at DIV7.

CGNs (DIV7) were treated with TSA (100-500 nM) for 24h, lysates prepared, separated by SDS-PAGE and immunoblotted for BIM, BID, BCL2, BCLxL, MCL1, BAX, GAPDH and APAF1 (**A**). CGNs were treated with TSA (100-500 nM) for 24 h. TSA was then removed by washing in PBS and then re-incubated with conditioned medium in the presence of MK-801 (2 μ M) and MgCl₂ (2 mM) for a further 24 h. Lysates were then prepared, separated by SDS-PAGE and immunoblotted for BCL2, BCLxL, MCL1, BIM, Ach3 and GAPDH (**B**; 2nd 24 h; -). Control CGNs were treated in the same way except after the PBS washes they were incubated in conditioned medium in the presence of TSA (2nd 24 h; TSA 0-500 nM).

therefore assessed. Consistent with the observations of Wright *et al.*, 2007, TSA alone had no effect on APAF1 in mature CGNs (Figure 5.2.7 A).

The increase in the levels of MCL1 and BIM_{EL} was also observed in CGNs at 48 h; removal and wash out of TSA abrogated the increased expression (Figure 5.2.7 B), indicating that this is a result of HDAC inhibition by TSA. There was a further reduction in the level of BCLxL in CGNs at 48 h and the expression of BCL2 was also decreased (Figure 5.2.7 B). This was potentially not a direct result of the TSA treatment as it continued to decline in the absence of TSA.

MCL1 and BIM are two examples of BCL2 family proteins that undergo proteasomal degradation (Ley *et al.*, 2003; Luciano *et al.*, 2003; Zhang *et al.*, 2002). To confirm that their increase was not the result of enhanced stability due to TSA inhibition of the proteasome, the accumulation of ubiquitinated proteins was assessed. The levels of ubiquitinated proteins in lysates from CGNs treated with TSA compared to those from control CGNs did not differ significantly (data not shown). This indicates that inhibition of the proteasome was not responsible for the increase in the protein levels of BIM_{EL}, BID, MCL1 and BAX.

In TSA treated CGNs at DIV1 there was a decline in the levels of BCL2, BCLxL, MCL1 and BIM_L (Figure 5.2.8 A). The expression levels of BIM_{EL} and APAF1 remained unchanged. This result is in contrast to the TSA-induced upregulation in the protein expression of APAF1 in immature neurons (Wright *et al.*, 2007). However, there appeared to be a decline in the level of APAF1 at DIV7 when compared to that at DIV1 (compare Figure 5.2.7 A with Figure 5.2.8 A), a finding that is consistent with previous investigations in neuronal systems (Wright *et al.*, 2004; Wright *et al.*, 2007; Yakovlev *et al.*, 2001).

BCL2, BCLxL and MCL1 have all been demonstrated to be substrates of caspase-3 (Cheng *et al.*, 1997; Clem *et al.*, 1998; Snowden *et al.*, 2003). In addition as discussed above, several BCL2 family proteins are degraded by the proteasome. In order to investigate whether the loss of BCL2, BCLxL and MCL1 in CGNs treated with TSA was caspase-dependent or a result of proteasomal degradation, CGNs (DIV1) were treated with TSA in the presence of z-VAD.fmk or PS-341. Lysates were then prepared for immunoblot.

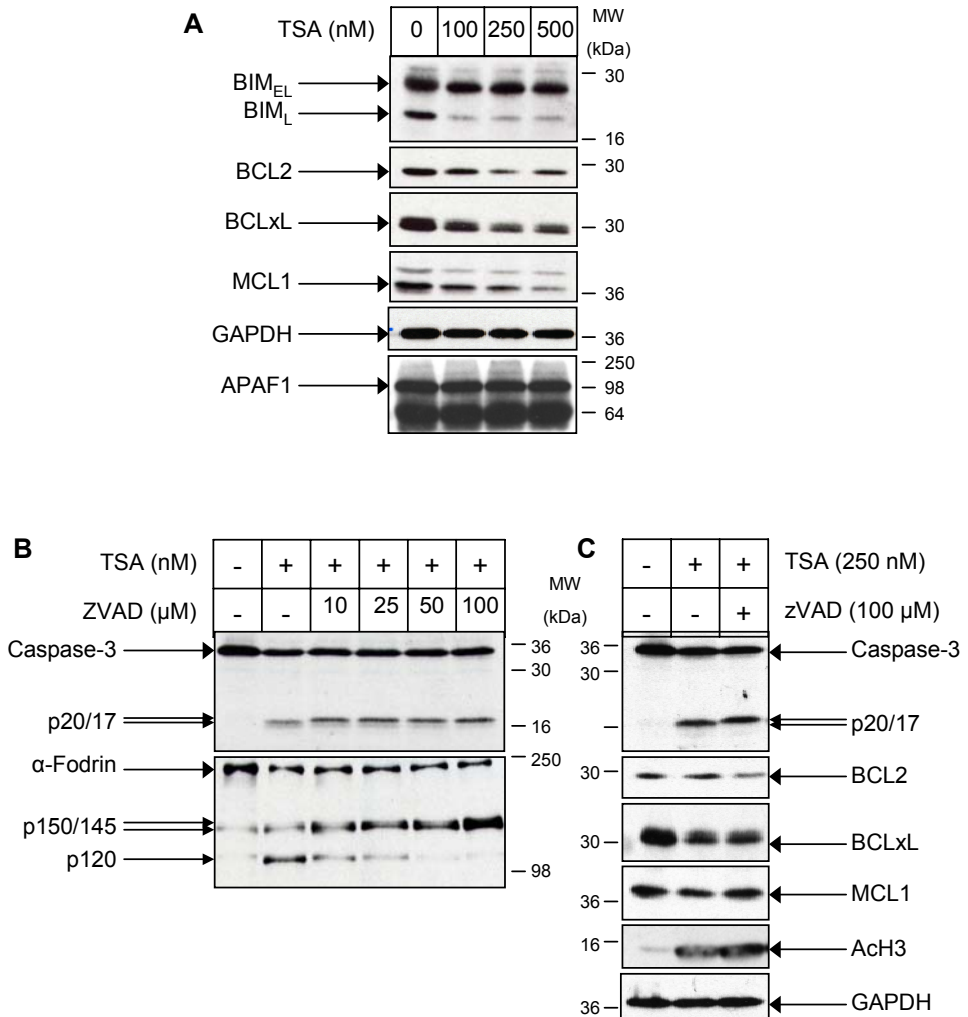


Figure 5.2.8. TSA induces the loss of BCL2 family proteins in CGNs at DIV1.

CGNs (18-24 h after plating) were treated with TSA for 24 h, lysates were prepared, run on SDS-PAGE and immunoblotted for BIM, BCL2, BCLxL, MCL1, GAPDH and APAF1 (**A**). CGNs (18-24 h after plating) were incubated with z-VAD.fmk (0-100 μM (**B**); 100 μM (**C**)) for 1 h and treated with TSA (250 nM) for 24 h. Lysates were then prepared, run on SDS-PAGE and immunoblotted for caspase-3, α-fodrin, BCL2, BCLxL, MCL1, Ach3 and GAPDH.

Caspase-3 was cleaved to its p17 active fragment in lysates from CGNs treated with TSA alone (Figure 5.2.8 B). The addition of zVAD.fmk abrogated the cleavage, halting the processing at the p20 form of caspase-3 (Sun *et al.*, 1999). In addition, the cleavage of α -fodrin by caspase-3 to its p120 fragment was attenuated in a concentration dependent manner, confirming the inhibition of caspase-3 activation. The presence of z-VAD.fmk did not reverse the loss of BCL2 and BCLxL in TSA treated CGNs; in fact the loss of BCL2 seemed to be further enhanced upon zVAD treatment (Figure 5.2.8 C). There was a slight abrogation in the reduction of MCL1 by zVAD.fmk, indicating that the loss of MCL1 was partially caspase dependent. The co-treatment of CGNs with TSA and the proteasome inhibitor PS-341 resulted in the almost complete loss of all proteins (data not shown), suggesting that the losses were not the result of proteasome degradation. As it is probable that TSA is altering the gene expression of the BCL2 family proteins, quantitative-PCR should have been employed to confirm this.

Taken together, these data suggest that the TSA-mediated increase in the level of the pro-survival BCL2 family protein, MCL1, is a possible candidate for the neuroprotection elicited by HDACi in neurons.

5.2.5. The majority of HDAC activity in CGNs is the result of Class I HDACs.

Many structurally diverse HDACi have been developed and most can be divided into classes based on their ability to inhibit specific HDACs or classes of HDACs and on their chemical structure (Bolden *et al.*, 2006). By exploiting the different inhibition efficiencies of HDACi, specific HDACs can be inhibited and non-specific effects can be reduced. It was therefore decided to establish the class of HDAC that was inhibited by TSA in CGNs. TSA was already demonstrated to inhibit class I HDACs, by the accumulation of Ach3 at DIV7 (Figure 5.2.4 B). To ensure that TSA was also mediating the inhibition of class II HDACs, its ability to induce the accumulation of acetylated tubulin (AcTub), was compared against the highly selective class II inhibitor MC1568 (Inoue *et al.*, 2006a; Mai *et al.*, 2005). AcTub is a substrate of the class II HDAC, HDAC6 (Hubbert *et al.*, 2002). CGNs (DIV7) were therefore treated with TSA and MC1568 and lysates were prepared for immunoblot.

There was an accumulation of Ach3 in the lysates from CGNs treated with TSA (Figure 5.2.9 A). This was expected due to the inhibitory properties of this inhibitor against the class I HDACs and was previously demonstrated earlier in this chapter (Figure 5.2.4 B). MC1568 was ineffective in increasing the levels of Ach3, consistent with this being

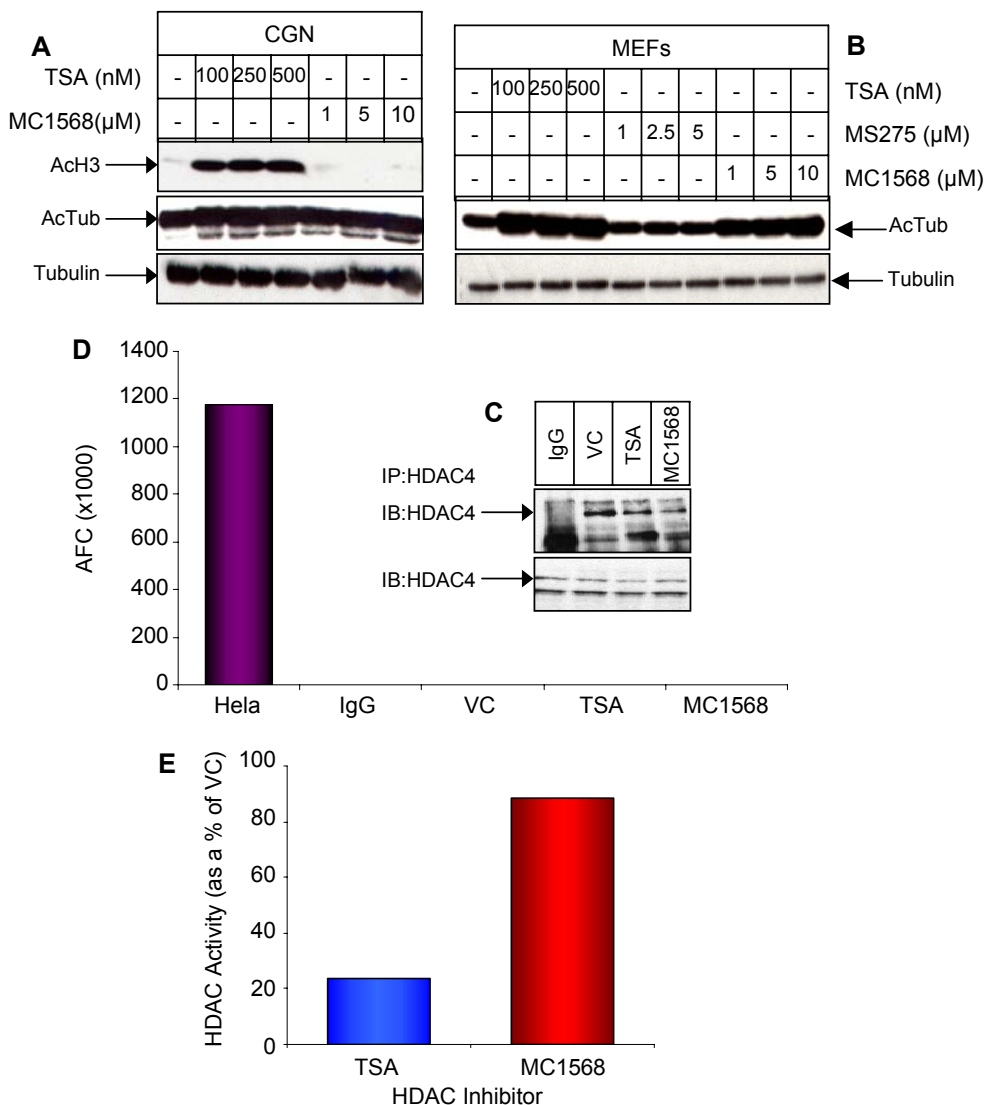


Figure 5.2.9. The accumulation of AcTub cannot be used to confirm Class II HDAC inhibition in CGNs. CGNs (DIV7) were treated with TSA (100-500 nM) or MC1568 for 24 h. Lysates were then prepared, separated by SDS-PAGE and immunoblotted for AcH3, AcTub and tubulin (**A**). MEFs were treated with TSA (100-500 nM), MC1568(1-10 μM) or MS-275 (1-5 μM) for 4h, lysates were prepared, separated by SDS-PAGE and immunoblotted for AcTub and tubulin (**B**). CGNs (DIV7) were treated with TSA (250 nM) or MC1568 (5 μM) for 24 h, lysates were prepared and an IP was performed using an antibody for HDAC4. Samples were then taken to run on SDS-PAGE and immunoblotted for HDAC4 (**C**) or assayed for HDAC4 activity (**D**). As a control, vehicle control (VC) CGN lysates were incubated with mouse IgG. CGNs (DIV7) were treated with TSA (250 nM) or MC1568 (5μM) for 24 h, lysates were prepared and directly assayed for HDAC activity (50 μg; **E**). Data expressed as the mean from two independent cultures; expressed as a % of the vehicle control.

a class II inhibitor. However, the accumulation of AcTub was absent in the lysates from CGNs treated with TSA and MC1568. Deacetylation of tubulin is closely coupled to depolymerisation. In CGNs the majority of tubulin is acetylated as microtubules in neurons are highly stable, (Black *et al.*, 1989). It is therefore not surprising that observable differences in AcTub levels in CGNs were not seen.

The inhibitor MC1568 has been demonstrated as an effective class II inhibitor in human cell-lines and in maize (Inoue *et al.*, 2006a; Mai *et al.*, 2005). To ensure that it was effective in cells of murine origin, it was necessary to investigate the ability of MC1568 to inhibit the class II HDACs in MEFs. A specific class I inhibitor – MS-275 was also employed for comparison. The treatment of MEFs with the HDACi TSA and MC1568 resulted in an enhanced accumulation of AcTub (Figure 5.2.9 B), indicative of class II inhibition and confirms that MC1568 is effective in murine cells. In contrast, the class I inhibitor MS-275 had no effect on AcTub levels.

Having established that the accumulation of AcTub could not be used to confirm the inhibition of class II HDACs by TSA or MC1568 in CGNs, it was necessary to investigate their ability to directly inhibit the class II HDAC, HDAC4. To isolate the desired HDAC in a cell lysate it was initially required to immunoprecipitate (IP) HDAC4, followed by a HDAC activity assay on the isolated enzyme. CGNs (DIV7) were therefore treated with TSA or MC1568. After 24 h lysates were prepared, immunoprecipitated using an anti-HDAC4 antibody and samples were taken for immunoblot or assayed for HDAC activity.

HDAC4 was detected at ~140 kDa following IP in control CGN lysates and in those from HDACi treated CGNs (Figure 5.2.9 C). In addition HDAC4 was absent from the control CGN lysates incubated with mouse IgG, confirming the IP had specifically isolated HDAC4. However, when the isolated enzymes were assayed for HDAC4 activity, it was absent in all the CGN lysates (Figure 5.2.9 D). The HeLa nuclear extract used as a positive control confirmed that the assay was functional.

Class II HDACs have a low level of expression in CGNs, as they are required for specialised tissue specific functions. It is possible that class I HDACs constitute the majority of the HDAC activity in the cell. Therefore by isolating HDAC4, it would represent a minimal level of the HDAC activity in the cell. To investigate this further, lysates were prepared from CGNs treated with TSA and MC1568 and the lysates were assayed for HDAC activity as a whole. HDAC activity was strongly inhibited in the

lysates from TSA treated CGNs (Figure 5.2.9 E), with only 22 % activity residing. The remaining HDAC activity may be that of the class III HDACs (SIRT1-7), which are not inhibited by TSA. In contrast, MC1568 inhibited only 18 % of the CGN HDAC activity, suggesting that the majority of HDAC activity is a result of class I HDACs in CGNs. This also explains the absence of HDAC activity in the post-IP HDAC4 samples. The contribution of the specific class I and class II HDACs to apoptotic cell death or in the maintenance of neuronal survival requires further characterisation.

5.2.6. BCL2 family protein expression is developmentally regulated in the cerebellum.

The differential protein expression of many of the BCL2 family proteins in cultured CGNs was demonstrated in Figure 5.2.6. *In vivo*, the formation of the cerebellar laminar structure occurs perinatally in the mouse and continues into the third week of postnatal life (Millen *et al.*, 1999; Wang and Zoghbi, 2001; Zhang and D'Ercole, 2004). To understand the postnatal developmental expression of the BCL2 family proteins *in vivo*, cerebellar were isolated from mice at different postnatal ages and lysates were prepared for immunoblot (Figure 5.2.10). While densitometry was performed on the data, this proved inaccurate as the immunoblots were highly overexposed. Therefore, only the trends in the BCL2 family protein expression are described below.

Early in the development of the cerebellum there was a high level in the protein expression of all the BCL2 family proteins, with the exception of PUMA α (Figure 5.2.10). The protein expression of BIM_{EL/L} was also low at postnatal day 3 (P3) in comparison to the expression of the other BCL2 family proteins, however its expression had increased by P9. This makes this time period one of extremely high BCL2 family protein expression. In the adult cerebellum, the expression of the majority of the pro-apoptotic BCL2 members had declined to almost undetectable levels (BAX, BIM_{EL/L}, BID). The exception was PUMA β and PUMA α , although the level of PUMA β seemed largely reduced in comparison to its expression at P3. The expression of PUMA α was relatively late in development when compared to the other BH3-only proteins, and it seemed to coincide with the reduction in the level of PUMA β . In addition, there was a much lower level of expression of the anti-apoptotic BCLxL and MCL1 in the adult cerebellum when compared to that of BCL2. Furthermore, their expression was reduced when compared to the protein levels at P3.

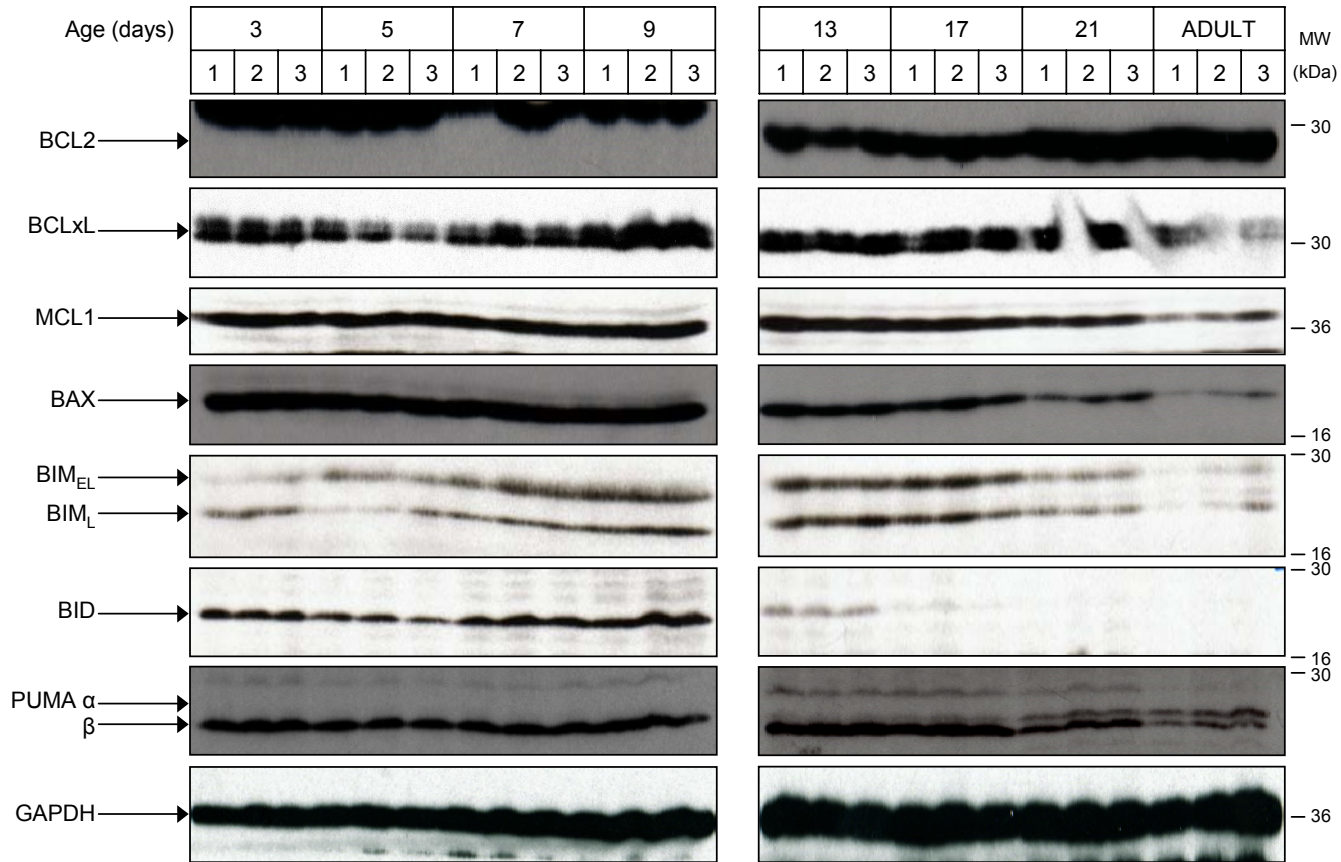


Figure 5.2.10. The BCL2 family proteins are differentially expressed during the development of the cerebellum. Cerebellar were isolated from mice at postnatal day 3, 5, 7, 9, 13, 17, 21 and from adult mice. The tissue was then lysed, separated by SDS-PAGE (50 μ g) and immunoblotted for BCL2, BCLxL, MCL1, BAX, BIM_{EL}, BIM_L, BID, PUMA α and PUMA β .

These data indicate that after an initial period of high BCL2 family protein expression, the majority of their protein levels fall to low levels in the adult cerebellum, the exception being PUMA α and BCL2.

5.3. Discussion

The regulation of gene transcription is carried out by various mechanisms, which include DNA methylation, RNA-associated silencing and post-translational histone modification; acetylation being primarily responsible for the latter (Glaser, 2007). An early feature in many polyglutamine diseases is a loss of gene transcription, linked to a reduction in the acetyltransferase activity of CBP and p300/CBP-associated factor (P/CAF) (Steffan *et al.*, 2000; Steffan *et al.*, 2001; Taylor *et al.*, 2003; Bates *et al.*, 2006). HDACi enhance the viability of the cells in these model systems. Furthermore they have been demonstrated to restore learning and memory, the result of neurodegeneration, in mice models (Fischer *et al.*, 2007). They are therefore promising agents for the treatment of many neurodegenerative conditions.

With this in mind, CGN survival in the presence of the HDACi TSA, in the absence of cell death stimuli and other survival factors, was investigated. High dose treatment of CGNs with TSA induced rapid apoptosis in immature, undifferentiated neurons, when treated at DIV1. In contrast, the survival of mature differentiated CGNs was maintained for more than 48 h when treated with TSA. In agreement, the differential response of immature and mature CGNs to thapsigargin and lithium has previously been described (D'Mello *et al.*, 1994; Levick *et al.*, 1995).

Postnatal granule neurons undergo proliferation in the external granule layer (EGL). Granule cell axons extend beneath the EGL, the cell bodies then migrate and settle in the internal granule layer (IGL). It is in the IGL that the mature granule neurons receive their first synaptic innervations from the mossy fibres. It seems that cultured CGNs at DIV1 represent a mixed population of immature EGL progenitor cells and postmitotic cells. The population of immature undifferentiated EGL cells then decline over time in culture; cultured granule neurons at DIV4 are thought represent differentiated, mature IGL-like neurons (Manzini *et al.*, 2006). This is consistent with the observations that several biochemical criteria also become apparent at DIV4. For example, the dependency for survival of cultured CGNs on non-physiological concentrations of extracellular K^+ (25 mM K^+) manifests after DIV4-5, after which the reduction in the concentration of K^+ to the physiological level of 5 mM results in apoptotic cell death as previously demonstrated (Figure 4.2.3) (Gallo *et al.*, 1987). Furthermore, several transcription factors including MEF2 and Zic 1 and 2 (markers of differentiation) are upregulated by DIV4 (Manzini *et al.*, 2007; Manzini *et al.*, 2006).

In this study, consistent with the time frame of differentiation of CGN cultures, the 'switch' in the ability to withstand HDACi treatment was also demonstrated between DIV3 and DIV5; further confirming the suggestion that after DIV4 CGNs have acquired the characteristics of differentiated neurons (Levick *et al.*, 1995). Furthermore, the differential protein expression of several anti- and pro-apoptotic BCL2 family proteins was demonstrated during the differentiation of the CGN cultures. For the majority of the BCL2 family proteins, their levels declined in CGNs with time in culture.

In the cerebellum there was a high level of protein expression of both the anti- and pro-apoptotic BCL2 family members early in development (P3 to P7). These data are in agreement with the period immediately after birth being one of active gene transcription, protein synthesis and protein folding; the gene expression of proteins involved in these functions decline steadily after this time (Lim *et al.*, 2004). In addition, the protein expression of the majority of the BCL2 family remained high throughout the period of granule cell neurogenesis around P13; a phase of active differentiation and cell migration (Lim *et al.*, 2004). Late postnatal development is characterised by an upregulation in the expression of neurotransmitter receptors and other genes that have a role in postsynaptic signal transduction and synaptic function. The maturation of synapses and the acquirement of the characteristics of the adult cerebellum is accomplished by the third postnatal week (Lim *et al.*, 2004). During this time, the protein expression of the majority of the BCL2 family proteins decreased to a low level. The protein levels of BCL2 and PUMA α were the only members of the BCL2 family that remained elevated in the adult cerebellum. While there is little information concerning the role of PUMA α in the development of the CNS, BCL2 has been extensively studied. BCL2 is required for the regulation of differentiation of neurons and axonal outgrowth early in development (Holm and Isacson, 1999; Middleton *et al.*, 1998; Zhang *et al.*, 1996). It is also thought that there are low basal levels of BCL2 in the adult CNS, BCLxL being critical in mediating cell survival in the adult brain (Shacka and Roth, 2006).

Although the protein expression of N-BAK was investigated in CGN cultures, its expression was not looked at in the developing cerebellum due to limited amounts of lysates. The expression of BAK in the cerebellum would have been interesting to examine given that it has previously been hypothesised to be expressed as the full-length form in neural/neuronal precursor cells, which is largely reduced upon maturation and differentiation when the mature neurons completely switch to the expression of N-BAK (Uo *et al.*, 2005). The differential function of full-length BAK/N-BAK

is also worthy of further assessment in granule neurons, given the conflicting views on their roles in neuronal apoptosis (Sun et al., 2003; Sun et al., 2001; Uo et al., 2005).

Overall, the expression of the BCL2 family proteins in the *in vitro* CGN cultures closely paralleled the trend in their expression in the cerebellum after P7, the point at which the cerebellar are isolated for the preparation of CGN cultures.

Several BCL2 family proteins were demonstrated to be modulated by TSA in CGNs, particularly at DIV7. In agreement, previous studies have described the modulation of many BCL2 proteins such as BCLxL (Cao *et al.*, 2001; Inoue *et al.*, 2007), BCL2 (Duan *et al.*, 2005), BIM (Inoue *et al.*, 2007; Zhao *et al.*, 2005), NOXA (Inoue *et al.*, 2007) and MCL1 (Inoue *et al.*, 2008) by HDACi in various cell lines. Most interestingly, TSA induced an increase in the expression of the anti-apoptotic MCL1, which may have contributed to the prolonged survival of the CGNs. While MCL1 has been shown to be a critical survival factor in natural killer (NK) cells and multiple myeloma cells (Huntington *et al.*, 2007; MacCallum *et al.*, 2005; Zhang *et al.*, 2002) and is responsible for the resistance displayed by various cell types to the BAD BH3 mimetic ABT737 (van Delft *et al.*, 2006), it is unlikely to mediate these effects alone in CGNs. The pro-apoptotic BIM_{EL}, BID and BAX were also increased and PUMA α was observed in CGN cultures at this time, although its expression did not change upon TSA treatment (data not shown). It is therefore possible that other anti-apoptotic proteins, not investigated in this study such as A1 and BCLW, also contribute to the survival of the CGN cultures, possibly by 'buffering' the increases in the BH3-only proteins. Due to inadequate commercial antibodies, particularly for A1, quantitative-PCR should be employed to assess their expression levels. In addition, the reduction in the expression of APAF1 between DIV1 and DIV7, and the potential loss of apoptosome activity as a result of this, as described previously (Wright *et al.*, 2004; Wright *et al.*, 2007; Yakovlev *et al.*, 2001), should also be examined further.

The modulation of MCL1 by HDACi and its potential role as a survival factor in CGNs requires further investigation to that presented here; this is discussed further in a later section (section 6.2). Several other proteins, modulated by HDACi have been proposed to be critical for the neuroprotection observed in previous studies. In one such investigation, an increase in the level of α -synuclein by VPA was demonstrated to mediate the neuroprotection against glutamate induced excitotoxicity in CGNs (Leng and Chuang, 2006). In contrast to the work presented here, the treatment regime was initiated at DIV1, glutamate being added at DIV7 for 24 h. In addition, a neuroprotective

role for the transcriptional upregulation of the cyclin-dependent kinase (Cdk) inhibitor p21^{waf1/cip1} by high dose 'pulse inhibition' of HDACs, has also been proposed in oxidative stress-induced cell death in cortical neurons and in a model of permanent ischemia *in vivo*. However, experiments using cortical neurons prepared from p21^{-/-} mice suggest that p21 is not essential for the HDACi mediated neuroprotection (Langley *et al.*, 2008). The co administration of VPA with lithium was demonstrated to protect aging CGNs from glutamate toxicity; inhibition of the activity of GSK-3, a target of lithium, being potentiated by VPA in this model (Leng *et al.*, 2008). This is interesting given that GSK-3 has been proposed to mediate the phosphorylation of MCL1, which results in its ubiquitination and degradation by the proteasome (Maurer *et al.*, 2006; Ding *et al.*, 2007).

While the majority of these studies have described the HDACi-induced protection against cell death there are a number of studies in which the inhibition of HDACs was demonstrated to be damaging to neuronal function. The TSA-induced cell death of CGNs was previously demonstrated by Boutillier and colleagues. The death was hypothesised to be the result of an enhanced transcription of E2F-1 and proposed to be controlled by HDAC3 (Boutillier *et al.*, 2002; Boutillier *et al.*, 2003; Panteleeva *et al.*, 2004). Whilst these data conflict with those presented here, a direct target of enhanced E2F-1 activity is BIM (Zhao *et al.*, 2005) and therefore corresponds with the TSA mediated increase in the level of BIM_{EL} (Figure 5.2.6). The source of the death vs. survival discrepancies is potentially a consequence of different culturing conditions and treatment regimes.

In addition, as previously described HDAC6 has been implicated in the transport of polyubiquitinated proteins to aggresomes and the induction of autophagy (Iwata *et al.*, 2005; Kawaguchi *et al.*, 2003; Pandey *et al.*, 2007). Given that the induction of autophagy is proposed to prolong the survival of the affected neuron by initiating the degradation of the accumulated proteins, inhibition of HDACs would be expected to prevent the corresponding autophagic response and induce cell death. HDACi have actually been demonstrated to induce autophagy in Apaf-1^{-/-} MEFs (Shao *et al.*, 2004). In this investigation, there was no indication of the induction of autophagy in response to HDAC inhibition (data not shown), however it cannot be ruled out that long term treatment with low dose HDACi would not induce an autophagic response.

While it was attempted to elucidate the class of HDAC that was inhibited by TSA in CGNs, it proved problematic. Given that the deacetylation of microtubules occurs

during depolymerisation and microtubules are highly stable in post-mitotic neurons (Black *et al.*, 1989), it was difficult to observe any change in the level of acetylated tubulin through the inhibition of HDAC6. A specific HDAC4 activity assay was also unsuccessful; thought to be due to the low level activity of the class II HDACs in CGNs. This was also indicated by the partial inhibition of whole cell HDAC activity by the class II specific inhibitor MC1568 compared to TSA.

It is likely that the treatment of CGNs with HDACi, particularly those which are universal HDAC inhibitors, modulates the expression of many different proteins, not only those of the BCL2 family. Class specific inhibitors are therefore attractive therapeutic considerations as they would be expected to reduce off target effects and may be targeted to specific brain regions, as demonstrated with MS-275 (Simonini *et al.*, 2006). Furthermore, MCL1 is an interesting candidate for the mediation of neuronal survival and deserves further investigation.

Chapter 6

General Discussion

6.1. General Discussion

The balance of protein synthesis and degradation is essential for cell growth and differentiation. The predominant pathways for short and long-lived protein degradation and organelle turnover are the ubiquitin-proteasome system and autophagy. Failure of either of these systems culminates in the death of the cell. This is particularly undesirable in neuronal systems, as shown in neurodegenerative diseases.

The initial aim of this study was to investigate the role of the proteasome during K^+ withdrawal induced cell death in CGNs and the functional significance of any caspase cleavage of the proteasome subunits. The cleavage of the proteasomal subunits S1, S5a, the ATPase S6' (Adrain *et al.*, 2004; Sun *et al.*, 2004) and the γ subunit of the 11S proteasome activator complex (PA28 γ) by caspase-3 in human cells and cleavage of the 20S complex subunits α 2, α 4, β 4 and S7 (19S) in *Drosophila* (Adrain *et al.*, 2004) have previously been demonstrated. In addition, the caspase-7 mediated cleavage of the 19S ATPase S7, α 2 and α 6, subunits of the 20S, was observed in the absence of caspase-3 (Jang *et al.*, 2007).

The role of the proteasome in CGNs during K^+ withdrawal-induced cell death was previously limited to showing an increase in its activity early in the apoptotic pathway and the subsequent decline in activity below that of the resting constitutive level (Atlante *et al.*, 2003; Canu *et al.*, 2000). This is in agreement with that demonstrated in this investigation (Chapter 3; Figure 6.1.1) and is hypothesised to represent a proteasome regulated response to the prior increase in the levels of reactive oxygen species (Atlante *et al.*, 2003; Valencia and Moran, 2001). The subsequent decrease in LLVYase activity was also observed, at a time that was consistent with the initial cleavage of the widely characterised caspase-3 substrate, α -fodrin. In addition, the loss in LLVYase activity seemed to be negated by the caspase inhibitors z-VAD.fmk and DEVD.fmk, consistent with that previously demonstrated (Canu *et al.*, 2000). In the absence of a pre-lysis centrifugation step, the cleavage fragments of the proteasome subunits S1 and S6' were not observed until ~16 h in low K^+ .

The observed cleavage fragments of S1 and S6' were abrogated in the presence of caspase inhibitors. Taken together, these data suggest that the observed cleavage of the proteasome subunits, S1 and S6' in CGNs during K^+ withdrawal-induced cell death is mediated by caspases and the loss of LLVYase activity may be attributable at least in part, to the activation of caspases in CGNs (Figure 6.1.1). In addition, the specific

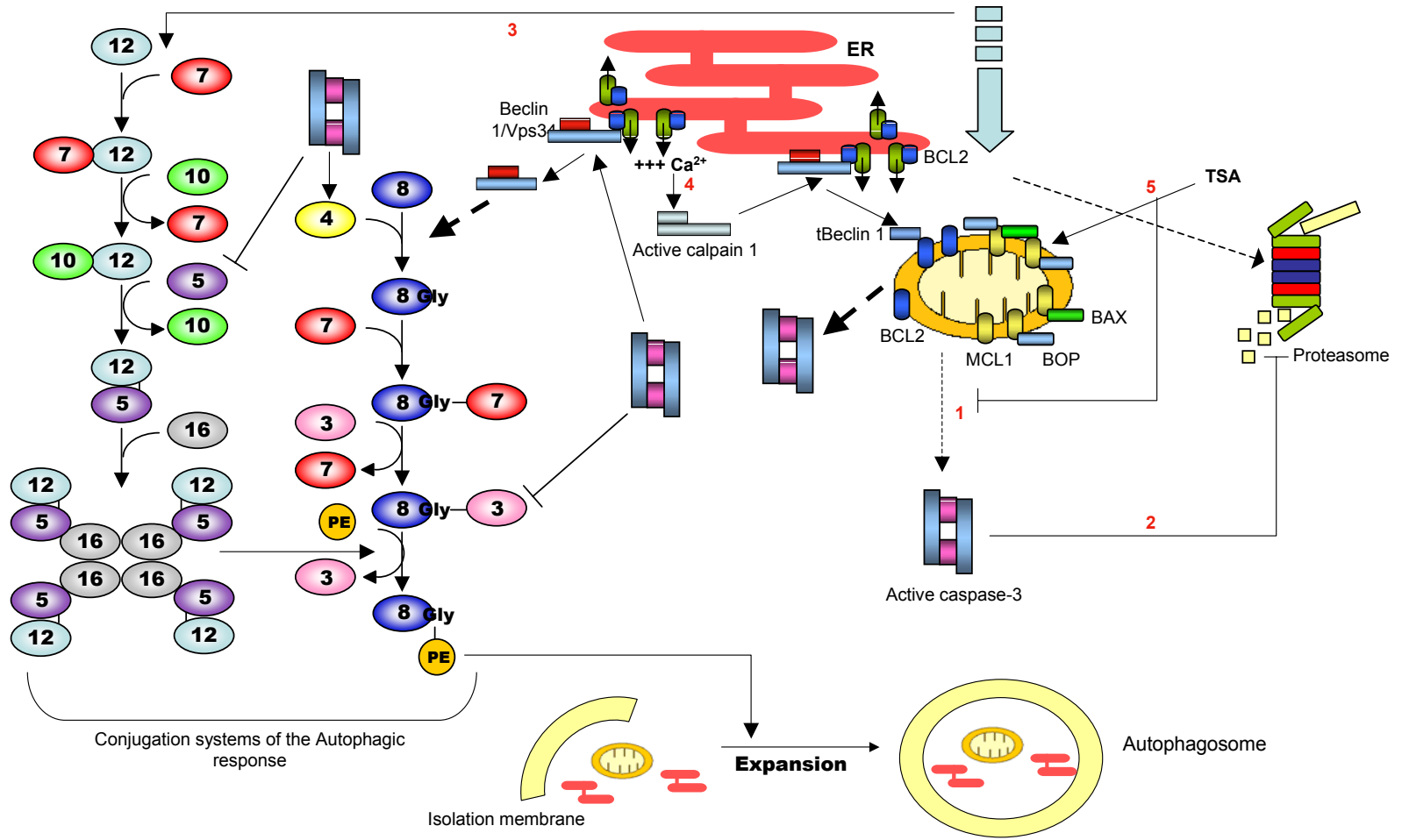


Figure 6.1.1. Schematic of the proposed processes in this investigation. Apoptotic stimuli induce the activation of caspase-3 downstream of the mitochondria (1). This is then capable of cleaving various substrates, in particular, the proteasome subunits S1 and S6', the activity of which is lost after an earlier increase in its activity (2). In addition, the autophagic response is induced simultaneously with the stimulation of apoptosis (3). The ability of the autophagy-related proteins, Atg3 and Atg5 to associate with their respective binding partners may be lost by caspase cleavage. In contrast, the activity of the autophagic proteins, Beclin 1 and Atg4 is enhanced. The activation of calpain 1 through the increase in the intracellular concentration of Ca^{2+} (4), mediates the processing of Beclin 1, which may remove its ability to interact with Vps34. Furthermore, the Beclin 1 BH3 domain may then be able to interact with BCL2 and stimulate the activation of BAX and hence the apoptotic response. The HDACi, TSA increases the expression of the anti-apoptotic protein MCL1 and several pro-apoptotic BCL2 family members (5; BOP (BH3-only proteins)). Caspase-3 activation is reduced.

calpain inhibitor, calpeptin, seemed to restore the loss of proteasomal LLVYase activity. This indicates that calpain activation potentially occurs upstream of caspase activation. However, calpeptin did not prevent the loss in the mitochondria's ability to reduce MTT or the level of apoptotic cells at a late stage in the cell death process (Chapter 3), suggesting a minimal role in the process.

Whilst the LLVYase assay was used as a measure of the chymotrypsin-like activity of the proteasome in this study, there are several drawbacks to its use. It does not accurately represent the activity of the proteasome as a whole; essentially it is a measure of 20S proteasomal activity, rather than that of the 26S holoenzyme. In addition, it is often used to measure other protease activities in cell lysates, such as that of calpain (Giguere and Schnellmann, 2008; Seidah *et al.*, 2003). Recently proteasome sensors have been designed and constructed for the assessment of proteasomal activity (Lindsten *et al.*, 2003; Lindsten *et al.*, 2006; Luker *et al.*, 2003; Neefjes and Dantuma, 2004; Stack *et al.*, 2000). An ubiquitinated-EYFP sensor was therefore constructed to accurately assess proteasomal activity and the contributions by caspase-3 to the loss observed in CGNs during cell death induced by K^+ withdrawal on a single cell level.

Active site directed probes (tagged irreversible inhibitors) are also used for the assessment of proteasomal activity. In contrast to the fluorescent reporters, these provide information of proteasomal activity, active subunit composition and the activity of deubiquitinating enzymes (Berkers *et al.*, 2005; Ovaa, 2007; Verdoes *et al.*, 2006). Whilst there may be several drawbacks to using the fluorescent reporter approach, I decided that it was more relevant for our purpose in assessing the proteolytic function on a single cell level. The sensor was demonstrated to be a *bona fide* proteasome sensor *in vitro* and in SH-SY5Y cells. However, its use in CGNs was restricted by its low transfection efficiency (discussed further in section 6.2).

The proteasome inhibitor MG132 was demonstrated to delay the loss in cell viability induced by the withdrawal of K^+ , prevented the cleavage of α -fodrin by calpain to the p145 fragment and largely reduced the activation of caspase-3 at 16 h (Chapter 3). This is in agreement with the results of previous investigations in CGNs (Bobba *et al.*, 2002; Butts *et al.*, 2005; Canu *et al.*, 2000). However, this study demonstrated that the ability of MG132 to delay cell death was the result of its relatively non-specific inhibition of numerous cellular proteases in addition to the constraints on the proteasome. Furthermore, the specific proteasome inhibitor, PS-341, had little effect on the induction

of cell death, suggesting the proteasomal role in K^+ withdrawal-induced cell death is restricted to the early increase in activity.

The potential induction of autophagy was examined early in the cell death process induced by K^+ withdrawal in CGNs. Given that the role of the proteasome during K^+ withdrawal was downstream of caspase activation and therefore considered 'past the point of no return' with regards to the death process, I decided to investigate the regulation of the autophagic response during apoptosis. Previous evidence suggests that several proteins including the pro-survival BCL2 family proteins, caspase-8, Atg5 and calpain 1 and 2 may be involved in the regulation of both apoptosis and autophagy (Demarchi *et al.*, 2006; Erlich *et al.*, 2007; Liang *et al.*, 2006; Liang *et al.*, 1998; Lin *et al.*, 1999; Madden *et al.*, 2007; Maiuri *et al.*, 2007a; Oberstein *et al.*, 2007; Pattingre *et al.*, 2005; Pyo *et al.*, 2005; Shimizu *et al.*, 2004; Yousefi *et al.*, 2006). Therefore the *in vitro* processing of the Atg proteins by the cell death proteases, caspase-3, -6, -7, -8 and calpain 1 was investigated.

While it is important to confirm the hAtg cleavage in cell culture models to ensure functional significance, the *in vitro* cleavage assay had three main advantages. Firstly, due to the limited availability of commercial antibodies, epitope tagged constructs for the Atg proteins were prepared. Prior to transfection into cells, their expression was confirmed in the *in vitro* TNT reaction; therefore the initial assay was straightforward. Secondly, the *in vitro* screen reduced the number of targets for further investigation in the cell culture models and finally, the prediction of protease cleavage sites and the design of uncleavable mutants will aid in the analysis of functional significance (see section 6.2).

The majority of the hAtg proteins were cleaved *in vitro* by rCalpain 1 and/or the active rCaspases. During K^+ withdrawal-induced cell death in CGNs the activation of caspases, in particular caspase-3, predominates. Therefore, the cleavage of the hAtg proteins by caspases-3, -6 and -8 in this cell death model would be of most importance. Recombinant active caspase-3 was demonstrated to cleave hAtg5, the hAtg4 homologues hAtg4A, 4B, 4C and 4D, hAtg3, hAtg7 and Beclin 1 in the *in vitro* screen. In addition, rCaspase-6 cleaved Beclin 1 and hAtg3, and rCaspase-8 cleaved hAtg3 (Chapter 4). The cleavage of hAtg5 and hAtg3 by caspase-3, -6 and -8 was hypothesised to interfere with their interactions with hAtg16 and hAtg7 respectively, both of which were predicted to disrupt the essential process of vesicle elongation in the autophagic pathway. In contrast, cleavage of Beclin 1 was hypothesised to disturb

its regulation by the anti-apoptotic BCL2 proteins, resulting in the unregulated induction of autophagy (Figure 6.1.1). The cleavage of Beclin 1 was confirmed in apoptotic CGN lysates and was partially abrogated in the presence of z-VAD.fmk (Chapter 4). In order to determine which of these cleavages was significant in apoptotic conditions, uncleavable mutants would be required (section 6.2). Given that the autophagic response is enhanced under apoptotic conditions in the presence of caspase inhibition, it is possible that the loss in the ability to disrupt the Atg5:Atg16 and Atg3:Atg7 interactions, contributes to the increased autophagy observed.

The role of calpain 1 cleavage of the hAtg proteins would be limited during K⁺ withdrawal induced cell death in CGNs. Activation of calpain 1 by an alternative stimulus such as thapsigargin or ionomycin would be predicted to disrupt the function of several of the hAtg proteins. In particular the calpain 1 cleavage of Beclin 1 was hypothesised to result in the loss of the ability of Beclin 1 to interact with UVRAG, Vps34 and nPIST. Disruption in the association of Beclin 1 with UVRAG and Vps34 was predicted to reduce the induction of autophagy. Furthermore, the BH3 domain of Beclin 1 would remain intact. It is then possible that truncated Beclin 1 acts as a BH3-only protein (and pro-apoptotic protein), interacting with the pro-survival BCL2 proteins and initiating the activation of BAX (Figure 6.1.1). This is similar to that shown by Yousefi *et al.*, 2006, in which calpain 1 and 2 cleave Atg5, resulting in a pro-apoptotic protein (Yousefi *et al.*, 2006). The interaction of Beclin 1 with nPIST has not been extensively studied; therefore it is difficult to predict the effect of the disruption in this interaction. The initiation of an autophagic response by the release of Beclin 1 from the complex with the GluR δ 2^{LC} was demonstrated previously in cerebellar Purkinje cells. Whether Beclin 1 is released alone or in complex with nPIST is yet to be determined (Yue *et al.*, 2002). The processing of hAtg3 by calpain 1 was also proposed to perturb the coordination of hAtg3 binding with hAtg7 and hAtg8, disabling one of the ubiquitin-like conjugation systems of vesicle expansion.

Roles for several histone deacetylases (HDACs) in neuronal systems have been described. In particular, HDAC6 was implicated in the transport of cytotoxic polyubiquitinated proteins to aggresomes and the recruitment of the autophagic machinery for their degradation in the absence of proteasomal function (Iwata *et al.*, 2005; Kawaguchi *et al.*, 2003; Pandey *et al.*, 2007). In addition, HDAC4 and HDAC5 are critical regulators of myocyte enhancer factor-2 (MEF2) transcription factors, which are essential for mediating neuronal survival, particularly in CGNs (Bolger and Yao, 2005; Linseman *et al.*, 2003; Mao *et al.*, 1999; Mao and Wiedmann, 1999).

Furthermore, HDAC5 and MEF2 have been implicated in the behavioural response to chronic cocaine or stress (Pulipparacharuvil *et al.*, 2008; Renthal *et al.*, 2007). HDACs therefore have an important role in the maintenance of neuronal survival and their inhibition in CGNs was investigated.

HDAC inhibitors (HDACi) were previously demonstrated to provide protection in neuronal models against a range of toxic insults (Langley *et al.*, 2008; Leng and Chuang, 2006; Leng *et al.*, 2008). Similarly, in this investigation, 'mature' CGNs survived high dose TSA treatment for up to 72 h (Chapter 5). In contrast, immature CGNs underwent rapid apoptotic cell death upon treatment with TSA. The differential response of immature and mature CGNs to TSA, is consistent with that reported by D'Mello *et al.*, 1994 and Levick *et al.*, 1995, in response to treatment with lithium and thapsigargin respectively (D'Mello *et al.*, 1994; Levick *et al.*, 1995). The shift in the inability of CGNs to withstand TSA was at ~DIV4, a time point in culture that corresponds with the differentiation of CGNs, after which CGNs resemble the fully differentiated neurons of the internal granule layer of the cerebellum *in vivo*. Consistent with this observation, the BCL2 family of proteins were differentially expressed in CGN cultures. Furthermore, the protein levels of the BCL2 family in CGN cultures largely correlated with the expression in the cerebellum *in vivo*. In particular, the expression of the BCL2 proteins in fully differentiated, mature CGNs (DIV7) closely paralleled the levels in the adult cerebellum. Additionally, the dependency of CGNs in culture on 25 mM K⁺, which is thought to mimic the first afferent stimulation by the glutamergic mossy fibres, is obvious by DIV4. This stage is equivalent to the period surrounding P13 *in vivo*, which is one of active differentiation when the massively excessive numbers of granule cells are matched to their target cells and the correct synaptic connections are established (Galli *et al.*, 1995; Gallo *et al.*, 1987; Hack *et al.*, 1993; Lim *et al.*, 2004). Taken together, these data further confirm that fully differentiated, mature CGNs are an ideal model system for the adult cerebellum, particularly with respect to the expression of the appropriate BCL2 family proteins as shown here.

While the reduction in the protein levels of BAX, BIM_{EL} and BID over time in culture correlated with the continued survival of mature CGNs (DIV7), the subsequent increase in BIM_{EL}, BID, BAX, and the decline in the level of BCLxL after TSA treatment did not. An additional TSA-induced elevation in the level of the pro-survival protein, MCL1 was also observed. The contribution of MCL1 to the survival of CGNs was suggested in this study. While the role of MCL1 in the CNS has not been extensively studied to date, previous reports have proposed an essential role for MCL1 in cortical development and

for the survival of neurons after seizure-induced injury and DNA damage (Arbour *et al.*, 2008; Mori *et al.*, 2004). Mcl-1 is unlikely to be the only potential neuronal survival factor induced by TSA given the enhanced expression of the pro-apoptotic proteins. The decline in the expression of APAF1 in mature neurons as previously demonstrated, is also an interesting candidate for further investigation (Wright *et al.*, 2004; Wright *et al.*, 2007; Yakovlev *et al.*, 2001). In addition, several other proteins have been demonstrated to be responsible for the protection mediated by HDACi in neuronal systems (Langley *et al.*, 2008; Leng and Chuang, 2006; Leng *et al.*, 2008). To conclude, elucidating the proteins responsible for the continued survival of CGNs is important to establish future drug targets, and identifying the HDACs involved will aid in the reduction of non-target effects.

6.2. Future Work

In this thesis I have demonstrated that the ubiquitinated proteasome sensor, 4xubi(G76V)-YFP, can be transfected into SH-SY5Y and behaves as a proteasome substrate for the effective measurement of proteasomal activity (Chapter 3). In addition, the technology was previously used in the generation of transgenic animals to assess the proteolytic activity in specific organs and tissues, including isolated neuronal cultures (Lindsten *et al.*, 2003). While attempts were made to transiently transfect the sensors into primary CGNs using calcium phosphate precipitation, nucleofection and lipofection, low transfection efficiency was observed by all methods. A viral delivery system may be more efficient and therefore could be employed to address this. This would then enable the assessment of proteasomal function in direct relation to caspase-3 activation at the single cell level.

A number of hAtg proteins were identified as *in vitro* substrates of the cell death proteases caspase-3, -6, -8 and calpain 1 (Chapter 4). The potential sites were predicted based on the molecular weights of the cleavage fragments and their detection by the epitope tags. As the guidelines for caspase and calpain cleavage of substrates is not absolute, all corresponding cleavage sites within a particular region were highlighted. Thus, in order to determine the cleavages that are functionally significant in terms of apoptosis and the corresponding regulation of the autophagic response it would be important to identify the specific sites required for the processing. Uncleavable mutant forms of the corresponding proteins could then be produced by site-directed mutagenesis. These would be transfected into a readily transducible cell line, ideally in the absence of the endogenous expression of the protein of interest,

such as MEFs derived from knockout mice. The processing of the protein could then be assessed in the presence of an apoptotic stimulus, the detection of which being aided by the epitope tags. The mutant forms will provide a more accurate idea as to the cleavages that are required for the regulation of the autophagic response during apoptosis and assist in the determination of the cleavage that predominates and is of most importance. However, caution should be used in the interpretation of results using overexpressed mutant forms of the Atg proteins. Fujita *et al.*, 2008 previously demonstrated the inhibition of the autophagic pathway while investigating the overexpression of a series of Atg16L deletion mutants. The autophagy inhibition observed was the result of the mistargeting of the Atg16L complex due to overexpression, which had an inhibitory effect on LC3 lipidation (Fujita *et al.*, 2008b).

Although the protease cleavage of the majority of the core autophagic machinery was assessed, several of the hAtg proteins were missing, in particular hAtg1, hAtg2, hAtg18 and hAtg16L. Attempts were made to clone these at the same time as the other Atg proteins, however this was unsuccessful in the time frame. Thus, to gain an accurate overall assessment of the regulation of the autophagic response it would be required to further attempt their preparation.

The survival of mature CGNs was maintained despite the presence of TSA even though the expression of the pro-apoptotic proteins, BIM_{EL}, BID, and BAX was enhanced and the level of BCLxL declined. The expression of the anti-apoptotic protein MCL1 was elevated and it was hypothesised that MCL1 may contribute to the prolonged survival of the neurons. In order to investigate this further the knockdown of MCL1 would be required. The cyclin-dependent kinase inhibitor Seliciclib (R-roscovitine/CYC202) was employed in an attempt to downregulate the expression of MCL1 in CGNs (MacCallum *et al.*, 2005). Unfortunately results were extremely preliminary therefore conclusions could not be drawn. In addition, it would be difficult to definitively determine that the effect mediated by a kinase inhibitor was solely the result of the loss of MCL1. Therefore the use of siRNA for MCL1 would be more appropriate. However, it is unlikely, that MCL1 is able to protect CGNs from the high levels of the anti-survival BH3-only proteins. The expression levels of the additional pro-survival BCL2 proteins, BCLW and A1 were unable to be assessed due to the lack of suitable antibodies, thus quantitative-PCR should be used to determine their expression upon TSA treatment. Furthermore, in order to elucidate the mechanism responsible for the prevention of BAX activation in mature CGNs, immunoprecipitation of the TSA-regulated BCL2 proteins could be employed.

References

- Abeliovich, H., Dunn, W. A., Jr., Kim, J., and Klionsky, D. J. (2000). Dissection of autophagosome biogenesis into distinct nucleation and expansion steps. *J Cell Biol* 151, 1025-1034.
- Adams, J., Behnke, M., Chen, S., Cruickshank, A. A., Dick, L. R., Grenier, L., Klunder, J. M., Ma, Y. T., Plamondon, L., and Stein, R. L. (1998). Potent and selective inhibitors of the proteasome: dipeptidyl boronic acids. *Bioorg Med Chem Lett* 8, 333-338.
- Adams, J., Palombella, V. J., Sausville, E. A., Johnson, J., Destree, A., Lazarus, D. D., Maas, J., Pien, C. S., Prakash, S., and Elliott, P. J. (1999). Proteasome inhibitors: a novel class of potent and effective antitumor agents. *Cancer Res* 59, 2615-2622.
- Adrain, C., Creagh, E. M., Cullen, S. P., and Martin, S. J. (2004). Caspase-dependent inactivation of proteasome function during programmed cell death in *Drosophila* and man. *J Biol Chem* 279, 36923-36930.
- Adrain, C., Creagh, E. M., and Martin, S. J. (2001). Apoptosis-associated release of Smac/DIABLO from mitochondria requires active caspases and is blocked by Bcl-2. *EMBO J* 20, 6627-6636.
- Allsopp, T. E., McLuckie, J., Kerr, L. E., Macleod, M., Sharkey, J., and Kelly, J. S. (2000). Caspase 6 activity initiates caspase 3 activation in cerebellar granule cell apoptosis. *Cell Death Differ* 7, 984-993.
- Almond, J. B., and Cohen, G. M. (2002). The proteasome: a novel target for cancer chemotherapy. *Leukemia* 16, 433-443.
- Arbour, N., Vanderluit, J. L., Le Grand, J. N., Jahani-Asl, A., Ruzhynsky, V. A., Cheung, E. C., Kelly, M. A., MacKenzie, A. E., Park, D. S., Opferman, J. T., and Slack, R. S. (2008). Mcl-1 is a key regulator of apoptosis during CNS development and after DNA damage. *J Neurosci* 28, 6068-6078.
- Aritomi, M., Kunishima, N., Inohara, N., Ishibashi, Y., Ohta, S., and Morikawa, K. (1997). Crystal structure of rat Bcl-xL. Implications for the function of the Bcl-2 protein family. *J Biol Chem* 272, 27886-27892.

- Ashford, T. P., and Porter, K. R. (1962). Cytoplasmic components in hepatic cell lysosomes. *J Cell Biol* 12, 198-202.
- Ashkenazi, A. (2002). Targeting death and decoy receptors of the tumour-necrosis factor superfamily. *Nat Rev Cancer* 2, 420-430.
- Atlante, A., Bobba, A., Calissano, P., Passarella, S., and Marra, E. (2003). The apoptosis/necrosis transition in cerebellar granule cells depends on the mutual relationship of the antioxidant and the proteolytic systems which regulate ROS production and cytochrome c release en route to death. *J Neurochem* 84, 960-971.
- Azuma, Y., Arnaoutov, A., and Dasso, M. (2003). SUMO-2/3 regulates topoisomerase II in mitosis. *J Cell Biol* 163, 477-487.
- Bali, P., Pranpat, M., Bradner, J., Balasis, M., Fiskus, W., Guo, F., Rocha, K., Kumaraswamy, S., Boyapalle, S., Atadja, P., *et al.* (2005). Inhibition of histone deacetylase 6 acetylates and disrupts the chaperone function of heat shock protein 90: a novel basis for antileukemia activity of histone deacetylase inhibitors. *J Biol Chem* 280, 26729-26734.
- Bampton, E. T., Goemans, C. G., Niranjana, D., Mizushima, N., and Tolkovsky, A. M. (2005). The dynamics of autophagy visualized in live cells: from autophagosome formation to fusion with endo/lysosomes. *Autophagy* 1, 23-36.
- Bano, D., Young, K. W., Guerin, C. J., LeFeuvre, R., Rothwell, N. J., Naldini, L., Rizzuto, R., Carafoli, E., and Nicotera, P. (2005). Cleavage of the Plasma Membrane Na⁺/Ca²⁺ Exchanger in Excitotoxicity. *Cell* 120, 275-285.
- Bates, E. A., Victor, M., Jones, A. K., Shi, Y., and Hart, A. C. (2006). Differential contributions of *Caenorhabditis elegans* histone deacetylases to huntingtin polyglutamine toxicity. *J Neurosci* 26, 2830-2838.
- Berkers, C. R., Verdoes, M., Lichtman, E., Fiebiger, E., Kessler, B. M., Anderson, K. C., Ploegh, H. L., Ovaas, H., and Galardy, P. J. (2005). Activity probe for in vivo profiling of the specificity of proteasome inhibitor bortezomib. *Nat Methods* 2, 357-362.

- Berliocchi, L., Fava, E., Leist, M., Horvat, V., Dinsdale, D., Read, D., and Nicotera, P. (2005). Botulinum neurotoxin C initiates two different programs for neurite degeneration and neuronal apoptosis. *J Cell Biol* 168, 607-618.
- Bernales, S., McDonald, K. L., and Walter, P. (2006). Autophagy counterbalances endoplasmic reticulum expansion during the unfolded protein response. *PLoS Biol* 4, e423.
- Beyette, J., Mason, G. G., Murray, R. Z., Cohen, G. M., and Rivett, A. J. (1998). Proteasome activities decrease during dexamethasone-induced apoptosis of thymocytes. *Biochem J* 332 (Pt 2), 315-320.
- Black, M. M., Baas, P. W., and Humphries, S. (1989). Dynamics of alpha-tubulin deacetylation in intact neurons. *J Neurosci* 9, 358-368.
- Boatright, K. M., Renatus, M., Scott, F. L., Sperandio, S., Shin, H., Pedersen, I. M., Ricci, J. E., Edris, W. A., Sutherlin, D. P., Green, D. R., and Salvesen, G. S. (2003). A unified model for apical caspase activation. *Mol Cell* 11, 529-541.
- Bobba, A., Canu, N., Atlante, A., Petragallo, V., Calissano, P., and Marra, E. (2002). Proteasome inhibitors prevent cytochrome c release during apoptosis but not in excitotoxic death of cerebellar granule neurons. *FEBS Lett* 515, 8-12.
- Bolden, J. E., Peart, M. J., and Johnstone, R. W. (2006). Anticancer activities of histone deacetylase inhibitors. *Nat Rev Drug Discov* 5, 769-784.
- Boldin, M. P., Goncharov, T. M., Goltsev, Y. V., and Wallach, D. (1996). Involvement of MACH, a novel MORT1/FADD-interacting protease, in Fas/APO-1- and TNF receptor-induced cell death. *Cell* 85, 803-815.
- Boldin, M. P., Varfolomeev, E. E., Pancer, Z., Mett, I. L., Camonis, J. H., and Wallach, D. (1995). A novel protein that interacts with the death domain of Fas/APO1 contains a sequence motif related to the death domain. *J Biol Chem* 270, 7795-7798.
- Bolger, T. A., and Yao, T. P. (2005). Intracellular trafficking of histone deacetylase 4 regulates neuronal cell death. *J Neurosci* 25, 9544-9553.

- Boutillier, A. L., Trinh, E., and Loeffler, J. P. (2002). Constitutive repression of E2F1 transcriptional activity through HDAC proteins is essential for neuronal survival. *Ann N Y Acad Sci* 973, 438-442.
- Boutillier, A. L., Trinh, E., and Loeffler, J. P. (2003). Selective E2F-dependent gene transcription is controlled by histone deacetylase activity during neuronal apoptosis. *J Neurochem* 84, 814-828.
- Boya, P., Gonzalez-Polo, R. A., Casares, N., Perfettini, J. L., Dessen, P., Larochette, N., Metivier, D., Meley, D., Souquere, S., Yoshimori, T., *et al.* (2005). Inhibition of macroautophagy triggers apoptosis. *Mol Cell Biol* 25, 1025-1040.
- Boyault, C., Gilquin, B., Zhang, Y., Rybin, V., Garman, E., Meyer-Klaucke, W., Matthias, P., Muller, C. W., and Khochbin, S. (2006). HDAC6-p97/VCP controlled polyubiquitin chain turnover. *EMBO J* 25, 3357-3366.
- Bradford, M. M. (1976). A rapid and sensitive method for the quantitation of microgram quantities of protein utilizing the principle of protein-dye binding. *Anal Biochem* 72, 248-254.
- Bras, M., Queenan, B., and Susin, S. A. (2005). Programmed cell death via mitochondria: different modes of dying. *Biochemistry (Mosc)* 70, 231-239.
- Bratton, S. B., MacFarlane, M., Cain, K., and Cohen, G. M. (2000). Protein complexes activate distinct caspase cascades in death receptor and stress-induced apoptosis. *Exp Cell Res* 256, 27-33.
- Bratton, S. B., Walker, G., Srinivasula, S. M., Sun, X. M., Butterworth, M., Alnemri, E. S., and Cohen, G. M. (2001). Recruitment, activation and retention of caspases-9 and-3 by Apaf-1 apoptosome and associated XIAP complexes. *EMBO J* 20, 998-1009.
- Brewster, J. L., Linseman, D. A., Bouchard, R. J., Loucks, F. A., Precht, T. A., Esch, E. A., and Heidenreich, K. A. (2006). Endoplasmic reticulum stress and trophic factor withdrawal activate distinct signaling cascades that induce glycogen synthase kinase-3 beta and a caspase-9-dependent apoptosis in cerebellar granule neurons. *Mol Cell Neurosci* 32, 242-253.

- Buss, R. R., Sun, W., and Oppenheim, R. W. (2006). Adaptive roles of programmed cell death during nervous system development. *Annu Rev Neurosci* 29, 1-35.
- Butler, R., and Bates, G. P. (2006). Histone deacetylase inhibitors as therapeutics for polyglutamine disorders. *Nat Rev Neurosci* 7, 784-796.
- Butts, B. D., Hudson, H. R., Linseman, D. A., Le, S. S., Ryan, K. R., Bouchard, R. J., and Heidenreich, K. A. (2005). Proteasome inhibition elicits a biphasic effect on neuronal apoptosis via differential regulation of pro-survival and pro-apoptotic transcription factors. *Mol Cell Neurosci*.
- Cain, K., Bratton, S. B., and Cohen, G. M. (2002). The Apaf-1 apoptosome: a large caspase-activating complex. *Biochimie* 84, 203-214.
- Campbell, D. S., and Holt, C. E. (2001). Chemotropic responses of retinal growth cones mediated by rapid local protein synthesis and degradation. *Neuron* 32, 1013-1026.
- Canu, N., Barbato, C., Ciotti, M. T., Serafino, A., Dus, L., and Calissano, P. (2000). Proteasome Involvement and Accumulation of Ubiquitinated Proteins in Cerebellar Granule Neurons Undergoing Apoptosis. *J Neurosci* 20, 589-599.
- Canu, N., Tufi, R., Serafino, A. L., Amadoro, G., Ciotti, M. T., and Calissano, P. (2005). Role of the autophagic-lysosomal system on low potassium-induced apoptosis in cultured cerebellar granule cells. *J Neurochem* 92, 1228-1242.
- Cao, X. X., Mohuiddin, I., Ece, F., McConkey, D. J., and Smythe, W. R. (2001). Histone deacetylase inhibitor downregulation of bcl-xl gene expression leads to apoptotic cell death in mesothelioma. *Am J Respir Cell Mol Biol* 25, 562-568.
- Cardozo, T., and Pagano, M. (2007). Wrenches in the works: drug discovery targeting the SCF ubiquitin ligase and APC/C complexes. *BMC Biochem* 8 *Suppl* 1, S9.
- Cerretti, D. P., Kozlosky, C. J., Mosley, B., Nelson, N., Van Ness, K., Greenstreet, T. A., March, C. J., Kronheim, S. R., Druck, T., Cannizzaro, L. A., and et al. (1992). Molecular cloning of the interleukin-1 beta converting enzyme. *Science* 256, 97-100.

- Certo, M., Del Gaizo Moore, V., Nishino, M., Wei, G., Korsmeyer, S., Armstrong, S. A., and Letai, A. (2006). Mitochondria primed by death signals determine cellular addiction to antiapoptotic BCL-2 family members. *Cancer Cell* 9, 351-365.
- Cha, J. H., Kosinski, C. M., Kerner, J. A., Alsdorf, S. A., Mangiarini, L., Davies, S. W., Penney, J. B., Bates, G. P., and Young, A. B. (1998). Altered brain neurotransmitter receptors in transgenic mice expressing a portion of an abnormal human huntington disease gene. *Proc Natl Acad Sci U S A* 95, 6480-6485.
- Chan, E. Y., Kir, S., and Tooze, S. A. (2007). siRNA screening of the kinome identifies ULK1 as a multidomain modulator of autophagy. *J Biol Chem* 282, 25464-25474.
- Chau, V., Tobias, J. W., Bachmair, A., Marriott, D., Ecker, D. J., Gonda, D. K., and Varshavsky, A. (1989). A multiubiquitin chain is confined to specific lysine in a targeted short-lived protein. *Science* 243, 1576-1583.
- Chen, M., He, H., Zhan, S., Krajewski, S., Reed, J. C., and Gottlieb, R. A. (2001). Bid is cleaved by calpain to an active fragment in vitro and during myocardial ischemia/reperfusion. *J Biol Chem* 276, 30724-30728.
- Chen, P., and Hochstrasser, M. (1996). Autocatalytic subunit processing couples active site formation in the 20S proteasome to completion of assembly. *Cell* 86, 961-972.
- Chen, P. S., Wang, C. C., Bortner, C. D., Peng, G. S., Wu, X., Pang, H., Lu, R. B., Gean, P. W., Chuang, D. M., and Hong, J. S. (2007). Valproic acid and other histone deacetylase inhibitors induce microglial apoptosis and attenuate lipopolysaccharide-induced dopaminergic neurotoxicity. *Neuroscience* 149, 203-212.
- Chen, Q., Gong, B., and Almasan, A. (2000). Distinct stages of cytochrome c release from mitochondria: evidence for a feedback amplification loop linking caspase activation to mitochondrial dysfunction in genotoxic stress induced apoptosis. *Cell Death Differ* 7, 227-233.
- Cheng, E. H., Kirsch, D. G., Clem, R. J., Ravi, R., Kastan, M. B., Bedi, A., Ueno, K., and Hardwick, J. M. (1997). Conversion of Bcl-2 to a Bax-like death effector by caspases. *Science* 278, 1966-1968.

- Cheong, H., Nair, U., Geng, J., and Klionsky, D. J. (2008). The Atg1 Kinase Complex Is Involved in the Regulation of Protein Recruitment to Initiate Sequestering Vesicle Formation for Nonspecific Autophagy in *Saccharomyces cerevisiae*. *Mol Biol Cell* 19, 668-681.
- Chinnaiyan, A. M., O'Rourke, K., Tewari, M., and Dixit, V. M. (1995). FADD, a novel death domain-containing protein, interacts with the death domain of Fas and initiates apoptosis. *Cell* 81, 505-512.
- Chung, C. H., and Baek, S. H. (1999). Deubiquitinating enzymes: their diversity and emerging roles. *Biochem Biophys Res Commun* 266, 633-640.
- Ciechanover, A. (1994). The ubiquitin-proteasome proteolytic pathway. *Cell* 79, 13-21.
- Ciechanover, A. (2005). Proteolysis: from the lysosome to ubiquitin and the proteasome. *Nat Rev Mol Cell Biol* 6, 79-87.
- Ciechanover, A., and Brundin, P. (2003). The Ubiquitin Proteasome System in Neurodegenerative Diseases: Sometimes the Chicken, Sometimes the Egg. *Neuron* 40, 427-446.
- Ciechanover, A., Elias, S., Heller, H., and Hershko, A. (1982). "Covalent affinity" purification of ubiquitin-activating enzyme. *J Biol Chem* 257, 2537-2542.
- Ciechanover, A., Finley, D., and Varshavsky, A. (1984). Ubiquitin dependence of selective protein degradation demonstrated in the mammalian cell cycle mutant ts85. *Cell* 37, 57-66.
- Ciechanover, A., Heller, H., Elias, S., Haas, A. L., and Hershko, A. (1980). ATP-dependent conjugation of reticulocyte proteins with the polypeptide required for protein degradation. *Proc Natl Acad Sci U S A* 77, 1365-1368.
- Ciechanover, A., Hod, Y., and Hershko, A. (1978). Heat-Stable Polypeptide Component of an Atp-Dependent Proteolytic System from Reticulocytes. *Biochem Biophys Res Commun* 81, 1100-1105.

- Clarke, P. G. (1990). Developmental cell death: morphological diversity and multiple mechanisms. *Anat Embryol (Berl)* 181, 195-213.
- Clem, R. J., Cheng, E. H., Karp, C. L., Kirsch, D. G., Ueno, K., Takahashi, A., Kastan, M. B., Griffin, D. E., Earnshaw, W. C., Veluona, M. A., and Hardwick, J. M. (1998). Modulation of cell death by Bcl-XL through caspase interaction. *Proc Natl Acad Sci U S A* 95, 554-559.
- Coffey, E. T., Smiciene, G., Hongisto, V., Cao, J., Brecht, S., Herdegen, T., and Courtney, M. J. (2002). c-Jun N-terminal protein kinase (JNK) 2/3 is specifically activated by stress, mediating c-Jun activation, in the presence of constitutive JNK1 activity in cerebellar neurons. *J Neurosci* 22, 4335-4345.
- Cohen, G. M. (1997). Caspases: the executioners of apoptosis. *Biochem J* 326 (Pt 1), 1-16.
- Conradt, B., and Horvitz, H. R. (1998). The *C. elegans* protein EGL-1 is required for programmed cell death and interacts with the Bcl-2-like protein CED-9. *Cell* 93, 519-529.
- Contestabile, A. (2002). Cerebellar granule cells as a model to study mechanisms of neuronal apoptosis or survival in vivo and in vitro. *Cerebellum* 1, 41-55.
- Cook, W. J., Jeffrey, L. C., Carson, M., Chen, Z., and Pickart, C. M. (1992). Structure of a diubiquitin conjugate and a model for interaction with ubiquitin conjugating enzyme (E2). *J Biol Chem* 267, 16467-16471.
- Cook, W. J., Jeffrey, L. C., Kasperek, E., and Pickart, C. M. (1994). Structure of tetraubiquitin shows how multiubiquitin chains can be formed. *J Mol Biol* 236, 601-609.
- Culmsee, C., and Mattson, M. P. (2005). p53 in neuronal apoptosis. *Biochem Biophys Res Commun* 331, 761-777.
- D'Mello, S. R., Anelli, R., and Calissano, P. (1994). Lithium induces apoptosis in immature cerebellar granule cells but promotes survival of mature neurons. *Exp Cell Res* 211, 332-338.

- D'Mello, S. R., Galli, C., Ciotti, T., and Calissano, P. (1993). Induction of apoptosis in cerebellar granule neurons by low potassium: inhibition of death by insulin-like growth factor I and cAMP. *Proc Natl Acad Sci U S A* *90*, 10989-10993.
- da Fonseca, P. C., and Morris, E. P. (2008). Structure of the human 26S proteasome: subunit radial displacements open the gate into the proteolytic core. *J Biol Chem* *283*, 23305-23314.
- de Ruijter, A. J., van Gennip, A. H., Caron, H. N., Kemp, S., and van Kuilenburg, A. B. (2003). Histone deacetylases (HDACs): characterization of the classical HDAC family. *Biochem J* *370*, 737-749.
- Degterev, A., and Yuan, J. (2008). Expansion and evolution of cell death programmes. *Nat Rev Mol Cell Biol* *9*, 378-390.
- Demarchi, F., Bertoli, C., Copetti, T., Tanida, I., Brancolini, C., Eskelinen, E. L., and Schneider, C. (2006). Calpain is required for macroautophagy in mammalian cells. *J Cell Biol* *175*, 595-605.
- DeMartino, G. N., and Slaughter, C. A. (1999). The proteasome, a novel protease regulated by multiple mechanisms. *J Biol Chem* *274*, 22123-22126.
- Deng, L., Wang, C., Spencer, E., Yang, L., Braun, A., You, J., Slaughter, C., Pickart, C., and Chen, Z. J. (2000). Activation of the I κ B kinase complex by TRAF6 requires a dimeric ubiquitin-conjugating enzyme complex and a unique polyubiquitin chain. *Cell* *103*, 351-361.
- Desagher, S., and Martinou, J. C. (2000). Mitochondria as the central control point of apoptosis. *Trends Cell Biol* *10*, 369-377.
- Desagher, S., Severac, D., Lipkin, A., Bernis, C., Ritchie, W., Le Digarcher, A., and Journot, L. (2005). Genes regulated in neurons undergoing transcription-dependent apoptosis belong to signaling pathways rather than the apoptotic machinery. *J Biol Chem* *280*, 5693-5702.
- Deveraux, Q. L., Roy, N., Stennicke, H. R., Van Arsdale, T., Zhou, Q., Srinivasula, S. M., Alnemri, E. S., Salvesen, G. S., and Reed, J. C. (1998). IAPs block apoptotic

- events induced by caspase-8 and cytochrome c by direct inhibition of distinct caspases. *EMBO J* 17, 2215-2223.
- Dice, J. F. (2007). Chaperone-mediated autophagy. *Autophagy* 3, 295-299.
- Donepudi, M., Mac Sweeney, A., Briand, C., and Grutter, M. G. (2003). Insights into the regulatory mechanism for caspase-8 activation. *Mol Cell* 11, 543-549.
- Du, C., Fang, M., Li, Y., Li, L., and Wang, X. (2000). Smac, a mitochondrial protein that promotes cytochrome c-dependent caspase activation by eliminating IAP inhibition. *Cell* 102, 33-42.
- Duan, H., Heckman, C. A., and Boxer, L. M. (2005). Histone deacetylase inhibitors down-regulate bcl-2 expression and induce apoptosis in t(14;18) lymphomas. *Mol Cell Biol* 25, 1608-1619.
- Eaton, E. M., and Sealy, L. (2003). Modification of CCAAT/enhancer-binding protein-beta by the small ubiquitin-like modifier (SUMO) family members, SUMO-2 and SUMO-3. *J Biol Chem* 278, 33416-33421.
- Eletr, Z. M., Huang, D. T., Duda, D. M., Schulman, B. A., and Kuhlman, B. (2005). E2 conjugating enzymes must disengage from their E1 enzymes before E3-dependent ubiquitin and ubiquitin-like transfer. *Nat Struct Mol Biol* 12, 933-934.
- Ellis, H. M., and Horvitz, H. R. (1986). Genetic control of programmed cell death in the nematode *C. elegans*. *Cell* 44, 817-829.
- Elsasser, S., Gali, R. R., Schwickart, M., Larsen, C. N., Leggett, D. S., Muller, B., Feng, M. T., Tubing, F., Dittmar, G. A., and Finley, D. (2002). Proteasome subunit Rpn1 binds ubiquitin-like protein domains. *Nat Cell Biol* 4, 725-730.
- Enari, M., Sakahira, H., Yokoyama, H., Okawa, K., Iwamatsu, A., and Nagata, S. (1998). A caspase-activated DNase that degrades DNA during apoptosis, and its inhibitor ICAD. *Nature* 391, 43-50.

- Erlich, S., Mizrachy, L., Segev, O., Lindenboim, L., Zmira, O., Adi-Harel, S., Hirsch, J. A., Stein, R., and Pinkas-Kramarski, R. (2007). Differential interactions between Beclin 1 and Bcl-2 family members. *Autophagy* 3, 561-568.
- Etlinger, J. D., and Goldberg, A. L. (1977). A soluble ATP-dependent proteolytic system responsible for the degradation of abnormal proteins in reticulocytes. *Proc Natl Acad Sci U S A* 74, 54-58.
- Fadok, V. A., Voelker, D. R., Campbell, P. A., Cohen, J. J., Bratton, D. L., and Henson, P. M. (1992). Exposure of phosphatidylserine on the surface of apoptotic lymphocytes triggers specific recognition and removal by macrophages. *J Immunol* 148, 2207-2216.
- Fang, S., Jensen, J. P., Ludwig, R. L., Vousden, K. H., and Weissman, A. M. (2000). Mdm2 is a RING finger-dependent ubiquitin protein ligase for itself and p53. *J Biol Chem* 275, 8945-8951.
- Fennell, D. A., Chacko, A., and Mutti, L. (2008). BCL-2 family regulation by the 20S proteasome inhibitor bortezomib. *Oncogene* 27, 1189-1197.
- Fimia, G. M., Stoykova, A., Romagnoli, A., Giunta, L., Di Bartolomeo, S., Nardacci, R., Corazzari, M., Fuoco, C., Ucar, A., Schwartz, P., *et al.* (2007). Ambra1 regulates autophagy and development of the nervous system. *Nature* 447, 1121-1125.
- Finley, D., Ciechanover, A., and Varshavsky, A. (1984). Thermolability of ubiquitin-activating enzyme from the mammalian cell cycle mutant ts85. *Cell* 37, 43-55.
- Finley, D., Tanaka, K., Mann, C., Feldmann, H., Hochstrasser, M., Vierstra, R., Johnston, S., Hampton, R., Haber, J., McCusker, J., *et al.* (1998). Unified nomenclature for subunits of the *Saccharomyces cerevisiae* proteasome regulatory particle. *Trends Biochem Sci* 23, 244-245.
- Fischer, A., Sananbenesi, F., Wang, X., Dobbin, M., and Tsai, L. H. (2007). Recovery of learning and memory is associated with chromatin remodelling. *Nature* 447, 178-182.
- Fuentes-Prior, P., and Salvesen, G. S. (2004). The protein structures that shape caspase activity, specificity, activation and inhibition. *Biochem J* 384, 201-232.

- Fujita, N., Itoh, T., Omori, H., Fukuda, M., Noda, T., and Yoshimori, T. (2008a). The Atg16L Complex Specifies the Site of LC3 Lipidation for Membrane Biogenesis in Autophagy. *Mol Biol Cell* *19*, 2092-2100.
- Fujita, N., Itoh, T., Omori, H., Fukuda, M., Noda, T., and Yoshimori, T. (2008b). The Atg16L Complex Specifies the Site of LC3 Lipidation for Membrane Biogenesis in Autophagy. *Mol Biol Cell* *19*, 2092-2100.
- Furumai, R., Komatsu, Y., Nishino, N., Khochbin, S., Yoshida, M., and Horinouchi, S. (2001). Potent histone deacetylase inhibitors built from trichostatin A and cyclic tetrapeptide antibiotics including trapoxin. *Proc Natl Acad Sci U S A* *98*, 87-92.
- Furuya, N., Yu, J., Byfield, M., Pattingre, S., and Levine, B. (2005). The evolutionarily conserved domain of Beclin 1 is required for Vps34 binding, autophagy and tumor suppressor function. *Autophagy* *1*, 46-52.
- Galli, C., Meucci, O., Scorziello, A., Werge, T. M., Calissano, P., and Schettini, G. (1995). Apoptosis in cerebellar granule cells is blocked by high KCl, forskolin, and IGF-1 through distinct mechanisms of action: the involvement of intracellular calcium and RNA synthesis. *J Neurosci* *15*, 1172-1179.
- Gallo, V., Kingsbury, A., Balazs, R., and Jorgensen, O. S. (1987). The role of depolarization in the survival and differentiation of cerebellar granule cells in culture. *J Neurosci* *7*, 2203-2213.
- Gao, L., Cueto, M. A., Asselbergs, F., and Atadja, P. (2002). Cloning and functional characterization of HDAC11, a novel member of the human histone deacetylase family. *J Biol Chem* *277*, 25748-25755.
- Gardian, G., Browne, S. E., Choi, D. K., Klivenyi, P., Gregorio, J., Kubilus, J. K., Ryu, H., Langley, B., Ratan, R. R., Ferrante, R. J., and Beal, M. F. (2005). Neuroprotective effects of phenylbutyrate in the N171-82Q transgenic mouse model of Huntington's disease. *J Biol Chem* *280*, 556-563.
- Gerhardt, E., Kugler, S., Leist, M., Beier, C., Berliocchi, L., Volbracht, C., Weller, M., Bahr, M., Nicotera, P., and Schulz, J. B. (2001). Cascade of caspase activation in

potassium-deprived cerebellar granule neurons: targets for treatment with peptide and protein inhibitors of apoptosis. *Mol Cell Neurosci* 17, 717-731.

Giguere, C. J., and Schnellmann, R. G. (2008). Limitations of SLLVY-AMC in calpain and proteasome measurements. *Biochem Biophys Res Commun* 371, 578-581.

Gill, G. (2004). SUMO and ubiquitin in the nucleus: different functions, similar mechanisms? *Genes Dev* 18, 2046-2059.

Glaser, K. B. (2007). HDAC inhibitors: clinical update and mechanism-based potential. *Biochem Pharmacol* 74, 659-671.

Glickman, M. H., and Ciechanover, A. (2002). The ubiquitin-proteasome proteolytic pathway: destruction for the sake of construction. *Physiol Rev* 82, 373-428.

Glickman, M. H., Rubin, D. M., Coux, O., Wefes, I., Pfeifer, G., Cjeka, Z., Baumeister, W., Fried, V. A., and Finley, D. (1998). A subcomplex of the proteasome regulatory particle required for ubiquitin-conjugate degradation and related to the COP9-signalosome and eIF3. *Cell* 94, 615-623.

Goldknopf, I. L., and Busch, H. (1977). Isopeptide linkage between nonhistone and histone 2A polypeptides of chromosomal conjugate-protein A24. *Proc Natl Acad Sci U S A* 74, 864-868.

Goldstein, G., Scheid, M., Hammerling, U., Schlesinger, D. H., Niall, H. D., and Boyse, E. A. (1975). Isolation of a polypeptide that has lymphocyte-differentiating properties and is probably represented universally in living cells. *Proc Natl Acad Sci U S A* 72, 11-15.

Goll, D. E., Thompson, V. F., Li, H., Wei, W., and Cong, J. (2003). The calpain system. *Physiol Rev* 83, 731-801.

Gonzalez, R., J., and Tarloff, J., B. (2001). Evaluation of hepatic subcellular fractions for Alamar blue and MTT reductase activity. *Toxicology in Vitro* 15, 257-259.

- Goping, I. S., Gross, A., Lavoie, J. N., Nguyen, M., Jemmerson, R., Roth, K., Korsmeyer, S. J., and Shore, G. C. (1998). Regulated targeting of BAX to mitochondria. *J Cell Biol* 143, 207-215.
- Graham, R. K., Deng, Y., Slow, E. J., Haigh, B., Bissada, N., Lu, G., Pearson, J., Shehadeh, J., Bertram, L., Murphy, Z., *et al.* (2006). Cleavage at the caspase-6 site is required for neuronal dysfunction and degeneration due to mutant huntingtin. *Cell* 125, 1179-1191.
- Griffiths, G. J., Dubrez, L., Morgan, C. P., Jones, N. A., Whitehouse, J., Corfe, B. M., Dive, C., and Hickman, J. A. (1999). Cell damage-induced conformational changes of the pro-apoptotic protein Bak in vivo precede the onset of apoptosis. *J Cell Biol* 144, 903-914.
- Groll, M., Bajorek, M., Kohler, A., Moroder, L., Rubin, D. M., Huber, R., Glickman, M. H., and Finley, D. (2000). A gated channel into the proteasome core particle. *Nat Struct Biol* 7, 1062-1067.
- Groll, M., Ditzel, L., Lowe, J., Stock, D., Bochtler, M., Bartunik, H. D., and Huber, R. (1997). Structure of 20S proteasome from yeast at 2.4 Å resolution. *Nature* 386, 463-471.
- Groll, M., Heinemeyer, W., Jager, S., Ullrich, T., Bochtler, M., Wolf, D. H., and Huber, R. (1999). The catalytic sites of 20S proteasomes and their role in subunit maturation: a mutational and crystallographic study. *Proc Natl Acad Sci U S A* 96, 10976-10983.
- Gutierrez, M. G., Munafo, D. B., Beron, W., and Colombo, M. I. (2004). Rab7 is required for the normal progression of the autophagic pathway in mammalian cells. *J Cell Sci* 117, 2687-2697.
- Haas, A. L., Warme, J. V., Hershko, A., and Rose, I. A. (1982). Ubiquitin-activating enzyme. Mechanism and role in protein-ubiquitin conjugation. *J Biol Chem* 257, 2543-2548.
- Hack, N., Hidaka, H., Wakefield, M. J., and Balazs, R. (1993). Promotion of granule cell survival by high K⁺ or excitatory amino acid treatment and Ca²⁺/calmodulin-dependent protein kinase activity. *Neuroscience* 57, 9-20.

- Haglund, K., and Dikic, I. (2005). Ubiquitylation and cell signaling. *EMBO J* 24, 3353-3359.
- Hamazaki, J., Iemura, S., Natsume, T., Yashiroda, H., Tanaka, K., and Murata, S. (2006). A novel proteasome interacting protein recruits the deubiquitinating enzyme UCH37 to 26S proteasomes. *EMBO J* 25, 4524-4536.
- Han, Z., Hendrickson, E. A., Bremner, T. A., and Wyche, J. H. (1997). A sequential two-step mechanism for the production of the mature p17:p12 form of caspase-3 in vitro. *J Biol Chem* 272, 13432-13436.
- Hanada, T., Noda, N. N., Satomi, Y., Ichimura, Y., Fujioka, Y., Takao, T., Inagaki, F., and Ohsumi, Y. (2007). The Atg12-Atg5 conjugate has a novel E3-like activity for protein lipidation in autophagy. *J Biol Chem* 282, 37298-37302.
- Hanada, T., and Ohsumi, Y. (2005). Structure-function relationship of Atg12, a ubiquitin-like modifier essential for autophagy. *Autophagy* 1, 110-118.
- Hanahan, D., and Weinberg, R. A. (2000). The hallmarks of cancer. *Cell* 100, 57-70.
- Handley, P. M., Mueckler, M., Siegel, N. R., Ciechanover, A., and Schwartz, A. L. (1991). Molecular cloning, sequence, and tissue distribution of the human ubiquitin-activating enzyme E1. *Proc Natl Acad Sci U S A* 88, 258-262.
- Hara, T., Nakamura, K., Matsui, M., Yamamoto, A., Nakahara, Y., Suzuki-Migishima, R., Yokoyama, M., Mishima, K., Saito, I., Okano, H., and Mizushima, N. (2006). Suppression of basal autophagy in neural cells causes neurodegenerative disease in mice. *Nature* 441, 885-889.
- Hara, T., Takamura, A., Kishi, C., Iemura, S., Natsume, T., Guan, J. L., and Mizushima, N. (2008). FIP200, a ULK-interacting protein, is required for autophagosome formation in mammalian cells. *J Cell Biol* 181, 497-510.
- Harper, N., Hughes, M., MacFarlane, M., and Cohen, G. M. (2003). Fas-associated death domain protein and caspase-8 are not recruited to the tumor necrosis factor receptor 1 signaling complex during tumor necrosis factor-induced apoptosis. *J Biol Chem* 278, 25534-25541.

-
- Harrington, L. S., Findlay, G. M., Gray, A., Tolkacheva, T., Wigfield, S., Rebholz, H., Barnett, J., Leslie, N. R., Cheng, S., Shepherd, P. R., *et al.* (2004). The TSC1-2 tumor suppressor controls insulin-PI3K signaling via regulation of IRS proteins. *J Cell Biol* 166, 213-223.
- Hatakeyama, S., and Nakayama, K. I. (2003). U-box proteins as a new family of ubiquitin ligases. *Biochem Biophys Res Commun* 302, 635-645.
- He, C., and Orvedahl, A. (2007). 2007 Keystone Symposium on Autophagy in Health and Disease. *Autophagy* 3, 527-536.
- Hendil, K. B., Khan, S., and Tanaka, K. (1998). Simultaneous binding of PA28 and PA700 activators to 20 S proteasomes. *Biochem J* 332 (Pt 3), 749-754.
- Hengartner, M. O. (2000). The biochemistry of apoptosis. *Nature* 407, 770-776.
- Hengartner, M. O., and Horvitz, H. R. (1994). *C. elegans* cell survival gene *ced-9* encodes a functional homolog of the mammalian proto-oncogene *bcl-2*. *Cell* 76, 665-676.
- Hershko, A., Ciechanover, A., Heller, H., Haas, A. L., and Rose, I. A. (1980). Proposed role of ATP in protein breakdown: conjugation of protein with multiple chains of the polypeptide of ATP-dependent proteolysis. *Proc Natl Acad Sci U S A* 77, 1783-1786.
- Hershko, A., Ciechanover, A., and Rose, I. A. (1979). Resolution of the ATP-dependent proteolytic system from reticulocytes: a component that interacts with ATP. *Proc Natl Acad Sci U S A* 76, 3107-3110.
- Hershko, A., Ciechanover, A., and Rose, I. A. (1981). Identification of the active amino acid residue of the polypeptide of ATP-dependent protein breakdown. *J Biol Chem* 256, 1525-1528.
- Hershko, A., Heller, H., Elias, S., and Ciechanover, A. (1983). Components of ubiquitin-protein ligase system. Resolution, affinity purification, and role in protein breakdown. *J Biol Chem* 258, 8206-8214.

- Hershko, A., and Rose, I. A. (1987). Ubiquitin-aldehyde: a general inhibitor of ubiquitin-recycling processes. *Proc Natl Acad Sci U S A* *84*, 1829-1833.
- Hirano, Y., Hendil, K. B., Yashiroda, H., Iemura, S., Nagane, R., Hioki, Y., Natsume, T., Tanaka, K., and Murata, S. (2005). A heterodimeric complex that promotes the assembly of mammalian 20S proteasomes. *Nature* *437*, 1381-1385.
- Hochstrasser, M. (2000). Evolution and function of ubiquitin-like protein-conjugation systems. *Nat Cell Biol* *2*, E153-157.
- Hol, E. M., Fischer, D. F., Ova, H., and Scheper, W. (2006). Ubiquitin proteasome system as a pharmacological target in neurodegeneration. *Expert Rev Neurother* *6*, 1337-1347.
- Holm, K., and Isacson, O. (1999). Factors intrinsic to the neuron can induce and maintain its ability to promote axonal outgrowth: a role for BCL2? *Trends Neurosci* *22*, 269-273.
- Hori, T., Osaka, F., Chiba, T., Miyamoto, C., Okabayashi, K., Shimbara, N., Kato, S., and Tanaka, K. (1999). Covalent modification of all members of human cullin family proteins by NEDD8. *Oncogene* *18*, 6829-6834.
- Hosfield, C. M., Elce, J. S., Davies, P. L., and Jia, Z. (1999). Crystal structure of calpain reveals the structural basis for Ca(2+)-dependent protease activity and a novel mode of enzyme activation. *EMBO J* *18*, 6880-6889.
- Houde, C., Banks, K. G., Coulombe, N., Rasper, D., Grimm, E., Roy, S., Simpson, E. M., and Nicholson, D. W. (2004). Caspase-7 expanded function and intrinsic expression level underlies strain-specific brain phenotype of caspase-3-null mice. *J Neurosci* *24*, 9977-9984.
- Hoyer-Hansen, M., Bastholm, L., Szyniarowski, P., Campanella, M., Szabadkai, G., Farkas, T., Bianchi, K., Fehrenbacher, N., Elling, F., Rizzuto, R., *et al.* (2007). Control of macroautophagy by calcium, calmodulin-dependent kinase kinase-beta, and Bcl-2. *Mol Cell* *25*, 193-205.

- Hsu, H., Huang, J., Shu, H. B., Baichwal, V., and Goeddel, D. V. (1996a). TNF-dependent recruitment of the protein kinase RIP to the TNF receptor-1 signaling complex. *Immunity* *4*, 387-396.
- Hsu, H., Shu, H. B., Pan, M. G., and Goeddel, D. V. (1996b). TRADD-TRAF2 and TRADD-FADD interactions define two distinct TNF receptor 1 signal transduction pathways. *Cell* *84*, 299-308.
- Hsu, H., Xiong, J., and Goeddel, D. V. (1995). The TNF receptor 1-associated protein TRADD signals cell death and NF-kappa B activation. *Cell* *81*, 495-504.
- Hsu, Y. T., and Youle, R. J. (1998). Bax in murine thymus is a soluble monomeric protein that displays differential detergent-induced conformations. *J Biol Chem* *273*, 10777-10783.
- Hu, Y., Ding, L., Spencer, D. M., and Nunez, G. (1998). WD-40 repeat region regulates Apaf-1 self-association and procaspase-9 activation. *J Biol Chem* *273*, 33489-33494.
- Huang, D. T., Hunt, H. W., Zhuang, M., Ohi, M. D., Holton, J. M., and Schulman, B. A. (2007). Basis for a ubiquitin-like protein thioester switch toggling E1-E2 affinity. *Nature* *445*, 394-398.
- Huang, D. T., Paydar, A., Zhuang, M., Waddell, M. B., Holton, J. M., and Schulman, B. A. (2005). Structural basis for recruitment of Ubc12 by an E2 binding domain in NEDD8's E1. *Mol Cell* *17*, 341-350.
- Huang, H., Joazeiro, C. A., Bonfoco, E., Kamada, S., Levenson, J. D., and Hunter, T. (2000). The inhibitor of apoptosis, cIAP2, functions as a ubiquitin-protein ligase and promotes in vitro monoubiquitination of caspases 3 and 7. *J Biol Chem* *275*, 26661-26664.
- Huang, Y., and Wang, K. K. (2001). The calpain family and human disease. *Trends Mol Med* *7*, 355-362.
- Hubbert, C., Guardiola, A., Shao, R., Kawaguchi, Y., Ito, A., Nixon, A., Yoshida, M., Wang, X. F., and Yao, T. P. (2002). HDAC6 is a microtubule-associated deacetylase. *Nature* *417*, 455-458.

- Huibregtse, J. M., Scheffner, M., Beaudenon, S., and Howley, P. M. (1995). A family of proteins structurally and functionally related to the E6-AP ubiquitin-protein ligase. *Proc Natl Acad Sci U S A* *92*, 2563-2567.
- Huibregtse, J. M., Scheffner, M., and Howley, P. M. (1991). A cellular protein mediates association of p53 with the E6 oncoprotein of human papillomavirus types 16 or 18. *EMBO J* *10*, 4129-4135.
- Huibregtse, J. M., Scheffner, M., and Howley, P. M. (1993). Cloning and expression of the cDNA for E6-AP, a protein that mediates the interaction of the human papillomavirus E6 oncoprotein with p53. *Mol Cell Biol* *13*, 775-784.
- Huntington, N. D., Puthalakath, H., Gunn, P., Naik, E., Michalak, E. M., Smyth, M. J., Tabarias, H., Degli-Esposti, M. A., Dewson, G., Willis, S. N., *et al.* (2007). Interleukin 15-mediated survival of natural killer cells is determined by interactions among Bim, Noxa and Mcl-1. *Nat Immunol* *8*, 856-863.
- Huttenlocher, A., Palecek, S. P., Lu, Q., Zhang, W., Mellgren, R. L., Lauffenburger, D. A., Ginsberg, M. H., and Horwitz, A. F. (1997). Regulation of cell migration by the calcium-dependent protease calpain. *J Biol Chem* *272*, 32719-32722.
- Ichimura, Y., Kirisako, T., Takao, T., Satomi, Y., Shimonishi, Y., Ishihara, N., Mizushima, N., Tanida, I., Kominami, E., Ohsumi, M., *et al.* (2000). A ubiquitin-like system mediates protein lipidation. *Nature* *408*, 488-492.
- Inoue, S., MacFarlane, M., Harper, N., Wheat, L. M., Dyer, M. J., and Cohen, G. M. (2004). Histone deacetylase inhibitors potentiate TNF-related apoptosis-inducing ligand (TRAIL)-induced apoptosis in lymphoid malignancies. *Cell Death Differ* *11 Suppl 2*, S193-206.
- Inoue, S., Mai, A., Dyer, M. J., and Cohen, G. M. (2006a). Inhibition of histone deacetylase class I but not class II is critical for the sensitization of leukemic cells to tumor necrosis factor-related apoptosis-inducing ligand-induced apoptosis. *Cancer Res* *66*, 6785-6792.

- Inoue, S., Riley, J., Gant, T. W., Dyer, M. J., and Cohen, G. M. (2007). Apoptosis induced by histone deacetylase inhibitors in leukemic cells is mediated by Bim and Noxa. *Leukemia* 21, 1773-1782.
- Inoue, S., Twiddy, D., Dyer, M. J., and Cohen, G. M. (2006b). Upregulation of TRAIL-R2 is not involved in HDACi mediated sensitization to TRAIL-induced apoptosis. *Cell Death Differ* 13, 2160-2162.
- Inoue, S., Walewska, R., Dyer, M. J., and Cohen, G. M. (2008). Downregulation of Mcl-1 potentiates HDACi-mediated apoptosis in leukemic cells. *Leukemia* 22, 819-825.
- Iwata, A., Riley, B. E., Johnston, J. A., and Kopito, R. R. (2005). HDAC6 and microtubules are required for autophagic degradation of aggregated huntingtin. *J Biol Chem* 280, 40282-40292.
- Jager, S., Bucci, C., Tanida, I., Ueno, T., Kominami, E., Saftig, P., and Eskelinen, E. L. (2004). Role for Rab7 in maturation of late autophagic vacuoles. *J Cell Sci* 117, 4837-4848.
- Jang, M., Park, B. C., Lee, A. Y., Na, K. S., Kang, S., Bae, K. H., Myung, P. K., Chung, B. C., Cho, S., Lee do, H., and Park, S. G. (2007). Caspase-7 mediated cleavage of proteasome subunits during apoptosis. *Biochem Biophys Res Commun* 363, 388-394.
- Jänicke, R. U., Ng, P., Sprengart, M. L., and Porter, A. G. (1998). Caspase-3 Is Required for α -Fodrin Cleavage but Dispensable for Cleavage of Other Death Substrates in Apoptosis. *J Biol Chem* 273, 15540-15545.
- Jeong, M. R., Hashimoto, R., Senatorov, V. V., Fujimaki, K., Ren, M., Lee, M. S., and Chuang, D. M. (2003). Valproic acid, a mood stabilizer and anticonvulsant, protects rat cerebral cortical neurons from spontaneous cell death: a role of histone deacetylase inhibition. *FEBS Lett* 542, 74-78.
- Jiang, X., and Wang, X. (2000). Cytochrome c promotes caspase-9 activation by inducing nucleotide binding to Apaf-1. *J Biol Chem* 275, 31199-31203.
- Jin, J., Li, X., Gygi, S. P., and Harper, J. W. (2007). Dual E1 activation systems for ubiquitin differentially regulate E2 enzyme charging. *Nature* 447, 1135-1138.

- Joazeiro, C. A., Wing, S. S., Huang, H., Levenson, J. D., Hunter, T., and Liu, Y. C. (1999). The tyrosine kinase negative regulator c-Cbl as a RING-type, E2-dependent ubiquitin-protein ligase. *Science* 286, 309-312.
- Johnson, E. S., Ma, P. C., Ota, I. M., and Varshavsky, A. (1995). A proteolytic pathway that recognizes ubiquitin as a degradation signal. *J Biol Chem* 270, 17442-17456.
- Johnson, J. A., Ward, C. W., and Kopito, R. R. (1998). Aggresomes: A cellular response to misfolded proteins. *Mol Biol Cell* 9, 260a-260a.
- Johnstone, R. W. (2002). Histone-deacetylase inhibitors: novel drugs for the treatment of cancer. *Nat Rev Drug Discov* 1, 287-299.
- Juhasz, G., Erdi, B., Sass, M., and Neufeld, T. P. (2007). Atg7-dependent autophagy promotes neuronal health, stress tolerance, and longevity but is dispensable for metamorphosis in *Drosophila*. *Genes Dev* 21, 3061-3066.
- Juhasz, G., and Neufeld, T. P. (2006). Autophagy: a forty-year search for a missing membrane source. *PLoS Biol* 4, e36.
- Kaasik, A., Rikk, T., Piirsoo, A., Zharkovsky, T., and Zharkovsky, A. (2005). Up-regulation of lysosomal cathepsin L and autophagy during neuronal death induced by reduced serum and potassium. *Eur J Neurosci* 22, 1023-1031.
- Kabeya, Y., Kamada, Y., Baba, M., Takikawa, H., Sasaki, M., and Ohsumi, Y. (2005). Atg17 functions in cooperation with Atg1 and Atg13 in yeast autophagy. *Mol Biol Cell* 16, 2544-2553.
- Kabeya, Y., Mizushima, N., Ueno, T., Yamamoto, A., Kirisako, T., Noda, T., Kominami, E., Ohsumi, Y., and Yoshimori, T. (2000). LC3, a mammalian homologue of yeast Apg8p, is localized in autophagosomal membranes after processing. *EMBO J* 19, 5720-5728.
- Kaiser, P., Flick, K., Wittenberg, C., and Reed, S. I. (2000). Regulation of transcription by ubiquitination without proteolysis: Cdc34/SCF(Met30)-mediated inactivation of the transcription factor Met4. *Cell* 102, 303-314.

- Kamada, Y., Funakoshi, T., Shintani, T., Nagano, K., Ohsumi, M., and Ohsumi, Y. (2000). Tor-mediated induction of autophagy via an Apg1 protein kinase complex. *J Cell Biol* *150*, 1507-1513.
- Kang, C., You, Y. J., and Avery, L. (2007). Dual roles of autophagy in the survival of *Caenorhabditis elegans* during starvation. *Genes Dev* *21*, 2161-2171.
- Kang, S. J., Wang, S., Hara, H., Peterson, E. P., Namura, S., Amin-Hanjani, S., Huang, Z., Srinivasan, A., Tomaselli, K. J., Thornberry, N. A., *et al.* (2000). Dual role of caspase-11 in mediating activation of caspase-1 and caspase-3 under pathological conditions. *J Cell Biol* *149*, 613-622.
- Kawaguchi, Y., Kovacs, J. J., McLaurin, A., Vance, J. M., Ito, A., and Yao, T. P. (2003). The deacetylase HDAC6 regulates aggresome formation and cell viability in response to misfolded protein stress. *Cell* *115*, 727-738.
- Kerr, J. F., Wyllie, A. H., and Currie, A. R. (1972). Apoptosis: a basic biological phenomenon with wide-ranging implications in tissue kinetics. *Br J Cancer* *26*, 239-257.
- Kihara, A., Noda, T., Ishihara, N., and Ohsumi, Y. (2001). Two distinct Vps34 phosphatidylinositol 3-kinase complexes function in autophagy and carboxypeptidase Y sorting in *Saccharomyces cerevisiae*. *J Cell Biol* *152*, 519-530.
- Kim, H. J., Rowe, M., Ren, M., Hong, J. S., Chen, P. S., and Chuang, D. M. (2007). Histone deacetylase inhibitors exhibit anti-inflammatory and neuroprotective effects in a rat permanent ischemic model of stroke: multiple mechanisms of action. *J Pharmacol Exp Ther* *321*, 892-901.
- Kim, J., Dalton, V. M., Eggerton, K. P., Scott, S. V., and Klionsky, D. J. (1999). Apg7p/Cvt2p is required for the cytoplasm-to-vacuole targeting, macroautophagy, and peroxisome degradation pathways. *Mol Biol Cell* *10*, 1337-1351.
- Kim, J., Huang, W. P., Stromhaug, P. E., and Klionsky, D. J. (2002). Convergence of multiple autophagy and cytoplasm to vacuole targeting components to a perivacuolar membrane compartment prior to de novo vesicle formation. *J Biol Chem* *277*, 763-773.

- Kimura, S., Noda, T., and Yoshimori, T. (2007). Dissection of the autophagosome maturation process by a novel reporter protein, tandem fluorescent-tagged LC3. *Autophagy* 3, 452-460.
- Kirisako, T., Baba, M., Ishihara, N., Miyazawa, K., Ohsumi, M., Yoshimori, T., Noda, T., and Ohsumi, Y. (1999). Formation process of autophagosome is traced with Apg8/Aut7p in yeast. *J Cell Biol* 147, 435-446.
- Kirisako, T., Ichimura, Y., Okada, H., Kabeya, Y., Mizushima, N., Yoshimori, T., Ohsumi, M., Takao, T., Noda, T., and Ohsumi, Y. (2000). The reversible modification regulates the membrane-binding state of Apg8/Aut7 essential for autophagy and the cytoplasm to vacuole targeting pathway. *J Cell Biol* 151, 263-276.
- Kisselev, A. F., Akopian, T. N., Castillo, V., and Goldberg, A. L. (1999). Proteasome active sites allosterically regulate each other, suggesting a cyclical bite-chew mechanism for protein breakdown. *Mol Cell* 4, 395-402.
- Kitada, T., Asakawa, S., Hattori, N., Matsumine, H., Yamamura, Y., Minoshima, S., Yokochi, M., Mizuno, Y., and Shimizu, N. (1998). Mutations in the parkin gene cause autosomal recessive juvenile parkinsonism. *Nature* 392, 605-608.
- Klionsky, D. J., Cregg, J. M., Dunn, W. A., Jr., Emr, S. D., Sakai, Y., Sandoval, I. V., Sibirny, A., Subramani, S., Thumm, M., Veenhuis, M., and Ohsumi, Y. (2003). A unified nomenclature for yeast autophagy-related genes. *Dev Cell* 5, 539-545.
- Kloetzel, P. M., and Ossendorp, F. (2004). Proteasome and peptidase function in MHC-class-I-mediated antigen presentation. *Curr Opin Immunol* 16, 76-81.
- Kluck, R. M., Bossy-Wetzel, E., Green, D. R., and Newmeyer, D. D. (1997). The release of cytochrome c from mitochondria: a primary site for Bcl-2 regulation of apoptosis. *Science* 275, 1132-1136.
- Kohler, A., Bajorek, M., Groll, M., Moroder, L., Rubin, D. M., Huber, R., Glickman, M. H., and Finley, D. (2001). The substrate translocation channel of the proteasome. *Biochimie* 83, 325-332.

- Komatsu, M., Tanida, I., Ueno, T., Ohsumi, M., Ohsumi, Y., and Kominami, E. (2001). The C-terminal region of an Apg7p/Cvt2p is required for homodimerization and is essential for its E1 activity and E1-E2 complex formation. *J Biol Chem* 276, 9846-9854.
- Komatsu, M., Waguri, S., Chiba, T., Murata, S., Iwata, J., Tanida, I., Ueno, T., Koike, M., Uchiyama, Y., Kominami, E., and Tanaka, K. (2006). Loss of autophagy in the central nervous system causes neurodegeneration in mice. *Nature* 441, 880-884.
- Komatsu, M., Waguri, S., Ueno, T., Iwata, J., Murata, S., Tanida, I., Ezaki, J., Mizushima, N., Ohsumi, Y., Uchiyama, Y., *et al.* (2005). Impairment of starvation-induced and constitutive autophagy in Atg7-deficient mice. *J Cell Biol* 169, 425-434.
- Komatsu, M., Wang, Q. J., Holstein, G. R., Friedrich, V. L., Jr., Iwata, J., Kominami, E., Chait, B. T., Tanaka, K., and Yue, Z. (2007). Essential role for autophagy protein Atg7 in the maintenance of axonal homeostasis and the prevention of axonal degeneration. *Proc Natl Acad Sci U S A* 104, 14489-14494.
- Kopito, R. R. (2000). Aggresomes, inclusion bodies and protein aggregation. *Trends Cell Biol* 10, 524-530.
- Kothakota, S., Azuma, T., Reinhard, C., Klippel, A., Tang, J., Chu, K., McGarry, T. J., Kirschner, M. W., Kohts, K., Kwiatkowski, D. J., and Williams, L. T. (1997). Caspase-3-generated fragment of gelsolin: effector of morphological change in apoptosis. *Science* 278, 294-298.
- Kouroku, Y., Fujita, E., Tanida, I., Ueno, T., Isoai, A., Kumagai, H., Ogawa, S., Kaufman, R. J., Kominami, E., and Momoi, T. (2007). ER stress (PERK/eIF2alpha phosphorylation) mediates the polyglutamine-induced LC3 conversion, an essential step for autophagy formation. *Cell Death Differ* 14, 230-239.
- Kovacs, J. J., Murphy, P. J., Gaillard, S., Zhao, X., Wu, J. T., Nicchitta, C. V., Yoshida, M., Toft, D. O., Pratt, W. B., and Yao, T. P. (2005). HDAC6 regulates Hsp90 acetylation and chaperone-dependent activation of glucocorticoid receptor. *Mol Cell* 18, 601-607.
- Kubbutat, M. H., Jones, S. N., and Vousden, K. H. (1997). Regulation of p53 stability by Mdm2. *Nature* 387, 299-303.

- Kuida, K., Haydar, T. F., Kuan, C. Y., Gu, Y., Taya, C., Karasuyama, H., Su, M. S., Rakic, P., and Flavell, R. A. (1998). Reduced apoptosis and cytochrome c-mediated caspase activation in mice lacking caspase 9. *Cell* 94, 325-337.
- Kuida, K., Zheng, T. S., Na, S., Kuan, C., Yang, D., Karasuyama, H., Rakic, P., and Flavell, R. A. (1996). Decreased apoptosis in the brain and premature lethality in CPP32-deficient mice. *Nature* 384, 368-372.
- Kuma, A., Hatano, M., Matsui, M., Yamamoto, A., Nakaya, H., Yoshimori, T., Ohsumi, Y., Tokuhisa, T., and Mizushima, N. (2004). The role of autophagy during the early neonatal starvation period. *Nature* 432, 1032-1036.
- Kuma, A., Mizushima, N., Ishihara, N., and Ohsumi, Y. (2002). Formation of the approximately 350-kDa Apg12-Apg5-Apg16 multimeric complex, mediated by Apg16 oligomerization, is essential for autophagy in yeast. *J Biol Chem* 277, 18619-18625.
- Kundu, M., and Thompson, C. B. (2008). Autophagy: basic principles and relevance to disease. *Annu Rev Pathol* 3, 427-455.
- Kuwana, T., Bouchier-Hayes, L., Chipuk, J. E., Bonzon, C., Sullivan, B. A., Green, D. R., and Newmeyer, D. D. (2005). BH3 domains of BH3-only proteins differentially regulate Bax-mediated mitochondrial membrane permeabilization both directly and indirectly. *Mol Cell* 17, 525-535.
- Lam, Y. A., Lawson, T. G., Velayutham, M., Zweier, J. L., and Pickart, C. M. (2002). A proteasomal ATPase subunit recognizes the polyubiquitin degradation signal. *Nature* 416, 763-767.
- Langley, B., D'Annibale, M. A., Suh, K., Ayoub, I., Tolhurst, A., Bastan, B., Yang, L., Ko, B., Fisher, M., Cho, S., *et al.* (2008). Pulse inhibition of histone deacetylases induces complete resistance to oxidative death in cortical neurons without toxicity and reveals a role for cytoplasmic p21(waf1/cip1) in cell cycle-independent neuroprotection. *J Neurosci* 28, 163-176.
- Lasher, R. S., and Zagon, I. S. (1972). The effect of potassium on neuronal differentiation in cultures of dissociated newborn rat cerebellum. *Brain Res* 41, 482-488.

- Lee, D. H., and Goldberg, A. L. (1998). Proteasome inhibitors: valuable new tools for cell biologists. *Trends Cell Biol* 8, 397-403.
- Lee, I., and Schindelin, H. (2008). Structural insights into E1-catalyzed ubiquitin activation and transfer to conjugating enzymes. *Cell* 134, 268-278.
- Lee, M. S., Kwon, Y. T., Li, M., Peng, J., Friedlander, R. M., and Tsai, L. H. (2000). Neurotoxicity induces cleavage of p35 to p25 by calpain. *Nature* 405, 360-364.
- Lee, S. J., Choi, D., Rhim, H., and Kang, S. (2005). E3 ubiquitin ligase RNF2 interacts with the S6' proteasomal ATPase subunit and increases the ATP hydrolysis activity of S6'. *Biochem J* 389, 457-463.
- Leggett, D. S., Hanna, J., Borodovsky, A., Crosas, B., Schmidt, M., Baker, R. T., Walz, T., Ploegh, H., and Finley, D. (2002). Multiple associated proteins regulate proteasome structure and function. *Mol Cell* 10, 495-507.
- Leist, M., Fava, E., Montecucco, C., and Nicotera, P. (1997). Peroxynitrite and nitric oxide donors induce neuronal apoptosis by eliciting autocrine excitotoxicity. *Eur J Neurosci* 9, 1488-1498.
- Leist, M., Volbracht, C., Fava, E., and Nicotera, P. (1998). 1-Methyl-4-phenylpyridinium induces autocrine excitotoxicity, protease activation, and neuronal apoptosis. *Mol Pharmacol* 54, 789-801.
- Leng, Y., and Chuang, D. M. (2006). Endogenous alpha-synuclein is induced by valproic acid through histone deacetylase inhibition and participates in neuroprotection against glutamate-induced excitotoxicity. *J Neurosci* 26, 7502-7512.
- Leng, Y., Liang, M. H., Ren, M., Marinova, Z., Leeds, P., and Chuang, D. M. (2008). Synergistic neuroprotective effects of lithium and valproic acid or other histone deacetylase inhibitors in neurons: roles of glycogen synthase kinase-3 inhibition. *J Neurosci* 28, 2576-2588.
- Leonard, J. R., Klocke, B. J., D'Sa, C., Flavell, R. A., and Roth, K. A. (2002). Strain-dependent neurodevelopmental abnormalities in caspase-3-deficient mice. *J Neuropathol Exp Neurol* 61, 673-677.

Letai, A., Bassik, M. C., Walensky, L. D., Sorcinelli, M. D., Weiler, S., and Korsmeyer, S. J. (2002). Distinct BH3 domains either sensitize or activate mitochondrial apoptosis, serving as prototype cancer therapeutics. *Cancer Cell* 2, 183-192.

Levick, V., Coffey, H., and D'Mello, S. R. (1995). Opposing effects of thapsigargin on the survival of developing cerebellar granule neurons in culture. *Brain Res* 676, 325-335.

Levine, B. (2007). Cell biology: autophagy and cancer. *Nature* 446, 745-747.

Levine, B., and Klionsky, D. J. (2004). Development by self-digestion: molecular mechanisms and biological functions of autophagy. *Dev Cell* 6, 463-477.

Levine, B., and Kroemer, G. (2008). Autophagy in the pathogenesis of disease. *Cell* 132, 27-42.

Levine, B., and Yuan, J. (2005). Autophagy in cell death: an innocent convict? *J Clin Invest* 115, 2679-2688.

Levkovitz, Y., and Baraban, J. M. (2001). A dominant negative inhibitor of the Egr family of transcription regulatory factors suppresses cerebellar granule cell apoptosis by blocking c-Jun activation. *J Neurosci* 21, 5893-5901.

Ley, R., Balmanno, K., Hadfield, K., Weston, C., and Cook, S. J. (2003). Activation of the ERK1/2 signaling pathway promotes phosphorylation and proteasome-dependent degradation of the BH3-only protein, Bim. *J Biol Chem* 278, 18811-18816.

Li, H., Zhu, H., Xu, C. J., and Yuan, J. (1998). Cleavage of BID by caspase 8 mediates the mitochondrial damage in the Fas pathway of apoptosis. *Cell* 94, 491-501.

Li, M., Ona, V. O., Guegan, C., Chen, M., Jackson-Lewis, V., Andrews, L. J., Olszewski, A. J., Stieg, P. E., Lee, J. P., Przedborski, S., and Friedlander, R. M. (2000). Functional role of caspase-1 and caspase-3 in an ALS transgenic mouse model. *Science* 288, 335-339.

- Li, P., Nijhawan, D., Budihardjo, I., Srinivasula, S. M., Ahmad, M., Alnemri, E. S., and Wang, X. D. (1997). Cytochrome c and dATP-dependent formation of Apaf-1/caspase-9 complex initiates an apoptotic protease cascade. *Cell* *91*, 479-489.
- Liang, C., Feng, P., Ku, B., Dotan, I., Canaani, D., Oh, B. H., and Jung, J. U. (2006). Autophagic and tumour suppressor activity of a novel Beclin1-binding protein UVRAG. *Nat Cell Biol* *8*, 688-699.
- Liang, C., Lee, J. S., Inn, K. S., Gack, M. U., Li, Q., Roberts, E. A., Vergne, I., Deretic, V., Feng, P., Akazawa, C., and Jung, J. U. (2008). Beclin1-binding UVRAG targets the class C Vps complex to coordinate autophagosome maturation and endocytic trafficking. *Nat Cell Biol* *10*, 776-787.
- Liang, X. H., Kleeman, L. K., Jiang, H. H., Gordon, G., Goldman, J. E., Berry, G., Herman, B., and Levine, B. (1998). Protection against fatal Sindbis virus encephalitis by beclin, a novel Bcl-2-interacting protein. *J Virol* *72*, 8586-8596.
- Lim, C. R., Fukakusa, A., and Matsubara, K. (2004). Gene expression profiling of mouse postnatal cerebellar development using cDNA microarrays. *Gene* *333*, 3-13.
- Lin, Y., Devin, A., Rodriguez, Y., and Liu, Z. G. (1999). Cleavage of the death domain kinase RIP by caspase-8 prompts TNF-induced apoptosis. *Genes Dev* *13*, 2514-2526.
- Lindsten, K., Menendez-Benito, V., Masucci, M. G., and Dantuma, N. P. (2003). A transgenic mouse model of the ubiquitin/proteasome system. *Nat Biotechnol* *21*, 897-902.
- Lindsten, K., Menendez-Benito, V., Masucci, M. G., Dantuma, N. P., Kumarapeli, A. R., Horak, K. M., Zheng, H., and Wang, X. (2006). GFP reporter mouse models of UPS proteolytic function. *FASEB J* *20*, 1027; author reply 1027-1028.
- Linseman, D. A., Bartley, C. M., Le, S. S., Laessig, T. A., Bouchard, R. J., Meintzer, M. K., Li, M., and Heidenreich, K. A. (2003). Inactivation of the myocyte enhancer factor-2 repressor histone deacetylase-5 by endogenous Ca(2+) //calmodulin-dependent kinase II promotes depolarization-mediated cerebellar granule neuron survival. *J Biol Chem* *278*, 41472-41481.

- Linseman, D. A., Butts, B. D., Precht, T. A., Phelps, R. A., Le, S. S., Laessig, T. A., Bouchard, R. J., Florez-McClure, M. L., and Heidenreich, K. A. (2004). Glycogen synthase kinase-3 β phosphorylates Bax and promotes its mitochondrial localization during neuronal apoptosis. *J Neurosci* 24, 9993-10002.
- Linseman, D. A., Phelps, R. A., Bouchard, R. J., Le, S. S., Laessig, T. A., McClure, M. L., and Heidenreich, K. A. (2002). Insulin-like growth factor-I blocks Bcl-2 interacting mediator of cell death (Bim) induction and intrinsic death signaling in cerebellar granule neurons. *J Neurosci* 22, 9287-9297.
- Liu, C. W., Li, X., Thompson, D., Wooding, K., Chang, T. L., Tang, Z., Yu, H., Thomas, P. J., and DeMartino, G. N. (2006). ATP binding and ATP hydrolysis play distinct roles in the function of 26S proteasome. *Mol Cell* 24, 39-50.
- Liu, X., Kim, C. N., Yang, J., Jemmerson, R., and Wang, X. (1996). Induction of apoptotic program in cell-free extracts: requirement for dATP and cytochrome c. *Cell* 86, 147-157.
- Love, K. R., Catic, A., Schlieker, C., and Ploegh, H. L. (2007). Mechanisms, biology and inhibitors of deubiquitinating enzymes. *Nat Chem Biol* 3, 697-705.
- Lowe, J., Stock, D., Jap, B., Zwickl, P., Baumeister, W., and Huber, R. (1995). Crystal structure of the 20S proteasome from the archaeon *T. acidophilum* at 3.4 Å resolution. *Science* 268, 533-539.
- Luciano, F., Jacquelin, A., Colosetti, P., Herrant, M., Cagnol, S., Pages, G., and Auberger, P. (2003). Phosphorylation of Bim-EL by Erk1/2 on serine 69 promotes its degradation via the proteasome pathway and regulates its proapoptotic function. *Oncogene* 22, 6785-6793.
- Luger, K., Mader, A. W., Richmond, R. K., Sargent, D. F., and Richmond, T. J. (1997). Crystal structure of the nucleosome core particle at 2.8 Å resolution. *Nature* 389, 251-260.
- Luker, G. D., Pica, C. M., Song, J., Luker, K. E., and Piwnicka-Worms, D. (2003). Imaging 26S proteasome activity and inhibition in living mice. *Nat Med* 9, 969-973.

Lum, J. J., Bauer, D. E., Kong, M., Harris, M. H., Li, C., Lindsten, T., and Thompson, C. B. (2005). Growth factor regulation of autophagy and cell survival in the absence of apoptosis. *Cell* 120, 237-248.

MacCallum, D. E., Melville, J., Frame, S., Watt, K., Anderson, S., Gianella-Borradori, A., Lane, D. P., and Green, S. R. (2005). Seliciclib (CYC202, R-Roscovitin) induces cell death in multiple myeloma cells by inhibition of RNA polymerase II-dependent transcription and down-regulation of Mcl-1. *Cancer Res* 65, 5399-5407.

MacFarlane, M. (2003). TRAIL-induced signalling and apoptosis. *Toxicol Lett* 139, 89-97.

MacFarlane, M., Cain, K., Sun, X. M., Alnemri, E. S., and Cohen, G. M. (1997). Processing/activation of at least four interleukin-1beta converting enzyme-like proteases occurs during the execution phase of apoptosis in human monocytic tumor cells. *J Cell Biol* 137, 469-479.

MacFarlane, M., Merrison, W., Bratton, S. B., and Cohen, G. M. (2002). Proteasome-mediated degradation of Smac during apoptosis: XIAP promotes Smac ubiquitination in vitro. *J Biol Chem* 277, 36611-36616.

Madden, D. T., Egger, L., and Bredesen, D. E. (2007). A calpain-like protease inhibits autophagic cell death. *Autophagy* 3, 519-522.

Mai, A., Massa, S., Pezzi, R., Simeoni, S., Rotili, D., Nebbioso, A., Scognamiglio, A., Altucci, L., Loidl, P., and Brosch, G. (2005). Class II (IIa)-selective histone deacetylase inhibitors. 1. Synthesis and biological evaluation of novel (aryloxopropenyl)pyrrolyl hydroxyamides. *J Med Chem* 48, 3344-3353.

Maiuri, M. C., Le Toumelin, G., Criollo, A., Rain, J. C., Gautier, F., Juin, P., Tasdemir, E., Pierron, G., Troulinaki, K., Tavernarakis, N., *et al.* (2007a). Functional and physical interaction between Bcl-X(L) and a BH3-like domain in Beclin-1. *EMBO J* 26, 2527-2539.

Maiuri, M. C., Zalckvar, E., Kimchi, A., and Kroemer, G. (2007b). Self-eating and self-killing: crosstalk between autophagy and apoptosis. *Nat Rev Mol Cell Biol* 8, 741-752.

- Majeski, A. E., and Dice, J. F. (2004). Mechanisms of chaperone-mediated autophagy. *Int J Biochem Cell Biol* 36, 2435-2444.
- Manzini, M. C., Joseph, D. J., MacDermott, A. B., and Mason, C. A. (2007). Differential effects of AMPA receptor activation on survival and neurite integrity during neuronal development. *Mol Cell Neurosci* 35, 328-338.
- Manzini, M. C., Ward, M. S., Zhang, Q., Lieberman, M. D., and Mason, C. A. (2006). The stop signal revised: immature cerebellar granule neurons in the external germinal layer arrest pontine mossy fiber growth. *J Neurosci* 26, 6040-6051.
- Mao, Z., Bonni, A., Xia, F., Nadal-Vicens, M., and Greenberg, M. E. (1999). Neuronal activity-dependent cell survival mediated by transcription factor MEF2. *Science* 286, 785-790.
- Mao, Z., and Wiedmann, M. (1999). Calcineurin enhances MEF2 DNA binding activity in calcium-dependent survival of cerebellar granule neurons. *J Biol Chem* 274, 31102-31107.
- Marino, G., Salvador-Montoliu, N., Fueyo, A., Knecht, E., Mizushima, N., and Lopez-Otin, C. (2007). Tissue-specific autophagy alterations and increased tumorigenesis in mice deficient in Atg4C/autophagin-3. *J Biol Chem* 282, 18573-18583.
- Marino, G., Uria, J. A., Puente, X. S., Quesada, V., Bordallo, J., and Lopez-Otin, C. (2003). Human autophagins, a family of cysteine proteinases potentially implicated in cell degradation by autophagy. *J Biol Chem* 278, 3671-3678.
- Martin, S. J., O'Brien, G. A., Nishioka, W. K., McGahon, A. J., Mahboubi, A., Saido, T. C., and Green, D. R. (1995). Proteolysis of fodrin (non-erythroid spectrin) during apoptosis. *J Biol Chem* 270, 6425-6428.
- Martinon, F., and Tschopp, J. (2007). Inflammatory caspases and inflammasomes: master switches of inflammation. *Cell Death Differ* 14, 10-22.
- Mason, G. G., Murray, R. Z., Pappin, D., and Rivett, A. J. (1998). Phosphorylation of ATPase subunits of the 26S proteasome. *FEBS Lett* 430, 269-274.

- Matsushita, M., Suzuki, N. N., Obara, K., Fujioka, Y., Ohsumi, Y., and Inagaki, F. (2007). Structure of Atg5.Atg16, a complex essential for autophagy. *J Biol Chem* 282, 6763-6772.
- McCampbell, A., Taylor, J. P., Taye, A. A., Robitschek, J., Li, M., Walcott, J., Merry, D., Chai, Y., Paulson, H., Sobue, G., and Fischbeck, K. H. (2000). CREB-binding protein sequestration by expanded polyglutamine. *Hum Mol Genet* 9, 2197-2202.
- McGinnis, K. M., Gnegy, M. E., and Wang, K. K. (1999). Endogenous bax translocation in SH-SY5Y human neuroblastoma cells and cerebellar granule neurons undergoing apoptosis. *J Neurochem* 72, 1899-1906.
- McGrath, J. P., Jentsch, S., and Varshavsky, A. (1991). UBA 1: an essential yeast gene encoding ubiquitin-activating enzyme. *EMBO J* 10, 227-236.
- Medema, J. P., Scaffidi, C., Kischkel, F. C., Shevchenko, A., Mann, M., Krammer, P. H., and Peter, M. E. (1997). FLICE is activated by association with the CD95 death-inducing signaling complex (DISC). *EMBO J* 16, 2794-2804.
- Menendez-Benito, V., Heessen, S., and Dantuma, N. P. (2005). Monitoring of ubiquitin-dependent proteolysis with green fluorescent protein substrates. *Methods Enzymol* 399, 490-511.
- Middleton, G., Pinon, L. G., Wyatt, S., and Davies, A. M. (1998). Bcl-2 accelerates the maturation of early sensory neurons. *J Neurosci* 18, 3344-3350.
- Millard, S. M., and Wood, S. A. (2006). Riding the DUBway: regulation of protein trafficking by deubiquitylating enzymes. *J Cell Biol* 173, 463-468.
- Millen, K. J., Millonig, J. H., Wingate, R. J., Alder, J., and Hatten, M. E. (1999). Neurogenetics of the cerebellar system. *J Child Neurol* 14, 574-581; discussion 581-572.
- Miller, T. M., Moulder, K. L., Knudson, C. M., Creedon, D. J., Deshmukh, M., Korsmeyer, S. J., and Johnson, E. M., Jr. (1997). Bax deletion further orders the cell death pathway in cerebellar granule cells and suggests a caspase-independent pathway to cell death. *J Cell Biol* 139, 205-217.

- Minucci, S., and Pelicci, P. G. (2006). Histone deacetylase inhibitors and the promise of epigenetic (and more) treatments for cancer. *Nat Rev Cancer* 6, 38-51.
- Mizushima, N. (2004). Methods for monitoring autophagy. *Int J Biochem Cell Biol* 36, 2491-2502.
- Mizushima, N., Kuma, A., Kobayashi, Y., Yamamoto, A., Matsubae, M., Takao, T., Natsume, T., Ohsumi, Y., and Yoshimori, T. (2003). Mouse Apg16L, a novel WD-repeat protein, targets to the autophagic isolation membrane with the Apg12-Apg5 conjugate. *J Cell Sci* 116, 1679-1688.
- Mizushima, N., Noda, T., and Ohsumi, Y. (1999). Apg16p is required for the function of the Apg12p-Apg5p conjugate in the yeast autophagy pathway. *EMBO J* 18, 3888-3896.
- Mizushima, N., Noda, T., Yoshimori, T., Tanaka, Y., Ishii, T., George, M. D., Klionsky, D. J., Ohsumi, M., and Ohsumi, Y. (1998). A protein conjugation system essential for autophagy. *Nature* 395, 395-398.
- Mizushima, N., Yamamoto, A., Hatano, M., Kobayashi, Y., Kabeya, Y., Suzuki, K., Tokuhisa, T., Ohsumi, Y., and Yoshimori, T. (2001). Dissection of autophagosome formation using Apg5-deficient mouse embryonic stem cells. *J Cell Biol* 152, 657-668.
- Moran, J., Itoh, T., Reddy, U. R., Chen, M., Alnemri, E. S., and Pleasure, D. (1999). Caspase-3 expression by cerebellar granule neurons is regulated by calcium and cyclic AMP. *J Neurochem* 73, 568-577.
- Mori, M., Burgess, D. L., Gefrides, L. A., Foreman, P. J., Opferman, J. T., Korsmeyer, S. J., Cavalheiro, E. A., Naffah-Mazzacoratti, M. G., and Noebels, J. L. (2004). Expression of apoptosis inhibitor protein Mcl1 linked to neuroprotection in CNS neurons. *Cell Death Differ* 11, 1223-1233.
- Motoyama, N., Wang, F., Roth, K. A., Sawa, H., Nakayama, K., Nakayama, K., Negishi, I., Senju, S., Zhang, Q., Fujii, S., and et al. (1995). Massive cell death of immature hematopoietic cells and neurons in Bcl-x-deficient mice. *Science* 267, 1506-1510.

- Munarriz, E., Bano, D., Sayan, A. E., Rossi, M., Melino, G., and Nicotera, P. (2005). Calpain cleavage regulates the protein stability of p73. *Biochem Biophys Res Commun* 333, 954-960.
- Munoz, L. E., van Bavel, C., Franz, S., Berden, J., Herrmann, M., and van der Vlag, J. (2008). Apoptosis in the pathogenesis of systemic lupus erythematosus. *Lupus* 17, 371-375.
- Muzio, M., Chinnaiyan, A. M., Kischkel, F. C., O'Rourke, K., Shevchenko, A., Ni, J., Scaffidi, C., Bretz, J. D., Zhang, M., Gentz, R., *et al.* (1996). FLICE, a novel FADD-homologous ICE/CED-3-like protease, is recruited to the CD95 (Fas/APO-1) death-inducing signaling complex. *Cell* 85, 817-827.
- Muzio, M., Salvesen, G. S., and Dixit, V. M. (1997). FLICE induced apoptosis in a cell-free system. Cleavage of caspase zymogens. *J Biol Chem* 272, 2952-2956.
- Muzio, M., Stockwell, B. R., Stennicke, H. R., Salvesen, G. S., and Dixit, V. M. (1998). An induced proximity model for caspase-8 activation. *J Biol Chem* 273, 2926-2930.
- Nagata, S. (1997). Apoptosis by death factor. *Cell* 88, 355-365.
- Nagata, S., Nagase, H., Kawane, K., Mukae, N., and Fukuyama, H. (2003). Degradation of chromosomal DNA during apoptosis. *Cell Death Differ* 10, 108-116.
- Namura, S., Zhu, J., Fink, K., Endres, M., Srinivasan, A., Tomaselli, K. J., Yuan, J., and Moskowitz, M. A. (1998). Activation and cleavage of caspase-3 in apoptosis induced by experimental cerebral ischemia. *J Neurosci* 18, 3659-3668.
- Nath, R., Raser, K. J., Stafford, D., Hajimohammadreza, I., Posner, A., Allen, H., Talanian, R. V., Yuen, P., Gilbertsen, R. B., and Wang, K. K. W. (1996). Non-erythroid α -spectrin breakdown by calpain and interleukin 1 β -converting-enzyme-like protease(s) in apoptotic cells: contributory roles of both protease families in neuronal apoptosis. *Biochem J* 319, 683-690.
- Nechushtan, A., Smith, C. L., Hsu, Y. T., and Youle, R. J. (1999). Conformation of the Bax C-terminus regulates subcellular location and cell death. *EMBO J* 18, 2330-2341.

- Neefjes, J., and Dantuma, N. P. (2004). Fluorescent probes for proteolysis: tools for drug discovery. *Nat Rev Drug Discov* 3, 58-69.
- Nemoto, T., Tanida, I., Tanida-Miyake, E., Minematsu-Ikeguchi, N., Yokota, M., Ohsumi, M., Ueno, T., and Kominami, E. (2003). The mouse APG10 homologue, an E2-like enzyme for Apg12p conjugation, facilitates MAP-LC3 modification. *J Biol Chem* 278, 39517-39526.
- Nicholson, D. W., Ali, A., Thornberry, N. A., Vaillancourt, J. P., Ding, C. K., Gallant, M., Gareau, Y., Griffin, P. R., Labelle, M., Lazebnik, Y. A., and et al. (1995). Identification and inhibition of the ICE/CED-3 protease necessary for mammalian apoptosis. *Nature* 376, 37-43.
- Nijman, S. M., Luna-Vargas, M. P., Velds, A., Brummelkamp, T. R., Dirac, A. M., Sixma, T. K., and Bernards, R. (2005). A genomic and functional inventory of deubiquitinating enzymes. *Cell* 123, 773-786.
- Noda, T., and Ohsumi, Y. (1998). Tor, a phosphatidylinositol kinase homologue, controls autophagy in yeast. *J Biol Chem* 273, 3963-3966.
- O'Hare, M. J., Hou, S. T., Morris, E. J., Cregan, S. P., Xu, Q., Slack, R. S., and Park, D. S. (2000). Induction and modulation of cerebellar granule neuron death by E2F-1. *J Biol Chem* 275, 25358-25364.
- Obara, K., Sekito, T., Niimi, K., and Ohsumi, Y. (2008). The Atg18-Atg2 complex is recruited to autophagic membranes via phosphatidylinositol 3-phosphate and exerts an essential function. *J Biol Chem* 283, 23972-23980.
- Oberstein, A., Jeffrey, P. D., and Shi, Y. (2007). Crystal structure of the Bcl-XL-Beclin 1 peptide complex: Beclin 1 is a novel BH3-only protein. *J Biol Chem* 282, 13123-13132.
- Onuki, R., Nagasaki, A., Kawasaki, H., Baba, T., Uyeda, T. Q., and Taira, K. (2002). Confirmation by FRET in individual living cells of the absence of significant amyloid beta -mediated caspase 8 activation. *Proc Natl Acad Sci U S A* 99, 14716-14721.
- Oppenheim, R. W. (1991). Cell death during development of the nervous system. *Annu Rev Neurosci* 14, 453-501.

- Orvedahl, A., and Levine, B. (2008). Eating the enemy within: autophagy in infectious diseases. *Cell Death Differ.*
- Ovaa, H. (2007). Active-site directed probes to report enzymatic action in the ubiquitin proteasome system. *Nat Rev Cancer* 7, 613-620.
- Padmanabhan, J., Park, D. S., Greene, L. A., and Shelanski, M. L. (1999). Role of cell cycle regulatory proteins in cerebellar granule neuron apoptosis. *J Neurosci* 19, 8747-8756.
- Pandey, U. B., Nie, Z., Batlevi, Y., McCray, B. A., Ritson, G. P., Nedelsky, N. B., Schwartz, S. L., DiProspero, N. A., Knight, M. A., Schuldiner, O., *et al.* (2007). HDAC6 rescues neurodegeneration and provides an essential link between autophagy and the UPS. *Nature* 447, 859-863.
- Pantelieva, I., Rouaux, C., Larmet, Y., Boutillier, S., Loeffler, J. P., and Boutillier, A. L. (2004). HDAC-3 participates in the repression of e2f-dependent gene transcription in primary differentiated neurons. *Ann N Y Acad Sci* 1030, 656-660.
- Pattingre, S., Espert, L., Biard-Piechaczyk, M., and Codogno, P. (2008). Regulation of macroautophagy by mTOR and Beclin 1 complexes. *Biochimie* 90, 313-323.
- Pattingre, S., Tassa, A., Qu, X., Garuti, R., Liang, X. H., Mizushima, N., Packer, M., Schneider, M. D., and Levine, B. (2005). Bcl-2 antiapoptotic proteins inhibit Beclin 1-dependent autophagy. *Cell* 122, 927-939.
- Paz, Y., Elazar, Z., and Fass, D. (2000). Structure of GATE-16, membrane transport modulator and mammalian ortholog of autophagocytosis factor Aut7p. *J Biol Chem* 275, 25445-25450.
- Pelzer, C., Kassner, I., Matentzoglou, K., Singh, R. K., Wollscheid, H. P., Scheffner, M., Schmidtke, G., and Groettrup, M. (2007). UBE1L2, a novel E1 enzyme specific for ubiquitin. *J Biol Chem* 282, 23010-23014.
- Petiot, A., Ogier-Denis, E., Blommaert, E. F., Meijer, A. J., and Codogno, P. (2000). Distinct classes of phosphatidylinositol 3'-kinases are involved in signaling pathways that control macroautophagy in HT-29 cells. *J Biol Chem* 275, 992-998.

- Petroski, M. D., and Deshaies, R. J. (2005). Mechanism of lysine 48-linked ubiquitin-chain synthesis by the cullin-RING ubiquitin-ligase complex SCF-Cdc34. *Cell* *123*, 1107-1120.
- Pettmann, B., and Henderson, C. E. (1998). Neuronal cell death. *Neuron* *20*, 633-647.
- Pickart, C. M. (2001). Mechanisms underlying ubiquitination. *Annu Rev Biochem* *70*, 503-533.
- Pickart, C. M., and Cohen, R. E. (2004). Proteasomes and their Kin: Proteases in the Machine Age. *Nature Reviews: Molecular Cell Biology* *5*, 177-187.
- Pickart, C. M., and Rose, I. A. (1985a). Functional heterogeneity of ubiquitin carrier proteins. *J Biol Chem* *260*, 1573-1581.
- Pickart, C. M., and Rose, I. A. (1985b). Ubiquitin carboxyl-terminal hydrolase acts on ubiquitin carboxyl-terminal amides. *J Biol Chem* *260*, 7903-7910.
- Pulipparacharuvil, S., Renthal, W., Hale, C. F., Taniguchi, M., Xiao, G., Kumar, A., Russo, S. J., Sikder, D., Dewey, C. M., Davis, M. M., *et al.* (2008). Cocaine regulates MEF2 to control synaptic and behavioral plasticity. *Neuron* *59*, 621-633.
- Putchu, G. V., Harris, C. A., Moulder, K. L., Easton, R. M., Thompson, C. B., and Johnson, E. M., Jr. (2002). Intrinsic and extrinsic pathway signaling during neuronal apoptosis: lessons from the analysis of mutant mice. *J Cell Biol* *157*, 441-453.
- Pyo, J. O., Jang, M. H., Kwon, Y. K., Lee, H. J., Jun, J. I., Woo, H. N., Cho, D. H., Choi, B., Lee, H., Kim, J. H., *et al.* (2005). Essential roles of Atg5 and FADD in autophagic cell death: dissection of autophagic cell death into vacuole formation and cell death. *J Biol Chem* *280*, 20722-20729.
- Qu, X., Zou, Z., Sun, Q., Luby-Phelps, K., Cheng, P., Hogan, R. N., Gilpin, C., and Levine, B. (2007). Autophagy gene-dependent clearance of apoptotic cells during embryonic development. *Cell* *128*, 931-946.

- Ram, D., Ziv, E., Lantner, F., and Schechter, I. (2003). Interaction of the proteasome S5a/Rpn10 multiubiquitin-binding protein and the 8 kDa calcium-binding protein of *Schistosoma mansoni*. *Parasitology* *127*, 337-347.
- Rao, L., Perez, D., and White, E. (1996). Lamin proteolysis facilitates nuclear events during apoptosis. *J Cell Biol* *135*, 1441-1455.
- Rechsteiner, M., and Hill, C. P. (2005). Mobilizing the proteolytic machine: cell biological roles of proteasome activators and inhibitors. *Trends Cell Biol* *15*, 27-33.
- Reggiori, F., and Klionsky, D. J. (2002). Autophagy in the eukaryotic cell. *Eukaryot Cell* *1*, 11-21.
- Reggiori, F., Shintani, T., Nair, U., and Klionsky, D. J. (2005). Atg9 cycles between mitochondria and the pre-autophagosomal structure in yeasts. *Autophagy* *1*, 101-109.
- Reggiori, F., Tucker, K. A., Stromhaug, P. E., and Klionsky, D. J. (2004). The Atg1-Atg13 complex regulates Atg9 and Atg23 retrieval transport from the pre-autophagosomal structure. *Dev Cell* *6*, 79-90.
- Ren, M., Leng, Y., Jeong, M., Leeds, P. R., and Chuang, D. M. (2004). Valproic acid reduces brain damage induced by transient focal cerebral ischemia in rats: potential roles of histone deacetylase inhibition and heat shock protein induction. *J Neurochem* *89*, 1358-1367.
- Renthal, W., Maze, I., Krishnan, V., Covington, H. E., 3rd, Xiao, G., Kumar, A., Russo, S. J., Graham, A., Tsankova, N., Kippin, T. E., *et al.* (2007). Histone deacetylase 5 epigenetically controls behavioral adaptations to chronic emotional stimuli. *Neuron* *56*, 517-529.
- Ricci, J. E., Munoz-Pinedo, C., Fitzgerald, P., Bailly-Maitre, B., Perkins, G. A., Yadava, N., Scheffler, I. E., Ellisman, M. H., and Green, D. R. (2004). Disruption of mitochondrial function during apoptosis is mediated by caspase cleavage of the p75 subunit of complex I of the electron transport chain. *Cell* *117*, 773-786.

- Rosenzweig, R., Osmulski, P. A., Gaczynska, M., and Glickman, M. H. (2008). The central unit within the 19S regulatory particle of the proteasome. *Nat Struct Mol Biol* 15, 573-580.
- Rouaux, C., Jokic, N., Mbebi, C., Boutillier, S., Loeffler, J. P., and Boutillier, A. L. (2003). Critical loss of CBP/p300 histone acetylase activity by caspase-6 during neurodegeneration. *EMBO J* 22, 6537-6549.
- Rubinsztein, D. C., Gestwicki, J. E., Murphy, L. O., and Klionsky, D. J. (2007). Potential therapeutic applications of autophagy. *Nat Rev Drug Discov* 6, 304-312.
- Sabatini, D. M. (2006). mTOR and cancer: insights into a complex relationship. *Nat Rev Cancer* 6, 729-734.
- Saeki, Y., Sone, T., Toh-e, A., and Yokosawa, H. (2002). Identification of ubiquitin-like protein-binding subunits of the 26S proteasome. *Biochem Biophys Res Commun* 296, 813-819.
- Saez, M. E., Ramirez-Lorca, R., Moron, F. J., and Ruiz, A. (2006). The therapeutic potential of the calpain family: new aspects. *Drug Discov Today* 11, 917-923.
- Sahara, S., Aoto, M., Eguchi, Y., Imamoto, N., Yoneda, Y., and Tsujimoto, Y. (1999). Acinus is a caspase-3-activated protein required for apoptotic chromatin condensation. *Nature* 401, 168-173.
- Saito, K., Elce, J. S., Hamos, J. E., and Nixon, R. A. (1993). Widespread activation of calcium-activated neutral proteinase (calpain) in the brain in Alzheimer disease: a potential molecular basis for neuronal degeneration. *Proc Natl Acad Sci U S A* 90, 2628-2632.
- Sakahira, H., Enari, M., and Nagata, S. (1998). Cleavage of CAD inhibitor in CAD activation and DNA degradation during apoptosis. *Nature* 391, 96-99.
- Sakata, E., Yamaguchi, Y., Kurimoto, E., Kikuchi, J., Yokoyama, S., Yamada, S., Kawahara, H., Yokosawa, H., Hattori, N., Mizuno, Y., *et al.* (2003). Parkin binds the Rpn10 subunit of 26S proteasomes through its ubiquitin-like domain. *EMBO Rep* 4, 301-306.

- Saleh, A., Srinivasula, S. M., Acharya, S., Fishel, R., and Alnemri, E. S. (1999). Cytochrome c and dATP-mediated oligomerization of Apaf-1 is a prerequisite for procaspase-9 activation. *J Biol Chem* 274, 17941-17945.
- Samejima, K., Tone, S., and Earnshaw, W. C. (2001). CAD/DFF40 nuclease is dispensable for high molecular weight DNA cleavage and stage I chromatin condensation in apoptosis. *J Biol Chem* 276, 45427-45432.
- Samejima, K., Tone, S., Kottke, T. J., Enari, M., Sakahira, H., Cooke, C. A., Durrieu, F., Martins, L. M., Nagata, S., Kaufmann, S. H., and Earnshaw, W. C. (1998). Transition from caspase-dependent to caspase-independent mechanisms at the onset of apoptotic execution. *J Cell Biol* 143, 225-239.
- Sanchez, I., Xu, C. J., Juo, P., Kakizaka, A., Blenis, J., and Yuan, J. (1999). Caspase-8 is required for cell death induced by expanded polyglutamine repeats. *Neuron* 22, 623-633.
- Santella, L., Kyojuka, K., De Riso, L., and Carafoli, E. (1998). Calcium, protease action, and the regulation of the cell cycle. *Cell Calcium* 23, 123-130.
- Sarkar, S., Davies, J. E., Huang, Z., Tunnacliffe, A., and Rubinsztein, D. C. (2007). Trehalose, a novel mTOR-independent autophagy enhancer, accelerates the clearance of mutant huntingtin and alpha-synuclein. *J Biol Chem* 282, 5641-5652.
- Sarkar, S., Floto, R. A., Berger, Z., Imarisio, S., Cordenier, A., Pasco, M., Cook, L. J., and Rubinsztein, D. C. (2005). Lithium induces autophagy by inhibiting inositol monophosphatase. *J Cell Biol* 170, 1101-1111.
- Sasaki, T., Kikuchi, T., Yumoto, N., Yoshimura, N., and Murachi, T. (1984). Comparative specificity and kinetic studies on porcine calpain I and calpain II with naturally occurring peptides and synthetic fluorogenic substrates. *J Biol Chem* 259, 12489-12494.
- Saucedo, L. J., Gao, X., Chiarelli, D. A., Li, L., Pan, D., and Edgar, B. A. (2003). Rheb promotes cell growth as a component of the insulin/TOR signalling network. *Nat Cell Biol* 5, 566-571.

Scheffner, M., Nuber, U., and Huibregtse, J. M. (1995). Protein ubiquitination involving an E1-E2-E3 enzyme ubiquitin thioester cascade. *Nature* 373, 81-83.

Scherz-Shouval, R., Sagiv, Y., Shorer, H., and Elazar, Z. (2003). The COOH terminus of GATE-16, an intra-Golgi transport modulator, is cleaved by the human cysteine protease HsApg4A. *J Biol Chem* 278, 14053-14058.

Scherz-Shouval, R., Shvets, E., Fass, E., Shorer, H., Gil, L., and Elazar, Z. (2007). Reactive oxygen species are essential for autophagy and specifically regulate the activity of Atg4. *EMBO J* 26, 1749-1760.

Schmidt, M., Hanna, J., Elsasser, S., and Finley, D. (2005). Proteasome-associated proteins: regulation of a proteolytic machine. *Biol Chem* 386, 725-737.

Schulz, J. B., Weller, M., and Klockgether, T. (1996). Potassium deprivation-induced apoptosis of cerebellar granule neurons: a sequential requirement for new mRNA and protein synthesis, ICE-like protease activity, and reactive oxygen species. *J Neurosci* 16, 4696-4706.

Schwartz, A. L., and Ciechanover, A. (1999). The ubiquitin-proteasome pathway and pathogenesis of human diseases. *Annu Rev Med* 50, 57-74.

Seemuller, E., Lupas, A., and Baumeister, W. (1996). Autocatalytic processing of the 20S proteasome. *Nature* 382, 468-471.

Seidah, N. G., Benjannet, S., Wickham, L., Marcinkiewicz, J., Jasmin, S. B., Stifani, S., Basak, A., Prat, A., and Chretien, M. (2003). The secretory proprotein convertase neural apoptosis-regulated convertase 1 (NARC-1): liver regeneration and neuronal differentiation. *Proc Natl Acad Sci U S A* 100, 928-933.

Shacka, J. J., and Roth, K. A. (2006). Bcl-2 family and the central nervous system: from rheostat to real complex. *Cell Death Differ* 13, 1299-1304.

Shao, Y., Gao, Z., Marks, P. A., and Jiang, X. (2004). Apoptotic and autophagic cell death induced by histone deacetylase inhibitors. *Proc Natl Acad Sci U S A* 101, 18030-18035.

- Sharon, M., Witt, S., Glasmacher, E., Baumeister, W., and Robinson, C. V. (2007). Mass spectrometry reveals the missing links in the assembly pathway of the bacterial 20 S proteasome. *J Biol Chem* 282, 18448-18457.
- Shi, L., Gong, S., Yuan, Z., Ma, C., Liu, Y., Wang, C., Li, W., Pi, R., Huang, S., Chen, R., *et al.* (2005). Activity deprivation-dependent induction of the proapoptotic BH3-only protein Bim is independent of JNK/c-Jun activation during apoptosis in cerebellar granule neurons. *Neurosci Lett* 375, 7-12.
- Shi, Y. (2002). Mechanisms of Caspase Activation and Inhibition during Apoptosis. *Mol Cell* 9, 459-470.
- Shimizu, S., Kanaseki, T., Mizushima, N., Mizuta, T., Arakawa-Kobayashi, S., Thompson, C. B., and Tsujimoto, Y. (2004). Role of Bcl-2 family proteins in a non-apoptotic programmed cell death dependent on autophagy genes. *Nat Cell Biol* 6, 1221-1228.
- Shinohara, K., Tomioka, M., Nakano, H., Tone, S., Ito, H., and Kawashima, S. (1996). Apoptosis induction resulting from proteasome inhibition. *Biochem J* 317 (Pt 2), 385-388.
- Siman, R., Baudry, M., and Lynch, G. (1984). Brain fodrin: Substrate for calpain I, an endogenous calcium-activated protease. *Proc Natl Acad Sci U S A* 81, 3572-3576.
- Simonini, M. V., Camargo, L. M., Dong, E., Maloku, E., Veldic, M., Costa, E., and Guidotti, A. (2006). The benzamide MS-275 is a potent, long-lasting brain region-selective inhibitor of histone deacetylases. *Proc Natl Acad Sci U S A* 103, 1587-1592.
- Slee, E. A., Adrain, C., and Martin, S. J. (2001). Executioner caspase-3,-6, and-7 perform distinct, non-redundant roles during the demolition phase of apoptosis. *J Biol Chem* 276, 7320-7326.
- Slee, E. A., Harte, M. T., Kluck, R. M., Wolf, B. B., Casiano, C. A., Newmeyer, D. D., Wang, H. G., Reed, J. C., Nicholson, D. W., Alnemri, E. S., *et al.* (1999). Ordering the cytochrome c-initiated caspase cascade: Hierarchical activation of caspases-2, -3, -6, -7, -8, and -10 in a caspase-9-dependent manner. *J Cell Biol* 144, 281-292.

Smith, D. M., Chang, S. C., Park, S., Finley, D., Cheng, Y., and Goldberg, A. L. (2007). Docking of the proteasomal ATPases' carboxyl termini in the 20S proteasome's alpha ring opens the gate for substrate entry. *Mol Cell* *27*, 731-744.

Smith, D. M., Kafri, G., Cheng, Y., Ng, D., Walz, T., and Goldberg, A. L. (2005). ATP binding to PAN or the 26S ATPases causes association with the 20S proteasome, gate opening, and translocation of unfolded proteins. *Mol Cell* *20*, 687-698.

Snowden, R. T., Sun, X. M., Dyer, M. J., and Cohen, G. M. (2003). Bisindolylmaleimide IX is a potent inducer of apoptosis in chronic lymphocytic leukaemic cells and activates cleavage of Mcl-1. *Leukemia* *17*, 1981-1989.

Spence, J., Gali, R. R., Dittmar, G., Sherman, F., Karin, M., and Finley, D. (2000). Cell cycle-regulated modification of the ribosome by a variant multiubiquitin chain. *Cell* *102*, 67-76.

Spence, J., Sadis, S., Haas, A. L., and Finley, D. (1995). A ubiquitin mutant with specific defects in DNA repair and multiubiquitination. *Mol Cell Biol* *15*, 1265-1273.

Srinivasula, S. M., Ahmad, M., Fernandes-Alnemri, T., and Alnemri, E. S. (1998). Autoactivation of procaspase-9 by Apaf-1-mediated oligomerization. *Mol Cell* *1*, 949-957.

Srinivasula, S. M., Ahmad, M., Fernandes-Alnemri, T., Litwack, G., and Alnemri, E. S. (1996a). Molecular ordering of the Fas-apoptotic pathway: the Fas/APO-1 protease Mch5 is a CrmA-inhibitable protease that activates multiple Ced-3/ICE-like cysteine proteases. *Proc Natl Acad Sci U S A* *93*, 14486-14491.

Srinivasula, S. M., Fernandes-Alnemri, T., Zangrilli, J., Robertson, N., Armstrong, R. C., Wang, L., Trapani, J. A., Tomaselli, K. J., Litwack, G., and Alnemri, E. S. (1996b). The Ced-3/interleukin 1beta converting enzyme-like homolog Mch6 and the lamin-cleaving enzyme Mch2alpha are substrates for the apoptotic mediator CPP32. *J Biol Chem* *271*, 27099-27106.

Srinivasula, S. M., Hegde, R., Saleh, A., Datta, P., Shiozaki, E., Chai, J., Lee, R. A., Robbins, P. D., Fernandes-Alnemri, T., Shi, Y., and Alnemri, E. S. (2001). A conserved

XIAP-interaction motif in caspase-9 and Smac/DIABLO regulates caspase activity and apoptosis. *Nature* **410**, 112-116.

Stabach, P. R., Cianci, C. D., Glantz, S. B., Zhang, Z., and Morrow, J. S. (1997). Site-directed mutagenesis of alpha II spectrin at codon 1175 modulates its mu-calpain susceptibility. *Biochemistry (Mosc)* **36**, 57-65.

Stack, J. H., Herman, P. K., Schu, P. V., and Emr, S. D. (1993). A membrane-associated complex containing the Vps15 protein kinase and the Vps34 PI 3-kinase is essential for protein sorting to the yeast lysosome-like vacuole. *EMBO J* **12**, 2195-2204.

Stack, J. H., Whitney, M., Rodems, S. M., and Pollok, B. A. (2000). A ubiquitin-based tagging system for controlled modulation of protein stability. *Nat Biotechnol* **18**, 1298-1302.

Steffan, J. S., Bodai, L., Pallos, J., Poelman, M., McCampbell, A., Apostol, B. L., Kazantsev, A., Schmidt, E., Zhu, Y. Z., Greenwald, M., *et al.* (2001). Histone deacetylase inhibitors arrest polyglutamine-dependent neurodegeneration in *Drosophila*. *Nature* **413**, 739-743.

Steffan, J. S., Kazantsev, A., Spasic-Boskovic, O., Greenwald, M., Zhu, Y. Z., Gohler, H., Wanker, E. E., Bates, G. P., Housman, D. E., and Thompson, L. M. (2000). The Huntington's disease protein interacts with p53 and CREB-binding protein and represses transcription. *Proc Natl Acad Sci U S A* **97**, 6763-6768.

Stennicke, H. R., Deveraux, Q. L., Humke, E. W., Reed, J. C., Dixit, V. M., and Salvesen, G. S. (1999). Caspase-9 can be activated without proteolytic processing. *J Biol Chem* **274**, 8359-8362.

Stennicke, H. R., Renatus, M., Meldal, M., and Salvesen, G. S. (2000). Internally quenched fluorescent peptide substrates disclose the subsite preferences of human caspases 1, 3, 6, 7 and 8. *Biochem J* **350 Pt 2**, 563-568.

Stennicke, H. R., and Salvesen, G. S. (1999). Caspases: preparation and characterization. *Methods* **17**, 313-319.

- Stocker, H., Radimerski, T., Schindelholz, B., Wittwer, F., Belawat, P., Daram, P., Breuer, S., Thomas, G., and Hafen, E. (2003). Rheb is an essential regulator of S6K in controlling cell growth in *Drosophila*. *Nat Cell Biol* 5, 559-565.
- Strassburger, K., and Bretz, F. (2008). Compatible simultaneous lower confidence bounds for the Holm procedure and other Bonferroni-based closed tests. *Stat Med* 27, 4914-4927.
- Strobl, S., Fernandez-Catalan, C., Braun, M., Huber, R., Masumoto, H., Nakagawa, K., Irie, A., Sorimachi, H., Bourenkow, G., Bartunik, H., *et al.* (2000). The crystal structure of calcium-free human m-calpain suggests an electrostatic switch mechanism for activation by calcium. *Proc Natl Acad Sci U S A* 97, 588-592.
- Sugawara, K., Suzuki, N. N., Fujioka, Y., Mizushima, N., Ohsumi, Y., and Inagaki, F. (2004). The crystal structure of microtubule-associated protein light chain 3, a mammalian homologue of *Saccharomyces cerevisiae* Atg8. *Genes Cells* 9, 611-618.
- Sugawara, K., Suzuki, N. N., Fujioka, Y., Mizushima, N., Ohsumi, Y., and Inagaki, F. (2005). Structural basis for the specificity and catalysis of human Atg4B responsible for mammalian autophagy. *J Biol Chem* 280, 40058-40065.
- Sun, X.-M., Butterworth, M., MacFarlane, M., Dubiel, W., Ciechanover, A., and Cohen, G. M. (2004). Caspase Activation Inhibits Proteasome Function during Apoptosis. *Mol Cell* 14, 81-93.
- Sun, X. M., MacFarlane, M., Zhuang, J., Wolf, B. B., Green, D. R., and Cohen, G. M. (1999). Distinct caspase cascades are initiated in receptor-mediated and chemical-induced apoptosis. *J Biol Chem* 274, 5053-5060.
- Sun, Y. F., Yu, L. Y., Saarma, M., and Arumae, U. (2003). Mutational analysis of N-Bak reveals different structural requirements for antiapoptotic activity in neurons and proapoptotic activity in nonneuronal cells. *Mol Cell Neurosci* 23, 134-143.
- Sun, Y. F., Yu, L. Y., Saarma, M., Timmusk, T., and Arumae, U. (2001). Neuron-specific Bcl-2 homology 3 domain-only splice variant of Bak is anti-apoptotic in neurons, but pro-apoptotic in non-neuronal cells. *J Biol Chem* 276, 16240-16247.

- Suzuki, K., Kirisako, T., Kamada, Y., Mizushima, N., Noda, T., and Ohsumi, Y. (2001). The pre-autophagosomal structure organized by concerted functions of APG genes is essential for autophagosome formation. *EMBO J* 20, 5971-5981.
- Takahashi, Y., Coppola, D., Matsushita, N., Cualing, H. D., Sun, M., Sato, Y., Liang, C., Jung, J. U., Cheng, J. Q., Mul, J. J., *et al.* (2007). Bif-1 interacts with Beclin 1 through UVRAG and regulates autophagy and tumorigenesis. *Nat Cell Biol* 9, 1142-1151.
- Talanian, R. V., Quinlan, C., Trautz, S., Hackett, M. C., Mankovich, J. A., Banach, D., Ghayur, T., Brady, K. D., and Wong, W. W. (1997). Substrate specificities of caspase family proteases. *J Biol Chem* 272, 9677-9682.
- Tanaka, K., Suzuki, T., Hattori, N., and Mizuno, Y. (2004). Ubiquitin, proteasome and parkin. *Biochim Biophys Acta* 1695, 235-247.
- Tanida, I., Komatsu, M., Ueno, T., and Kominami, E. (2003). GATE-16 and GABARAP are authentic modifiers mediated by Apg7 and Apg3. *Biochem Biophys Res Commun* 300, 637-644.
- Tanida, I., Minematsu-Ikeguchi, N., Ueno, T., and Kominami, E. (2005). Lysosomal turnover, but not a cellular level, of endogenous LC3 is a marker for autophagy. *Autophagy* 1, 84-91.
- Tanida, I., Mizushima, N., Kiyooka, M., Ohsumi, M., Ueno, T., Ohsumi, Y., and Kominami, E. (1999). Apg7p/Cvt2p: A novel protein-activating enzyme essential for autophagy. *Mol Biol Cell* 10, 1367-1379.
- Tanida, I., Sou, Y. S., Ezaki, J., Minematsu-Ikeguchi, N., Ueno, T., and Kominami, E. (2004a). HsAtg4B/HsApg4B/autophagin-1 cleaves the carboxyl termini of three human Atg8 homologues and delipidates microtubule-associated protein light chain 3- and GABAA receptor-associated protein-phospholipid conjugates. *J Biol Chem* 279, 36268-36276.
- Tanida, I., Tanida-Miyake, E., Komatsu, M., Ueno, T., and Kominami, E. (2002). Human Apg3p/Aut1p homologue is an authentic E2 enzyme for multiple substrates, GATE-16, GABARAP, and MAP-LC3, and facilitates the conjugation of hApg12p to hApg5p. *J Biol Chem* 277, 13739-13744.

- Tanida, I., Ueno, T., and Kominami, E. (2004b). Human light chain 3/MAP1LC3B is cleaved at its carboxyl-terminal Met121 to expose Gly120 for lipidation and targeting to autophagosomal membranes. *J Biol Chem* 279, 47704-47710.
- Taylor, J., Gatchalian, C. L., Keen, G., and Rubin, L. L. (1997). Apoptosis in cerebellar granule neurones: involvement of interleukin-1 beta converting enzyme-like proteases. *J Neurochem* 68, 1598-1605.
- Taylor, J. P., Tanaka, F., Robitschek, J., Sandoval, C. M., Taye, A., Markovic-Plese, S., and Fischbeck, K. H. (2003a). Aggresomes protect cells by enhancing the degradation of toxic polyglutamine-containing protein. *Hum Mol Genet* 12, 749-757.
- Taylor, J. P., Taye, A. A., Campbell, C., Kazemi-Esfarjani, P., Fischbeck, K. H., and Min, K. T. (2003b). Aberrant histone acetylation, altered transcription, and retinal degeneration in a *Drosophila* model of polyglutamine disease are rescued by CREB-binding protein. *Genes Dev* 17, 1463-1468.
- Taylor, R. C., Cullen, S. P., and Martin, S. J. (2008). Apoptosis: controlled demolition at the cellular level. *Nat Rev Mol Cell Biol* 9, 231-241.
- Thorburn, A. (2008). Apoptosis and autophagy: regulatory connections between two supposedly different processes. *Apoptosis* 13, 1-9.
- Thornberry, N. A., Bull, H. G., Calaycay, J. R., Chapman, K. T., Howard, A. D., Kostura, M. J., Miller, D. K., Molineaux, S. M., Weidner, J. R., Aunins, J., and et al. (1992). A novel heterodimeric cysteine protease is required for interleukin-1 beta processing in monocytes. *Nature* 356, 768-774.
- Thornberry, N. A., Rano, T. A., Peterson, E. P., Rasper, D. M., Timkey, T., Garcia-Calvo, M., Houtzager, V. M., Nordstrom, P. A., Roy, S., Vaillancourt, J. P., et al. (1997). A combinatorial approach defines specificities of members of the caspase family and granzyme B. Functional relationships established for key mediators of apoptosis. *J Biol Chem* 272, 17907-17911.
- Thrower, J. S., Hoffman, L., Rechsteiner, M., and Pickart, C. M. (2000). Recognition of the polyubiquitin proteolytic signal. *EMBO J* 19, 94-102.

- Thumm, M., Egner, R., Koch, B., Schlumpberger, M., Straub, M., Veenhuis, M., and Wolf, D. H. (1994). Isolation of autophagocytosis mutants of *Saccharomyces cerevisiae*. *FEBS Lett* **349**, 275-280.
- Tompa, P., Buzder-Lantos, P., Tantos, A., Farkas, A., Szilagyi, A., Banoczi, Z., Hudecz, F., and Friedrich, P. (2004). On the sequential determinants of calpain cleavage. *J Biol Chem* **279**, 20775-20785.
- Trotter, L., Panton, W., Hajimohamadreza, I., Petalidis, L., Ward, R., Fleming, Y., Armstrong, C. G., Cohen, P., Karran, E. H., and Kinloch, R. A. (2002). Mitogen-activated protein kinase kinase 7 is activated during low potassium-induced apoptosis in rat cerebellar granule neurons. *Neurosci Lett* **320**, 29-32.
- Tsukada, M., and Ohsumi, Y. (1993). Isolation and characterization of autophagy-defective mutants of *Saccharomyces cerevisiae*. *FEBS Lett* **333**, 169-174.
- Twiddy, D. (2005). Molecular and Proteomic Characterisation of the ~700 kDa Apoptosome. PhD Thesis.
- Twiddy, D., Cohen, G. M., Macfarlane, M., and Cain, K. (2006). Caspase-7 is directly activated by the approximately 700-kDa apoptosome complex and is released as a stable XIAP-caspase-7 approximately 200-kDa complex. *J Biol Chem* **281**, 3876-3888.
- Uo, T., Kinoshita, Y., and Morrison, R. S. (2005). Neurons exclusively express N-Bak, a BH3 domain-only Bak isoform that promotes neuronal apoptosis. *J Biol Chem* **280**, 9065-9073.
- Valencia, A., and Moran, J. (2001). Role of oxidative stress in the apoptotic cell death of cultured cerebellar granule neurons. *J Neurosci Res* **64**, 284-297.
- van Delft, M. F., Wei, A. H., Mason, K. D., Vandenberg, C. J., Chen, L., Czabotar, P. E., Willis, S. N., Scott, C. L., Day, C. L., Cory, S., *et al.* (2006). The BH3 mimetic ABT-737 targets selective Bcl-2 proteins and efficiently induces apoptosis via Bak/Bax if Mcl-1 is neutralized. *Cancer Cell* **10**, 389-399.
- van der Vaart, A., Mari, M., and Reggiori, F. (2008). A picky eater: exploring the mechanisms of selective autophagy in human pathologies. *Traffic* **9**, 281-289.

- van Tijn, P., Hol, E. M., van Leeuwen, F. W., and Fischer, D. F. (2008). The neuronal ubiquitin-proteasome system: murine models and their neurological phenotype. *Prog Neurobiol* 85, 176-193.
- Vecsey, C. G., Hawk, J. D., Lattal, K. M., Stein, J. M., Fabian, S. A., Attner, M. A., Cabrera, S. M., McDonough, C. B., Brindle, P. K., Abel, T., and Wood, M. A. (2007). Histone deacetylase inhibitors enhance memory and synaptic plasticity via CREB:CBP-dependent transcriptional activation. *J Neurosci* 27, 6128-6140.
- Veis, D. J., Sorenson, C. M., Shutter, J. R., and Korsmeyer, S. J. (1993). Bcl-2-deficient mice demonstrate fulminant lymphoid apoptosis, polycystic kidneys, and hypopigmented hair. *Cell* 75, 229-240.
- Verdecia, M. A., Joazeiro, C. A., Wells, N. J., Ferrer, J. L., Bowman, M. E., Hunter, T., and Noel, J. P. (2003). Conformational flexibility underlies ubiquitin ligation mediated by the WWP1 HECT domain E3 ligase. *Mol Cell* 11, 249-259.
- Verdoes, M., Florea, B. I., Menendez-Benito, V., Maynard, C. J., Witte, M. D., van der Linden, W. A., van den Nieuwendijk, A. M., Hofmann, T., Berkers, C. R., van Leeuwen, F. W., *et al.* (2006). A fluorescent broad-spectrum proteasome inhibitor for labeling proteasomes in vitro and in vivo. *Chem Biol* 13, 1217-1226.
- Verhagen, A. M., Ekert, P. G., Pakusch, M., Silke, J., Connolly, L. M., Reid, G. E., Moritz, R. L., Simpson, R. J., and Vaux, D. L. (2000). Identification of DIABLO, a mammalian protein that promotes apoptosis by binding to and antagonizing IAP proteins. *Cell* 102, 43-53.
- Verma, P., Chierzi, S., Codd, A. M., Campbell, D. S., Meyer, R. L., Holt, C. E., and Fawcett, J. W. (2005). Axonal protein synthesis and degradation are necessary for efficient growth cone regeneration. *J Neurosci* 25, 331-342.
- Verma, R., Aravind, L., Oania, R., McDonald, W. H., Yates, J. R., 3rd, Koonin, E. V., and Deshaies, R. J. (2002). Role of Rpn11 metalloprotease in deubiquitination and degradation by the 26S proteasome. *Science* 298, 611-615.

- Verma, R., Oania, R., Graumann, J., and Deshaies, R. J. (2004). Multiubiquitin chain receptors define a layer of substrate selectivity in the ubiquitin-proteasome system. *Cell* 118, 99-110.
- Walden, H., Podgorski, M. S., and Schulman, B. A. (2003). Insights into the ubiquitin transfer cascade from the structure of the activating enzyme for NEDD8. *Nature* 422, 330-334.
- Walensky, L. D. (2006). BCL-2 in the crosshairs: tipping the balance of life and death. *Cell Death Differ* 13, 1339-1350.
- Walker, N. P., Talanian, R. V., Brady, K. D., Dang, L. C., Bump, N. J., Ferez, C. R., Franklin, S., Ghayur, T., Hackett, M. C., Hammill, L. D., and et al. (1994). Crystal structure of the cysteine protease interleukin-1 beta-converting enzyme: a (p20/p10)₂ homodimer. *Cell* 78, 343-352.
- Wang, M., Cheng, D., Peng, J., and Pickart, C. M. (2006). Molecular determinants of polyubiquitin linkage selection by an HECT ubiquitin ligase. *EMBO J* 25, 1710-1719.
- Wang, M., and Pickart, C. M. (2005). Different HECT domain ubiquitin ligases employ distinct mechanisms of polyubiquitin chain synthesis. *EMBO J* 24, 4324-4333.
- Wang, V. Y., and Zoghbi, H. Y. (2001). Genetic regulation of cerebellar development. *Nat Rev Neurosci* 2, 484-491.
- Watson, A., Eilers, A., Lallemand, D., Kyriakis, J., Rubin, L. L., and Ham, J. (1998). Phosphorylation of c-Jun is necessary for apoptosis induced by survival signal withdrawal in cerebellar granule neurons. *J Neurosci* 18, 751-762.
- Watts, R. J., Hoopfer, E. D., and Luo, L. (2003). Axon pruning during *Drosophila* metamorphosis: evidence for local degeneration and requirement of the ubiquitin-proteasome system. *Neuron* 38, 871-885.
- Wee, L. J., Tan, T. W., and Ranganathan, S. (2006). SVM-based prediction of caspase substrate cleavage sites. *BMC Bioinformatics* 7 *Suppl* 5, S14.

- Wei, Y., Pattingre, S., Sinha, S., Bassik, M., and Levine, B. (2008). JNK1-mediated phosphorylation of Bcl-2 regulates starvation-induced autophagy. *Mol Cell* 30, 678-688.
- Weissman, A. M. (2001). Themes and variations on ubiquitylation. *Nat Rev Mol Cell Biol* 2, 169-178.
- Welchman, R. L., Gordon, C., and Mayer, R. J. (2005). Ubiquitin and ubiquitin-like proteins as multifunctional signals. *Nat Rev Mol Cell Biol* 6, 599-609.
- Whitby, F. G., Masters, E. I., Kramer, L., Knowlton, J. R., Yao, Y., Wang, C. C., and Hill, C. P. (2000). Structural basis for the activation of 20S proteasomes by 11S regulators. *Nature* 408, 115-120.
- Wilkinson, K. D. (2004). Ubiquitin: a Nobel protein. *Cell* 119, 741-745.
- Wilkinson, K. D., Urban, M. K., and Haas, A. L. (1980). Ubiquitin is the ATP-dependent proteolysis factor I of rabbit reticulocytes. *J Biol Chem* 255, 7529-7532.
- Willis, S. N., Chen, L., Dewson, G., Wei, A., Naik, E., Fletcher, J. I., Adams, J. M., and Huang, D. C. (2005). Proapoptotic Bak is sequestered by Mcl-1 and Bcl-xL, but not Bcl-2, until displaced by BH3-only proteins. *Genes Dev* 19, 1294-1305.
- Willis, S. N., Fletcher, J. I., Kaufmann, T., van Delft, M. F., Chen, L., Czabotar, P. E., Ierino, H., Lee, E. F., Fairlie, W. D., Bouillet, P., *et al.* (2007). Apoptosis initiated when BH3 ligands engage multiple Bcl-2 homologs, not Bax or Bak. *Science* 315, 856-859.
- Wilson, K. P., Black, J. A., Thomson, J. A., Kim, E. E., Griffith, J. P., Navia, M. A., Murcko, M. A., Chambers, S. P., Aldape, R. A., Raybuck, S. A., and *et al.* (1994). Structure and mechanism of interleukin-1 beta converting enzyme. *Nature* 370, 270-275.
- Wolf, D. H., and Hilt, W. (2004). The proteasome: a proteolytic nanomachine of cell regulation and waste disposal. *Biochim Biophys Acta* 1695, 19-31.
- Wolter, K. G., Hsu, Y. T., Smith, C. L., Nechushtan, A., Xi, X. G., and Youle, R. J. (1997). Movement of Bax from the cytosol to mitochondria during apoptosis. *J Cell Biol* 139, 1281-1292.

- Wright, K. M., Linhoff, M. W., Potts, P. R., and Deshmukh, M. (2004). Decreased apoptosome activity with neuronal differentiation sets the threshold for strict IAP regulation of apoptosis. *J Cell Biol* *167*, 303-313.
- Wright, K. M., Smith, M. I., Farrag, L., and Deshmukh, M. (2007). Chromatin modification of Apaf-1 restricts the apoptotic pathway in mature neurons. *J Cell Biol* *179*, 825-832.
- Xie, Z., and Klionsky, D. J. (2007). Autophagosome formation: core machinery and adaptations. *Nat Cell Biol* *9*, 1102-1109.
- Xirodimas, D. P., Saville, M. K., Bourdon, J. C., Hay, R. T., and Lane, D. P. (2004). Mdm2-mediated NEDD8 conjugation of p53 inhibits its transcriptional activity. *Cell* *118*, 83-97.
- Xue, L., Fletcher, G. C., and Tolkovsky, A. M. (1999). Autophagy is activated by apoptotic signalling in sympathetic neurons: an alternative mechanism of death execution. *Mol Cell Neurosci* *14*, 180-198.
- Xue, L., Fletcher, G. C., and Tolkovsky, A. M. (2001). Mitochondria are selectively eliminated from eukaryotic cells after blockade of caspases during apoptosis. *Curr Biol* *11*, 361-365.
- Yakovlev, A. G., Ota, K., Wang, G., Movsesyan, V., Bao, W. L., Yoshihara, K., and Faden, A. I. (2001). Differential expression of apoptotic protease-activating factor-1 and caspase-3 genes and susceptibility to apoptosis during brain development and after traumatic brain injury. *J Neurosci* *21*, 7439-7446.
- Yamada, T., Carson, A. R., Caniggia, I., Umebayashi, K., Yoshimori, T., Nakabayashi, K., and Scherer, S. W. (2005). Endothelial nitric-oxide synthase antisense (NOS3AS) gene encodes an autophagy-related protein (APG9-like2) highly expressed in trophoblast. *J Biol Chem* *280*, 18283-18290.
- Yamada, Y., Suzuki, N. N., Hanada, T., Ichimura, Y., Kumeta, H., Fujioka, Y., Ohsumi, Y., and Inagaki, F. (2007). The crystal structure of Atg3, an autophagy-related ubiquitin carrier protein (E2) enzyme that mediates Atg8 lipidation. *J Biol Chem* *282*, 8036-8043.

- Yamamoto, A., Tagawa, Y., Yoshimori, T., Moriyama, Y., Masaki, R., and Tashiro, Y. (1998). Bafilomycin A1 prevents maturation of autophagic vacuoles by inhibiting fusion between autophagosomes and lysosomes in rat hepatoma cell line, H-4-II-E cells. *Cell Struct Funct* 23, 33-42.
- Yan, G. M., Ni, B., Weller, M., Wood, K. A., and Paul, S. M. (1994). Depolarization or glutamate receptor activation blocks apoptotic cell death of cultured cerebellar granule neurons. *Brain Res* 656, 43-51.
- Yan, J., Kuroyanagi, H., Kuroiwa, A., Matsuda, Y., Tokumitsu, H., Tomoda, T., Shirasawa, T., and Muramatsu, M. (1998). Identification of mouse ULK1, a novel protein kinase structurally related to *C. elegans* UNC-51. *Biochem Biophys Res Commun* 246, 222-227.
- Yan, J., Kuroyanagi, H., Tomemori, T., Okazaki, N., Asato, K., Matsuda, Y., Suzuki, Y., Ohshima, Y., Mitani, S., Masuho, Y., *et al.* (1999). Mouse ULK2, a novel member of the UNC-51-like protein kinases: unique features of functional domains. *Oncogene* 18, 5850-5859.
- Yang, J., Liu, X., Bhalla, K., Kim, C. N., Ibrado, A. M., Cai, J., Peng, T. I., Jones, D. P., and Wang, X. (1997). Prevention of apoptosis by Bcl-2: release of cytochrome c from mitochondria blocked. *Science* 275, 1129-1132.
- Yang, Y., and Yu, X. (2003). Regulation of apoptosis: the ubiquitous way. *FASEB J* 17, 790-799.
- Yao, T., and Cohen, R. E. (2002). A cryptic protease couples deubiquitination and degradation by the proteasome. *Nature* 419, 403-407.
- Yoshida, H., Kong, Y. Y., Yoshida, R., Elia, A. J., Hakem, A., Hakem, R., Penninger, J. M., and Mak, T. W. (1998). Apaf1 is required for mitochondrial pathways of apoptosis and brain development. *Cell* 94, 739-750.
- Yoshimori, T., Yamamoto, A., Moriyama, Y., Futai, M., and Tashiro, Y. (1991). Bafilomycin A1, a specific inhibitor of vacuolar-type H(+)-ATPase, inhibits acidification and protein degradation in lysosomes of cultured cells. *J Biol Chem* 266, 17707-17712.

- Youle, R. J., and Strasser, A. (2008). The BCL-2 protein family: opposing activities that mediate cell death. *Nat Rev Mol Cell Biol* 9, 47-59.
- Young, A. R., Chan, E. Y., Hu, X. W., Kochl, R., Crawshaw, S. G., High, S., Hailey, D. W., Lippincott-Schwartz, J., and Tooze, S. A. (2006). Starvation and ULK1-dependent cycling of mammalian Atg9 between the TGN and endosomes. *J Cell Sci* 119, 3888-3900.
- Young, P., Deveraux, Q., Beal, R. E., Pickart, C. M., and Rechsteiner, M. (1998). Characterization of two polyubiquitin binding sites in the 26 S protease subunit 5a. *J Biol Chem* 273, 5461-5467.
- Yousefi, S., Perozzo, R., Schmid, I., Ziemiecki, A., Schaffner, T., Scapozza, L., Brunner, T., and Simon, H. U. (2006). Calpain-mediated cleavage of Atg5 switches autophagy to apoptosis. *Nat Cell Biol* 8, 1124-1132.
- Yu, L., Alva, A., Su, H., Dutt, P., Freundt, E., Welsh, S., Baehrecke, E. H., and Lenardo, M. J. (2004). Regulation of an ATG7-beclin 1 program of autophagic cell death by caspase-8. *Science* 304, 1500-1502.
- Yuan, J., and Horvitz, H. R. (1992). The *Caenorhabditis elegans* cell death gene *ced-4* encodes a novel protein and is expressed during the period of extensive programmed cell death. *Development* 116, 309-320.
- Yuan, J., Shaham, S., Ledoux, S., Ellis, H. M., and Horvitz, H. R. (1993). The *C. elegans* cell death gene *ced-3* encodes a protein similar to mammalian interleukin-1 beta-converting enzyme. *Cell* 75, 641-652.
- Yuan, J., and Yankner, B. A. (2000). Apoptosis in the nervous system. *Nature* 407, 802-809.
- Yue, Z., Horton, A., Bravin, M., DeJager, P. L., Selimi, F., and Heintz, N. (2002). A novel protein complex linking the delta 2 glutamate receptor and autophagy: implications for neurodegeneration in *lurcher* mice. *Neuron* 35, 921-933.

- Yue, Z., Jin, S., Yang, C., Levine, A. J., and Heintz, N. (2003). Beclin 1, an autophagy gene essential for early embryonic development, is a haploinsufficient tumor suppressor. *Proc Natl Acad Sci U S A* *100*, 15077-15082.
- Zavrski, I., Jakob, C., Schmid, P., Krebbel, H., Kaiser, M., Fleissner, C., Rosche, M., Possinger, K., and Sezer, O. (2005). Proteasome: an emerging target for cancer therapy. *Anticancer Drugs* *16*, 475-481.
- Zeng, X., Overmeyer, J. H., and Maltese, W. A. (2006). Functional specificity of the mammalian Beclin-Vps34 PI 3-kinase complex in macroautophagy versus endocytosis and lysosomal enzyme trafficking. *J Cell Sci* *119*, 259-270.
- Zhang, B., Gojo, I., and Fenton, R. G. (2002). Myeloid cell factor-1 is a critical survival factor for multiple myeloma. *Blood* *99*, 1885-1893.
- Zhang, J., and D'Ercole, A. J. (2004). Expression of Mcl-1 in cerebellar granule neurons is regulated by IGF-I in a developmentally specific fashion. *Brain Res Dev Brain Res* *152*, 255-263.
- Zhang, K. Z., Westberg, J. A., Holtta, E., and Andersson, L. C. (1996). BCL2 regulates neural differentiation. *Proc Natl Acad Sci U S A* *93*, 4504-4508.
- Zhao, Y., Tan, J., Zhuang, L., Jiang, X., Liu, E. T., and Yu, Q. (2005). Inhibitors of histone deacetylases target the Rb-E2F1 pathway for apoptosis induction through activation of proapoptotic protein Bim. *Proc Natl Acad Sci U S A* *102*, 16090-16095.
- Zheng, N., Schulman, B. A., Song, L., Miller, J. J., Jeffrey, P. D., Wang, P., Chu, C., Koepf, D. M., Elledge, S. J., Pagano, M., *et al.* (2002). Structure of the Cul1-Rbx1-Skp1-F boxSkp2 SCF ubiquitin ligase complex. *Nature* *416*, 703-709.
- Zheng, N., Wang, P., Jeffrey, P. D., and Pavletich, N. P. (2000). Structure of a c-Cbl-UbcH7 complex: RING domain function in ubiquitin-protein ligases. *Cell* *102*, 533-539.
- Zhu, Q. Z., Wani, G., Wang, Q. E., El-mahdy, M., Snapka, R. M., and Wani, A. A. (2005). Deubiquitination by proteasome is coordinated with substrate translocation for proteolysis in vivo. *Exp Cell Res* *307*, 436-451.

Zou, H., Henzel, W. J., Liu, X., Lutschg, A., and Wang, X. (1997). Apaf-1, a human protein homologous to *C. elegans* CED-4, participates in cytochrome c-dependent activation of caspase-3. *Cell* 90, 405-413.

Zuhl, F., Seemuller, E., Golbik, R., and Baumeister, W. (1997). Dissecting the assembly pathway of the 20S proteasome. *FEBS Lett* 418, 189-194.

Zwickl, P., Ng, D., Woo, K. M., Klenk, H. P., and Goldberg, A. L. (1999). An archaeobacterial ATPase, homologous to ATPases in the eukaryotic 26 S proteasome, activates protein breakdown by 20 S proteasomes. *J Biol Chem* 274, 26008-26014.